The role of *EZH2* mutation in paediatric myelodysplasia



Nicholas James Fordham

St Catherine's College

University of Oxford

A thesis submitted for the degree of

Doctor of Philosophy

Hilary 2021

Dedication

For Matilda and Harriet, who hopefully noticed no difference.
And for Gemma, who will have done, and tolerated more than the failed trips.
Without their support and inspiration, I could not have achieved this work.

Abstract

Background: Fetal haematopoiesis has clear functional and molecular differences to adult haematopoiesis. Some leukaemias, such as juvenile myelomonocytic leukaemia (JMML), are believed to originate in fetal cells, and frequently have a poor prognosis. The majority of patients with JMML have a RAS activating mutation, and where mouse models exist, these primarily involve post-natal induction of mutations, which may not be suitable given the fetal origin of the disorder. Children with JMML develop recurrent mutations involving loss of function in the enhancer of zeste homolog 2 (*EZH2),* which is known to control developmental pathways, either through direct mutations or through loss of chromosomal material (monosomy 7). These are particularly associated with *Kras* mutations. It is not clear whether these mutations are gained in post-natal or adult life, however they worsen the prognosis. In other mouse models of myeloid disorders *Ezh2* loss leads to reactivation of fetal pathways, but their role in JMML remains unclear.

Aim: The overarching aim of this project was to investigate the fetal origins of JMML by creating a *Kras* mutant mouse model derived from fetal cells. This would allow me to study whether fetal versus adult induction of mutations affected the phenotype of the leukaemia and the effect of secondary *Ezh2* mutation in this model.

My specific aims were:
1. To develop a mouse model to investigate the fetal origins of JMML;
2. To investigate the effect of the acquisition of leukaemogenic mutations at differing stages of murine development;
3. To identify if mutation of *Ezh2* alters or enhances leukaemogenesis in a JMML model system.

Results:

1. Developing a mouse model to study the fetal origins of JMML: Initial experiments with Vav-iCre induction of mutations demonstrated the proof of principle that $Kras^{G12D}$ mutant cells from the fetal liver (FL) can cause a myelomonocytic leukaemia. *Ezh2* knock-out (KO) in combination with $Kras^{G12D}$, however, led to a cellular defect with no engraftment. Therefore, spontaneous induction in a small clone with Mx1Cre was

used. Transplantation experiments showed a possible combinatorial effect of *Kras* and *Ezh2* mutations, but there was a high rate of T-cell leukaemia as well as difficulty in proving a fetal origin of mutation. Fgd5CreERT2 induction was optimised, showing no spontaneous deletion in adult or fetal life, and *Fgd5* surface expression on yolk sac (YS) erythro-myeloid progenitors (EMPs), as well as FL, and adult bone marrow (aBM) haematopoietic stem cells (HSCs). Optimised dosing allowed delivery of induced FL mice, as well as induction in the aBM for comparison.

2. The effect of acquisition of mutations at differing stages of ontogeny: Kras mutation in the FL created a good model for JMML, with splenomegaly, thrombocytopenia, and monocytosis with evidence of lung infiltration, as seen in children with JMML. $Kras^{G12D}$ mutant FL mice had a significantly shortened latency of disease to adult mice, accompanied by a change in phenotype. The fetal induction allowed an almost universally penetrant myelomonocytic leukaemia, however on adult induction these mice developed a range of disorders, including a T-cell leukaemia not seen in the fetal cohort. Further, where the adult mice had phenotypic HSC depletion, the FL-induced mice did not.
3. Does *Ezh2* alter or enhance leukaemogenesis? Induction of *Ezh2* in adult and fetal mice altered the phenotype of disease, with adult mice developing a more 'fetal-like' increase in myelomonocytic leukaemia, whereas fetal loss of *Ezh2* led to a diminishing of the penetrance as well as alteration of the phenotype. On analysis of the HSPC compartment, *Ezh2* loss in adult leukaemic mice appeared to rescue the stem cell phenotype, but in fetal life depleted the stem cell compartment. This suggests a clear differential role of *Ezh2* and points towards a post-natal acquisition of *Ezh2* loss.

Conclusion: This project demonstrates a novel model for JMML with a clear fetal origin. Mice induced with $Kras^{G12D}$ in the FL develop a JMML phenotype with an alteration in phenotype with mutational gain in adult life. This suggests an important role of ontogeny in the timing of these mutations, and the model is the first model to allow study of fetal versus adult gain of mutations. The loss of *Ezh2* suggests that this may be a post-natal acquired secondary mutation, but clearly changes the phenotype of both adult and fetal mice, whilst accelerating disease. This project has been impacted by the COVID-19 pandemic, particularly due to cancellation of RNA sequencing, which is being planned to further investigate differences in the gene expression programs in the fetal and adult leukaemic mice.

Acknowledgements

I am forever indebted to my supervisors, Prof. Adam Mead and Prof. Irene Roberts for their amazing supervision; they were always available, however busy, and without their kindness, patience and guidance -- and good humour -- I would not have known where to begin. Thank you for taking a chance on me, and spending too much on mice.

Secondly I would like to thank all the members of the Mead and Roberts laboratories for their teaching, help, support and company. Thank you especially to Sorcha, Neo, Natalina, Chris, Siobhan, Ruggiero, Lucy, Catherine, Gemma, Joana, Bishan, Eleni, Andi, Ben, Beth, Nikos, Jen, Charlotte, Cristina, Helene, and Alba. Thank you to members of the other groups who helped, Chris Fisher, Prof. Marella De Bruijn, Prof. Tom Milne and James Davies, as well as the facilities team within the WIMM.

This project would not have been possible without the staff in the biomedical sciences department. Thank you so much for the care and attention from all in the JR BSB, as well as the sporadic weekend procedures. Andrew, Sara, Jordan without you the fostering could not have happened, and all in Wing B, thank you for the chat and the *extreme* patience with my handling. I hope someone beats my scruffing record soon.

To the flow cytometry facility, where the bulk of my analysis took place, thank you. Particularly to Paul, Sally and Kevin who helped with sorting and troubleshooting. Thank you to the X50, with which for many weeks I spent longer with than my wife.

I am very grateful to the funders of this project, the Kay Kendall Leukaemia Fund, who provided the funds which allowed me to pursue this project.

Thank you especially to all at the WIMM who kept me sane, tolerated my rants, and shared photos. Thank you Emma and Sarah for the gossip. Thank you Sorcha, Natalina, Lucy and Siobhan for the times away from the bench, your friendship, and your ears. I hope we stay in touch. A final acknowledgement to Jennie, who drew the mouse.

Publications and Presentations

Publications

Fordham, N., Baker, E., Forton, D., Klammer, M., Patel, K., Qadir, D., Reyal, Y., Willis, F. and Koh, M.B. First reported case of safe and efficacious use of tocilizumab for treatment of hyperinflammatory syndrome associated with COVID-19 in an allogeneic stem cell transplant patient. eJHaem. 2016; 2: 143-146.

Louka E, Povinelli B, Rodriguez-Meira A, Buck G, Wen WX, Wang G, Sousos N, Ashley N, Hamblin A, Booth CAG, Roy A, Elliott N, Iskander D, de la Fuente J, **Fordham N**, O'Byrne S, Inglott S, Norfo R, Salio M, Thongjuea S, Rao A, Roberts I, Mead AJ. Heterogeneous disease-propagating stem cells in juvenile myelomonocytic leukemia. J Exp Med. 2021 Feb 1;218(2):e20180853. doi: 10.1084/jem.20180853.

O'Byrne S, Elliott N, Rice S, Buck G, **Fordham N**, Garnett C, Godfrey L, Crump NT, Wright G, Inglott S, Hua P, Psaila B, Povinelli B, Knapp DJHF, Agraz-Doblas A, Bueno C, Varela I, Bennett P, Koohy H, Watt SM, Karadimitris A, Mead AJ, Ancliff P, Vyas P, Menendez P, Milne TA, Roberts I, Roy A. Discovery of a CD10-negative B-progenitor in human fetal life identifies unique ontogeny-related developmental programs. Blood. 2019 Sep 26;134(13):1059-1071.

Roberts I, **Fordham NJ**, Rao A, Bain BJ. Neonatal leukaemia. Br J Haematol. 2018 Jul;182(2):170-184. doi: 10.1111/bjh.15246. Epub 2018 May 28.

Mead AJ, Neo WH, Barkas N, Matsuoka S, Giustacchini A, Facchini R, Thongjuea S, Jamieson L, Booth CAG, **Fordham N**, Di Genua C, Atkinson D, Chowdhury O, Repapi E, Gray N, Kharazi S, Clark SA, Bouriez T, Woll P, Suda T, Nerlov C, Jacobsen SEW. Niche-mediated depletion of the normal hematopoietic stem cell reservoir by Flt3-ITD-induced myeloproliferation. J Exp Med. 2017 Jul 3;214(7):2005-2021.

Presentations

Roy, A., Psaila, B., Thongjuea, S., Ashley, N., Buck, G., O'Byrne, S., Elliott, N., Louka, E., **Fordham, N**., Hua, P., Povinelli, B., Heuston, E., Iskander, D., Karadimitris, A., Bodine, D., Mead, A., Roberts, I. (2018). Single cell profiling reveals key differences in the cellular architecture of human haematopoietic stem and progenitor cells throughout fetal and adult life. EHA 2018.

Louka, E., Povinelli, B., Rodriguez-Meira, A., Buck, G., Hamblin, A., Booth, C., Roy, A., Elliott, N., Iskander, D., de la Fuente, J., **Fordham, N**., O'Byrne, S., Inglott, S., Rao, A., Roberts, I., Mead, A. (2017). Molecular and Functional Characterization of Disease-Propagating Stem Cells in Juvenile Myelomonocytic Leukemia. Blood 130, 379.

O'Byrne, S., Elliott, N., Rice, S., **Fordham, N**., O'Connor, D., Taylor, S., Roy, A., Roberts, I. The impact of trisomy 21 on fetal B-lymphopoiesis. WIMM day 2018, Oxford.

O'Byrne, S., Elliott, N., Buck, G., Liu, B., Povinelli, B., **Fordham, N**., Louka, E., Bartolovic, K., Karadimitris, A., Mead, A., Roberts, I., Roy, A. (2017). Re-ordering the B cell development hierarchy in human fetal bone marrow: characterisation of a novel human fetal B progenitor. EHA 2017.

O'Byrne, S., Elliott, N., Buck, G., Liu, B., Povinelli, B., **Fordham, N**., Louka, E., Bartolovic, K., Karadimitris, A., Mead, A., Roberts, I., Roy, A. Reordering the B cell development hierarchy in human fetal bone marrow: characterisation of a novel human fetal B progenitor. WIMM day 2017, Oxford.

Elliott, N., O'Connor, D., Roy, A., Labbett, E., O'Byrne, S., Rice, S., **Fordham, N.**, Liu, B., Cowan, G., Karadimitris, A., Vyas, P., Roberts, I. (2018). Perturbation of fetal liver stromal cell function by trisomy 21 promotes increased erythro-megakaryopoiesis by fetal HSPC. EHA 2018.

List of abbreviations

6-MP	6 Mercaptopurine
aBM	Adult bone marrow
AGM	Aorto-gonad-mesonephros
ALL	Acute lymphoblastic leukaemia
AML	Acute myeloid leukaemia
BM	Bone marrow
BFU-E	Burst Forming Unit - Erythroid
CFU-E	Colony Forming Unit - Erythroid
CFU-GM	Colony Forming Unit - Granulocyte, monocyte
CMML	Chronic Myelomonocytic leukaemia
CS	Caesarian Section
DMEM	Dulbecco's Modified Eagle Medium
dpc	Days post-coitum
DS	Down Syndrome
E	Embryonic day
EMP	Erythro-myeloid precursor
EZH1/2	Enhancer of Zeste Homologue 1 or 2
FAB	French-American-British
FACS	Fluoresence activated cell sorting
FCS	Fetal calf serum
FL	Fetal Liver
FMO	Fluorsence minus one
G-CSF	Granulocyte colony stimulating factor
GM-CSF	Granulocyte-macrophage colony stimulating factor
GMP	Granulocyte-monocyte precursor
H3K27	Histone 3 Lysine 27
HSC	Haematopoietic Stem Cell
HSCT	Haematopoietic Stem Cell Transplant
HSPC	Haematopoietic stem and progenitor cell
IL	Interleukin
IMDM	Iscove's Modified Dulbecco's Medium

IP	Intraperitoneal
iPSC	Induced pluripotent stem cell
JCML	Juvenile Chronic Myelogenous Leukaemia
JMML	Juvenile Myelomonocytic Leukaemia
KI	Knock-in
KO	Knock-out
LMPP	Lymphoid primed multipotent progenitor
LOF	Loss of function
LOH	Loss of heterozygosity
MFI	Mean fluorescence intensity
ML	Myeloid Leukaemia
me(1-3)	Methylation 1-3
MPNST	Malignant peripheral nerve sheath tumours
MPP	Multi-potent progenitor
NSG	NOD-scid-IL2Rgnull
PB	Peripheral blood
PBS	Phosphate buffered saline
pcw	Post-conception weeks
Pen/Strep	Penicillin/Streptomycin
PND	Postnatal day
PolyI:C	Polyinosinic:polycytidylic acid
PRC2	Polycomb Repressive Complex 2
ProE	Proerythroid precursors
RNAseq	RNA sequencing
SEM	Standard error of mean
sp	Somite pairs
TAM	Transient Abnormal Myelopoiesis
YS	Yolk sac
WHO	World Health Organisation
WT	Wild type

List of figures

1.1	Summary of fetal murine haematopoiesis	2
1.2	Overview of the traditional view of the human, HSC derived, haematopoietic hierarchy	3
1.3	Hypothesis of fetal and postnatal clonal progression	9
1.4	Summary of RAS pathway mutations and frequency of occurrence in JMML	16
1.5	Summary of PRC2 and associated proteins	23
2.1	Example genotyping PCR products	51
2.2	Example gating strategy for lineage panel, showing gating from PB from adult transplanted mouse	64
2.3	Example gating strategy for HSC panel showing gating on fresh adult BM	64
3.1	Vav-iCre genotypes at birth	74
3.2	Fetal liver analysis of Vav-iCre embryos	75
3.3	Fetal liver induction with Vav-iCre and Tie2Cre	76
3.4	HSPCs in the FL with Vav-iCre induction	76
3.5	The Vav-iCre FL extended myeloid phentoype alters with mutant *Kras*	78
3.6	Erythroid precursors in E12.5 FL	79
3.7	FL Pre-GM population analysis	80
3.8	E9.5 EMP immunophenotype	82
3.9	Yolk sac cell counts	82
3.10	Overview of Vav-iCre FL transplantation experiments	83
3.11	Outcome of E12.5 FL cryopreserved transplants	84
3.12	Transplanting with fresh E12.5 FL leads to T-cell leukaemia	85
3.13	*Ezh2* loss can lead to a myeloid leukaemia in *Kras* mutant cells	86
3.14	Vav-iCre FL transplants using a million experimental cells	87
3.15	Pooled data from terminal readouts of mice transplanted with E12.5 FL	88
3.16	Peripheral blood phenotype of mice transplanted with fresh FL	89
3.17	Total engraftment from Vav-iCre FL fresh experiments is reduced in *Ezh2*-KO mice	90
3.18	Overview of Mx1Cre transplantation experiments	91

3.19 Mx1Cre induction leads to dTomato expression in all genotypes, despite different leukaemias 92
3.20 Haematological phenotype of Mx1Cre FL transplanted mice 93
3.21 Mixed phenotype disease following transplant 94
3.22 Summary of terminal readouts from FL Mx1Cre transplants 94
3.23 Summary of BM terminal readouts from FL Mx1Cre transplants 95
3.24 Deletion on Ezh2 and Kras FL 97
3.25 Sort gates to investigate LSK *Ezh2* deletion 98
3.26 Mx1Cre spontaneous expression in E15.5 FL 99
3.27 Ezh2 expression in dTomato positive FL LSKs 100
3.28 Optimisation of deletion protocols for dosing Mx1Cre neonatal mice 102
3.29 Summary of Mx1Cre neonatal mice 103
3.30 Tissue analysis of neonatal induced mice 104
3.31 Summary of adult Mx1Cre induced adult primary mice 105
3.32 Summary of genotypes and nomenclatures used for Fgd5CreERT2 phenotyping, transplantation and primary mice 106
3.33 Fluorescence of FL and adult Fgd5CreERT transgenic LSKs 107
3.34 Fgd5CreERT2 lacks spontaneous deletion 108
3.35 Proof of principle that tamoxifen can be used for dual stage deletions 110
3.36 Overview of tandem transplantation experiments using Fgd5CreERT2 induction in FL 111
3.37 Fgd5CreERT2 transplanted FL and adult mice 112
3.38 FL induced transplants, with expansion *in-utero* until E19.5 113
3.39 Optimising fetal induction with tamoxifen 114
3.40 FL induced at E12.5 and E13.5 with 4mg tamoxifen 115
3.41 Fetal deletion and weaning using a single dose of tamoxifen at E14.5 116

4.1 Overview of mating strategy and tamoxifen administration to achieve WT and K-F pups 125
4.2 Survival of mice from induction 127
4.3 Phenotype of fetal and adult-induced mice 127
4.4 Haematological findings at terminal readout 129
4.5 Haemoglobin analysis 130
4.6 PB morphology of primary mice 131

4.7	Histopathology of BM	132
4.8	Histopathology of lungs	133
4.9	Bone marrow LSKs in K-F mice	134
4.10	BM LK and myeloid HSPCs	135
4.11	Deletion in the LSK compartment in FL- and aBM-induced mutant Kras and Ezh2 deficient mice	136
4.12	Overview of transplantation experiments using cryopreserved BM from primary induced mice	137
4.13	Despite the findings in primary mice, T cell leukaemia is still prevalent in the transplantation setting	138
4.14	Myelomonocytic leukaemia can be transplanted from both adult and fetal and adult induced K-F mice	139
4.15	Transplantation of secondary transplanted mice into tertiary transplant recipients	140
4.16	Experimental overview of re-plating assays	141
4.17	Colony replating assays	142
4.18	Fetal induction leads to borderline GM-CSF hypersensitivity	143
4.19	FACS sorting of cell populations	144
4.20	Engraftment of HSPC populations from fetally-induced and adult-induced K-F and WT mice	145
4.21	Optimisation of yolk sac HSPC transplantation in NSG mice	148
4.22	Summary of single Vav-iCre YS experiments	148
4.23	Single whole YS transplantations into NSG mice	149
4.24	Data from pooled YS transplants	150
4.25	Analysis of PB, BM and spleen from the YS-derived K-F leukaemia	151
4.26	Analysis of PB, BM and spleen from the YS-derived EEK-V leukaemia	152
4.27	EMPs have surface expression of Fgd5	154
4.28	Fgd5 transgenic EMPs are inducible with tamoxifen	155
4.29	Induction of E8.5 YS shows persistence of dTomato in the E16.5 FL	155
4.30	Optimisation of tamoxifen dosing	156
4.31	Induction of Kras mutant embryos at E7.5 with 1.5mg Tamoxifen	157
4.32	YS EK-F mouse, induced with 1.5mg tamoxifen at E7.5	158
4.33	Induction of mutant *Kras* and *Ezh2* deletion at E7.5 with 0.5mg tamoxifen	159

5.1 Overview of transplantation experiments of mutant *Kras* with or without *Ezh2* loss using cryopreserved BM from mice transplanted with Mx1Cre induced FL 168
5.2 Ezh2-KO permits the transplantation of myeloid leukaemia 169
5.3 Phenotypic switching on serial transplantation of BM cells from myeloid primary mice 169
5.4 Overview of serial, rapid, sequential transplantation experiments 170
5.5 Ezh2-KO alone permits serial transplantability 171
5.6 $Kras^{G12D}$ depletes myeloid engraftment 172
5.7 Serial transplantation diminishes but does not abolish T cell leukaemia 172
5.8 Using a sublethal irradiation protocol to investigate the interaction between mutant Kras and Ezh2 loss in leukaemogenesis 173
5.9 Ezh2 loss in $Kras^{G12D}$ mutant mice accelerates disease and alters the phenotype 175
5.10 Adult mice with Kras induced leukaemia develop a myeloid leukaemia with loss of Ezh2 177
5.11 BM histology of adult induced mice consistent with flow cytometry 178
5.12 *Ezh2* loss rescues the stem cell depletion of K-F mice 178
5.13 Outcome of transplantation of adult induced BM into CD45.1 recipients 179
5.14 Design of experiments to investigate the impact of Ezh2 loss on mutant Kras-driven leukaemia by induction in fetal cells 180
5.15 Ezh2 loss in fetal induced $Kras^{G12D}$ mutant mice accelerates disease and alters the phenotype 181
5.16 Ezh2 loss changes the PB phenotypic findings in fetal induced mice 182
5.17 Fetal Ezh2 loss affects the morphology of Kras mutated leukaemia 183
5.18 Tissue infiltration in BM and Lungs of myelo-monocytic cells 184
5.19 Ezh2 loss depletes the LSK and HSC compartments 185
5.20 Transplantation of BM from fetal induced mice with myelomonocytic leukaemia into CD45.1 recipients 187
5.21 The effects of Ezh2 loss alter depending when in ontogeny the loss occurs 188
5.22 Ezh2 loss expands or depletes HSCs, depending on cellular context at acquisition 189

Contents

Dedication *iii*

Abstract *iv*

Acknowledgements *vi*

Publications and presentations *vii*

List of abbreviations *ix*

List of figures *xi*

Contents *xv*

1. **Introduction** **1**

1-1 Comparisons of fetal and adult haematopoiesis 1

1-1.1 Normal fetal haematopoiesis throughout development 1

1-1.2 Differences between fetal and adult haematopoiesis 5

1-2 The fetal origins of leukaemia 7

1-2.1 Current evidence for leukaemia originating *in-utero* 7

1-2.2 Recurring characteristics of leukaemia of fetal origin 8

1-3 Juvenile myelomonocytic leukaemia (JMML) 10

1-3.1 The clinical and haematological features of JMML 10

1-3.2 Cellular and molecular pathogenesis 14

1-3.3 Factors affecting the prognosis of JMML 18

1-3.4 Mouse model systems available for JMML 19

1-4 How aberrations in *Ezh2* disturb haematopoiesis 23

1-4.1 The normal function of Ezh2 23

1-4.2 *EZH2* mutations in human haematopoietic disease 27

1-4.3 Therapeutic targeting of *EZH2* alterations 30

1-5 Hypothesis and aims 31

2. Methods 48

2-1 Murine strains 48

2-2 Generation of embryos 51

2-3 Administration of substances 52

i) Tamoxifen +/- Progesterone 52

ii) PolyI:C 53

2-4 Delivery and fostering of pups following tamoxifen administration *in utero* 54

2-5 Isolation and processing of tissues 55

i) Peripheral blood 55

ii) Bone marrow (BM) 56

iii) Spleen 56

iv) Fetal liver (FL) 56

v) Yolk sac (YS) 57

vi) Genomic DNA 57

vii) Cryopreservation and thawing of cells and tissues 57

2-6 Transplantation analyses 58

i) Transplantation of bulk BM or FL 58

ii) Transplantation of specific cell populations 60

iii) Transplantation of YS 60

2-7 Histology and morphological assessment 61

2-8 Flow cytometric analysis and fluorescent assistant cell sorting (FACS) 61

2-9 *In-vitro* assays 65

i) Methocult assays to isolate colonies for DNA analysis 65

ii) Re-plating assays 65

iii) GM-CSF hypersensitivity assays 66

2-10 Molecular assays 67

i) qPCR of Ezh2 in FL 67

ii) RNAseq of murine haematopoietic stem and progenitor cells 67

iii) Isoelectric focussing of haemoglobins 68

2-11 Statistics 68

3. The development of a mouse model to investigate the fetal origins of leukaemia 71

3-1 The fetal phenotype associated with $Kras^{G12D}$ mutation and *Ezh2* knock out using Vav-iCre 74

i) Analysis of HSC and progenitor numbers in fetal liver (FL) 74

ii) Analysis of haematopoiesis in the murine yolk sac 81

3-2 Transplantation of FL actiaved using Vav-iCre 83

i) Optimising the transplant protocols 83

ii) The effect of cell dosage 86

3-3 Using Mx1Cre to activate mutations in a small number of FL cells 90

i) A transplantation based model of leukaemia derived from FL HSPCs 90

3-4 Limitations of using Mx1Cre to study the development of leukaemia at different stages of ontogeny 96

i) Quantifying fetal *Kras/Ezh2* deletion 97

ii) Is dTomato an accurate marker of recombination of other transgenes? 99

iii) Limitations of Mx1Cre and transplantation based model systems 100

3-5 The potential to use primary mice: pilot experiments using Mx1Cre induced mice 101

i) Neonatal mice 101

ii) Adult mice 104

3-6 Optimisation of an Fgd5CreERT2 based model 106

i) Leakiness in FL and aBM 107

ii) Induction of mutations using tamoxifen in FL and adult BM (aBM) 109

iii) Transplantation of HSPCs induced in FL or aBM 110

iv) The effect of expansion within the FL microenvironment 112

v) Identifying the correct dosage for FL induction to allow pups to survive fostering 113

3-7 Summary and Discussion 117

i) The effect of *Ezh2* in combination with mutant *Kras* 117

ii) Developing a model to study the timing of mutations using Fgd5CreERT2 118

iii) Future work 119

4. The effect of leukaemogenic mutation at different stages of gestation 124

4-1. Survival and phenotypic changes associated with the timing of induction of $Kras^{G12D}$ mutation 125

i) Comparison of survival of FL and aBM-induced mice 126
ii) High frequency of myelomonocytic leukaemia in FL-induced K-F mice 128
iii) Histological changes in tissues from FL- and aBM-induced K-F mice 131
iv) Alterations in the HSPC compartments 133
v) Deletion efficiency using a reporter and molecular methods 135
4-2 The functional consequence of *Kras* mutation in fetal HSPC 137
i) Serial transplantability of mutant *Kras* HSPC 137
ii) *In-vitro* studies: re-plating and GM-CSF hypersensitivity of fetally-induced K-F LSKs 140
4-3 Cellular origins of fetal induced myelomonocytic leukaemia 143
i) Identifying leukaemia-propagating cells by transplantation of purified HSPC populations 143
4-4 Molecular changes associated with induction of $Kras^{G12D}$ in fetal or adult life 146
4-5 Don't forget the yolk sac (YS)! 146
i) Proof of principle: YS derived leukaemia from Vav-iCre transplantation 147
ii) YS Erythro-myeloid progenitors (EMPs) have surface expression of Fgd5, which is inducible 153
iii) Optimising the induction of EMPs 155
iv) Preliminary data from primary YS induced mice: could JMML arise earlier in ontogeny than the FL? 156
4-6 Summary and Discussion 159

i) Phenotypic differences between adult and fetal induction methods 160

ii) The effect of ontogeny on function of malignant HSPCs 161

iii) The leukemic potential of YS HSPC 162

iv) Future work 162

5. The effect of *Ezh2* knock-out on a mouse model of JMML 167

5-1 Using the Mx1Cre model to assess serial transplantability of mutant *Kras* with or without *Ezh2* loss 168

i) The phenotypic consequence of *Ezh2* KO in a $Kras^{G12D}$ mouse model 168

ii) Does *Ezh2* loss in a fetal cell enhance self-renewal? 170

5-2 Does *Ezh2* knock-out in adult life alter the phenotype in a JMML model? 174

i) Leukaemia from primary mice induced to express mutant *Kras*, with or without *Ezh2* loss, in adult life 174

ii) Does *Ezh2* loss permit transplantation of a leukaemia derived from adult cells 179

5-3 How does *Ezh2* loss in fetal life affect the $Kras^{G12D}$ model of leukaemia 180

i) Impact of Ezh2 on the phenotype of mutant Kras driven disease in fetal cells 181

ii) Does *Ezh2* loss alter the function of Kras mutated leukaemia? 186

iii) Does *Ezh2* loss have differential effects in fetal and adult leukaemic mice? 187

5-4 Molecular alterations associated with *Ezh2* loss in $Kras^{G12D}$ mutated HSPCs 188

5-5 Summary and Discussion 190

i) Does *Ezh2* loss alter the $Kras^{G12D}$ driven leukaemia? 190

ii) Is there a differential effect between adult and fetal *Ezh2* loss? 191

iii) Future work 192

6. Discussion **196**

6-1 The development of a mouse model to investigate the fetal origins of leukaemia 197

i) The advantages and disadvantages of the different models used 197

ii) Future directions and possibilities of the Fgd5CreERT2 model 198

6-2 Does the timing of acquisition of mutations matter? 198

6-3 The effect of Ezh2 knock-out on a mouse model of JMML 201

i) Does *Ezh2* loss alter the phenotype of the mouse model? 202

ii) Does the Fgd5CreERT2 model inform us about the timing of acquisition of *Ezh2* loss? 204

iii) The implications of *Ezh2* loss for patient care and potential therapeutic targets 205

6-4 Limitations of the work in this project 205

6-5 Future work 208

6-6 Conclusions 209

7. **Appendices** **215**

7-1 Appendix 1: Vav-iCre 215

7-2 Appendix 2: Mx1Cre 218

7-3 Appendix 3: Fgd5CreERT2 optimisation 221

7-4 Appendix 4: Fgd5CreERT2 primary mice 223

7-5 Appendix 5: Methods 226

8 **Bibliography** **228**

Chapter 1: Introduction

1-1 Comparisons of fetal and adult haematopoiesis

1-1.1 Normal fetal haematopoiesis throughout development

i) Murine haematopoietic development

During fetal haematopoiesis, in both the human and the mouse, the sites of haematopoiesis change as cells migrate from the yolk sac (YS), through to the fetal liver (FL) and to the bone marrow (BM). Haematopoietic potential in the mouse embryo (figure 1.1) can be identified as early as embryonic day 7 (E7) with the first phase, which is transient, known as 'primitive' erythroid development, defined by both by cellular morphology and haemoglobin expression [Barker, 1968] [Moore, 1970] [Palis, 1999].

Definitive erythroid precursors are identified at E8.25 [Palis, 1999], which derive from the onset of definitive haematopoiesis in the form of YS derived erythro-myeloid progenitors (EMPs) [Moore, 1970] [Palis, 1999] [Gomez Perdiguero, 2015] [McGrath, 2015]. This EMP wave of definitive precursors show different gene expression patterns to primitive precursors, with ßH1 globin and c-myb expression [Palis, 1999] [McGrath, 2011], and have been shown to seed the FL as well as persist into post-natal life as tissue resident macrophages [Gomez Perdiguero, 2015] [Hoeffel, 2015][McGrath, 2015]. EMPs have been demonstrated to have in-vitro erythroid, myeloid and megakaryocytic potential [Gomez Perdiguero, 2015] [McGrath, 2015] (figure 1.1), however transplantation into irradiated recipients shows limited engraftment potential, with only transient engraftment of both erythroid and myeloid lineages into immunodeficient irradiated mice [McGrath, 2015].

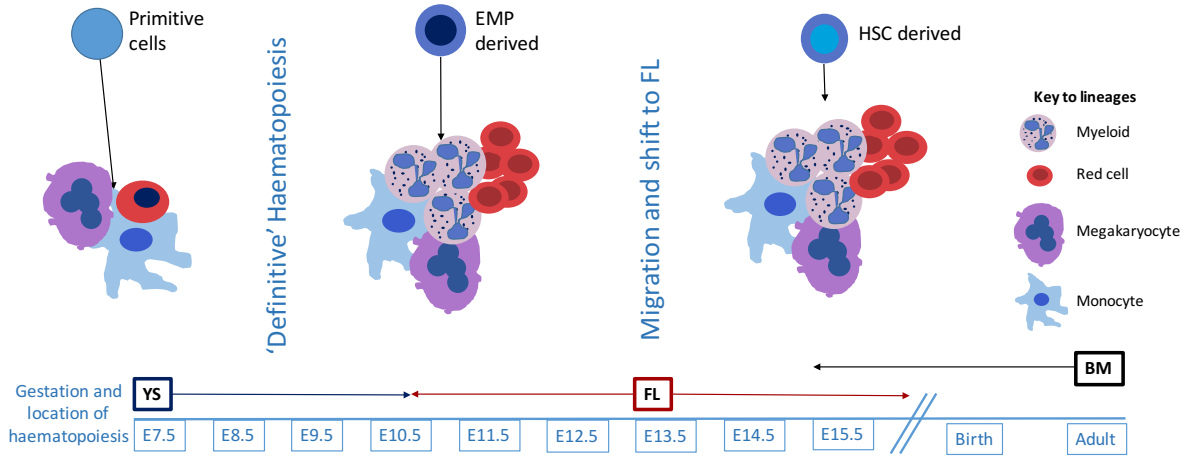


Fig 1.1 Summary of fetal murine haematopoiesis. Yolk sac (YS); Fetal liver (FL); Bone marrow (BM); Erythro-myeloid progenitor (EMP); Haematopoietic stem cell (HSC)

Further studies have clearly shown other haematopoietic progenitor cells within the YS, particularly IL7Rα and Rag1 expressing lympho-myeloid progenitors [Boiers, 2013], and transplantation experiments of whole YS have demonstrated long-term lymphoid potential, particularly when using either neonatal recipients or intra-peritoneal administration, but a persistent lack of long-term myeloid or erythroid engraftment [Cumano 1996] [Cumano 2001] [Yoder, 1997] [Yoshimoto, 2011] [McGrath, 2015]. Lineage tracing suggests that EMPs only develop myeloid potential *in-vivo* once they migrate to the FL [Gomez-Perdiguero, 2015], which may be a partial explanation for a lack of long-term myeloid engraftment from YS derived EMPs. The developmental role of the EMP has not been clearly identified, however EMP erythropoiesis is clearly important since it is sufficient to support a mouse embryo to term even though haematopoietic stem cell (HSC) development is absent [Chen, 2012]. In contrast, a conditional *Ezh2* knock-out (KO) using a *Tie2* system showed that EMP derived erythropoiesis is vital for bridging the early fetus to support HSC haematopoiesis [Neo, 2018], thus suggesting a potential bridging role in evolutionary development for EMP haematopoiesis. Although lineage tracing has suggested that EMPs contribute primarily to erythropoiesis prior to colonisation of the FL, where they develop myeloid potential [Gomez Perdiguero, 2015],

their evolving transcriptome and immunophenotype in the FL is not yet published, and therefore the role of EMPs in this haematopoietic environment is still unclear.

True HSC development takes place outside of the yolk sac, as shown in embryos lacking a functional circulation, *Ncx1*-/- mice, that cleanly show that YS emergence is separate from HSC development [Yoshimoto, 2011], reinforcing previous work demonstrating long-term HSC reconstitution from AGM [Medvinsky, 1996][de Bruijn, 2000]. These HSCs then seed the FL, with rapid expansion until E14.5, followed by migration to the BM at E15.5 [Morrison, 1995][Dzierzak, 2008][Dzierzak, 2018]. The traditional hierarchy of haematopoietic stem and progenitor cells (HSPCs) (Figure 1.2) differentiates from the FL HSCs, and although it is thought a similar hierarchy remains despite the site of haematopoiesis -- FL, BM, adult BM (aBM) -- recent studies have suggested there is more variability within each compartment, and that differentiation pathways are more diverse than previously thought with alternative hierarchies suggested [Pronk, 2007][Carrelha, 2018][Drissen, 2019].

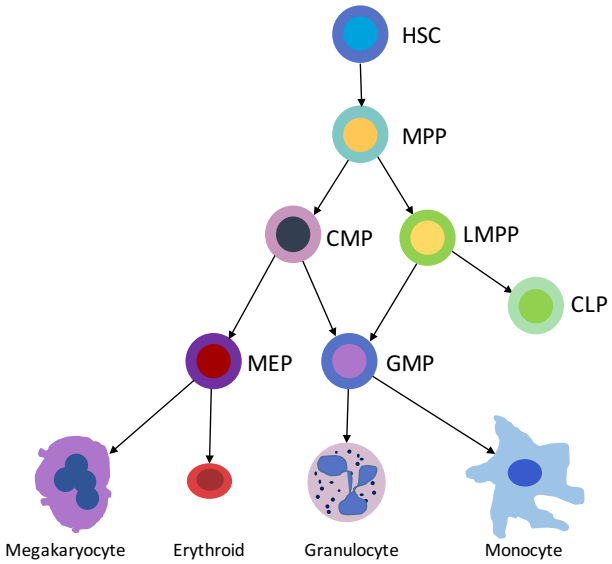


Fig 1.2 Overview of the traditional view of the human, HSC derived, haematopoietic hierarchy. Haematopoietic stem cell (HSC); Multipotent progenitor (MPP); Common Myeloid Progenitor (CMP); Lymphoid primed multipotent progenitor (LMPP); Megakaryocyte-erythroid progenitor (MEP); Granulocyte-monocyte progenitor (GMP); Common Lymphoid Progenitor (CLP)

ii) Differences between murine and human fetal haematopoiesis

Much of what we know about human fetal haematopoiesis has first been studied in mice. However, some caution is necessary using mouse models of fetal haematopoiesis as they have important differences as well as similarities to human fetal haematopoiesis. For example, although they have embryonic globins, there is no fetal haemoglobin [Sankaran, 2010]. Nevertheless, genes such as, *KLF1* and *BCL11a*, which are vital for human haemoglobin control and switching, are conserved in mice [Sankaran, 2010], as well as other fetal genes such as the HSPC regulatory gene *LIN28B* which appears to share functions between mice and humans [Shyh-Chang, 2013][Rowe, 2016]. In addition, the changes in the sites of haematopoiesis during development in humans mirror those during murine development, with emergence of HSCs from the AGM, followed by migration to the FL at 4-5 post-conception weeks (pcw) [Tavian, 1999][Oberlin, 2002]. Multi-potent cells can be identified in the human fetal BM at 10 weeks [Migliaccio, 1986][Sinka, 2012] although HSCs are not seen until 12 pcw [O'Byrne et al, 2019].

The immunophenotypic classification of murine HSPCs is different to human HSCs, with murine HSCs classified as Lineage (Lin)-, cKit+, Sca1+ve, then defined by markers including CD150+CD48-, PROCR, ESAM, as well as alternative markers [Kiel, 2005][Balazs, 2006][Ooi, 2009][Oguro, 2013]. These serial repopulating cells appear to be CD34 low or negative and therefore this is not a useful marker for murine studies [Osawa, 1996]. In contrast, human HSPCs are generally enriched with CD34+ [Dick, 1995][O'Byrne, 2019], although CD34- stem cells have been shown to exist, with distinct characteristics [Wang, 2003][Sonoda, 2021]. The accepted functional definition of an HSC, however, of long term engraftment on

transplantation into secondary murine recipients, remains the same between murine and human HSCs [Siminovitch, 1963][Spangrude, 1988][Kollman, 1994] [Fraser, 1995][Dick, 1995].

1-1.2 Differences between fetal and adult haematopoiesis

i) Functional characteristics of haematopoietic stem and progenitor cells

Although the HSPC hierarchy (Figure 1.2) is used to model both fetal and adult haematopoiesis there are a number of fetal-specific progenitors and precursors which do not fit in this traditional model. EMPs, as mentioned above, contribute to fetal haematopoiesis and persist in adults as tissue resident macrophages [Gomez-Perdiguero, 2015][McGrath, 2015], and may have a unique function [Epelman, 2014]. Evidence suggests some lymphoid progenitors show either fetal specificity or fetal-adult differences in phenotype: for example PreProB cells in human FL and BM [O'Byrne, 2019]; differences in murine B1 and B2 lymphoid progenitors with independent YS B1 cells [Montecino-Rodriguez, 2016]; YS derived lymphoid-primed multipotent progenitors [Boiers, 2013]; murine fetal-specific multipotent HSCs which preferentially give rise to lymphocytes, but do not persist into adult life [Beaudin, 2016].

Fetal HSCs are highly proliferative in comparison to adult HSCs. Adult stem cells are generally quiescent [Cheshier, 1999], and in cycling experiments using tamoxifen administration, fetal HSCs rapidly report fluorescent markers, whereas adult HSCs are more languorous [Busch, 2015]. Morrison *et al*, demonstrated that FL cells reconstitute irradiated recipients faster than adult donors as well as 25% of fetal HSCs being in S/G2/M phases [Morrison. 1995]. In this paper the authors also described how fetal HSCs express Mac-1 (CD11b) [Morrison, 1995], however this difference with adult HSCs may be because Mac-1 can also be a proliferative marker, as it has been shown that adult HSCs upregulate Mac1 on treatment with 5-fluorouracil

[Randall, 1997]. However, other phenotypic differences exist, with CD144 being expressed by 5% of E13.5 FL HSCs, and <1% of adult HSCs [Kim, 2005].

The fetal proliferative characteristics appears to last until 3 weeks postnatally, when transplantation experiments have demonstrated that HSCs assume adult repopulation velocities [Bowie, 2006][Bowie, 2007].

ii) Molecular differences between fetal and adult haematopoiesis

Several studies have shown that fetal HSPCs are reliant on signalling pathways which are not required for HSC maintenance in adult life. Some of these may be important at developmental stages, such as involvement in HSC emergence and maintenance: for example *Runx1* and *Gata2* genes [Tsai, 1994][North, 2002][Mikkola, 2006]. Another example, in human development, is *LIN28B* and *BCL11A,* which are selectively expressed in fetal life for vital developmental processes such as haemoglobin switching [Basak, 2020]. For some genes, the fetal function is unclear at present. For example, *Sox17,* which is over-expressed in HSPC in fetal mice when compared to adult counterparts, is clearly functionally vital in fetal life as deletion leads to embryonic loss due to HSPC failure [Kim, 2007]; some data show that it is necessary for maintaining AGM HSPCs and that it might do so by activating Notch1 (Saito, Nobuhisa et al, 2018) but the mechanism is unclear. Other genes, such as Lmo2 [Warren, 1994], Scl [Porcher, 1996], Aml1 [Okuda, 1996] and Mll [Ernst, 2004], appear to be vital for HSC development *in utero*, but genes involved in stem cell quiescence such as Bmi-1 and Hfi1, appear to be selectively important for adult HSCs [Park, 2003][Hock, 2004].

Not all of these genes have an important role in oncogenesis, but it is clear that some fetal specific gene pathways and fetal associated genes include important oncogenes. Warren *et al*,

demonstrate the dependence of fetal haematopoietic development on *Lmo2* [Warren, 1994], which has since been shown to be an important site of mutation in T-cell leukaemia [Hacein-Bey-Abina, 2003][Dave, 2004]. Other important genes in leukaemia are also important fetal genes: for example *Meis1* [Azcoitia, 2005], and *Ezh2* (discussed below in Section 1-4.1). Importantly, mutation of these fetal specific genes can lead to reactivation of fetal pathways even when mutated in adult life [Oshima, 2016][Sashida, 2016].

When modelling fetal-specific acquisition of mutations, or comparing fetal and adult acquisition, it is therefore vital to understanding the molecular and biological context in which these mutations lead to subsequent dysregulation of pathways. This approach could identify whether the dysregulated genes are expressed by *bona fide* fetal cells, or whether mutation in adult cells has led to re-animation of fetal molecular signatures.

1-2 The fetal origins of leukaemia

1-2.1 Current evidence for leukaemia originating *in-utero*

Although neonatal acute leukaemia can generally be assumed to have its origins *in-utero* [Roberts, 2018], other leukaemias have been traced back to pre-natal origins. Down syndrome (DS) is well recognised to cause a transient neonatal preleukaemia associated with *in-utero* *GATA1* mutations, which then can progress to myeloid leukaemia (ML) in later childhood [Roberts, 2013][Roberts, 2014][Labuhn, 2019]. Somatic mutations in other leukaemias, such as MLL-rearranged infant leukaemia [Ford, 1993][Gale, 1997][Greaves, 2018], B-cell precursor acute lymphoblastic leukaemia (ALL) [Greaves, 2018], and Juvenile Myelomonocytic Leukaemia (JMML) [Matsuda, 2010][Caye, 2015][Stieglitz, 2015] have been traced to the cord blood, where available, or neonatal blood spots. Twin studies in infant leukaemia have reinforced this finding [Greaves, 2003]. Therefore, a clone created by mutation

in a fetal-derived cell, can persist and lead to leukaemia later in life. From these studies it is clear that in JMML the somatic clone originates *in-utero* in the majority of cases [Matsuda, 2010][Stieglitz, 2015].

1-2.2 Recurring characteristics of leukaemia of fetal origin

A characteristic but unusual finding is that leukaemias of fetal origin have a significant spontaneous remission rate [Bader-Meunier, 1997][Bhatnager, 2016][Roberts, 2018]. Further, there is a relatively silent mutation landscape, with driver mutations occurring in a small family of genes for each condition, and at times these can occur without identifiable secondary mutations [Caye, 2015][Stieglitz, 2015][Bhatnager, 2016][Greaves, 2018][Labuhn, 2019]. This is in stark contrast to adult leukaemia, where mutation in multiple genes is common [Papaemmanuil, 2013][Papaemmanuil, 2016]. Where secondary mutations occur, these appear frequently in epigenetic modifiers: in the case of DS TAM and ML-DS in cohesin complexes and polycomb repressive complex 2 (PRC2) [Bhatnager, 2016] [Labuhn, 2019]; in the case of JMML PRC2 also features highly [Caye, 2015][Stieglitz, 2015].

One could hypothesise that this relative lack of mutations compared to adult leukaemia is due to the fact that fetal cells already exhibit a competitive advantage over adult cells -- through the rapid cycling, and proliferative stress described above. Thus speculatively, cells mutated in fetal life would exhibit a significant expansion early in the postnatal period followed by exhaustion and extinction following the loss of the fetal environment: as summarised in figure 1.3. This is demonstrated by the neonatal leukaemias in Down syndrome and Noonan's syndrome [Bader-Meunier, 1992][Hasle, 2009][Bhatnager, 2016]. Further, particular mutations or cellular contexts may require secondary mutations to lead to leukaemia: perhaps

explaining the way that solitary mutations are associated with progression to overt disease in some leukaemias but require secondary mutations in others.

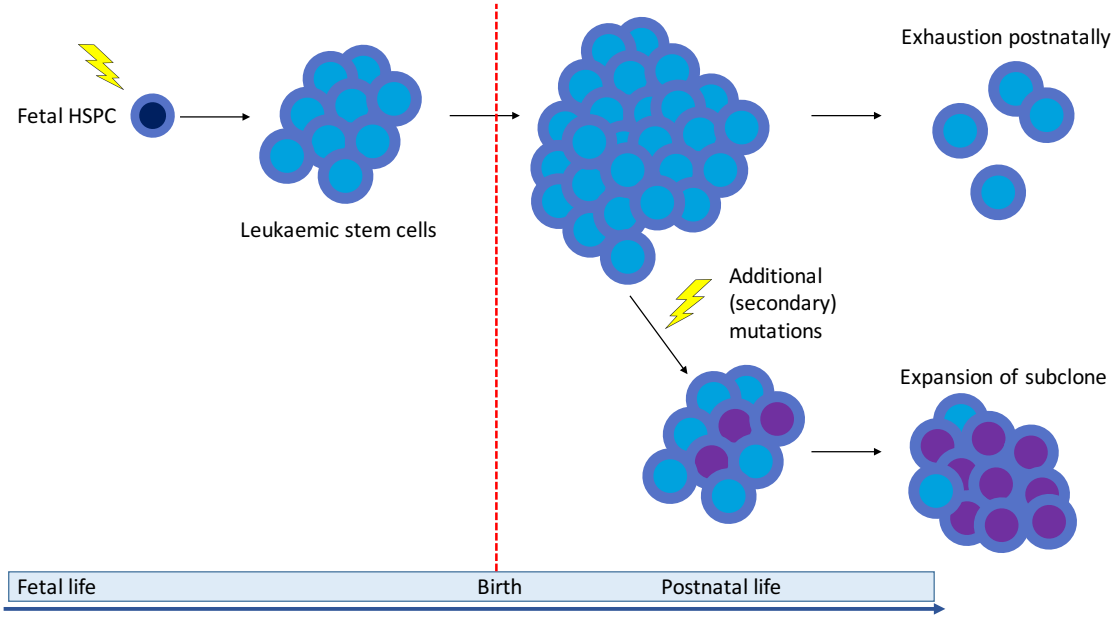


Fig 1.3 Hypothesis of fetal and postnatal clonal progression. Haematopoietic stem and progenitor cell (HSPC)

1-2.3 Importance of identifying fetal-specific disease: the prognosis and treatment options for fetal-derived leukaemia

Regardless of the pathophysiology of these disorders, their prognosis is often poor. Infant leukaemia and JMML are considered amongst the poorest prognosis of any childhood haematological disorder [Brown, 2013][Niemeyer, 2014][Brown, 2019]. Neonatal leukaemia is also regarded as having a particularly poor prognosis, when compared to other childhood leukaemias, even accounting for the small number of children achieving a spontaneous remission [Roberts, 2018]. One potential factor for this apparent poor prognosis is the high rate of relapse following transplant: most noted in JMML and ML-DS [Bhatnager, 2016][Locatelli, 2005][Locatelli, 2015], but also a problem in infant leukaemia [Brown, 2016].

Given the poor prognosis and frequency of relapse, new treatment options are essential. Some patients, such as those with ML-DS, respond well to initial chemotherapy, but require low dose chemotherapy due to therapy toxicities [Bhatnager, 2016]. Fetal cells exhibit unique programs and molecular expression pathways, so using these as targets for new therapies could be beneficial in reducing side-effects from current treatments. Using a model comparing adult and fetal malignant haematopoiesis could therefore help to identify fetal specific targets for these disorders.

1-3 Juvenile Myelomonocytic Leukaemia (JMML)

1-3.1 The clinical and haematological features of JMML

i) Clinical features and associated syndromes

JMML is defined as a clonal haematopoietic proliferation in childhood, characterised by monocytosis with or without granulocytosis [Baumann, 2017]. Although recent studies have clearly defined criteria based on the World Health Organisation (WHO) [Baumann, 2017], it is fair to say that historically, based on the French-American-British (FAB) classifications, the varied definitions as either chronic myelomonocytic leukaemia (CMML) [Castro-Malaspina, 1984][Hasle, 1994][Niemeyer, 1997], juvenile chronic myelogenous leukaemia (JCML) [Hardisty, 1964][Castleberry, 1994], or juvenile myelomonocytic leukaemia (JMML) [Passmore, 2003][Hasle, 1999][Niemeyer, 2014] led to some confusion.

JMML is a rare disease affecting ~1-2 per million children, of primarily young children, with ~50% of cases presenting before 2 years of age [Arico, 1997][Niemeyer, 1997][Hasle, 1999][Passmore, 2003]. Occasional cases present in the neonatal period [Hasle, 2009][Lee, 2016], although these appear to be associated with syndromes. There is a male preponderance,

with a male:female incidence ratio variously reported between 2.1 to 4 [Arico, 1997][Niemeyer, 1997][Hasle, 1999][Passmore, 2003]. The reasons for this are unknown.

Children almost uniformly present with splenomegaly [Castro-Malaspina, 1984][Arico, 1997][Niemeyer, 1997][Passmore, 1995], and the majority also have hepatomegaly and/or lymphadenopathy [Arico, 1997][Niemeyer, 1997][Hasle, 1999][Niemeyer, 2014][Passmore, 1995]. Skin infiltration, most often as a nodular rash, is frequent [Hasle, 1999][Arico, 1997], but unlike acute leukaemia, appears in older children with JMML as well as infants [Matsumoto, 2004][Gupta, 2014][Roberts, 2018]. Central nervous system involvement is incredibly rare, with occasional cases in series [Niemeyer, 1997], and only a single case report: however, this patient also had complex chromosomal translocations with an abnormal B-cell receptor, suggesting potential alternative pathology [Smith, 2007]. Ocular presentation and relapse has been documented [Nambu, 1999], as well as gastro-intestinal tract infiltration [Niemeyer, 1997].

ii) Haematological markers and parameters

The hallmark of JMML is leucocytosis, particularly monocytosis, as per the diagnostic criteria (Table 1.1), with a median monocyte count of ~5-10x10^9/L [Arico, 1997][Niemeyer, 1997]. Nevertheless, other abnormalities in the white blood cell counts are common with an increase in immature myeloid or erythroid precursors, but infrequent blast cells: generally <2% of total nucleated cells [Castro-Malaspina, 1984][Arico, 1997][Niemeyer, 1997][Niemeyer, 2008]. The bone marrow findings mirror the peripheral blood with an increase in myeloid precursors, but only an infrequent rise in blasts [Arico, 1997][Niemeyer, 1997][Niemeyer, 2008].

An important finding is thrombocytopenia, with only ~20% of patients having a platelet count >100 x 10^9/L [Castro-Malaspina, 1984][Arico, 1997][Niemeyer, 1997]. And, although most patients are anaemic, the finding of raised fetal haemoglobin for age is of importance both diagnostically and prognostically [Castro-Malaspina, 1984][Arico, 1997][Niemeyer, 1997][Owen, 1992][Passmore, 1995]. Although generally considered as evidence of fetal origin, the cause of the raised fetal haemoglobin is unclear. Recent data suggests that Lin28B is overexpressed in the majority of patients with raised fetal haemoglobin [Caye, 2020], but this is in conflict with previous studies suggesting no clear correlation [Helsmoortel, 2016]. It is known, however, that dysregulation of the Lin28B axis can lead to reactivation of fetal haemoglobin [Sankaran, 2008][Lee, 2013], and that Lin28B is frequently disturbed in JMML [Helsmoortel, 2016]. Given the finding that fetal haemoglobin elevation is not completely reliant upon the LIN28B or BCL11a axes, it may be that there are alternative mechanisms for the raised fetal haemoglobin, either derived directly from the fetal gene signatures within mutant fetal cells, or which involve post-natal reactivation due to genetic dysregulation in control pathways, for example LIN28B.

iii) The diagnosis of JMML

The current diagnosis of JMML is based on the WHO diagnostic criteria of haematological malignancies [Baumann, 2017], summarised in Table 1.1. Patients must fill all category 1 criteria, including <20% blasts, which would lead to exclusion of a small number of patients from the larger phenotyping studies [Niemeyer, 1997][Arico, 1997]. Criteria in category 2 are genetic and a mutation in at least one of the listed genes is normally considered necessary for a diagnosis of JMML. In the absence of a single genetic mutation described in criteria 2, or where mutational analysis is not possible, Baumann *et al* suggest that the criteria in category 3 can be applied instead [Baumann, 2017].

Chronic myeloid leukaemia (CML) occasionally presents in a similar fashion to JMML, hence the requirement for a negative BCR-ABL translocation, although in practice the age of the child and typical blood picture in CML rarely cause confusion [Baumann, 2017]. Case reports demonstrate that immunological or infectious disorders can mimic or accompany JMML and comprehensive investigations may be necessary to elucidate the exact diagnosis [Lorenzana, 2002][Moritaki, 2009][Yoshimi, 2013].

Diagnostic criteria for JMML (as per World Health Organisation)

Criteria 1 (Clinical-haematological) *All 4 required*	**Criteria 2 (Genetic)** *1 required*
PB monocytosis (>1x10^9/L)	Somatic mutation of PTPN11, NRAS or KRAS
Splenomegaly	Germline NF1 mutation, or diagnosis of Neurofibromatosis 1
Blast percentage <20% (PB and BM)	Germline CBL mutation AND loss of heterozygosity of CBL
No BCR-ABL rearrangement	
	Criteria 3 (In absence of genetic criteria)
	Monosomy 7 (fulfils criteria 3) OR two of following: *Raised fetal haemoglobin for age* *Myeloid and/or erythroid precursors on blood film* *GM-CSF Hypersensitivity in colony assays* *STAT5 Hyperphosphorylation*

(adapted from Baumann, 2017)

Table 1.1 Diagnostic Criteria for JMML. Criteria 1 must be met, and either criteria 2 or, in the absence of genetic confirmation then criteria 3. Adapted from Baumann, 2017. Granulocyte-macrophage colony stimulating factor (GM-CSF). Peripheral Blood (PB)

iv) Current treatment options for JMML

Historically, therapies for JMML have included radiation [Cooke, 1953] or older chemotherapeutic drugs, such as 6-mercaptopurine (6-MP) [Reisman, 1963], either as single agents or combination therapy, all of which offer transient, if any benefit [Bergstraesser, 2007]. The mainstay of treatment remains allogeneic HSCT, with a 4-5 year survival of ~55% [Locatelli, 1997][Macmillan, 1998][Manabe, 2002][Yabe, 2008]. Some recent studies have shown improved outcomes, perhaps associated with improvements in the transplantation

protocols [Locatelli, 2013][Yabe, 2015]. Nevertheless, disease relapse following transplant is a significant problem, occurring in ~25-35% of patients [Manabe, 2002][Locatelli, 2005][Locatelli, 2015][Yabe, 2015], with some mutations, such as PTPN11, having an even higher risk of relapse [Yoshida, 2009]. Importantly, not all patients seem to require HSCT. Small studies have demonstrated that some patients with NRAS mutations do well without HSCT [Matsuda, 2007] [Flotho, 2008] and systematic studies to evaluate the natural history of such cases are now underway.

Unfortunately, following relapse, the only option for most patients is a second transplant [Locatelli, 2015][Sakashita, 2016]. Recent advances, based on the observation that JMML patients have aberrant methylation (discussed below), suggest that hypomethylating agents may be of some benefit although most likely as a bridge to transplant rather than as curative therapy [Furlan, 2009][Cseh, 2015]. MEK inhibitors in mouse studies have also shown potential benefit [Chang, 2013], with improvement of white cell count (WCC), spleen size, and STAT5 phosphorylation in NF1 KO mice, however this effect is less marked in mice with other RAS pathway mutations. Both of these options are currently undergoing clinical trials [Sakashita, 2016][Niemeyer, 2018].

1-3.2 Cellular and molecular pathogenesis

i) Cellular origins and characteristics

It has long been established that JMML cells display spontaneous growth with low seeding densities and little or no growth factor additives [Emanuel, 1996], but the established finding in JMML is Granulocyte-macrophage colony stimulating factor (GM-CSF) hypersensitivity. Emmanuel *et al* first demonstrated this in Colony Forming Units-Granulocyte, Monocyte (CFU-GM), and Burst forming unit erythroid (BFU-E) assays where cells demonstrated

exaggerated growth with low levels of GM-CSF but not granulocyte colony stimulating factor (G-CSF) or interleukin (IL) 3 [Emanuel, 1991]. Further, patient-derived induced pluripotent stem cells (iPSCs), are also hypersensitive to GM-CSF [Gandre-Babba, 2013]. This, however, is likely an effect of an overactive RAS pathway as can be demonstrated by haematopoietic cells from mouse models with RAS activating mutations developing GM-CSF hypersensitivity [Araki, 2004][Braun, 2004][Li, 2011][Lyubynska, 2011]. This GM-CSF hypersensitivity is of use diagnostically as CD33+, CD14+ cells demonstrate increased phosphorylation of STAT5 by flow cytometry [Hasegawa, 2013].

The cell of origin of JMML had remained unclear until very recently. Early studies demonstrated clonality, using differential patterns of X-chromosome methylation, in the myeloid and erythroid lineages, but not all lymphoid lineages; some patients demonstrated no lymphoid clonality, but occasional patients showed B-cell clonality [Busque, 1995][Flotho, 1999]. From these reports, a stem cell or HSPC with myeloid and some lymphoid potential was suggested to be the cell of origin. Recent studies, however, have demonstrated that the disease initiating cells may be heterogenous, with propagation in patient derived xenografts from either haematopoietic stem cells (HSC), multi-potent progenitors (MPP), or other HSPCs [Caye, 2020][Louka, 2019]. Nevertheless detailed study at the single cell level has now confirmed that leukaemia-propagating cells can be traced back to the HSC compartment in all cases indicating that JMML is a stem cell disorder.

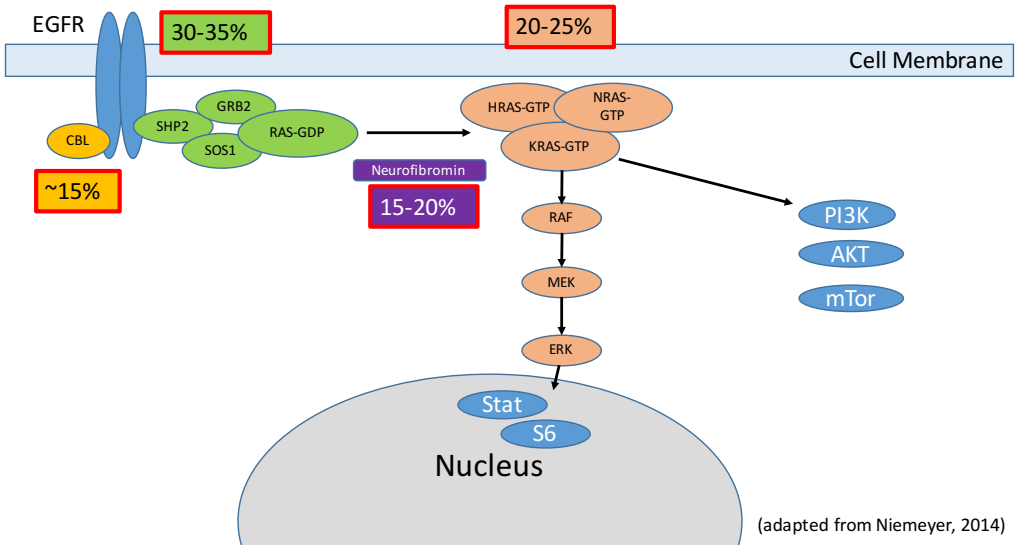
ii) Genomic changes in JMML

Prior to the advent of sequencing, identification of genomic aberrations relied on cytogenetics. Early large case series of JMML mirror the findings from more recent series in that monosomy

7 is found in around 20-30% of cases [Passmore, 1995[Arico, 1997][Niemeyer, 1997][Hasle, 1999][Passmore, 2003][Caye, 2015][Stieglitz, 2015].

Activating mutations in the RAS pathway have now been defined in ~85-90% of patients with JMML [Niemeyer, 2014][Caye, 2015][Stieglitz, 2015]. These mutations occur in the various RAS proteins with differing incidence [Miyauchi, 1994][Flotho, 1999][Yoshida, 2009][Loh, 2014] [Niemeyer, 2014][Caye, 2015][Stieglitz, 2015][Louka, 2019], and are shown in figure 1.4. The majority of these mutations are somatic, however approximately 30% of JMML cases are associated with a germline mutation, most commonly in children with Noonan's syndrome or Neurofibromatosis [Shannon, 1994][Bader-Meunier, 1997][Perez, 2010][Caye, 2020], however cases with germline CBL mutations occur in ~10%, the majority of which require loss of heterozygosity (LOH) to develop JMML [Stieglitz, 2015][Caye, 2015]. In the minority of patients who do not have a RAS pathway mutation identifiable by current sequencing techniques there are few published studies. Nevertheless, other mutations and fusion genes can be identified, such as ALK gene fusions, including those with ROS1 [Rottgers, 2010][Murakami, 2018].

Fig 1.4 Summary of RAS pathway mutations and frequency of occurrence in JMML. Adapted from Niemeyer, 2014



(adapted from Niemeyer, 2014)

Although single RAS pathway mutations are sufficient to cause disease, as mentioned above, secondary mutations do occur [Stieglitz, 2015][Caye, 2015][Louka, 2019][Caye, 2020]. These are commonly in epigenetic regulators such as polycomb complex genes, discussed below, but also in spliceosome (particularly *ZRSR2*) or transcription factor genes [Stieglitz, 2015][Caye, 2015]. Some RAS pathway mutations are specifically associated with certain secondary mutations; for example activating *KRAS* mutations are often accompanied by large chromosomal deletions, particularly chromosome 7 in ~56% of cases, whereas other initiating mutations are associated with secondary point mutations [Stieglitz, 2015][Caye, 2015]. The reasons for this are unclear at present, but *KRAS* mutations also appear to be associated with a young age at presentation [Stieglitz, 2015][Caye, 2015][Louka, 2019][Caye, 2020]. *KRAS* mutation appears associated with chromosome 7 and thereby *EZH2* loss in a number of studies [Caye, 2015][Stieglitz, 2015][Lipka, 2017], occurs generally at a young age, [Louka, 2019] and the majority of these mutations can be traced to fetal life [Matsuda, 2010][Stieglitz, 2015].

iii) Epigenetic aberrations in JMML

Two seminal papers described the mutational spectrum in JMML, highlighting the importance of epigenetic alterations, particularly affecting PRC2, as secondary mutations in JMML [Stieglitz, 2015][Caye, 2015]. These findings are also supported by two recent studies [Louka, 2019][Caye, 2020]. The PRC2 abnormalities are subclonal mutations [Stieglitz, 2015][Caye, 2015], but occur frequently, either through direct mutations in PRC2 genes, or loss of chromosomal material such as chromosome 7, carrying *EZH2* [Stieglitz, 2015][Caye, 2015][Caye, 2020]. In one series, all patients with a point mutation in *EZH2* had associated LOH with loss of chromosomal material on chromosome 7 [Stieglitz, 2015]. The PRC2 associated genes, such as ASXL1, are also mutated in 5-10% of individuals [Stieglitz,

2015][Caye, 2015], as well as LOF mutations in spliceosome genes which can lead to nonsense mediated *EZH2* mRNA decay [Kim, 2015][Stieglitz, 2015][Caye, 2015].

The biological effect of PRC2 related mutations is unclear. It has been proposed in other tumour types that RAS mutations and PRC mutations combine to allow hyperactive transcription pathways [De Raedt, 2014]. It is clear that these mutations have a functional effect on PRC2, as methylation is effected, with loss of trimethylation on histone 3, lysine 27 [Caye, 2015]. There may also be non-canonical effects of mutation, in that ASXL1 mutations lead to a global hypermethylated state [Stieglitz, 2015]. Other papers have identified aberrant DNA methylation in JMML and found that DNA hypermethylation is linked to a poor prognosis [Olk-Batz, 2011][Stieglitz, 2015][Lipka, 2017]. This hypermethylation may explain why hypomethylating agents are of potential benefit [Furlan, 2009][Sakashita, 2016][Niemeyer, 2018].

1-3.3 Factors affecting the prognosis of JMML

Overall, the survival of JMML patients is around 60% at 5 years [Manabe, 2002][Niemeyer, 2008][Locatelli, 2005][Locatelli, 2015]. Many studies have reported on clinical and haematological prognostic features, however the major recurring poor prognostic features are older age, male sex, thrombocytopenia, and the presence of an increased number of blasts in either the BM or peripheral blood (PB) [Castro-Malaspina, 1984][Owen, 1992][Passmore, 1995][Arico, 1997][Niemeyer, 1997][Niemeyer, 2014][Lipka, 2017]. Bleeding at presentation has also been associated with decreased survival, however this may be reflective of thrombocytopenia [Castro-Malaspina, 1984][Owen, 1992][Niemeyer, 1997]. Elevated fetal haemoglobin to varying degrees has been reported as a prognostic feature [Castro-Malaspina, 1984][Owen, 1992][Passmore, 1995][Arico, 1997][Niemeyer, 1997][Helsmoortel, 2016], but

these patients are often associated with older age, and other factors, such as LIN28B expression, playing a role [Niemeyer, 1997][Helsmoortel, 2016].

Although certain somatic RAS pathway mutations, particularly $NRAS^{G12S}$, have been associated with a mild disease course demonstrating long term survival without transplantation, this is not universal [Matusda, 2007][Niemeyer, 2014][Locatelli, 2015]. Patients with *KRAS* mutations appear to relapse less frequently leading some groups to modify transplant protocols to take this into account [Locatelli, 2015]. There have not been enough patients in studies to ascertain whether specific secondary mutations lead to a worse prognosis, however what has been demonstrated is that any additional mutation, including RAS double mutation, leads to an unfavourable outcome [Caye, 2015][Stieglitz, 2015].

1-3.4 Model systems available for JMML

i) Mouse models

Mouse models of JMML are summarised in Table 1.2. Most of these are knock-in (KI) activating RAS mutations. The models with PTPN11 mutations lead to relatively faithful recapitulation of Noonan's syndrome [Araki, 2004][Mohi, 2005], but the leukaemia associated with either constitutional or conditional $PTPN11^{E76K}$ or ^{D61Y} has only some features of JMML (leucocytosis, GM-CSF hypersensitivity, splenomegaly) and a large proportion developing T-cell leukaemia, which also occurs only after a long latency [Araki, 2004][Mohi, 2005][Chan, 2009]. Of note, there is some mouse model evidence that the BM niche can drive the disease in $PTPN11^{E76K}$ mice in that WT cells transplanted into recipient mice with niche cells expressing $PTPN11^{E76K}$ developed a JMML phenotype in the donor WT cells. [Dong, 2016]. This suggests that the microenvironment, and location of acquisition of mutations can contribute to JMML development.

Other RAS mutations give a similar outcome, with a long latency of disease, intermixed T-cell leukaemia, with some biological features of JMML (Table 1.2) [Zhang, 2001][Le, 2004][Li, 2011][Li, 2013][An, 2016]. Earlier induction using Tie2Cre activation in an NF1 mutant mouse model did not alter the latency of disease [Gitler, 2004].

Given the long latency, and conditional KI during adult life, these models do not represent a fetal origin of leukaemia. Table 3.1 (in chapter 3) summarises the difficulties of using the different Cre systems. In brief, the majority of these either do not cleanly allow fetal activation or are not haematopoietic specific (such as the 'leaky' Mx1Cre) or are constitutive and as such do not allow comparison of fetal and adult haematopoiesis (such as Flt3Cre, Tie2Cre and VavCre, the latter is also fetally lethal with $Kras^{G12D}$). To address this, Tarnawsky *et al* used conditional KI with either constitutive Flt3Cre or inducible Csf1rCre to induce $PTPN11^{E76K}$ in fetal life, however these mice still demonstrated a long latency of disease: with no disease until adult life and no monocytic phenotype.

ii) $Kras^{G12D}$ model

The problems with heterogenous diseases and long latency of disease onset can somewhat be addressed using a $Kras^{G12D}$ model [Johnson, 2001]. This shows, with conditional Mx1Cre induction at 3-4 weeks, the development of a fully penetrant, aggressive myeloproliferative disease resembling JMML [Braun, 2004]. When, however, cells from these mice are used for transplantation experiments, the mice almost uniformly succumb to T-cell leukaemia/lymphoma [Sabnis, 2009][Zhang, 2009] which is clearly completely different from the natural history of JMML.

Although conditional KI of $Kras^{G12D}$ throughout haematopoiesis from early fetal life is lethal [Tang, 2013], recently one group used Flt3Cre induction of $Kras^{G12D}$ from fetal MPPs to model

Experimental approach	Reference	Outcome	Pros	Cons
$Kras^{G12D}$, Mx1Cre Primary mice	Braun, 2004	Induction at 3-4 weeks leads to fully penetrant myelomonocytic leukaemia	1. Rapid disease onset 2. Reproducible 3. Myelomonocytic disease	1. Mx1Cre is 'leaky' 2. Not fetal
$Kras^{G12D}$, Mx1Cre Transplantation	Sabnis, 2009 Zhang, 2009	Transplantation of HSCs followed by induction leads to entirely T-cell disease. Induction followed by transplantation 8% myelomonocytic	1. Suggests role for environment in disease evolution	1. Transplantation leads to majority T-cell leukaemia
$Kras^{G12D}$, Flt3Cre from fetal MPP	Tarnawsky*, 2017	Short latency myeloid leukaemia	1. Fetal origin 2. Myeloid disease	1. Not inducible (constitutional Cre line) 2. Not monocytic leukaemia 3. MPP may not be human cell of origin
NSG Xenografts	Louka, 2019 Caye, 2020	Engraftment and propagation of human disease Suggests HSC compartment involved in leukaemogenesis	1. Recapitulates human disease 2. Close study of human mutational interactions	1. Not readily reproducible 2. Not able to study ontogenic timing of mutation acquisition
Ptpn11 transplants using Mx1Cre, VavCre and niche specific Cre lines	Dong, 2016	Role for niche cells with cytokine (CCL3 and IL-1ß) overexpression	1. Suggests role for niche cells 2. Reproduces JMML phenotype	1. Not able to study fetal origins 2. Long latency
Ptpn11 mutated primary mice	Araki, 2004	Constitutional $Ptpn11^{D61G}$ leads to long latency myeloproliferation	1. Mouse model of germline JMML/Noonan's MPD	1. Extremely long latency of disease 2. Not able to study ontogenic timings
Viral transduction of *Shp2* mutant gene	Mohi, 2005	Transplantation of viral transduced BM cells causes leukaemia	1. Would be able to use in fetal cells	1. Long latency of disease 2. Transplantation model (with $Kras^{G12D}$ may cause T-cell leukaemia)
Nf1 mutation	Zhang, 2001	Homozygous NF1 mutation in a transplantation model causes long-latency myeloproliferative disorder	1. Germline mouse model	1. Long latency of disease 2. Not able to study fetal origin (uses Nf1-/-)
$Nras^{G12D}$, Mx1Cre	Li, 2011	$Nras^{G12D}$ mutation in Mx1Cre primary mice develop long latency myelomonocytic leukaemia	1. Could use $Nras^{G12D}$ to compare with $Kras^{G12D}$	1. Extremely long latency of disease 2. Mainly in-vitro studies on induced BM cells 3. Not fetal in origin
CBL mutation	An, 2016	CBL loss causing myeloproliferation	1. Only CBL model	2. Poor correlation with human disease

Table 1.2: Summary of current available mouse models for JMML showing $Kras^{G12D}$ mutant models at top followed by other mutations

JMML [Tarnawsky*, 2017]. This paper showed that *Kras* mutation in fetal cells could cause a JMML phenotype with a short latency. Importantly, however, the disease achieved was a neutrophilic disease, with CD11b+, Gr1+ expansion and neutrophilic morphology [Tarnawsky*, 2017] very different from human JMML. Further, as discussed above, JMML initiating mutations are gained in HSCs [Louka, 2021][Caye, 2020], rather than solely in MPPs, which this paper does not address. This model also does not allow a study of timing of acquisition of mutations: the Flt3Cre model is constitutional and as such, any MPP expressing Flt3, which are present even from the YS stage of gestation [Boiers, 2013], will be activated. Finally, this model was not used to explain unanswered questions regarding the biology of JMML [Tarnawsky*, 2017].

Whilst the different mouse model systems share phenotypic and functional characteristics of JMML, no model has successfully induced the mutation in fetal HSCs. HSPCs from the $Kras^{G12D}$ mice have the requisite GM-CSF hypersensitivity [Braun, 2004][Akutgawa, 2016], and demonstrate an upregulation of proliferative genes at the expense of quiescence gene transcription [Sabnis, 2009][Di Genua, 2019]. This may explain the relative depletion of phenotypic HSCs in the BM [Sabnis, 2009][Melo-Cardenas, 2018], but the phenotypic and functional HSCs can be rescued with the addition of relevant secondary mutations [Melo-Cardenas, 2018][Di Genua, 2019]. Further, treatment of $Kras^{G12D}$ mice with targeted therapies successfully reduces their myeloproliferative phenotype [Lyubynska, 2011][Akutgawa, 2016].

iii) Other model systems

Recently, patient derived xenograft (PDX) models [Yoshimi, 2017][Louka, 2019][Caye, 2020] have allowed vital insights into the biology of JMML. However, these rely on established disease and cannot model disease initiation, although they do allow expansion of leukaemia

propagating cells, and trials of treatments. Alternative models include *in-vitro* culture systems, such as co-cultures [Louka, 2019] or induced pluripotent stem cells, which show *in-vitro* characteristics of JMML but do not readily allow study of *in-vivo* biology [Gandre-Babbe, 2013][Gagne, 2018][Tasian, 2019]. Whilst these may allow limited validation of treatment targets, they are not suitable to address questions relating to the impact of initiation of mutations at alternative stages of development.

1-4 How aberrations in *Ezh2* disturb haematopoiesis

1-4.1 The normal function of Ezh2

i) The role of Ezh2 and the Polycomb Repressive Complex 2 (PRC2)

The Enhancer of Zeste Homologue 2 (EZH2) forms PRC2 along with the major subunits EED, SUZ12, RbAp46/48 [Margueron, 2011][Lund, 2014][Herviou, 2016]. Other polycomb associated components, eg JARID2, AEBP2, ASXL1, play an apparent role in PRC2 recruitment and localisation to the correct site for gene repression, demonstrated in Figure 1.5 [Boultwood, 2010][Margueron, 2011][Abdel-Wahab, 2012].

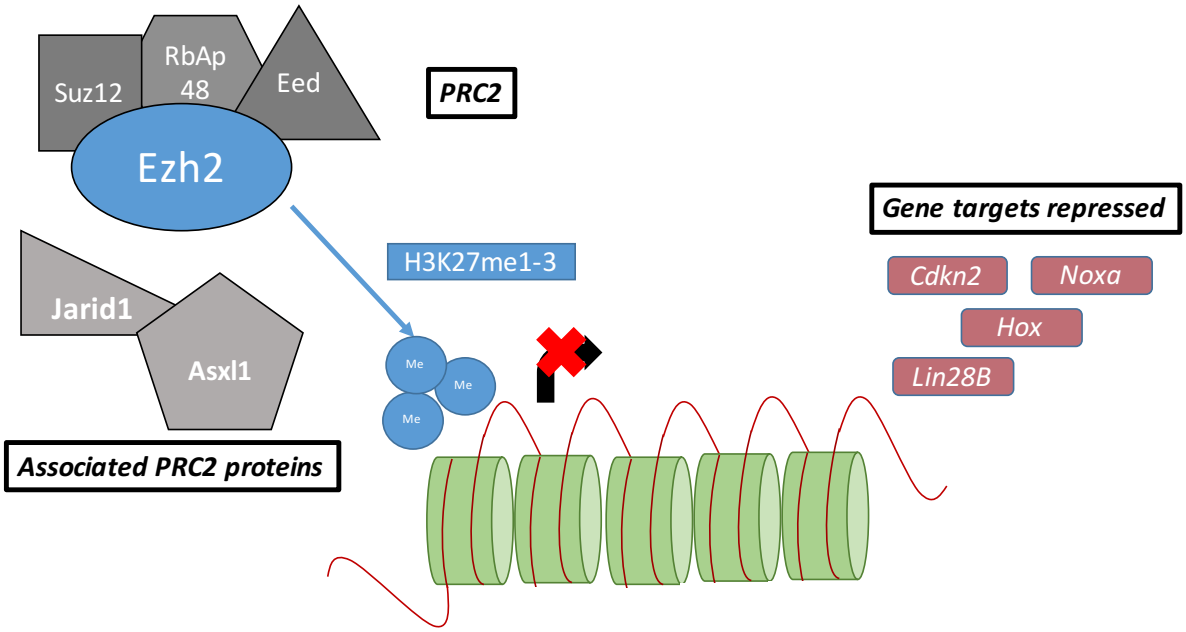


Fig 1.5 Summary of PRC2 and associated proteins. Canonical mechanism of action shown with methylation of histone 3 and subsequent repression of genetic transcription

Initially the polycomb group and enhancer of zeste proteins were described in Drosophila [Lewis, 1978][Duncan, 1982][Margueron, 2011], and are important for determining cell fate, acting in antagonism with the drosophila trithorax proteins [Schuettengruber, 2009][Simon, 2009][Margueron, 2011].

EZH2 acts as the main catalyst for the role of PRC2 in methylation, but is not necessarily solely responsible for this as evidence suggests that *Ezh1,* a close homologue, can compensate for *Ezh2* loss in mice [Margueron, 2008][Shen, 2008][Ezhkova, 2011]. Knock-out mouse models, discussed in more detail below, reinforce this finding as, on loss of *Ezh2*, PRC2 based methylation in HSCs is partially preserved [Shen, 2008][Mochizuki-Kashio, 2011][Xie, 2014]. This is in contrast to the other major subunits, EED or SUZ12, where knock-out leads to a complete loss of methylation [Xie, 2014][Lee, 2015].

ii) The role of Ezh2 and PRC2 in normal adult mouse haematopoiesis

The polycomb repressive complex 2 leads to repression of gene transcription through methylation (me) of histone 3 at lysine 27 (H3K27) [Cao, 2002][Czermin, 2002][Muller, 2002][Lund, 2014][Herviou, 2016]. Ezh2 acts mainly to place di- or tri-methylation marks (me2-3), but in its absence Ezh1 compensates with a degree of mono-methylation (me1) [Cao, 2002][Shen, 2008] [Margueron, 2011][Mochizuki-Kashio, 2011][Xie, 2014]. These methylation marks, particularly H3K27me3 lead to gene repression, although the mechanism is not fully established.

Classically, canonical PRC2 places H3K27me3 via the SET domain of EZH2 which then allows recruitment of other enzymes and complexes, such as PRC1, the role of which is to

ubiquitinate histone 2a at lysine 119 [Cao, 2002][Wang, 2004][Margueron, 2011][Lund, 2014][Herviou, 2016] leading to gene repression. However, the majority of this work was initially performed in *Drosophila* or embryonic stem cells [Cao, 2002][Wang, 2004][Margueron, 2011] and work in mouse HSPCs suggests the role in haematopoiesis may be more varied [Majewski, 2010]. These studies suggest that although many targets for PRC1 and PRC2 are similar, they may have alternating roles in gene activation or repression. In addition, while in mouse HSCs the complexes may target different genes, in lymphoid development they may work in tandem [Majewski, 2010] [Beguelin, 2016] [Kim, 2016][Rinke, 2020]. PRC2 has been shown to target cell cycle genes such as CDKN2a, developmental regulators such as HOX genes, regulators of apoptosis [Xie, 2014][Herviou, 2016], and potentially cKit, by recruitment to genes expressed at low levels [Berrozpe, 2017].

Although the majority of work on the role of EZH2 focusses on the canonical role within PRC2, in certain cell contexts EZH2 appears to have non-canonical effects [Kim, 2016]. However, the vast majority of these relate to the role of either mutated or wild type (WT) *EZH2* in malignancy [Kim, 2016][Rinke, 2020]. These findings demonstrate the potential importance of cell context in the roles of EZH2 and PRC2, but emphasise that their roles are not fully understood. What, however, is clear is that amongst other targets, both complexes appear to control genes important in fetal life and embryogenesis [Majewski, 2010].

iii) Differences in the role of Ezh2 during fetal development to steady-state adult haematopoiesis

Ezh2 has a role in lymphocyte maturation; adult mice with Ezh2 deletion demonstrate a profound loss of both B- and T-lymphocytes [Su, 2003][Su, 2005]. In adult mouse HSCs, Ezh2 overexpression prevents stress induced exhaustion [Kamminga, 2006], and even dysregulation

through heterozygous loss of function (LOF) mutations increases PB cell counts in MPL-/- mice [Majewski, 2010], suggesting a role in maintaining steady-state HSC differentiation or senescence. The polycomb groups have been further implicated in maintenance of functional and phenotypic HSC in post-natal life [Park, 2003][Xie, 2014][Lee, 2015]. However, the importance of functional Ezh2 in adult mice is disputed due to the putative compensation by Ezh1. Despite complete loss of functional Ezh2 protein, studies in adult mice deleting *Ezh2* genes demonstrate surprisingly little effect on HSC function, thus suggesting this compensatory mechanism [Mochizuki-Kashio, 2011][Hidalgo, 2012][Xie, 2014].

In fetal haematopoiesis the role of Ezh2 is unclear. Studies demonstrate increased expression of *Ezh2* in long-term HSCs, with rapidly decreasing expression post-natally [Xie, 2014]. *Ezh2* loss in fetal life leads to HSC expansion, whereas deletion in adult life predisposes to a mild decrease in phenotypic HSCs [Neo, 2018]. These fetal HSC are functional, with no loss of myeloid reconstitution despite serial transplantation [Neo, 2018]. On the other hand, others have suggested a significant role for Ezh2 in embryonic HSC survival with early deletion, but not leading to a functional defect on transplantation [Mochizuki-Kashio, 2011]. Nevertheless, other groups showed no such effect despite deletion in fetal life [Xie, 2014], and these discrepancies remain unexplained.

The stage of murine development appears to be important in PRC2 function, even differentiating between the role in the YS and FL. When deleted in the YS stage of development, *Ezh1* appears to have significant impact, even with heterozygous loss [Vo, 2018], whereas at the AGM stage *Ezh2* may be more important [Vo, 2018], and the stage of development at which the inducing Cre line acts alters the phenotype [Mochizuki-Kashio, 2011][Hidalgo, 2012][Neo, 2018][Vo, 2018]. What seems likely, therefore, is that polycomb

group proteins have differential roles throughout fetal and adult life, further emphasising the importance of cell context in polycomb group gene repression.

1-4.2 *EZH2* mutations in human haematopoietic disease

i) Characteristics and patterns of *Ezh2* disturbance in human haematopoietic disease

In humans, germline *EZH2* and PRC2 mutations cause Weaver syndrome, a condition characterised by bony overgrowth as well as an increased incidence of malignancy, including leukaemia [Basel-Vanagaite, 2010][Gibson, 2012][Deevy, 2019]. Somatic mutation of, or overexpression of WT *EZH2* is seen in many tumours including non-haematopoietic malignancies [Herviou, 2016][Kim, 2016][Nakagawa, 2018]. Most non-haematopoietic malignancies and lymphomas appear to require overexpression of EZH2, but in T-ALL, myeloid malignancies, myelodysplasia, and rare other tumours such as malignant peripheral nerve sheath tumours (MPNST) the major mutation is in-fact LOF [Ntziachristos, 2012][Papaemmanuil, 2013][De Raedt, 2014][Lund, 2014][Herviou, 2016][Kim, 2016] [Papaemmanuil, 2016][Nakagawa, 2018]. Although LOF point mutations are relatively rare in adult MDS [Papaemmanuil, 2013], in AML and JMML the *EZH2* gene is often lost in a heterozygous fashion through loss of large chromosomal material, such as monosomy 7 or deletion 7q [Caye, 2015][Stieglitz, 2015][Rinke, 2020]. Other polycomb associated genes can also be mutated in JMML and other malignant myeloid conditions, suggesting an important role of the canonical function of PRC2 in their biology, however to a lesser extent than *EZH2* [Score, 2012][Papaemmanuil, 2015][Caye, 2015][Stieglitz, 2015]. A further mechanism of *EZH2* loss in malignancy is through post-transcriptional modifications. Kim *et al* demonstrated that spliceosome mutations in MDS, such as *SRSF2*, lead to *EZH2* mRNA degradation and therefore loss of functional protein [Kim, 2015]; spliceosome genes are also recurrently

mutated in AML, MDS and JMML [Papaemmanuil, 2013][Papaemmanuil, 2015][Caye, 2015][Stieglitz, 2015].

Regardless of the malignancy, *EZH2* mutations of any sort appear to lead to a proliferative state and poor prognosis [Herviou, 2016][Nakagawa, 2018]. Again, even in haematopoietic malignancies, the role of cell context is vital as in certain contexts, such as lymphoma, *EZH2* may be an oncogene, but in light of the recurrent LOF in myeloid malignancies, eg in JMML, *EZH2* is more accurately described as a tumour suppressor.

ii) The functional and molecular characteristics of *Ezh2* mutation in human myeloid leukaemias

The functional effect of *EZH2* mutation in JMML has not been studied. Other malignancies, however, share RAS pathway mutations and polycomb inactivation, and although there are no clear findings some theories regarding the interaction have been suggested. In MPNST, RAS mutation and PRC2 LOF lead to decreased survival in a mouse model [De Raedt, 2014]. This suggests that hyperactive RAS mediated transcription may be exacerbated by excess H3K27ac following the loss of PRC2 and *EZH2*. Support for this comes from the effects of bromodomain inhibitors, preventing the increased acetylation leading to transcription, which may lead to reversal of this hyperactive state [De Raedt, 2014][Booth, 2018]. Due to the relative rarity of patients with combinations of mutations, the molecular characteristics of secondary *Ezh2* loss have been best demonstrated in mouse models.

iii) Mouse models of *Ezh2* knock-out in myeloid disease

As discussed above *Ezh2* KO alone in either fetal or adult life, leads to a potential but not reproducible enhancement in HSC function. *Ezh2* deletion alone can lead to haematological

malignancies in mice, albeit with a heterogenous phenotype and long latency [Mochizuki-Kashio, 2015]. However, recurrently mouse models have drawn into question the effect of deleting *Ezh2* due to compensation by *Ezh1* [Mochizuki-Kashio, 2011][Hidalgo, 2012][Xie, 2014]. The additive impact of *Ezh2* KO in malignant disease, however, can be less disputed. Basheer *et al*., demonstrate the varying roles of *Ezh2* in an AML mouse model, using deletion of *Ezh2* at varying stages of disease to demonstrate its role as a tumour suppressor or oncogene depending on the stage of disease, thus further emphasising the importance of cell context in *EZH2* mutant disease [Basheer, 2019].

Myelodysplasia and myelofibrosis mouse models demonstrate that *Ezh2* deletion enhances the phenotype in cooperation with initiating events; showing decreased survival and worsening of haematological parameters [Muto, 2013][Yang, 2016][Sashida, 2016][Shimizu, 2016]. Further, *Ezh2* KO enhanced the stem cell phenotype of the models with an additive effect when combined with mutated *Jak2* [Shimizu, 2016][Yang, 2016] or *Tet2* [Muto, 2013] on serial transplantation, which treatment with bromodomain inhibitors appeared to diminish [Sashida, 2016]. Although the gene mutated in the *Jak2* myelofibrosis model is obviously different to the *Kras* myelomonocytic disease model, they share some molecular characteristics.

HSPCs from the $Kras^{G12D}$ mutant mouse model downregulate stem cell genes, whilst activating a proliferative gene signature [Di Genua, 2019], which is similar to the *Jak2* myelofibrosis models [Shimizu, 2016][Yang, 2016]. *Ezh2* loss in the *Jak2* models then acts synergistically to reactivate repressed Ezh2 targets and, despite being lost in adult life, allows HSCs to develop a fetal signature, particularly increased expression of *Hmga2* and *Lin28b.* Although the synergistic effect of *Ezh2* loss has not been studied in the $Kras^{G12D}$ mouse model, secondary mutations do alter function. Despite losing transplantability rapidly, *Kras* mutant HSCs are

only able to be serially transplanted with the addition of *AML1-ETO* mutation, correlating with a relevant change in gene expression [Di Genua, 2019]. This suggests that secondary mutations are important factors in propagating these myeloid diseases, and perhaps have a role in chemo-resistance.

These models are a good demonstration of the cooperation between mutations. However, they are associated with important limitations, such as the initiation of disease in the entire BM, by using pan-activating Cre lines, such as Mx1Cre or Cre-ERT2. Therefore, they may not be ideal to study a leukaemia known to arise high up the HSPC hierarchy with mutations initiated in a single cell, in fetal life. A further problem lies in that Mx1Cre has spontaneous activation [Sabnis, 2009], thereby impeding comparative investigation between induction of mutations between fetal or adult life.

1-4.3 Therapeutic targeting of *Ezh2* alterations

Current methods of targeting aberrations in *EZH2* revolve around overexpression and hyperactive mutations [Xu, 2015][Kim, 2016], which have shown some promise. Loss of function, however, becomes more difficult to target directly as EZH2 replacement would lead to systemic overexpression. Presently, therefore, targeting relies on mitigating the downstream effects of *EZH2* loss.

One such mechanism, discussed above, uses inhibition of bromodomain enzymes, which reduces the overactive transcription contributed to by the increased activating mark H3K27ac. An impressive imaginative attempt is in acute myeloid leukaemia, where EZH2 loss leads to increased expression of EZH2 targets -- such as HOXA9 -- and knockdown of these genes in leukaemic cells increased sensitivity to cytotoxics [Gollner, 2017]. The same group also

identified novel methods of EZH2 protein degradation and managed to target the proteasome with bortezomib [Gollner, 2017].

Currently, however, direct treatment options specifically for LOF somatic mutations in *EZH2* remain elusive. These described attempts are more focussed on either alternative EZH2 protein loss or downstream effects. This is partly due to the difficulties in addressing an imbalance in PRC2 in a single organ system, resulting in overexpression elsewhere, but perhaps as the effect of *EZH2* loss will be distinct in different malignancies. In fetal-derived leukaemias, loss of a gene known to repress fetal targets, such as *EZH2,* may have distinct transcriptional effects on a fetal-derived cell of origin.

1-5 Hypothesis and aims

In summary, JMML is a fetal-derived leukaemia, usually associated with mutations in the RAS pathway, and carries a poor prognosis with few treatment options. There is no ideal model which recapitulates the fetal derived nature of the leukaemia, and it is not known whether the same mutation at different stages of ontogeny will lead to alternative outcomes.

Recurrent somatic mutations in *EZH2* are common secondary mutations in JMML, but it is not known whether these secondary mutations occur antenatally. Again, there may be an important role of cell context, as suggested by the differential effects of PRC2 in fetal life, and as such the development of these mutations at different stages of ontogeny or in different cell types may lead to different outcomes.

1-5.1 Hypotheses

i) RAS pathway mutations in fetal haematopoietic stem or progenitors cause JMML.

ii) The acquisition of leukaemogenic mutations at differing stages of ontogeny alters phenotypic, functional, and/or molecular properties of resulting leukaemias.

iii) Ezh2 knock-out enhances or alters the develoment of RAS mutation-associated leukaemia.

1-5.2 Aims

i) To develop a mouse model to investigate the fetal origins of JMML.

ii) To investigate the effect of the acquisition of leukaemogenic mutations at differing stages of murine development.

iii) To identify if mutation of Ezh2 alters or enhances leukaemogenesis in a JMML model system.

References

Abdel-Wahab O, Adli M, LaFave LM, et al. ASXL1 mutations promote myeloid transformation through loss of PRC2-mediated gene repression. *Cancer Cell*. 2012;22(2):180-193.

Akutagawa J, Huang TQ, Epstein I, et al. Targeting the PI3K/Akt pathway in murine MDS/MPN driven by hyperactive Ras. *Leukemia*. 2016;30(6):1335-1343.

An W, Mohapatra BC, Zutshi N, et al. VAV1-Cre mediated hematopoietic deletion of CBL and CBL-B leads to JMML-like aggressive early-neonatal myeloproliferative disease. *Oncotarget*. 2016;7(37):59006-59016.

Araki T, Mohi MG, Ismat FA, et al. Mouse model of Noonan syndrome reveals cell type- and gene dosage-dependent effects of Ptpn11 mutation. *Nat Med*. 2004;10(8):849-85.

Aricò M, Biondi A, Pui CH. Juvenile myelomonocytic leukemia. *Blood*. 1997;90(2):479-488.

Azcoitia V, Aracil M, Martinez AC, Torres M. The homeodomain protein Meis1 is essential for definitive hematopoiesis and vascular patterning in the mouse embryo. *Dev Biol*. 2005;280:307–320.

Bader-Meunier B, Tchernia G, Miélot F, et al. Occurrence of myeloproliferative disorder in patients with Noonan syndrome. *J Pediatr*. 1997;130(6):885-889.

Balazs AB, Fabian AJ, Esmon CT, Mulligan RC. Endothelial protein C receptor (CD201) explicitly identifies hematopoietic stem cells in murine bone marrow. *Blood*. 2006;107(6):2317-2321.

Basak A, Munschauer M, Lareau CA, et al. Control of human hemoglobin switching by LIN28B-mediated regulation of BCL11A translation. *Nat Genet*. 2020;52(2):138-145.

Basel-Vanagaite L. Acute lymphoblastic leukemia in Weaver syndrome. *Am J Med Genet A*. 2010;152A(2):383-386.

Basheer F, Giotopoulos G, Meduri E, et al. Contrasting requirements during disease evolution identify EZH2 as a therapeutic target in AML. *J Exp Med*. 2019;216(4):966-981.

Baumann I, Bennett JM, Niemeyer CM. Thiele J. Juvenile myelomonocytic leukaemia. In: Swerdlow SH, Campo E, Harris NL, et al, eds. WHO Classification of Tumors of Haematopoietic and Lymphoid Tissues. Lyon, France: International Agency for Research on Cancer (IARC); 2017:89-92.

Barker JE. Development of the mouse hematopoietic system. I. Types of hemoglobin produced in embryonic yolk sac and liver. *Dev Biol*. 1968;18(1):14-29.

Beaudin AE, Boyer SW, Perez-Cunningham J, et al. A Transient Developmental Hematopoietic Stem Cell Gives Rise to Innate-like B and T Cells. *Cell Stem Cell*. 2016;19(6):768-783.

Béguelin W, Teater M, Gearhart MD, et al. EZH2 and BCL6 Cooperate to Assemble CBX8-BCOR Complex to Repress Bivalent Promoters, Mediate Germinal Center Formation and Lymphomagenesis. *Cancer Cell*. 2016;30(2):197-213.

Bergstraesser E, Hasle H, Rogge T, et al. Non-hematopoietic stem cell transplantation treatment of juvenile myelomonocytic leukemia: a retrospective analysis and definition of response criteria. *Pediatr Blood Cancer*. 2007;49(5):629-633.

Berrozpe G, Bryant GO, Warpinski K, et al. Polycomb Responds to Low Levels of Transcription. *Cell Rep*. 2017;20(4):785-793.

Bhatnagar N, Nizery L, Tunstall O, Vyas P, Roberts I. Transient Abnormal Myelopoiesis and AML in Down Syndrome: an Update. *Curr Hematol Malig Rep*. 2016;11(5):333-341.

Böiers C, Carrelha J, Lutteropp M, et al. Lymphomyeloid contribution of an immune-restricted progenitor emerging prior to definitive hematopoietic stem cells. *Cell Stem Cell*. 2013;13(5):535-548.

Booth CAG, Barkas N, Neo WH, et al. Ezh2 and Runx1 Mutations Collaborate to Initiate Lympho-Myeloid Leukemia in Early Thymic Progenitors. *Cancer Cell*. 2018;33(2):274-291.e8.

Boultwood J, Perry J, Pellagatti A, et al. Frequent mutation of the polycomb-associated gene ASXL1 in the myelodysplastic syndromes and in acute myeloid leukemia. *Leukemia*. 2010;24(5):1062-1065.

Bowie MB, McKnight KD, Kent DG, McCaffrey L, Hoodless PA, Eaves CJ. Hematopoietic stem cells proliferate until after birth and show a reversible phase-specific engraftment defect. *J Clin Invest*. 2006;116(10):2808-2816.

Bowie MB, Kent DG, Dykstra B, et al. Identification of a new intrinsically timed developmental checkpoint that reprograms key hematopoietic stem cell properties. *Proc Natl Acad Sci U S A*. 2007;104(14):5878-5882.

Braun BS, Tuveson DA, Kong N, et al. Somatic activation of oncogenic Kras in hematopoietic cells initiates a rapidly fatal myeloproliferative disorder. *Proc Natl Acad Sci U S A*. 2004;101(2):597-602.

Brown P. Treatment of infant leukemias: challenge and promise. *Hematology Am Soc Hematol Educ Program*. 2013;2013:596-600.

Brown P, Pieters R, Biondi A. How I treat infant leukemia. *Blood*. 2019;133(3):205-214.

Buijs A, Bruin M. Fusion of FIP1L1 and RARA as a result of a novel t(4;17)(q12;q21) in a case of juvenile myelomonocytic leukemia. *Leukemia*. 2007;21(5):1104-1108.

Busch K, Klapproth K, Barile M, et al. Fundamental properties of unperturbed haematopoiesis from stem cells in vivo. *Nature*. 2015;518(7540):542-546.

Busque L, Gilliland DG, Prchal JT, et al. Clonality in juvenile chronic myelogenous leukemia. *Blood*. 1995;85(1):21-30.

Cao R, Wang L, Wang H, et al. Role of histone H3 lysine 27 methylation in Polycomb-group silencing. *Science*. 2002;298(5595):1039-1043.

Castleberry RP, Emanuel PD, Zuckerman KS, et al. A pilot study of isotretinoin in the treatment of juvenile chronic myelogenous leukemia. *N Engl J Med*. 1994;331(25):1680-1684.

Castro-Malaspina H, Schaison G, Passe S, et al. Subacute and chronic myelomonocytic leukemia in children (juvenile CML). Clinical and hematologic observations, and identification of prognostic factors. *Cancer*. 1984;54(4):675-686.

Carrelha J, Meng Y, Kettyle LM, et al. Hierarchically related lineage-restricted fates of multipotent haematopoietic stem cells. *Nature*. 2018;554(7690):106-111.

Caye A, Strullu M, Guidez F, et al. Juvenile myelomonocytic leukemia displays mutations in components of the RAS pathway and the PRC2 network. *Nat Genet*. 2015;47(11):1334-1340.

Caye A, Rouault-Pierre K, Strullu M, et al. Despite mutation acquisition in hematopoietic stem cells, JMML-propagating cells are not always restricted to this compartment [published correction appears in Leukemia. 2020 Jan 31;:]. *Leukemia*. 2020;34(6):1658-1668.

Chan G, Kalaitzidis D, Usenko T, et al. Leukemogenic Ptpn11 causes fatal myeloproliferative disorder via cell-autonomous effects on multiple stages of hematopoiesis. *Blood*. 2009;113(18):4414-4424.

Chang T, Krisman K, Theobald EH, et al. Sustained MEK inhibition abrogates myeloproliferative disease in Nf1 mutant mice [published correction appears in J Clin Invest. 2016 Jan;126(1):404]. *J Clin Invest*. 2013;123(1):335-339.

Chen MJ, Li Y, De Obaldia ME, et al. Erythroid/myeloid progenitors and hematopoietic stem cells originate from distinct populations of endothelial cells [published correction appears in Cell Stem Cell. 2012 Mar 2;10(3):345-6].

Cheshier, S. H., Morrison, S. J., Liao, X. and Weissman, I. L. (1999). In vivo proliferation and cell cycle kinetics of long-term self-renewing hematopoietic stem cells. *Proc. Natl. Acad. Sci. USA* 96,3120 -3125

COOKE JV. Chronic myelogenous leukemia in children. *J Pediatr*. 1953;42(5):537-550.

Cseh A, Niemeyer CM, Yoshimi A et al . Bridging to transplant with azacitidine in juvenile myelomonocytic leukemia: a retrospective analysis of the EWOG-MDS study group. *Blood* 2015; 125: 2311–3.

Cumano A, Dieterlen-Lievre F, Godin I. Lymphoid potential, probed before circulation in mouse, is restricted to caudal intraembryonic splanchnopleura. *Cell*. 1996;86(6):907-916.

Cumano A, Ferraz JC, Klaine M, Di Santo JP, Godin I. Intraembryonic, but not yolk sac hematopoietic precursors, isolated before circulation, provide long-term multilineage reconstitution. *Immunity*. 2001;15(3):477-485.

Czermin B, Melfi R, McCabe D, Seitz V, Imhof A, Pirrotta V. Drosophila enhancer of Zeste/ESC complexes have a histone H3 methyltransferase activity that marks chromosomal Polycomb sites. *Cell*. 2002;111(2):185-196.

Davé UP, Jenkins NA, Copeland NG. Gene therapy insertional mutagenesis insights. *Science*. 2004;303(5656):333.

de Bruijn MF, Speck NA, Peeters MC, Dzierzak E. Definitive hematopoietic stem cells first develop within the major arterial regions of the mouse embryo. *EMBO J.* 2000;19(11):2465-2474.

De Raedt T, Beert E, Pasmant E, et al. PRC2 loss amplifies Ras-driven transcription and confers sensitivity to BRD4-based therapies. *Nature*. 2014;514(7521):247-251.

Deevy O, Bracken AP. PRC2 functions in development and congenital disorders. *Development*. 2019;146(19):dev181354.

Dick JE. Normal and leukemic human stem cells assayed in SCID mice. *Semin Immunol*. 1996;8(4):197-206.

Di Genua C, Norfo R, Rodriguez-Meira A, et al. Cell-intrinsic depletion of Aml1-ETO-expressing pre-leukemic hematopoietic stem cells by K-Ras activating mutation. *Haematologica*. 2019;104(11):2215-2224.

Dong L, Yu WM, Zheng H, et al. Leukaemogenic effects of Ptpn11 activating mutations in the stem cell microenvironment. *Nature*. 2016;539(7628):304-308.

Drissen R, Buza-Vidas N, Woll P, et al. Distinct myeloid progenitor-differentiation pathways identified through single-cell RNA sequencing. *Nat Immunol*. 2016;17(6):666-676.

Dzierzak E, Speck NA. Of lineage and legacy: the development of mammalian hematopoietic stem cells. *Nat Immunol*. 2008;9(2):129-136.

Dzierzak E, Bigas A. Blood Development: Hematopoietic Stem Cell Dependence and Independence. *Cell Stem Cell*. 2018;22(5):639-651.

Duncan, I. M. Polycomblike: a gene that appears to be required for the normal expression of the bithorax and antennapedia gene complexes of Drosophila melanogaster. *Genetics.* 1982;102:49 -70.

Emanuel PD, Bates LJ, Castleberry RP, Gualtieri RJ, Zuckerman KS. Selective hypersensitivity to granulocyte-macrophage colony-stimulating factor by juvenile chronic myeloid leukemia hematopoietic progenitors. *Blood*. 1991;77(5):925-929.

Emanuel PD, Shannon KM, Castleberry RP. Juvenile myelomonocytic leukemia: molecular understanding and prospects for therapy. *Mol Med Today*. 1996;2(11):468-475.

Epelman S, Lavine KJ, Beaudin AE, et al. Embryonic and adult-derived resident cardiac macrophages are maintained through distinct mechanisms at steady state and during inflammation. *Immunity*. 2014;40(1):91-104.

Ernst P, Fisher JK, Avery W, Wade S, Foy D, Korsmeyer SJ. Definitive hematopoiesis requires the mixed-lineage leukemia gene. *Dev Cell*. 2004;6:437–443.

Ezhkova E, Lien WH, Stokes N, Pasolli HA, Silva JM, Fuchs E. EZH1 and EZH2 cogovern histone H3K27 trimethylation and are essential for hair follicle homeostasis and wound repair. *Genes Dev*. 2011;25(5):485-498.

Flotho C, Valcamonica S, Mach-Pascual S, et al. RAS mutations and clonality analysis in children with juvenile myelomonocytic leukemia (JMML). *Leukemia*. 1999;13(1):32-37.

Flotho C, Kratz CP, Bergsträsser E, et al. Genotype-phenotype correlation in cases of juvenile myelomonocytic leukemia with clonal RAS mutations. *Blood*. 2008;111(2):966-968.

Ford AM, Ridge SA, Cabrera ME, et al. In utero rearrangements in the trithorax-related oncogene in infant leukaemias. *Nature*. 1993;363(6427):358-360.

Fraser CC, Kaneshima H, Hansteen G, Kilpatrick M, Hoffman R, Chen BP. Human allogeneic stem cell maintenance and differentiation in a long-term multilineage SCID-hu graft. *Blood*. 1995;86(5):1680-1693.

Furlan I, Batz C, Flotho C et al . Intriguing response to azacitidine in a patient with juvenile myelomonocytic leukemia and monosomy 7. *Blood* 2009; 113: 2867–8.

Gagne AL, Maguire JA, Gandre-Babbe S, et al. Generation of a human Juvenile myelomonocytic leukemia iPSC line, CHOPi001-A, with a mutation in CBL. *Stem Cell Res*. 2018;31:157-160.

Gale KB, Ford AM, Repp R, et al. Backtracking leukemia to birth: identification of clonotypic gene fusion sequences in neonatal blood spots. *Proc Natl Acad Sci U S* A. 1997;94(25):13950-13954.

Gandre-Babbe S, Paluru P, Aribeana C, et al. Patient-derived induced pluripotent stem cells recapitulate hematopoietic abnormalities of juvenile myelomonocytic leukemia. *Blood*. 2013;121(24):4925-4929.

Gibson WT, Hood RL, Zhan SH, et al. Mutations in EZH2 cause Weaver syndrome. *Am J Hum Genet*. 2012;90(1):110-118.

Gitler AD, Kong Y, Choi JK, Zhu Y, Pear WS, Epstein JA. Tie2-Cre-induced inactivation of a conditional mutant Nf1 allele in mouse results in a myeloproliferative disorder that models juvenile myelomonocytic leukemia. *Pediatr Res*. 2004;55(4):581-584.

Göllner S, Oellerich T, Agrawal-Singh S, et al. Loss of the histone methyltransferase EZH2 induces resistance to multiple drugs in acute myeloid leukemia. *Nat Med*. 2017;23(1):69-78.

Gomez Perdiguero E, Klapproth K, Schulz C, et al. Tissue-resident macrophages originate from yolk-sac-derived erythro-myeloid progenitors. *Nature*. 2015;518(7540):547-551.

Greaves MF, Maia AT, Wiemels JL, Ford AM. Leukemia in twins: lessons in natural history. Blood. 2003;102(7):2321-2333.

Greaves M. A causal mechanism for childhood acute lymphoblastic leukaemia [published correction appears in Nat Rev Cancer. 2018 May 30;:]. *Nat Rev Cancer*. 2018;18(8):471-484.

Gupta RK, Qureshi A, Choi JK. Histologic findings in skin biopsy in a JMML rash: a case report and review of literature. *Pediatr Dev Pathol*. 2014;17(2):130-133.

Hacein-Bey-Abina S, Von Kalle C, Schmidt M, et al. LMO2-associated clonal T cell proliferation in two patients after gene therapy for SCID-X1 [published correction appears in Science. 2003 Oct 24;302(5645):568]. *Science*. 2003;302(5644):415-419.

HARDISTY RM, SPEED DE, TILL M. GRANULOCYTIC LEUKAEMIA IN CHILDHOOD. *Br J Haematol*. 1964;10:551-566.

Hasegawa D, Bugarin C, Giordan M, et al. Validation of flow cytometric phospho-STAT5 as a diagnostic tool for juvenile myelomonocytic leukemia. *Blood Cancer J.* 2013;3(11):e160.

Hasle H. Myelodysplastic syndromes in childhood--classification, epidemiology, and treatment. *Leuk Lymphoma*. 1994;13(1-2):11-26.

Hasle H, Wadsworth LD, Massing BG, McBride M, Schultz KR. A population-based study of childhood myelodysplastic syndrome in British Columbia, Canada. *Br J Haematol*. 1999;106(4):1027-1032.

Hasle H. Malignant diseases in Noonan syndrome and related disorders. *Horm Res*. 2009;72 Suppl 2:8-14.

Helsmoortel HH, Bresolin S, Lammens T, et al. LIN28B overexpression defines a novel fetal-like subgroup of juvenile myelomonocytic leukemia. *Blood*. 2016;127(9):1163-1172.

Herviou L, Cavalli G, Cartron G, Klein B, Moreaux J. EZH2 in normal hematopoiesis and hematological malignancies. *Oncotarget*. 2016;7(3):2284-2296.

Hidalgo I, Herrera-Merchan A, Ligos JM, et al. Ezh1 is required for hematopoietic stem cell maintenance and prevents senescence-like cell cycle arrest. *Cell Stem Cell*. 2012;11(5):649-662.

Hock H, Hamblen MJ, Rooke HM, Schindler JW, Saleque S, Fujiwara Y, Orkin SH. Gfi-1 restricts proliferation and preserves functional integrity of haematopoietic stem cells. *Nature*. 2004a;431:1002–1007.

Hoeffel G, Chen J, Lavin Y, et al. C-Myb(+) erythro-myeloid progenitor-derived fetal monocytes give rise to adult tissue-resident macrophages. *Immunity*. 2015;42(4):665-678.

Johnson L, Mercer K, Greenbaum D, et al. Somatic activation of the K-ras oncogene causes early onset lung cancer in mice. *Nature*. 2001;410(6832):1111-1116.

Kamminga LM, Bystrykh LV, de Boer A, et al. The Polycomb group gene Ezh2 prevents hematopoietic stem cell exhaustion. *Blood*. 2006;107(5):2170-2179.

Kiel MJ, Yilmaz OH, Iwashita T, Yilmaz OH, Terhorst C, Morrison SJ. SLAM family receptors distinguish hematopoietic stem and progenitor cells and reveal endothelial niches for stem cells. *Cell*. 2005;121(7):1109-1121.

Kim E, Ilagan JO, Liang Y, et al. SRSF2 Mutations Contribute to Myelodysplasia by Mutant-Specific Effects on Exon Recognition. *Cancer Cell*. 2015;27(5):617-630.

Kim I, Yilmaz OH, Morrison SJ. CD144 (VE-cadherin) is transiently expressed by fetal liver hematopoietic stem cells. *Blood*. 2005;106(3):903-905.

Kim I, Saunders TL, Morrison SJ. Sox17 dependence distinguishes the transcriptional regulation of fetal from adult hematopoietic stem cells. *Cell*. 2007;130(3):470-483.

Kim KH, Roberts CW. Targeting EZH2 in cancer. *Nat Med*. 2016;22(2):128-134.

Kollmann TR, Kim A, Zhuang X, Hachamovitch M, Goldstein H. Reconstitution of SCID mice with human lymphoid and myeloid cells after transplantation with human fetal bone marrow without the requirement for exogenous human cytokines. *Proc Natl Acad Sci U S A*. 1994;91(17):8032-8036.

Labuhn M, Perkins K, Matzk S, et al. Mechanisms of Progression of Myeloid Preleukemia to Transformed Myeloid Leukemia in Children with Down Syndrome. *Cancer Cell*. 2019;36(3):340.

Le DT, Kong N, Zhu Y, et al. Somatic inactivation of Nf1 in hematopoietic cells results in a progressive myeloproliferative disorder. *Blood*. 2004;103(11):4243-4250.

Lee ML, Yen HJ, Chen SJ, Hung GY, Tsao PC, Soong WJ. Juvenile Myelomonocytic Leukemia in a Premature Neonate Mimicking Neonatal Sepsis. *Pediatr Neonatol*. 2016;57(2):149-152.

Lee SC, Miller S, Hyland C, et al. Polycomb repressive complex 2 component Suz12 is required for hematopoietic stem cell function and lymphopoiesis. *Blood*. 2015;126(2):167-175.

Lee YT, de Vasconcellos JF, Yuan J, et al. LIN28B-mediated expression of fetal hemoglobin and production of fetal-like erythrocytes from adult human erythroblasts ex vivo. *Blood*. 2013;122(6):1034-1041.

Lewis EB. A gene complex controlling segmentation in Drosophila. *Nature*. 1978;276(5688):565-570.

Li Q, Haigis KM, McDaniel A, et al. Hematopoiesis and leukemogenesis in mice expressing oncogenic NrasG12D from the endogenous locus. *Blood*. 2011;117(6):2022-2032.

Li Q, Bohin N, Wen T, et al. Oncogenic Nras has bimodal effects on stem cells that sustainably increase competitiveness. *Nature*. 2013;504(7478):143-147.

Lipka DB, Witte T, Toth R, et al. RAS-pathway mutation patterns define epigenetic subclasses in juvenile myelomonocytic leukemia. *Nat Commun*. 2017;8(1):2126.

Locatelli F, Niemeyer C, Angelucci E, et al. Allogeneic bone marrow transplantation for chronic myelomonocytic leukemia in childhood: a report from the European Working Group on Myelodysplastic Syndrome in Childhood. *J Clin Oncol*. 1997;15(2):566-573.

Locatelli F, Nöllke P, Zecca M, et al. Hematopoietic stem cell transplantation (HSCT) in children with juvenile myelomonocytic leukemia (JMML): results of the EWOG-MDS/EBMT trial. *Blood*. 2005;105(1):410-419.

Locatelli F, Crotta A, Ruggeri A et al . Analysis of risk factors influencing outcomes after cord blood transplantation in children with juvenile myelomonocytic leukemia: a EUROCORD, EBMT, EWOG-MDS. CIBMTR study. *Blood* 2013; 122: 2135–41.

Locatelli F, Niemeyer CM. How I treat juvenile myelomonocytic leukemia. *Blood*. 2015;125(7):1083-1090.

Loh ML, Vattikuti S, Schubbert S, et al. Mutations in PTPN11 implicate the SHP-2 phosphatase in leukemogenesis. *Blood*. 2004;103(6):2325-2331.

Lorenzana A, Lyons H, Sawaf H, Higgins M, Carrigan D, Emanuel PD. Human herpesvirus 6 infection mimicking juvenile myelomonocytic leukemia in an infant. *J Pediatr Hematol Oncol*. 2002;24(2):136-141.

Louka E, Povinelli B, Meira AR. Heterogeneous disease-propagating stem cells in juvenile myelomonocytic leukemia. *BioRXiv*. 2019; May 07. https://doi.org/10.1101/628479.

Lund K, Adams PD, Copland M. EZH2 in normal and malignant hematopoiesis. *Leukemia*. 2014;28(1):44-49.

Lutz P, Zix-Kieffer I, Souillet G, et al. Juvenile myelomonocytic leukemia: analyses of treatment results in the EORTC Children's Leukemia Cooperative Group (CLCG). *Bone Marrow Transplant*. 1996;18(6):1111-1116.

Lyubynska N, Gorman MF, Lauchle JO, et al. A MEK inhibitor abrogates myeloproliferative disease in Kras mutant mice. *Sci Transl Med*. 2011;3(76):76ra27.

MacMillan ML, Davies SM, Orchard PJ, Ramsay NK, Wagner JE. Haemopoietic cell transplantation in children with juvenile myelomonocytic leukaemia. *Br J Haematol*. 1998;103(2):552-558.

Majewski IJ, Ritchie ME, Phipson B, et al. Opposing roles of polycomb repressive complexes in hematopoietic stem and progenitor cells. *Blood*. 2010;116(5):731-739.

Manabe A, Okamura J, Yumura-Yagi K, et al. Allogeneic hematopoietic stem cell transplantation for 27 children with juvenile myelomonocytic leukemia diagnosed based on the criteria of the International JMML Working Group. *Leukemia*. 2002;16(4):645-649.

Margueron R, Li G, Sarma K, et al. Ezh1 and Ezh2 maintain repressive chromatin through different mechanisms. *Mol Cell*. 2008;32(4):503-518.

Margueron R, Reinberg D. The Polycomb complex PRC2 and its mark in life. *Nature*. 2011;469(7330):343-349

Matsuda K, Shimada A, Yoshida N, et al. Spontaneous improvement of hematologic abnormalities in patients having juvenile myelomonocytic leukemia with specific RAS mutations. *Blood*. 2007;109(12):5477-5480.

Matsuda K, Sakashita K, Taira C, et al. Quantitative assessment of PTPN11 or RAS mutations at the neonatal period and during the clinical course in patients with juvenile myelomonocytic leukaemia. *Br J Haematol*. 2010;148(4):593-599.

Matsumoto K, Miki J, Matsuzaki S, Koike K, Saida T. Skin infiltration of juvenile myelomonocytic leukemia. *J Dermatol*. 2004;31(9):748-751.

McGrath KE, Frame JM, Fromm GJ, et al. A transient definitive erythroid lineage with unique regulation of the β-globin locus in the mammalian embryo. *Blood*. 2011;117(17):4600-4608.

McGrath KE, Frame JM, Fegan KH, et al. Distinct Sources of Hematopoietic Progenitors Emerge before HSCs and Provide Functional Blood Cells in the Mammalian Embryo. *Cell Rep*. 2015;11(12):1892-1904.

Medvinsky A, Dzierzak E. Definitive hematopoiesis is autonomously initiated by the AGM region. *Cell*. 1996;86(6):897-906.

Melo-Cardenas J, Xu Y, Wei J, et al. USP22 deficiency leads to myeloid leukemia upon oncogenic Kras activation through a PU.1-dependent mechanism. *Blood*. 2018;132(4):423-434.

Migliaccio G, Migliaccio AR, Petti S, et al. Human embryonic hemopoiesis. Kinetics of progenitors and precursors underlying the yolk sac----liver transition. *J Clin Invest*. 1986;78(1):51-60.

Mikkola HK, Orkin SH. The journey of developing hematopoietic stem cells. *Development*. 2006;133(19):3733-3744.

Miyauchi J, Asada M, Sasaki M, Tsunematsu Y, Kojima S, Mizutani S. Mutations of the N-ras gene in juvenile chronic myelogenous leukemia. *Blood*. 1994;83(8):2248-2254.

Mochizuki-Kashio M, Mishima Y, Miyagi S, et al. Dependency on the polycomb gene Ezh2 distinguishes fetal from adult hematopoietic stem cells [published correction appears in *Blood*. 2012 Jul 26;120(4):924]. *Blood*. 2011;118(25):6553-6561.

Mohi MG, Williams IR, Dearolf CR, et al. Prognostic, therapeutic, and mechanistic implications of a mouse model of leukemia evoked by Shp2 (PTPN11) mutations. *Cancer Cell*. 2005;7(2):179-191.

Montecino-Rodriguez E, Fice M, Casero D, Berent-Maoz B, Barber CL, Dorshkind K. Distinct Genetic Networks Orchestrate the Emergence of Specific Waves of Fetal and Adult B-1 and B-2 Development. *Immunity*. 2016;45(3):527-539.

Moore, M.A.S. and Metcalf, D. Ontogeny of the Haemopoietic System: Yolk Sac Origin of In Vivo and In Vitro Colony Forming Cells in the Developing Mouse Embryo*. *British Journal of Haematology*. 1970;18: 279-296.

Moritake H, Ikeda T, Manabe A, Kamimura S, Nunoi H. Cytomegalovirus infection mimicking juvenile myelomonocytic leukemia showing hypersensitivity to granulocyte-macrophage colony stimulating factor. *Pediatr Blood Cancer*. 2009;53(7):1324-1326.

Morrison SJ, Hemmati HD, Wandycz AM, Weissman IL. The purification and characterization of fetal liver hematopoietic stem cells. *Proc Natl Acad Sci U S A*. 1995;92(22):10302-10306.

Müller J, Hart CM, Francis NJ, et al. Histone methyltransferase activity of a Drosophila Polycomb group repressor complex. *Cell*. 2002;111(2):197-208.

Murakami N, Okuno Y, Yoshida K, et al. Integrated molecular profiling of juvenile myelomonocytic leukemia. *Blood*. 2018;131(14):1576-1586.

Muto T, Sashida G, Oshima M, et al. Concurrent loss of Ezh2 and Tet2 cooperates in the pathogenesis of myelodysplastic disorders. *J Exp Med*. 2013;210(12):2627-2639.

Nakagawa M, Kitabayashi I. Oncogenic roles of enhancer of zeste homolog 1/2 in hematological malignancies. *Cancer Sci*. 2018;109(8):2342-2348.

Nambu M, Shimizu K, Ito S, Ohta S. A case of juvenile myelomonocytic leukemia with ocular infiltration. *Ann Hematol*. 1999;78(12):568-570.

Neo WH, Booth CAG, Azzoni E, et al. Cell-extrinsic hematopoietic impact of Ezh2 inactivation in fetal liver endothelial cells. *Blood*. 2018;131(20):2223-2234.

Niemeyer CM, Arico M, Basso G, et al. Chronic myelomonocytic leukemia in childhood: a retrospective analysis of 110 cases. European Working Group on Myelodysplastic Syndromes in Childhood (EWOG-MDS). *Blood*. 1997;89(10):3534-3543.

Niemeyer CM, Kratz CP. Paediatric myelodysplastic syndromes and juvenile myelomonocytic leukaemia: molecular classification and treatment options. *Br J Haematol*. 2008;140(6):610-624.

Niemeyer CM. RAS diseases in children. *Haematologica*. 2014;99(11):1653-1662.

Niemeyer CM. JMML genomics and decisions. *Hematology Am Soc Hematol Educ Program*. 2018;2018(1):307-312.

North TE, de Bruijn MF, Stacy T, et al. Runx1 expression marks long-term repopulating hematopoietic stem cells in the midgestation mouse embryo. *Immunity*. 2002;16(5):661-672.

Ntziachristos P, Tsirigos A, Van Vlierberghe P, et al. Genetic inactivation of the polycomb repressive complex 2 in T cell acute lymphoblastic leukemia. *Nat Med*. 2012;18(2):298-301.

Oberlin E, Tavian M, Blazsek I, Péault B. Blood-forming potential of vascular endothelium in the human embryo. *Development*. 2002;129(17):4147-4157.

O'Byrne S, Elliott N, Rice S, et al. Discovery of a CD10-negative B-progenitor in human fetal life identifies unique ontogeny-related developmental programs. *Blood*. 2019;134(13):1059-1071.

Oguro H, Ding L, Morrison SJ. SLAM family markers resolve functionally distinct subpopulations of hematopoietic stem cells and multipotent progenitors. *Cell Stem Cell*. 2013;13(1):102-116.

Okuda T, Vandeursen J, Hiebert SW, Grosveld G, Downing JR. AML1, the target of multiple chromosomal translocations in human leukemia, is essential for normal fetal liver hematopoiesis. *Cell*. 1996;84:321–330.

Olk-Batz C, Poetsch AR, Nöllke P, et al. Aberrant DNA methylation characterizes juvenile myelomonocytic leukemia with poor outcome. *Blood*. 2011;117(18):4871-4880.

Ooi AG, Karsunky H, Majeti R, et al. The adhesion molecule esam1 is a novel hematopoietic stem cell marker. *Stem Cells*. 2009;27(3):653-661.

Osawa M, Hanada K, Hamada H, Nakauchi H. Long-term lymphohematopoietic reconstitution by a single CD34-low/negative hematopoietic stem cell. *Science*. 1996;273(5272):242-245.

Oshima M, Hasegawa N, Mochizuki-Kashio M, et al. Ezh2 regulates the Lin28/let-7 pathway to restrict activation of fetal gene signature in adult hematopoietic stem cells. *Exp Hematol*. 2016;44(4):282-96.e3.

Owen G, Lewis IJ, Morgan M, Robinson A, Stevens RF. Prognostic factors in juvenile chronic granulocytic leukaemia. *Br J Cancer Suppl*. 1992;18:S68-S71.

Palis, J., Robertson, S., Kennedy, M., Wall, C. and Keller, G., 1999. Development of erythroid and myeloid progenitors in the yolk sac and embryo proper of the mouse. *Development*, *126*(22), pp.5073-5084.

Papaemmanuil E, Gerstung M, Malcovati L, et al. Clinical and biological implications of driver mutations in myelodysplastic syndromes. *Blood*. 2013;122(22):3616-3699.

Papaemmanuil E, Gerstung M, Bullinger L, et al. Genomic Classification and Prognosis in Acute Myeloid Leukemia. *N Engl J Med*. 2016;374(23):2209-2221.

Park IK, Qian D, Kiel M, Becker M, Pihalja M, Weissman IL, Morrison SJ, Clarke M. Bmi-1 is required for the maintenance of adult self-renewing hematopoietic stem cells. *Nature*. 2003;423:302–305.

Passmore SJ, Hann IM, Stiller CA, et al. Pediatric myelodysplasia: a study of 68 children and a new prognostic scoring system. *Blood*. 1995;85(7):1742-1750.

Passmore SJ, Chessells JM, Kempski H, Hann IM, Brownbill PA, Stiller CA. Paediatric myelodysplastic syndromes and juvenile myelomonocytic leukaemia in the UK: a population-based study of incidence and survival. *Br J Haematol*. 2003;121(5):758-767.

Pérez B, Kosmider O, Cassinat B, et al. Genetic typing of CBL, ASXL1, RUNX1, TET2 and JAK2 in juvenile myelomonocytic leukaemia reveals a genetic profile distinct from chronic myelomonocytic leukaemia. *Br J Haematol*. 2010;151(5):460-468.

Porcher C, Swat W, Rockwell K, Fujiwara Y, Alt FW, Orkin SH. The T cell leukemia oncoprotein SCL/tal-1 is essential for development of all hematopoietic lineages. *Cell*. 1996;86:47–57.

Pronk CJ, Rossi DJ, Månsson R, et al. Elucidation of the phenotypic, functional, and molecular topography of a myeloerythroid progenitor cell hierarchy. *Cell Stem Cell.* 2007;1(4):428-442.

Randall TD, Weissman IL. Phenotypic and functional changes induced at the clonal level in hematopoietic stem cells after 5-fluorouracil treatment. *Blood*. 1997;89(10):3596-3606.

REISMAN LE, TRUJILLO JM. Chronic granulocytic leukemia of childhood. Clinical and cytogenetic studies. *J Pediatr*. 1963;62:710-723.

Rinke J, Chase A, Cross NCP, Hochhaus A, Ernst T. EZH2 in Myeloid Malignancies. *Cells*. 2020;9(7):E1639. Published 2020 Jul 8.

Roberts I, Alford K, Hall G, et al. GATA1-mutant clones are frequent and often unsuspected in babies with Down syndrome: identification of a population at risk of leukemia. *Blood*. 2013;122(24):3908-3917.

Roberts I, Izraeli S. Haematopoietic development and leukaemia in Down syndrome. *Br J Haematol*. 2014;167(5):587-599.

Roberts I, Fordham NJ, Rao A, Bain BJ. Neonatal leukaemia [published correction appears in Br J Haematol. 2019 Jul;186(1):196]. *Br J Haematol*. 2018;182(2):170-184.

Röttgers S, Gombert M, Teigler-Schlegel A, et al. ALK fusion genes in children with atypical myeloproliferative leukemia. *Leukemia*. 2010;24(6):1197-1200.

Rowe RG, Wang LD, Coma S, et al. Developmental regulation of myeloerythroid progenitor function by the Lin28b-let-7-Hmga2 axis. *J Exp Med*. 2016;213(8):1497-1512.

Sabnis AJ, Cheung LS, Dail M, et al. Oncogenic Kras initiates leukemia in hematopoietic stem cells. *PLoS Biol*. 2009;7(3):e59.

Sakashita K, Matsuda K, Koike K. Diagnosis and treatment of juvenile myelomonocytic leukemia. *Pediatr Int*. 2016;58(8):681-690.

Sankaran VG, Menne TF, Xu J, et al. Human fetal hemoglobin expression is regulated by the developmental stage-specific repressor BCL11A. *Science*. 2008;322(5909):1839-1842.

Sankaran VG, Xu J, Orkin SH. Advances in the understanding of haemoglobin switching. *Br J Haematol*. 2010;149(2):181-194.

Sashida G, Wang C, Tomioka T, et al. The loss of Ezh2 drives the pathogenesis of myelofibrosis and sensitizes tumor-initiating cells to bromodomain inhibition. *J Exp Med*. 2016;213(8):1459-1477.

Schuettengruber B, Cavalli G. Recruitment of polycomb group complexes and their role in the dynamic regulation of cell fate choice. *Development*. 2009;136(21):3531-3542.

Score J, Hidalgo-Curtis C, Jones AV, et al. Inactivation of polycomb repressive complex 2 components in myeloproliferative and myelodysplastic/myeloproliferative neoplasms. *Blood*. 2012;119(5):1208-1213.

Shen X, et al. EZH1 mediates methylation on histone H3 lysine 27 and complements EZH2 in maintaining stem cell identity and executing pluripotency. *Mol Cell*. 2008;32:491–502.

Simon JA, Kingston RE. Mechanisms of polycomb gene silencing: knowns and unknowns. *Nat Rev Mol Cell Biol*. 2009;10(10):697-708.

SIMINOVITCH L, MCCULLOCH EA, TILL JE. THE DISTRIBUTION OF COLONY-FORMING CELLS AMONG SPLEEN COLONIES. J Cell Comp Physiol. 1963;62:327-336.

Shannon KM, O'Connell P, Martin GA, et al. Loss of the normal NF1 allele from the bone marrow of children with type 1 neurofibromatosis and malignant myeloid disorders. *N Engl J Med*. 1994;330(9):597-601.

Shimizu T, Kubovcakova L, Nienhold R, et al. Loss of Ezh2 synergizes with JAK2-V617F in initiating myeloproliferative neoplasms and promoting myelofibrosis. *J Exp Med*. 2016;213(8):1479-1496.

Shyh-Chang N, Daley GQ. Lin28: primal regulator of growth and metabolism in stem cells. *Cell Stem Cell*. 2013;12(4):395-406.

Sinka L, Biasch K, Khazaal I, Péault B, Tavian M. Angiotensin-converting enzyme (CD143) specifies emerging lympho-hematopoietic progenitors in the human embryo. *Blood*. 2012;119(16):3712-3723.

Smith LB, Valdes Y, Check WE, Britt PM, Frankel LS. Juvenile myelomonocytic leukemia presenting with facial nerve paresis: a unique presentation. *J Pediatr Hematol Oncol*. 2007;29(11):770-773.

Sonoda Y. Human CD34-negative hematopoietic stem cells: The current understanding of their biological nature. *Exp Hematol*. 2021 Apr;96:13-26.

Spangrude GJ, Heimfeld S, Weissman IL. Purification and characterization of mouse hematopoietic stem cells [published correction appears in Science 1989 Jun 2;244(4908):1030]. *Science*. 1988;241(4861):58-62.

Stieglitz E, Taylor-Weiner AN, Chang TY, et al. The genomic landscape of juvenile myelomonocytic leukemia [published correction appears in Nat Genet. 2015 Nov;47(11):1333] [published correction appears in Nat Genet. 2016 Jan;48(1):101]. *Nat Genet*. 2015;47(11):1326-1333.

Su IH, Basavaraj A, Krutchinsky AN, et al. Ezh2 controls B cell development through histone H3 methylation and Igh rearrangement. *Nat Immunol*. 2003;4(2):124-131.

Su IH, Dobenecker MW, Dickinson E, et al. Polycomb group protein ezh2 controls actin polymerization and cell signaling. *Cell*. 2005;121(3):425-436.

Tang P, Gao C, Li A, Aster J, Sun L, Chai L. Differential roles of Kras and Pten in murine leukemogenesis. *Leukemia*. 2013;27(5):1210-1214.

Tarnawsky SP, Yoshimoto M, Deng L, Chan RJ, Yoder MC. Yolk sac erythromyeloid progenitors expressing gain of function PTPN11 have functional features of JMML but are not sufficient to cause disease in mice. *Dev Dyn*. 2017;246(12):1001-1014.

Tarnawsky* SP, Kobayashi M, Chan RJ, Yoder MC. Mice expressing KrasG12D in hematopoietic multipotent progenitor cells develop neonatal myeloid leukemia. *J Clin Invest*. 2017;127(10):3652-3656.

Tarnawsky SP, Yu WM, Qu CK, Chan RJ, Yoder MC. Hematopoietic-restricted Ptpn11E76K reveals indolent MPN progression in mice. *Oncotarget*. 2018;9(31):21831-21843.

Tasian SK, Casas JA, Posocco D, et al. Mutation-specific signaling profiles and kinase inhibitor sensitivities of juvenile myelomonocytic leukemia revealed by induced pluripotent stem cells. *Leukemia*. 2019;33(1):181-190.

Tavian M, Hallais MF, Péault B. Emergence of intraembryonic hematopoietic precursors in the pre-liver human embryo. *Development*. 1999;126(4):793-803.

Tsai FY, Keller G, Kuo FC, Weiss M, Chen J, Rosenblatt M, Alt FW, Orkin SH. An early haematopoietic defect in mice lacking the transcription factor GATA-2. *Nature*. 1994;371:221–226.

Vo LT, Kinney MA, Liu X, et al. Regulation of embryonic haematopoietic multipotency by EZH1. *Nature*. 2018;553(7689):506-510.

Wang J, Kimura T, Asada R, Harada S, Yokota S, Kawamoto Y, Fujimura Y, Tsuji T, Ikehara S, Sonoda Y. SCID-repopulating cell activity of human cord blood-derived CD34- cells assured by intra-bone marrow injection. *Blood*. 2003 Apr 15;101(8):2924-31.

Wang H, Wang L, Erdjument-Bromage H, et al. Role of histone H2A ubiquitination in Polycomb silencing. *Nature*. 2004;431(7010):873-878.

Warren AJ, Colledge WH, Carlton MB, Evans MJ, Smith AJ, Rabbitts TH. The oncogenic cysteine-rich LIM domain protein rbtn2 is essential for erythroid development. *Cell*. 1994;78(1):45-57.

Xie H, Xu J, Hsu JH, et al. Polycomb repressive complex 2 regulates normal hematopoietic stem cell function in a developmental-stage-specific manner. *Cell Stem Cell*. 2014;14(1):68-80.

Xu B, On DM, Ma A, et al. Selective inhibition of EZH2 and EZH1 enzymatic activity by a small molecule suppresses MLL-rearranged leukemia. *Blood*. 2015;125(2):346-357.

Yabe M, Sako M, Yabe H, et al. A conditioning regimen of busulfan, fludarabine, and melphalan for allogeneic stem cell transplantation in children with juvenile myelomonocytic leukemia. *Pediatr Transplant*. 2008;12(8):862-867.

Yabe M, Ohtsuka Y, Watanabe K et al . Transplantation for juvenile myelomonocytic leukemia: a retrospective study of 30 children treated with a regimen of busulfan, fludarabine, and melphalan. *Int. J. Hematol*. 2015; 101: 184–90.

Yang Y, Akada H, Nath D, Hutchison RE, Mohi G. Loss of Ezh2 cooperates with Jak2V617F in the development of myelofibrosis in a mouse model of myeloproliferative neoplasm. *Blood*. 2016;127(26):3410-3423.

Yoder MC, Hiatt K. Engraftment of Embryonic Hematopoietic Cells in Conditioned Newborn Recipients. *Blood* 1997; 89 (6): 2176–2183.

Yoshida N, Yagasaki H, Xu Y, et al. Correlation of clinical features with the mutational status of GM-CSF signaling pathway-related genes in juvenile myelomonocytic leukemia. *Pediatr Res*. 2009;65(3):334-340.

Yoshimi A, Kamachi Y, Imai K, et al. Wiskott-Aldrich syndrome presenting with a clinical picture mimicking juvenile myelomonocytic leukaemia. *Pediatr Blood Cancer*. 2013;60(5):836-841.

Yoshimi A, Balasis ME, Vedder A, et al. Robust patient-derived xenografts of MDS/MPN overlap syndromes capture the unique characteristics of CMML and JMML [published correction appears in Blood. 2017 Sep 28;130(13):1602]. *Blood*. 2017;130(4):397-407. doi:10.1182/blood-2017-01-763219

Yoshimoto M, Montecino-Rodriguez E, Ferkowicz MJ, et al. Embryonic day 9 yolk sac and intra-embryonic hemogenic endothelium independently generate a B-1 and marginal zone progenitor lacking B-2 potential. *Proc Natl Acad Sci U S A*. 2011;108(4):1468-1473.

Zhang Y, Taylor BR, Shannon K, Clapp DW. Quantitative effects of Nf1 inactivation on in vivo hematopoiesis. *J Clin Invest*. 2001;108(5):709-715.

Zhang J, Wang J, Liu Y, et al. Oncogenic Kras-induced leukemogeneis: hematopoietic stem cells as the initial target and lineage-specific progenitors as the potential targets for final leukemic transformation. *Blood*. 2009;113(6):1304-1314.

Chapter 2: Methods

2-1 Murine strains

Mice were cared for in a specific-pathogen-free facility in individually ventilated cages within the John Radcliffe Biomedical Sciences Building, University of Oxford. Soft bedding and nesting material in addition to stimulation were provided. Mice were fed with a solid diet, except where stated below, and water. All procedures and protocols were followed as per the home office licences (30/3103 Sept 2016 - Aug 2018; P2FF90EE8 Aug 2018 onwards). Personal licence (I1B775543; PILABC) obtained from the Home Office through the University of Oxford training facility.

i) $Kras^{LSL\text{-}G12D}$ conditional knock-in

The $Kras^{LSL\text{-}G12D}$ mouse model (JAX: 008179), designed by Johnson *et al* [Johnson, 2001], described with haematopoietic activation [Braun, 2004], was obtained from Terry Rabbitts and has been well established in the Mead Laboratory [Booth, 2018][Di Genua, 2019]. Cre recombinase leads to removal of a Lox-Stop-Lox codon and activation of $Kras^{G12D}$. It was backcrossed onto a C57Bl/6 background for >15 generations prior to my project and were maintained on a pure C57Bl/6 background. Homozygous carriage is lethal, so mice were bred to heterozygosity.

ii) *Ezh2* conditional knock-out

The $Ezh2^{fl/fl}$ mouse (JAX: 022616), has previously been described in Su *et al*, 2003. A floxed area of the *Ezh2* SET domain is removed when $Ezh2^{fl/fl}$ occurs with a Cre recombinase, leading to production a truncated mRNA and subsequent decreased Ezh2 protein expression [Su, 2003]. These mice were maintained on a pure C57Bl/6 background and are well established in

the Mead Laboratory [Booth, 2018][Neo, 2018]. Mice were bred to WT, *Ezh2*$^{fl/+}$ or *Ezh2*$^{fl/fl}$, depending on experimental need.

iii) Ai9-Rosa26 inducible tdTomato

The Ai9 mouse (JAX: 007909) is a reporter mouse for Cre expression. Cre recombinase leads to removal of a Lox-Stop-Lox codon and expression of the tdTomato reporter protein [Madisen, 2010] from the Rosa26 locus. Mice were obtained from the Jackson Laboratory and have been previously backgrossed to C57Bl/6 background, on which they were maintained. Mice were bred aiming for homozygous expression, however heterozygous and homozygous mice were used for experiments.

iv) Cre recombinase lines

Vav-iCre: The Vav-iCre transgenic mouse (JAX: 008610), developed by De Boer, *et al*, 2003 leads to haematopoietic specific constitutive expression of an optimised Cre Recombinase enzyme (iCre), under control of the Vav1 promotor [De Boer, 2003]. Mice were maintained on a C57Bl/6 background and were bred to heterozygosity. Where possible, Vav-iCre was maintained on the male mice, to minimise germline deletion, as per the Jackson laboratory breeding suggestions at the time.

Tie2Cre: The Tie2Cre transgenic mouse (JAX: 008863), developed by Kisanuki *et al* uses the Tie2 (Tek) promotor to achieve Cre expression in endothelial cells [Kisanuki, 2001]. Mice were maintained on a C57Bl/6 background and were bred to heterozygosity. Where possible, Tie2Cre was maintained on the male mice, to minimise germline deletion, as per the Jackson laboratory breeding suggestions at the time.

Mx1Cre: The Mx1Cre transgene (JAX: 003556) uses the interferon pathway to allow induction of Cre Recombinase with Polyinosinic:polycytidylic acid (PolyI:C). Mice were obtained from the Jackson laboratory, and had previously been backcrossed into a C57Bl/6 background. Mice were maintained on a C57Bl/6 background and were bred to heterozygosity.

Fgd5CreERT2: Fgd5CreERT2 (JAX 027789) is expressed only in CD150+ LSK HSCs [Gazit, 2014]. A Cre cassette along with ZsGreen (a green fluorescent protein) was inserted into the *Fgd5* locus by the developing laboratory [Gazit, 2014]. With tamoxifen administration Cre expression is induced due to translocation of the Cre to the nucleus and expression of the transgene can be monitored with ZsGreen by flow cytometry of HSCs. Mice were obtained from the Jacobsen laboratory and have been previously backcrossed to a C57Bl/6 background. Mice were maintained on a C57Bl/6 background and were bred to heterozygosity.

v) NOD-*scid*-IL2Rg^{null} (NSG) mice

NOD-*scid*-IL2Rg^{null} (NSG) mice (JAX: 005557) immunodeficient mice were obtained from the Jackson laboratory and used for YS transplantations [McGrath, 2015]. Mice were bred to other NSG mice as per Jackson laboratory recommendations. Care was taken to clean NSG cages prior to other cages, and monitoring of NSG mice first during routine cage checks to avoid cross-infection from C57Bl/6 mice.

vi) Breeding protocol

Breeding pairs or trios (one male to maximum two females) were maintained for 6-12 months, to a maximum of 6 litters, or until 12 months of age when they were replaced. Mice were earclipped at 10 days to 3 weeks for identification and litters were weaned at ~3 weeks, once

able to survive on normal diet. At this point male and female mice were separated. See section 2-2.1 for generation of timed embryos.

vii) Genotyping and DNA extraction

DNA was extracted from earclips by a DNA extraction kit (Omega Bio-Tek: Cat# R6731-01). For fetal mice DNA was extracted from a sample of embryonic material using a commercially available kit (Thermofischer: Cat# F170S). PCRs were then performed using established protocols within the laboratory (appendix 5.1), using Kapa2G PCR mastermix (Kapa Biosystems: Cat# KK5103), using known positive and negative controls in addition to water. Amplified DNA was run on agarose gel electrophoresis to delineate the genotype of the mice (figure 2.1).

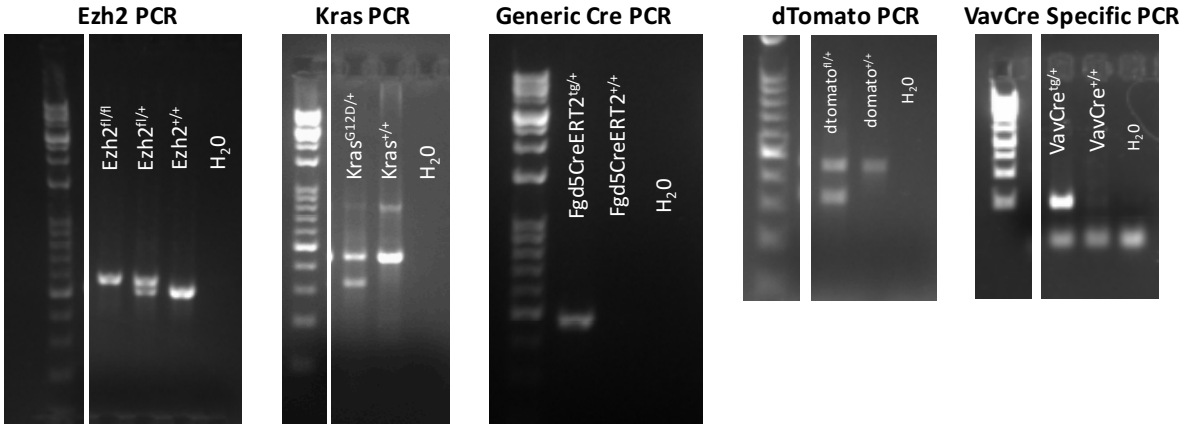


Figure 2.1: Example genotyping PCR products. Agarose gels showing products from (a) Ezh2, controls for homozygous, heterozygous, WT and water (b) Kras heterozygous, WT and water (c) Generic Cre, used for Tie2, Fgd5CreERT2 and Mx1Cre. Shown Fgd5CreERT transgenic, WT and water(d) dTomato controls for heterozygous, WT and water and (e) VavCre transgenic, WT, water.

2-2. Generation of embryos

Female cycles were synchronised with male bedding for 4-5 days prior to plugging. Males were separated from their breeding cage. For generation of timed embryos single male mice were placed in a cage with between one and four females in the evening of day 0. The following

morning females were checked for a vaginal plug, and the day of plug formation termed 0.5 days post-coitum (dpc).

Dams were culled at the appropriate dpc by rising concentration of CO_2 and cervical dislocation. Uterine horns were dissected, kept on ice, and embryos >E12.5 were decapitated prior to dissection under a light microscope, submerged in phosphate buffered saline (PBS, Thermofisher: Cat# 10010023) supplemented with 10% fetal calf serum (FCS, Sigma: Cat# F7524). Tissues were placed in PBS+10% FCS and kept on ice until use. Experimental embryos were assessed using established criteria to confirm gestational age, and somite pairs (sp) or tail somites were counted [Palis, 1999]. E9.5 embryos were counted to include 20-29sp and E10.5 30-37sp. Tail somites were counted for E12 to E14.5. After E14 gestational stage (>60sp) was assessed using morphological criteria (ie separation of digits at E14.5-15.5).

2-3. Administration of substances

i) Tamoxifen +/- Progesterone

Embryonic administration: Dams were dosed with tamoxifen (Sigma: Cat# T5648-1G), dissolved in corn oil (Sigma: Cat# C8267) by oral gavage (100μL) at the appropriate time point in gestation. Final FL induction used 2mg tamoxifen at E14.5, however for phenotyping 4mg was given at E12.5 and 13.5. Prior to E12.5, tamoxifen was mixed with progesterone (Sigma: Cat# P0130) in a 2:1 ratio, due to the potential abortive actions of oestrogen agonists early in gestation and protective effect of progesterone [McGrath, 2015]. Embryonic ranges for YS induction of E7.5 and E9.5 received as little as 0.5mg tamoxifen (with 0.25mg progesterone) to a maximum of 2.5mg tamoxifen (with 1.25mg progesterone), as described in Chapter 4. An alternative, but not used, technique would be to use the active metabolite of tamoxifen (4-OH-Tamoxifen), which needs to be given parenterally, but has a much shorter half-life, so may be

able to be given later in gestation (E8.5-9.5) without inducing HSCs. Dams receiving tamoxifen were kept in separate cages until delivery to minimise the transfer of tamoxifen in faeces. Mice were monitored daily after tamoxifen administration to ensure no side effects or miscarriage.

Adult administration: Adult mice aged 6-8 weeks were given 4mg tamoxifen (100μL) daily for 5 day by oral gavage. Given the problems with weight loss following tamoxifen administration [Ye, 2015], mice were supplemented with formula milk (TESCO: SMA Pro1) and crushed solid diet. Adult male or female mice were randomly chosen, and where possible whole cages were induced. Mice were weighed daily for up to 14 days following tamoxifen administration and inspected daily for signs of ill health. Mice which lost >15% of weight by day 10 following induction were culled as per the Home Office licence and were excluded from future analysis. Mice were followed up for up to 6 months following tamoxifen administration.

ii) PolyI:C

Experimental adult $Mx1Cre^{tg/+}$ or $Mx1Cre^{+/+}$ mice were induced with three doses of 200μg PolyI:C (GE Healthcare: Cat# 27473201) by intraperitoneal injection (made up in PBS to 1mg/1ml), at 2 day intervals. Neonatal mice were induced with 20μg (~20μg/g) for two or three doses over five days by intraperitoneal injection. Male and female mice were randomly chosen, or where possible, whole litters were induced. Mice were monitored for up to 6 months following induction with PolyI:C.

2-4. Delivery and fostering of pups following tamoxifen administration *in-utero*

Delivery: As oestrogen interferes with the natural parturition of mice, dams who received tamoxifen were delivered by caesarean section (CS) prior to term, as detailed in the Home Office licence. Dams were monitored daily until E19.5 (for 3 experiments during optimisation E18.5 was used) for signs of premature delivery. Where mice appeared to be delivering or miscarrying prior to E18.5, dams were culled. In the morning of E19.5 dams were induced with anaesthesia with 3-4% isofluorane (obtained by prescription from Oxford University Veterinary Services). Once surgical anaesthesia was achieved dams were culled by cervical dislocation. Pups were removed by caesarean section, dried and resuscitated by continuous stimulation with warmed paper towels within a heat box at 38^{o}C. Umbilical cord, yolk sac and placental material was removed as much as possible.

Fostering: Day 0-1 postnatal day (pnd) foster mothers were chosen. Initially, where possible, alternative coat colours (agouti/white coated) were chosen and 2-4 pups from the original litter left. The foster mother's urine and bedding from the cage was rubbed over the experimental pups, which were placed with the host litter. Due to sparsity of alternative colours, later C57Bl/6 foster mothers were used and in this case whole litters were removed and replaced with experimental litters. The cages were not disturbed for 5 days and were inspected carefully externally only. At day 5pnd the number of remaining pups were counted. Pups were genotyped as close to day 10pnd as possible, and weaned ~3 weeks. Where whole litters were WT or $Ezh2^{fl/+};Kras^{G12D+/+};Fgd5CreERT2^{tg/+}$ the litters were culled and not included in further analysis. Optimisation over time to improve maternal acceptance of foster pups included:

- Rapid delivery and resuscitation with two experienced operators (one for delivery, one focussed on resuscitation)

- Prolonged resuscitation and not placing in foster cage until pups pink and wriggling
- Removal of any remnants of products of conception, blood and umbilical cords
- Rubbing pups with foster maternal bedding and urine
- Removal of entire host litter and replacement with foster litter, placing neatly in cage, together
- Not opening cage until day 5pnd

On 2 occasions mice receiving YS induction of tamoxifen delivered in the night between E18.5 and E19.5. There were no ill effects and after discussion with the veterinary team, these mice were allowed to be kept. The pups were not fostered and left with the dams. None of these pups developed illness. All pups delivered by CS were followed up until >16 weeks, or until showing signs of ill health. Pups were culled prior to 19 weeks, as delineated in the Home Office licence.

2-5. Isolation and processing of tissues

i) Peripheral blood

PB was obtained either through tail vein bleeding for serial monitoring or cardiac puncture at terminal readouts into EDTA coated tubes. Where enough blood was obtained (>100μL) then blood counts were undiluted. Otherwise blood was diluted 4-5x with PBS. PB parameters were obtained using a Sysmex KX-21N analyser. At terminal readouts, or where required, 5μL blood was used to make a PB film.

Processing for analysis: Whole blood was incubated with equal volume 2% Dextran (Sigma: Cat# D4876) at 37^{o}C for 20-25minutes to red cell deplete. The supernatant was removed and placed in a clean Eppendorf tube, which was then washed with 1ml PBS+10%FCS and spun at 4^{o}C, 1000rcf for 4minutes. The supernatant was removed by suction pump and the pellet

resuspended in 200μL ammonium chloride (Stemcell: Cat# 07850) and incubated at 20^{o}C for 1.5minutes. This was then washed in 1ml PBS+10%FCS and spun at 4^{o}C, 1000rcf for 4minutes. The supernatant discarded and the pellet resuspended in the appropriate solution for the experiment.

ii) Bone marrow (BM)

Whole legs were dissected and musculature and ligaments removed and kept on ice in PBS+10% FCS. Single legs were crushed with 5ml PBS+10% FCS and the resulting single cell suspension filtered through a 70μm filter. An aliquot of 80μL was taken for a cell count on the Sysmex KX-21N analyser and the tube weighed for total cell count.

iii) Spleen

Spleens were dissected, kept on ice in PBS+10% FCS, and weighed; on occasion they were photographed. Whole spleens were then macerated through with PBS+10% FCS through a 70μm filter. An 80μL aliquot of the resultant single cell suspension was taken for a cell count on the Sysmex KX-21N analyser and the tube weighed for total cell count.

iv) Fetal liver (FL)

Uterine horns were dissected and kept on ice in PBS+10% FCS. Fetal livers were dissected under a light microscope and kept on ice in 1ml PBS+10% FCS. Whole FL were disrupted sequentially with syringe suction using a 25-26G needle then 27G needle. An 80μL aliquot of the resultant single cell suspension was taken for a cell count on the Sysmex KX-21N analyser.

v) Yolk sac (YS)

Uterine horns were dissected and kept on ice in PBS+10% FCS. Yolk sacs were dissected under a light microscope and kept on ice in 200μL PBS+10% FCS. The PBS was removed by pipette and the YS incubated for 20min at 37^{o}C in Dulbecco's Modified Eagle Medium (DMEM, Thermofisher: Cat# 31966021) + 10%FCS + 3mg/ml Collagenases IV (Worthington: Cat# LS004186) and 200units/ml DNase I (Sigma: Cat# 11284932001). The resultant YS was disrupted by pipette and washed with 1ml PBS+10% FCS before centrifugation at 4^{o}C, 300rcf for 6minutes. The supernatant was discarded and the pellet reconstituted in the appropriate medium for the required experiment. Cells were counted using a Neubauer haemocytometer and trypan blue (Thermofisher: Cat# 15250061).

vi) Genomic DNA

Earclips for mouse identification were kept at -20^{o}C until required. At dissection of embryos a sample was taken for genotyping (head at <12 days and portion of tail >12 days gestation) and kept on ice until DNA extracted. DNA was extracted as per chapter 2.1-vii. For deletion analysis in PB and BM, processed PB and BM (>2million cells) were spun and pelleted. The pellet was frozen at -20^{o}C before DNA extracted as per the embryonic material (see chapter 2.1-vii, Thermofischer: Cat# F170S).

vii) Cryopreservation and thawing of cells and tissues

Cryopreservation: Processed BM and spleen suspensions were spun at 4^{o}C, 500rcf for 5 mins and the resultant pellet reconstituted in Freezing media FCS+10%DMSO (Sigma: Cat# 472301), aiming for a cell concentration of ~10million/ml. Aliquots of 1ml were placed in cryovials and frozen using Nalgene (Sigma: Cat# C1562) or CoolCell technology (Corning: Cat# CLS432001) at -80^{o}C, then placed into liquid nitrogen tanks for long term storage.

Thawing: Required cryovials were removed from liquid nitrogen storage on dry ice and placed in a waterbath at 37 ^{o}C. Once thawed, cryovial tubes were washed and contents placed in 50ml Iscove's Modified Dulbecco's Medium (IMDM, Thermofisher: Cat# 21056023)+20%FCS+DNase and spun at 4^{o}C for 10 mins at 500rcf. The supernatant was discarded and pellet resuspended in the appropriate medium for the following experiment. Where required cells were counted using a Neubauer haemocytometer, as per the YS protocol.

2-6. Transplantation analyses

Throughout the transplantation experiments >7 week old female recipient C57Bl/6 mice, obtained from the same colony, were used as preference for husbandry reasons; however, where these were not available on occasion male mice were used (for FL and aBM cryopreserved Fgd5CreERT2 transplantation experiments: figure 3.36; NSG males used for some YS transplantations: chapter 4-5). Where used, no male mice had to be culled or separated for fighting and engraftment was comparable to other experiments where female mice were used.

Irradiated mice were weighed at baseline, earclipped for identification and water supplemented with Baytril Enrofloxacin 2.5% antibacterial solution at ~0.5mg/mouse/day for 14 days post-irradiation.

i) Transplantation of bulk BM or FL

Irradiation and competitor cells: On the day of transplantation age matched (7-14 week old, depending on experiment) C57Bl/6 CD45.1 mice were irradiated with 5gray on two occasions separated by 4 hours, for a total of 10gray. For one experiment (chapter 5-1) a single dose of

5gray irradiation was used. Mice were warmed to 40^{o}C in a heatbox for 15-20 minutes prior to transplantation. A single CD45.1 mouse for each experiment was culled prior to irradiation and a leg taken as a source of competitor BM cells. This was processed as per section 2-4.ii and kept on ice until required. When required, the required number of cells was removed and centrifuged at 4^{o}C, 500rcf for 5minutes, supernatant removed and the pellet resuspended in transplantation medium (PBS+1%FCS), at 200μL per dose.

Experimental cells: Thawed or fresh cells from C57Bl/6 CD45.2 BM or FL were made into a single cell suspension and cells counted (via Sysmex or haemocytometer). Required aliquots were spun at 4^{o}C, 500rcf for 5 mins and the supernatant removed. The pellet was resuspended with the required number of competitor cells in transplant medium at 200μL per dose. This transplantation mixture was filtered through a 50μL filter prior to transplantation to remove clumps of cells. It was then placed on ice until transplantation. A range (defined in figures) of 0.25-5x10^{6} experimental cells and 0.25-0.5x10^{6} competitor cells were used, depending on experimental considerations.

Transplantation: Warmed mice were removed, restrained, tails cleaned with 70% Ethanol, and cells injected via tail vein injection. Where this was not possible or mice were surplus, the mice were culled immediately. Where injection was possible, but difficult, a note was made and mice were monitored carefully for signs of ill health. Following transplantation mice were weighed and inspected daily for 14 days and thereafter inspected at least 4x per week for signs of ill health.

ii) Transplantation of specific cell populations

Irradiation and competitor cells: Female C57Bl/6 mice were irradiated and competitor cells were prepared as above. When making the competitor cell suspension for transplantation the transplant medium was IMDM+1%FCS (rather than PBS), due to the extended length of time the cells needed to spend on ice prior to transplant.

Cell preparation: Selected BM samples from leukaemic primary mice were selected and thawed as per section 2-4.vii and stained as per the flow cytometry protocol in section 2-6.i-ii. The resulting suspension was resuspended in IMDM+10%FCS+2mM EDTA (Sigma: Cat# 03690) to prevent clumping in addition to filtering through 50μm mesh filters prior to FACS sorting. Requisite cell populations (see chapter 4-3 for numbers) were FACS sorted into 50μL IMDM and then the requisite number filtered competitor cells added in IMDM transplant media. The transplantation and follow-up of mice was as 2-5.i.

iii) Transplantation of YS

Irradiation: NSG CD45.1 mice were given a single irradiation at 1.5gray, clipped for identification and weighed at baseline. No competitor cells were used for these experiments. Mice were warmed prior to transplant for 15minutes at 37 ^{o}C.

YS Preparation and transplantation: YS were dissected and disrupted as per 2-4.v. Pellets were resuspended in 200μL PBS+1%FCS and filtered through a 50μm filter, and left on ice. Embryos were selected for transplant according to genotype. Transplantation was then performed as soon as possible after disruption (minimum of 2 hours post-irradiation). Mice were transplanted and followed-up as per transplantation protocol, section 2-5-i.

2-7 Histology and morphological assessment

Peripheral blood films: 5μL whole blood was spread on a slide and air dried. Films were stained as soon as possible on a Bayer Hema-Tek with Wright-Giemsa stain. Slides were mounted with a coverslip using Pertex® mounting media (Pioneer: Cat# PRC/R/750), and analysed by light microscopy All differentials and percentage dysplasia were assessed using 200 manual cell counts.

Cytospins: Slides were prepared by moistening filter paper with 80μL PBS for 2minutes at 350rpm (Thermoscientific cytospin centrifuge 4). Aliquots of 1-10x10^4 cells were placed in 80μL PBS and transferred to the cytofunnels on the centrifuge. Slides were centrifuged for 10minutes at 350rpm, then stained and mounted as per PB films.

Histology (BM, spleen, lung): Whole tissues were submerged in 4% paraformaldehyde (EMS: Cat# 15710) and kept at 4^{o}C. Tissues then underwent decalcification with EDTA for BM, embedding in paraffin wax, sectioned and stained with Haematoxylin and Eosin by the Histology Facility at the Kennedy Centre, University of Oxford. Slides were then assessed by light microscopy.

2-8 Flow cytometric analysis and fluorescent assisted cell sorting (FACS)

i) Flow cytometric analysis

Staining: For PB and YS the entirety remaining after counting was used; for FL, BM and spleen, aliquots of ~2-5x10^6cells were selected for lineage panels. For HSC and Bryder panels ~ 5-10x10^6cells were used where possible, although for E12.5 FL and below ~0.5-1x10^6cells were used. Erythroid panels used between 100 and 500,000 cells. Cell pellets were resuspended in 25μL PBS+10%FCS+FcBlock (Lab manufactured, use at 1:200 dilution). Cells were

incubated for >10minutes at 4°C. Then, 25μL of the appropriate antibody cocktail (table 2.1) was added (in PBS+10%FCS: total staining volume 50μL), and the cells were mixed and incubated for 20minutes at 4°C. Cells were washed in 1ml PBS+10%FCS and centrifuged at 4°C, 500rcf for 5minutes. The supernatant was removed, and if a second stain (streptavidin conjugated antibody) was used, this was added at this point (50μL of second stain was added) and the cells were mixed and incubated for 20minutes at 4°C. Cells were washed in 1ml PBS+10%FCS and centrifuged at 4°C, 500rcf for 5minutes. Once staining was complete cells were resuspended in 200μL of FBC+10%FCS, YS and FL samples were filtered through a 50μm filter, and kept in the dark at 4°C until analysis.

Acquisition: Acquisition was almost exclusively on a BD LSR Fortessa X50 flow cytometer, however on occasion when this was not available a BD LSR Fortessa, X20-2 or LSRII was used. FACSDiva software was used for acquisition. Each panel was set using beads (BD: Cat# 552843, 552844) stained with single stains, except where cell fluorescent markers were used in which case unstained fluorescent cells were used. Each panel had fluorescence minus one (FMO) compensation controls (see Example panel in appendix 5.2) to aid in compensation between fluorochromes.

Table 2.1: Antibodies used for flow cytometry

Antigen	Conjugate	Clone	Company	Cat#
7AAD	Pe-Cy5	(viability)	Sigma	A9400
CD93	PE	AA4.1	BD	558039
CD93	APC	AA4.1	BioL	136510
B220	PE-TxR	RA3-6B2	BD	551489
B220*	Pe-Cy5	RA3-6B2	BioL	103210
CD105	Bi	MJ7/18	BioL	120404
CD11c	FITC	N418	BioL	117316

CD150	Pe-Cy7	TC15-12F12.2	BioL	115914
CD16/32 (FcGR)	APC	93	eBio	17-0161-82
CD16/32 (FcGR)	PE	93	eBio	12-0161-81
CD19	Pe-Cy7	ID3	eBIo	15-0193-83
CD25	PE	3C7	BD	553075
CD31	APC	390	eBIo	17-0311-82
CD34	AF700	RAM34	eBio	56-0341-82
CD3e	APC	145-2C11	eBio	17-0031-83
CD3e*	Pe-Cy5	145-2C11	BioL	100310
CD4	APC-ef780	RM4-5	eBio	17-0042-83
CD41	Pe-Cy7	MWReg30	eBio	25-0411-82
CD41	BV605	MWReg30	BD	563317
CD44	FITC	IM7	BioL	103006
CD45.1	BV650	A20	BioL	110736
CD45.1	PE	A20	eBio	12-0453-81
CD45.2	AF700	104	BioL	109822
CD48	APC	HM48-1	BioL	103412
CD48	BV510	HM48-1	BioL	563536
CD71	FITC	R17217	BioL	113805
CD71	Bi	R17217	eBio	13-0711-82
CD8a	APC-ef780	53-6.7	eBio	47-0081-82
cKit	APC-ef780	2B8	eBio	47-1171-82
cKit	PE	2B8	eBio	12-1171-81
DAPI	PB	(viablity)	Invitrogen	D3571
f4/80*	Pe-Cy5	BM8	BioL	123112
Flt3	PE	A2F10	eBio	12-1351-83
Gr-1	PO	RB6-8C5	Caltag	RM3030
Gr-1*	Pe-Cy5	RB6-8C5	BioL	108410
IL7r*	Pe-Cy5	A7R34	eBio	15-1271-81
Mac-1	APC	M1/70	BioL	101212
Mac-1*	Pe-Cy5	M1/70	BioL	101210
NK1-1	PB	PK136	BioL	108740
Sca-1	PB	D7	BioL	108120
Sca-1	BV786	D7	BD	563991
Streptavidin	PE-TxR		BD	551487
Ter119	FITC	TER-119	eBio	11-5921-85
Ter119	BV650	TER-119	BioL	116232
Ter119	Pe-Cy5	TER-119	BioL	116210

*used in lineage cocktail

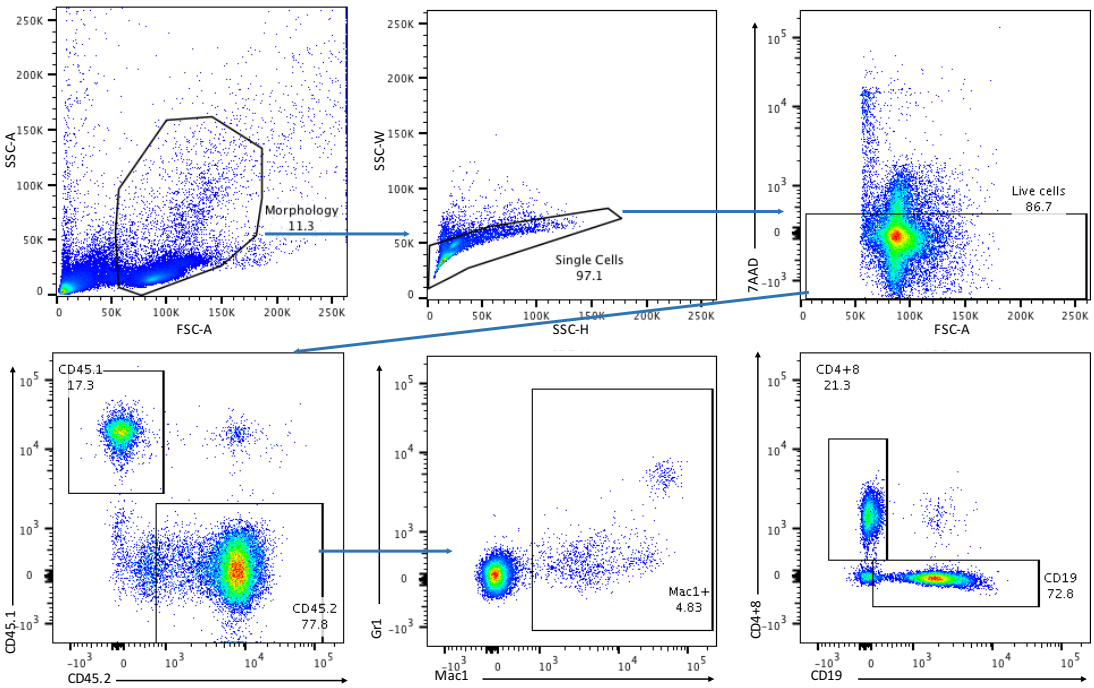


Figure 2.2: Example gating strategy for lineage panel, showing gating from PB from adult transplanted mouse (from transplant experiments – including CD45.1 and CD45.2 gating)

Analysis: Analysis and compensation was on FloJo v10 software and statistical analysis on GraphPad Prism v7.00 (licenced through WIMM). Example gating strategies are shown in figures 2.2 and 2.3.

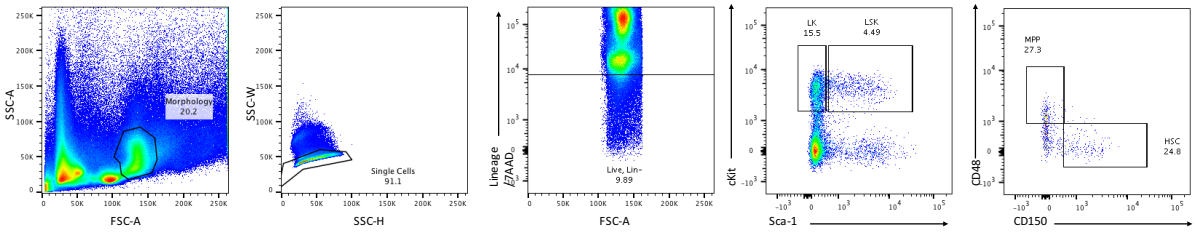


Figure 2.3: Example gating strategy for HSC panel showing gating on fresh adult BM

ii) FACS

For fluorescence activated cell sorting (FACS) cells were stained as per the protocol in 2-7.i, except resuspended in sorting buffer of PBS+10%FCS+2mM EDTA and all filtered through a 50µm filter prior to analysis. Acquisition was on a BD FACSAria II or III, or BD Fusion machine. Machines were set up and sorting assisted by a member of the WIMM FACS Facility.

Cells were sorted into single well plates or Eppendorfs supplemented according to the relevant protocol (see chapter 2-8 and 2-9). Example sort gating for HSCs can be seen in figure 4.22.

2-9 *In-vitro* assays

i) Methocult assays to isolate colonies for DNA analysis

In order to extract DNA to assess recombination of floxed genes in single cell derived colonies 1000 fresh E15.5 FL LSKs were FACS sorted as per 2-8.ii into 1000ml IMDM+2%FCS in a sterile Eppendorf tube. These were mixed and 250µl (~250 LSKs) plated into 2.5ml of Methocult GF M3434 culture medium (Stemcell: Cat# 03434), supplemented with 25µl 1% Penicillin/Streptomycin (Pen/Strep) at final concentration 100units/ml (Sigma: Cat# 11074440001). These were vortexed for 2minutes before 1ml plated into 2.5cm culture plates and cultured at 37^{o}C in 5% CO_2 for 7 days. On day 8, 96 single-cell derived colonies per replicate were plucked and placed in 10µl H_2O before being flash frozen at -20^{o}C [Sabnis, 2009]. After 24 hours the plates were thawed, vortexed, and 2µl used in $Kras^{LSL\text{-}G12D}$ and $Ezh2^{fl/fl}$ deletion PCRs (appendix 2.4 and 5.1).

ii) Re-plating assays

To assess the serial replating potential of fetal and adult cells, frozen BM cells from primary mice were thawed according to 2-4.vii and prepared for FACS as per 2-8.ii. 400 LSK BM cells from fetal and adult WT or $Kras^{G12D\ tg/+}$ mice were sorted per replicate into 400µl IMDM+1%FCS. This was added to 4ml of MethoCult GF M3434 culture medium, supplemented with 40µl Penicillin/Streptomycin, vortexed and 1ml plated into 2.5cm culture plates (4 plates per replicate with ~100LSKs per plate). They were cultured at 37^{o}C in 5% CO_2 for 7 days.

At Day 7, 60 wells of 96 well flat-bottomed culture plates were prepared with 100microL/well of MethoCult GF3434 (supplemented with 1% pen/strep) solution. The external wells were filled with water for humidity. Single cell colonies were plucked and dissociated with 10µl PBS and mixed by pipetting into individual MethoCult wells, then cultured at 37^{o}C in 5% CO_2 for 7 days. Every 7 days until the 6th replating wells with growth were counted and each well with growth (derived from a single LSK colony) removed, dissociated and washed in PBS, spun at 500rcf for 5mins at 4 ^{o}C before being resuspended in 10µl and replated into 100µl /well of MethoCult solution (prepared as above). Initially 4 replicates were genotype were used in 2 separate experiments, however during replating 2 plates had apparent bacterial contamination affecting 1 each from fetal and adult WT and Kras mutant replicates. These cells were counted but not replated.

iii) GM-CSF hypersensitivity assays

To assess the different GM-CSF sensitivity of fetal and adult cells, frozen BM cells from primary mice were thawed according to 2-4.vii and prepared for FACS as per 2-8.ii. 500 LSK BM cells from fetal and adult WT or Kras$^{G12D\ tg/+}$ mice were sorted per replicate into 500µl IMDM+1%FCS. Five 1ml aliquots of MethoCult M3134 (plain, to avoid any stimulation by other cytokines such as IL-3). Each 40ml M3134 was supplemented with 40ml IMDM and 20ml BIT 9500 (Stemcell: Cat# 09500), in addition to 1% pen/strep. Each 1ml replicate was supplemented with decreasing concentrations of GM-CSF (1ng/ml, 0.1ng/ml. 0.01ng/ml, 0.001ng/ml, No GM-CSF). 100µl of LSK suspension was added to 1ml M3134 (~100LSK cells), vortexed then plated into 2.5cm culture plates. Cells were cultured at 37^{o}C in 5% CO_2 for 7 days, and colony growth assessed at days 3, 5 and 7. Growth was very poor overall so colonies were defined as a cluster of >5 cells.

2-10 Molecular assays

i) qPCR of Ezh2 in FL

Sorting and pre-amplification: Cryopreserved E15.5 from $Ezh2^{fl/fl;}$ $dtomato^{fl/fl}$;$Mx1Cre^{tg/+}$ were thawed according to 2-4.vii and prepared for FACS as per 2-8.ii. 100 FL LSK, either dTomato+ve or -ve were sorted into 10µl pre-amplification PCR mixture, prepared immediately prior to sort and kept at 4°C (appendix 5.3). Sorting lasted ~1.5 hours and immediately after sort, PCR plate run on cDNA preamplification protocol for 16 cycles (appendix 5.3), followed by freezing at -20°C. Controls for complete deletion (known Ezh2-KO), no deletion ($Ezh2^{fl/fl}$;$Mx1Cre^{+/+}$), template negative (no sorted cells) and RT negative control (no polymerase enzyme) (appendix 5.3).

RT-PCR: The pre-amplified cDNA was thawed and mastermixes made for each probe (Gapdh/Actin/Ezh2:1/Ezh2:2, appendix 5.3). Each 20µl reaction contained 4µl cDNA, 5µl RNAse free water, 1µl of probes for relevant assay and 10µl Taqman fast reagent (Thermofisher: Cat# 4444557). RT-PCR run for total of 40 cycles and then total Ezh2 proportion calculated by proportion of Ezh2 probes to housekeeping genes ($2^{-\Delta CT}$) followed by ratio of *Ezh2 probe2 (*only Ezh2 WT only) *to Ezh2 probe1 (*Ezh2 WT and deleted). As mRNA is still produced by floxed SET domain deletion, two probes are required to assess proportion of SET domain Ezh2 mRNA: No SET domain Ezh2 protein.

ii) RNAseq of murine haematopoietic stem and progenitor cells

This was not performed due to COVID-19 restrictions, but I hope to perform this in the future. 50 (HSCs) and 100 (LSKs) will be sorted into prepared lysis buffer from thawed BM from primary mice: both adult and fetal cohorts, all genotypes, 5 replicates where possible -- and prepared for FACS as per 2-8.ii, then flash frozen on dry ice then -80°C. The lysis buffer with

cells will be thawed, heat inactivated and RT-PCR performed. Libraries will then be prepared and sequenced by Illumina™ technology. For these experiments, experienced members of the Mead/Roberts laboratories will help with the RNA preparation.

iii) Isoelectric focussing of haemoglobins

Fresh unprocessed PB in EDTA from fetal or adult induced mice, with controls of fetal mice (E10.5) or WT adult mice, was frozen at -20 ^{o}C. Chris Fisher (Higgs/Gibbons laboratories, WIMM) kindly processed and performed the isoelectric focussing, stained with horseradish peroxidase, and processed the images.

2-11 Statistics

Data shown in bar charts is expressed as mean +/- standard error of mean (SEM), unless otherwise stated. Statistical significance was defined by Mann-Whitney U tests or ANOVA to compare experimental groups, as indicated in the relevant figures. Survival analysis was performed with Mantel-Cox log-rank test. All statistical analysis was performed using GraphPad Prism v7.00.

References

Booth CAG, Barkas N, Neo WH, et al. Ezh2 and Runx1 Mutations Collaborate to Initiate Lympho-Myeloid Leukemia in Early Thymic Progenitors. *Cancer Cell*. 2018;33(2):274-291.e8.

Braun BS, Tuveson DA, Kong N, et al. Somatic activation of oncogenic Kras in hematopoietic cells initiates a rapidly fatal myeloproliferative disorder. *Proc Natl Acad Sci U S A*. 2004;101(2):597-602.

de Boer J, Williams A, Skavdis G, Harker N, Coles M, Tolaini M, Norton T, Williams K, Roderick K, Potocnik AJ, Kioussis D. Transgenic mice with hematopoietic and lymphoid specific expression of Cre. *Eur J Immunol*. 2003 Feb;33(2):314-25.

Di Genua C, Norfo R, Rodriguez-Meira A, et al. Cell-intrinsic depletion of Aml1-ETO-expressing pre-leukemic hematopoietic stem cells by K-Ras activating mutation. *Haematologica*. 2019;104(11):2215-2224.

Gazit R, Mandal PK, Ebina W, Ben-Zvi A, Nombela-Arrieta C, Silberstein LE, Rossi DJ. Fgd5 identifies hematopoietic stem cells in the murine bone marrow. *J Exp Med*. 2014 Jun 30;211(7):1315-31.

Johnson L, Mercer K, Greenbaum D, et al. Somatic activation of the K-ras oncogene causes early onset lung cancer in mice. *Nature*. 2001;410(6832):1111-1116.

Kisanuki YY, Hammer RE, Miyazaki J, Williams SC, Richardson JA, Yanagisawa M. Tie2-Cre transgenic mice: a new model for endothelial cell-lineage analysis in vivo. *Dev Biol*. 2001 Feb 15;230(2):230-42.

Kühn R, Schwenk F, Aguet M, Rajewsky K. Inducible gene targeting in mice. *Science*. 1995 Sep 8;269(5229):1427-9.

Madisen L, Zwingman TA, Sunkin SM, Oh SW, Zariwala HA, Gu H, Ng LL, Palmiter RD, Hawrylycz MJ, Jones AR, Lein ES, Zeng H. A robust and high-throughput Cre reporting and characterization system for the whole mouse brain. *Nat Neurosci*. 2010 Jan;13(1):133-40.

McGrath KE, Frame JM, Fegan KH, et al. Distinct Sources of Hematopoietic Progenitors Emerge before HSCs and Provide Functional Blood Cells in the Mammalian Embryo. *Cell Rep*. 2015;11(12):1892-1904.

Neo WH, Booth CAG, Azzoni E, et al. Cell-extrinsic hematopoietic impact of Ezh2 inactivation in fetal liver endothelial cells. *Blood*. 2018;131(20):2223-2234.

Palis J, Robertson S, Kennedy M, Wall C, Keller G. Development of erythroid and myeloid progenitors in the yolk sac and embryo proper of the mouse. *Development*. 1999 Nov;126(22):5073-84.

Sabnis AJ, Cheung LS, Dail M, et al. Oncogenic Kras initiates leukemia in hematopoietic stem cells. *PLoS Biol*. 2009;7(3):e59.

Su IH, Basavaraj A, Krutchinsky AN, et al. Ezh2 controls B cell development through histone H3 methylation and Igh rearrangement. *Nat Immunol*. 2003;4(2):124-131.

Ye R, Wang QA, Tao C, Vishvanath L, Shao M, McDonald JG, Gupta RK, Scherer PE. Impact of tamoxifen on adipocyte lineage tracing: Inducer of adipogenesis and prolonged nuclear translocation of Cre recombinase. *Mol Metab*. 2015 Aug 29;4(11):771-8.

Chapter 3: The development of a mouse model to investigate the fetal origins of leukaemia

Mouse models of JMML currently utilise either activating mutations induced in young adult life [Braun, 2004], xenografts [Yoshimi, 2017][Louka, 2019][Caye, 2020], or widespread activation of mutations in fetal life [Tarnawsky*, 2017]. Fetal activation of $Kras^{G12D}$ in MPPs has been used to create a potentially useful model but as it develops a more neutrophilic disease and utilises constitutive activation, which makes it inappropriate for the comparison of fetal and adult origins of JMML, or the study of mutational gain in HSCs [Tarnawsky*, 2017]. Other currently available models are adult derived, and a number demonstrate an incredibly long latency (see Table 1.2, introduction). Of the current models available, a fetal derived, inducible model with a faithful phenotype does not exist.

A fetal-derived model is vital to study the biology of JMML. The differences between fetal and adult haematopoiesis are described in chapter 1, and it is well known that many fetal derived leukaemias, such as JMML, have driver mutations that can be traced to early life [Matsuda, 2010][Stieglitz, 2015]. The persistence into adult life of a fetal-like leukaemic HSPC, with a fetal molecular signature, suggests that only a model induced at the correct stage and site for leukaemia development in JMML can model the disease accurately. A model allowing comparison of fetal and adult induced leukaemic stem cells would permit the study of functional and molecular differences between these leukaemias, and could be used to develop fetal-specific therapies or biomarkers for JMML. Nevertheless, the development of such a model is fraught with both scientific and technical obstructions. A summary of methods used in this chapter, showing the advantages and disadvantages is shown in table 3.1.

Experimental approach	Section	Outcome	Pros	Cons
Vav-iCre transplantations	3.2	Some JMML-Like disease in K-V and EK-V Majority T-cell leukaemia	1. Haematopoietic Activation 2. Fetal origin of mutations 3. JMML-like disease in some mice	1. EEK-V cells do not engraft 2. Requires transplantation (primary mice fetal lethality) 3. Pan-activation (not reflective of clonal expansion)
Mx1Cre transplantations	3.3	Majority T-cell leukaemia *Ezh2* loss required for myelomonocytic disease	1. Models clonal growth 2. Fetal cell of origin 3. JMML-like disease	1. Unable to compare adult and fetal 2. Not definitively fetal derived mutagenesis
Mx1Cre primary mice	3.5	Skin lesions universal in neonatal mice Difference between neonatal and adult induction	1. Both adult and fetal mice develop JMML-like disease 2. Proof of principle of ontogenic effect on disease	1. Inability to study fetal mice 2. Activation may occur at any point in ontogeny
Fgd5CreERT2 Transplantations (E14.5)	3.6	No spontaneous activation T-cell leukaemia predominant	1. No 'leakiness' 2. Engraftment and leukaemia in all genotypes	1. Almost universally T-cell leukaemia 2. No difference despite Fetal/Adult induction or genotype
Fgd5CreERT2 Transplantations (E19.5)	3.6	More JMML-like disease	1. Proof of principle that expansion in-utero prior to transplantation permits JMML	1. Higher cell dose used than previous 2. No adult comparison
Fgd5CreERT2 Primary mice	3.6 (expanded in chapter 4)	JMML-like phenotype Ability to induce in FL and adult life with no spontaneous activation (full results in chapter 4)	1. Ability to compare adult and fetal induction 2. No spontaneous induction 3. Can use in YS (see chapter 4.5)	1. Difficult experimental procedures with fostering required 2. Tamoxifen to dams (and spontaneous abortions)

Table 3.1: Summary of optimisation experiments and methods used to identify the best method

I selected $Kras^{G12D}$ mutation as it is known that patients with Kras mutations often present early in childhood, and the mutations are generally acquired as somatic mutations, allowing study of mutational gain within a specific cell group rather than constitutionally [Caye, 2015][Stieglitz, 2015][Louka, 2019][Caye, 2020]. Other driver mutations could have been chosen, however the $Kras^{G12D}$ model is well described with Mx1Cre activation, with an aggressive and highly prevalent phenotype in young, 3-4 week old, mice [Braun, 2004]. Further, Kras mutations are associated with loss of chromosome 7 in up to 56% of patients [Stieglitz, 2015], and therefore

at least heterozygous loss of *EZH2*. Inactivation of both copies of *EZH2* has been described in patients [Caye, 2015][Stieglitz, 2015], and as EZH2 and polycomb group proteins are known to have a role in controlling developmental pathways [Xie, 2014][Herviou, 2016], loss of function of *EZH2* in JMML may therefore help control reactivation of fetal pathways. Therefore, to create a model to study my hypotheses, I initially used fetal HSPCs from $Kras^{G12D}$ transgenic mice either alone or with loss of one or both *Ezh2* genes.

I first used a haematopoietic pan-activating constitutive Cre, Vav-iCre, to assess the fetal haemopoietic phenotype and the potential for a fetal onset model. Vav-Cre conditionally induces floxed mutations from ~E9.5, which becomes fully penetrant from E12.5-13.5 [Gan, 2010][Neo, 2018]. Unfortunately, Vav-iCre with $Kras^{G12D}$ leads to a fetally lethal phenotype with an apparent erythoid block in differentiation [Tang, 2013] while *Ezh2*-KO with Vav-iCre also leads to fetal death, later at ~E19.5-20 [Neo, 2018]. However, by using this Vav-Cre based model I hoped to be able to study the effects of $Kras^{G12D}$ mutation in combination with *Ezh2*-KO on fetal HSPC phenotype and pilot a potential transplant-based model examining the combination of $Kras^{G12D}$ and $Ezh2^{fl/fl}$.

To achieve this, I crossed $Kras^{LSL\text{-}G12D}$, *Ezh2* and wild type (WT) mice to be able to study fetuses obtained from five different genotypes, shown in figure 3.1a. As Vav-iCre with $Kras^{G12D}$ conditional mutation is fetally lethal by E14.5-15.5 [Tang, 2013], embryos were obtained by timed matings to obtain E12.5 FL from each genotype. In keeping with the expected fetal lethality, no live pups were born from any of the $Kras^{G12D}$ or *Ezh2* knock out mice (figure 3.1b-c).

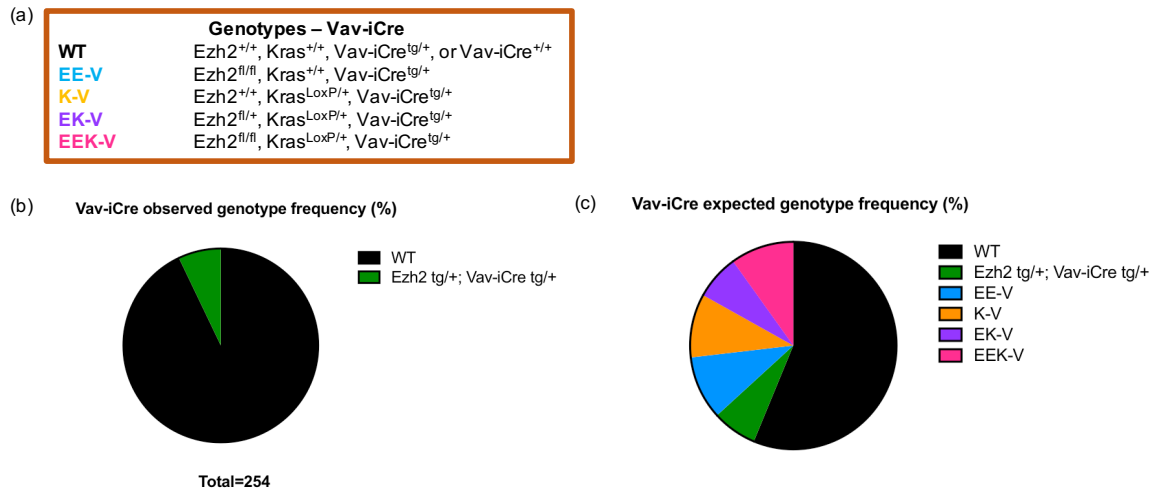


Fig 3.1: Vav-iCre genotypes at birth. (a) Overview of sought Vav-iCre genotypes and abbreviations used (b) observed frequencies, including *Ezh2* heterozygous mutation alone and (c) expected frequencies of genotyped pups. Genotypes colour matched throughout. Legend: WT ($Ezh2^{+/+}$, $Kras^{+/+}$, $Vav\text{-}iCre^{tg/+}$, or $Vav\text{-}iCre^{+/+}$), EE-V ($Ezh2^{fl/fl}$, $Kras^{+/+}$, $Vav\text{-}iCre^{tg/+}$), K-V ($Ezh2^{+/+}$, $Kras^{LoxP/+}$, $Vav\text{-}iCre^{tg/+}$), EK-V ($Ezh2^{fl/+}$, $Kras^{LoxP/+}$, $Vav\text{-}iCre^{tg/+}$), EEK-V ($Ezh2^{fl/fl}$, $Kras^{LoxP/+}$, $Vav\text{-}iCre^{tg/+}$).

3-1 The fetal phenotype associated with $Kras^{G12D}$ mutation and *Ezh2* knock out using Vav-iCre

i) Analysis of HSC and progenitor numbers in fetal liver (FL)

The cellularity of the FL at E12.5 showed a modest decrease in cellularity in both of the genotypes with mutant *Kras* and *Ezh2*-LOF (EK-V or EEK-V) compared to WT controls and an additional decrease in the EEK-V mice compared to the homozygous *Ezh2*-KO mice without a *Kras* mutation (EE-V) (figure 3.2a). Given the low cellularity overall of ~$3x10^6$, and the need to cryopreserve cells for future transplants, I designed a single panel incorporating the extended myeloid HSPC panel known as the Bryder panel [Pronk, 2007], and in addition encorporated extended markers to further analyse LSK, HSC and MPP. Initial attempts did not permit proper evaluation of Sca-1 expression, so after optimisation I developed a panel allowing me to use a single smaller aliquot of cells to study the cellular hierarchy in the FL in more detail (gating strategy figure 3.2b-c).

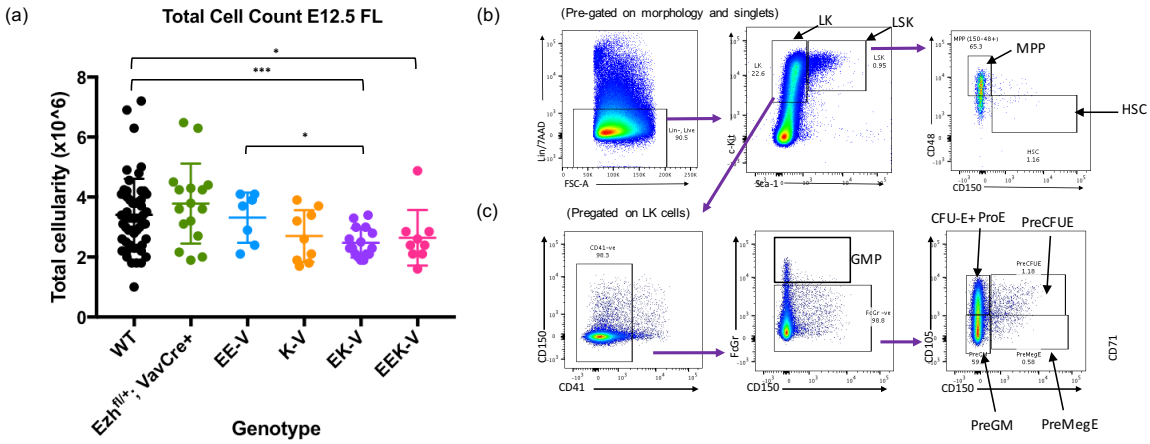


Fig 3.2: Fetal liver analysis of Vav-iCre embryos. (a) Total cell counts of E12.5 FL. Each point represents a biological replicate. Example gating strategy of FL modifed Bryder panel for (b) LSKs including HSCs and MPPs and (c) LK cells for Bryder panel. LK (Lin-, cKit+), LSK (Lin-, cKit+, Sca-1+), MPP (Multipotent progenitor; LSK, CD48+, CD150-), HSC (Haematopoeitic stem cell (LSK; CD150+, CD48-), GMP (Granulocyte monocyte progenitor; LK, CD41-, FcGr+), PreGM (LK, CD41-, CD150-, CD105-), PreCFUE (Pre-colony forming unit-Erythroid; LK, CD41-, CD150+, CD105+), PreMegE (Pre-Megakaryocyte erythroid progenitor; LK, CD41-, CD150+, CD105-), CFU-E (Colony forming unit-erythroid; LK, CD41-, CD150-, CD105+, Ter119-), ProE (ProErythroid progenitor; LK, CD41-, CD150-, CD105+, Ter119+). Statistical significance determined by Mann-Whitney U test. * p<0.05, *** p<0.001

In a series of fourteen experiments, timed matings were used to generate embryos at E12.5. Fetal livers were harvested from each embryo, and processed for both cryopreservation and fetal phenotyping, whilst germline tissue was taken for genotyping of each embryo. Macroscopic appearances were striking, with *Kras* mutant embryos (K-V) demonstrating pale livers with haemorrhagic foci (figure 3.3a). To assess earlier conditional deletion, I also used Tie2Cre -- which recombines from ~E7.5 -- however when assessing *Ezh2*$^{fl/fl}$ embryos these demonstrated marked pallor (data not shown) as previously described secondary to a failure of erythroid development between the YS and FL [Neo, 2018]. Further, no *Kras* mutant embryos were identified at E12.5 (figure 3.3b), suggestive of earlier fetal lethality than induction with Vav-iCre. Evaluation of Tie2Cre induction at the FL stage was therefore discontinued.

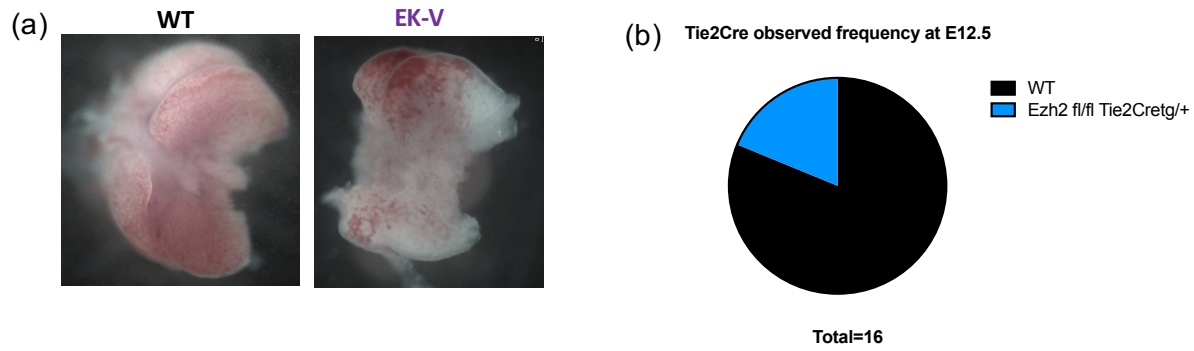


Fig 3.3: Fetal liver induction with Vav-iCre and Tie2Cre. a) Representative images of FL from WT (n=8) and *Kras* transgenic (n=2) embryos (b) Embryo frequency at E12.5 from WT and *Ezh2*$^{fl/fl}$, Tie2Cre$^{tg/+}$ pups (3 experiments)

On analysis of the disrupted FL there were significantly reduced LSK cells in the K-V and EK-V embryos, shown in figure 3.4a. EEK-V was not significant, however trended to a similar reduced number as the K-V and EK-V mice. To investigate this in more detail, I evaluated the numbers of HSC and MPP within the LSK compartment using the gating strategy and surface marker definition in figure 3.2b. Phenotypic HSCs were significantly reduced in number in K-V mice, but not decreased in EK-V or EEK-V mice (figure 3.4b). This is in keeping with the previously described poor transplantability and function of the *Kras*^{G12D} stem cells [Di Genua, 2019], but suggests that *Ezh2* loss may also affect the HSC compartment.

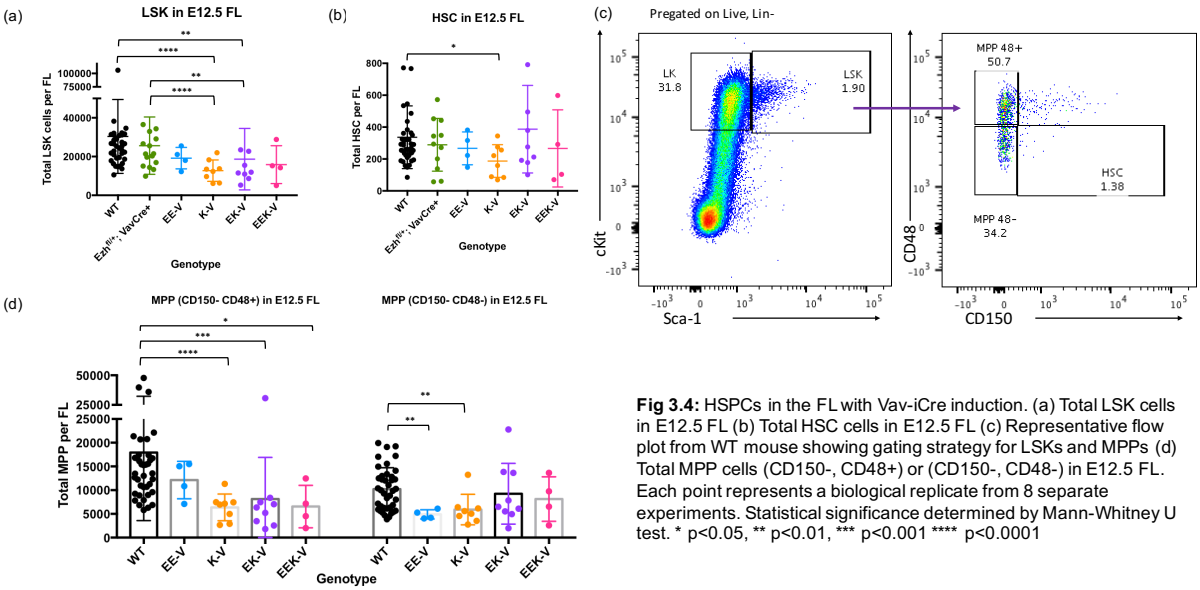


Fig 3.4: HSPCs in the FL with Vav-iCre induction. (a) Total LSK cells in E12.5 FL (b) Total HSC cells in E12.5 FL (c) Representative flow plot from WT mouse showing gating strategy for LSKs and MPPs (d) Total MPP cells (CD150-, CD48+) or (CD150-, CD48-) in E12.5 FL. Each point represents a biological replicate from 8 separate experiments. Statistical significance determined by Mann-Whitney U test. * p<0.05, ** p<0.01, *** p<0.001 **** p<0.0001

I also found a significantly reduced number of MPPs (figure 3.4c; LSKs, CD150-, CD48+) with all of the genotypes with mutant *Kras* with or without *Ezh2* loss, but with no alteration of phenotype with *Ezh2* loss alone. However, other cell populations within the LSK compartment were also reduced with mutant Kras alone, but not with EK-V or EEK-V genotypes (figure 3.4d). The reduction within all LSK compartments with $Kras^{G12D}$ mutation may represent the proliferative drive from this mutation. Particularly, however, the CD150-, CD48+ MPPs have previously been shown to have a myeloid bias [Pietras, 2015][Oguro, 2013], and thus it may be that these MPPs are most affected by the hyperactive Kras mutation.

Unexpectedly, *Ezh2*-KO alone appeared to also significantly reduce CD150-CD48- MPPs (see figure 3.4c), sometimes termed short term HSCs (ST-HSCs) (figure 3.4c-d). This may be because of the 'stem cell phenotype' of *Ezh2* loss, but my data cannot fully explain this decrease in phenotypic numbers. The effect of *Ezh2* on this HSPC compartment has not been previously published, but there is a discrepant decrease of CD150-, CD48+ve MPPs, on *Ezh2* loss between fetal and adult life, which these data may demonstrate further [Booth, 2018][Neo, 2018].

The 'Bryder panel' is well established in phenotypic analysis of murine adult BM as a method of subcharacterising myeloid and erythroid HSPCs [Pronk, 2007]. However, the application of this panel to the analysis of FL cells is untested. My data shows that these compartments can be seen in FL, but with vastly altered appearance (figure 3.5a), and the phenotypic-functional correlation is not established. Across compartments, many of the HSPC compartments show a moderate decrease in the experimental genotypes (see appendix 1.1).

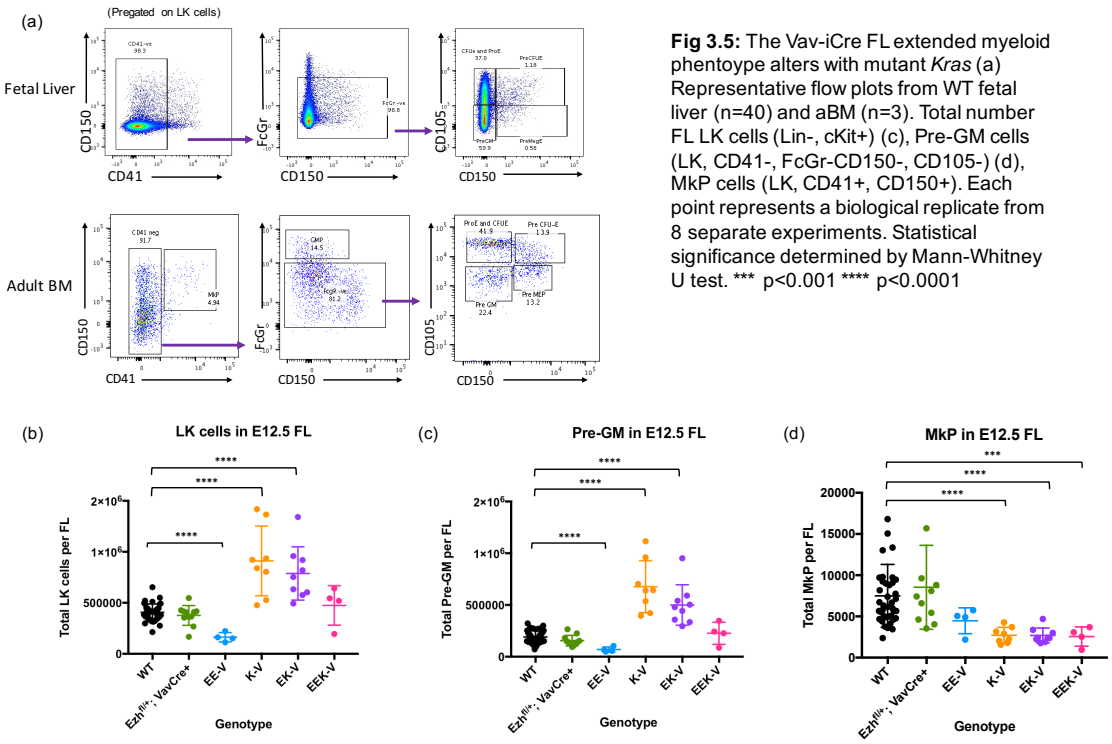


Fig 3.5: The Vav-iCre FL extended myeloid phentoype alters with mutant *Kras* (a) Representative flow plots from WT fetal liver (n=40) and aBM (n=3). Total number FL LK cells (Lin-, cKit+) (c), Pre-GM cells (LK, CD41-, FcGr-CD150-, CD105-) (d), MkP cells (LK, CD41+, CD150+). Each point represents a biological replicate from 8 separate experiments. Statistical significance determined by Mann-Whitney U test. *** p<0.001 **** p<0.0001

Overall, however the lineage negative, cKit +ve (LK) cells are markedly expanded in K-V and EK-V genotypes, mainly due to an expansion in the Pre-GM population (figure3.5b-c). There is also a significant reduction in megakaryocyte precursors (MkP) in all *Kras* mutant FL genotypes regardless of *Ezh2* status, as shown in figure 3.5d, which may explain the haemorrhagic phenotype on macroscopic examination.

Finally, I evaluated the impact of K-ras mutation and Ezh2 knockout on the FL erythroid compartment. Previously, $Kras^{G12D}$ mutation induced with Vav-iCre has been shown to be fetally lethal due to aberrant erythropoiesis [Tang, 2013], but the changes are only sparsely described in this paper. In my model I demonstrate an almost total block in erythroid differentiation, with a vast increase in CD71+Ter119- early erythroid precursors in Kras mutant embryos, and a decrease in CD71+Ter119+ve precursors (figure 3.6a-c).

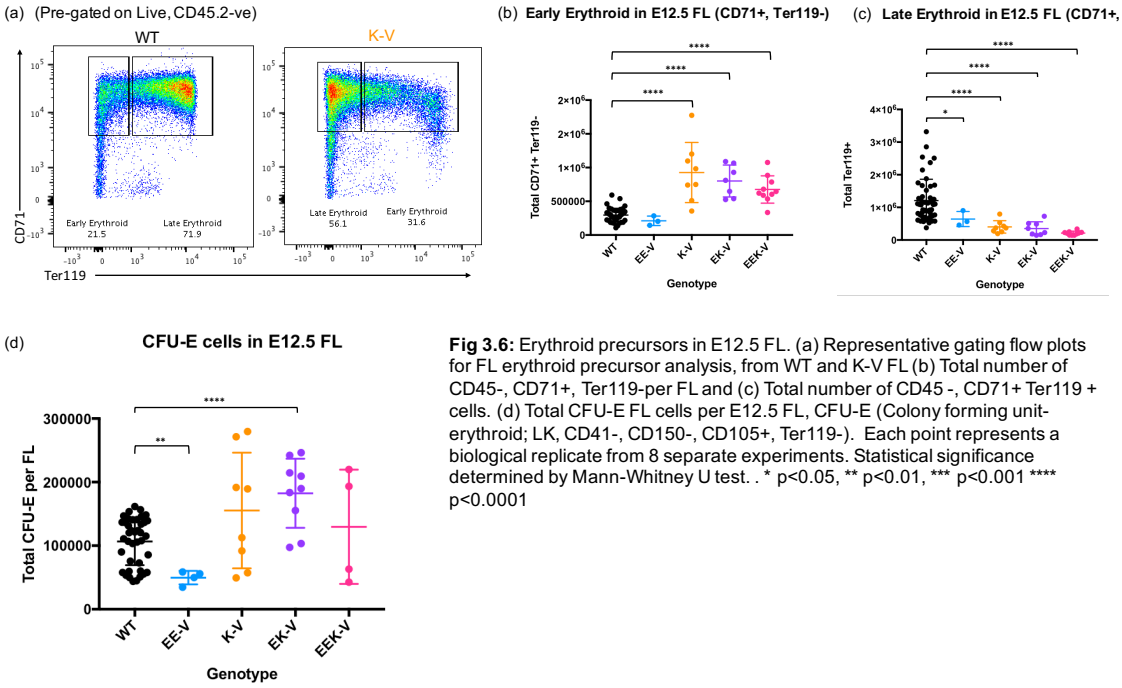


Fig 3.6: Erythroid precursors in E12.5 FL. (a) Representative gating flow plots for FL erythroid precursor analysis, from WT and K-V FL (b) Total number of CD45-, CD71+, Ter119-per FL and (c) Total number of CD45 -, CD71+ Ter119 + cells. (d) Total CFU-E FL cells per E12.5 FL, CFU-E (Colony forming unit-erythroid; LK, CD41-, CD150-, CD105+, Ter119-). Each point represents a biological replicate from 8 separate experiments. Statistical significance determined by Mann-Whitney U test. . * p<0.05, ** p<0.01, *** p<0.001 **** p<0.0001

This is in keeping with, but more marked than the findings from the 'Bryder' panel erythroid colony-forming units (CFU-E) (figure 3.6d). This erythroid block has been previously shown in the context of *Hras* oncogenes leading to a hyperactive RAS pathway, with potential mechanisms including EpoR independent growth of early erythroid precursors [Zhang, 2003]. In addition, *Kras* has previously been shown to be vital for erythroid differentiation in the E13.5 FL [Khalaf, 2005].

One of the most surprising and interesting findings was the large percentage of cells falling into the negative gate, within the Pre-GM population, even in the WT embryos -- but expanded in *Kras* mutant FL. This is different to the pattern in adult murine BM (figure 3.5a,c). Using the optimised FL panel, I assessed the composition of this compartment, and found them to be mainly CD71+ cells, likely erythroid precursors (figure 3.7). As this was apparent in WT embryos, this is likely to represent the physiological expansion of these cells during normal development and it is interesting that this expansion of early erythroid precursors was further

enhanced in *Kras* mutant mice, as described above in figure 3.6. Another interesting observation was seen in the FL from *Ezh2*$^{fl/+}$ embryos. These showed little change in the major HSPC compartments, but in Granulocyte-Monocyte precursors (GMPs) demonstrated a marginal increase, where *Ezh2*-KO did not (appendix 1.1). This discrepancy further suggests that there may be a differential role in FL for *Ezh2* and that this varies in different cell populations.

In order to show that these changes involve Kras^{G12D} alterations, I performed deletion PCR on DNA extracted from bulk FL cells. This demonstrated a deleted band, in keeping with the proportion from adult BM cells and the control positive cells, although not all experiments were tested (appendix 1.2).

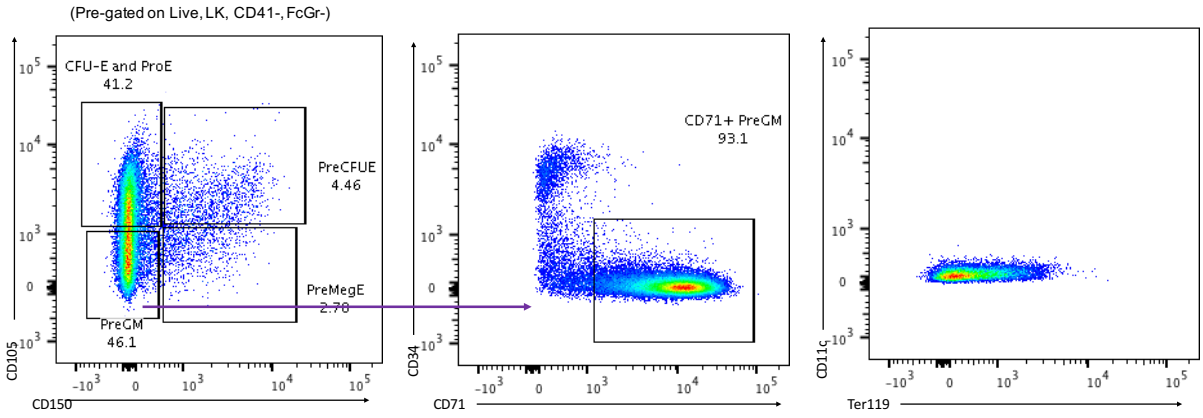


Fig 3.7: FL Pre-GM population analysis. Representative flow plots of WT FL (n=6) showing CD71 expression in Pre-GM population but not CD34, Ter119 or CD11c. Each fluorchrome from a single experiment. Showing CD71 positivity in Pre-GM population.

In summary, these data show a distinct effect of *Kras*^{G12D} mutation on the haematopoietic compartment within the FL. Some of the major changes, such as the erythroid expansion and differentiation block (figure 3.6) [Khalaf, 2005][Tang, 2013] have been previously described. The decrease in HSCs in *Kras*^{G12D} mice (figure 3.4) have been suggested by functional data, but phenotypic evaluation of the FL has not been published [Di Genua, 2019]. In addition to

this my data using this model reveal a clear interaction between mutant *Kras* and *Ezh2* loss, with potential rescue of the mild HSC decrease, but also suppression of the LK expansion (figure 3.4). The reasoning for this is not clear at present, but one hypothesis from other models may be that *Ezh2* loss allows quiescent genes to become expressed which *Kras* mutations alone suppress, at the expense of proliferation [Di Genua, 2019].

ii) Analysis of haematopoiesis in the murine yolk sac

Given that the main manifestation of JMML is the presence of abnormal monocytes and erythroid cells [Niemeyer, 2008][Niemeyer, 2014], I hypothesized that EMPs within the YS were a potential candidate cell for transformation in JMML due to their restricted lineage output [McGrath, 2015]. However other progenitors, including LMPP-like cells, also exist in the YS, leading to other potential targets [Boiers, 2013]. In order to investigate the effects of $Kras^{G12D}$ mutation alone, or in combination with *Ezh2*KO, in YS EMPs I used timed matings with either Tie2Cre or Vav-iCre activation. Embryos were assessed at both E9.5, prior to the emergence of HSCs at E10.5, utilising a validated flow cytometry immunophenotypic strategy for EMPs (lineage-Kit+Sca-1-CD41+FcGR (CD16/32)+) as shown in figure 3.8a [McGrath, 2015][Neo, 2018]. Although other strategies are available, I chose this approach as this was already used within our laboratory. Although I attempted to further refine this by using alternative markers such as CD93 [Gomez Perdiguero, 2015], the staining using the same antibody was ineffective in my hands (figure 3.8b). However, the additional markers did allow me to identify cell surface staining for several alternative EMP markers, including CD71 (transferrin), and CD31 (appendix 1.3), as well as to show the expression of CD105 (endoglin) on murine yolk sac EMPs for the first time (figure 3.8c).

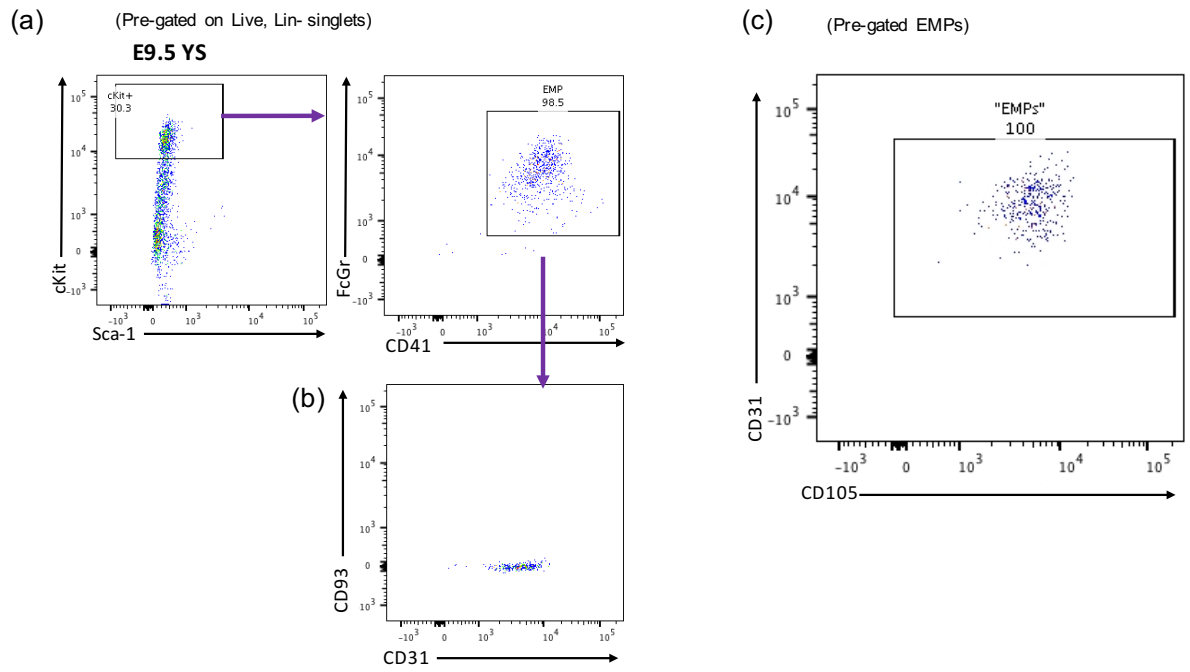


Fig 3.8: E9.5 EMP immunophenotype (a) Example gating strategy and (b) representative flow plot (n=18) from 3 separate experiments with CD93 demonstrating no EMP expression but CD31 positivity. (c) Representative flow plot from 2 separate experiements (n=11) demonstrating CD105 positivity by immunophenotyping in EMPs

Using Vav-iCre there were no significant differences between the cell counts of disrupted E9.5 YS between the 5 genotypes (figure 3.9a). However, there was a mild decrease in cKit+ve cells and total EMPs in K-V embryos (figure 3.9b-c). This difference was not present in EK-V or EEK-V embryos. This is in keeping with my FL data, suggesting a decrease in early HSPCs in K-V mice. As discussed above, published data suggests that *Kras*^{G12D} decreases functional stem cells, again in keeping with my data [Di Genua, 2019].

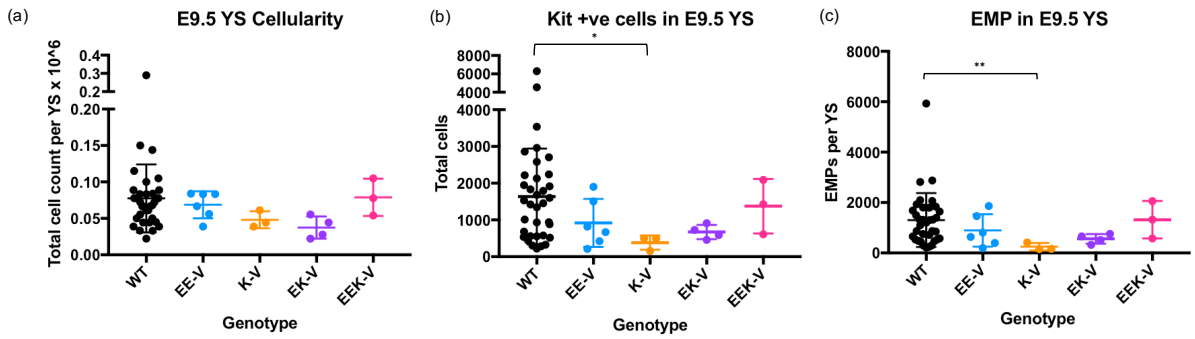


Fig 3.9: Yolk sac cell counts. (a) Total cell count of digested YS, counted by haemocytometer (b) Total number of Live, Lin-, cKit+ve cells per YS and (c) Total number EMPs per YS, Each point represents a biological replicate from 5 separate experiments. Statistical significance determined by Mann-Whitney U test. . * p<0.05, ** p<0.01

Brief analysis of earlier induction with Tie2Cre was uninformative and further experiments were abandoned after functional experiments showed no clear evidence that any of the genotypes caused leukaemia after transplantation (see Chapter 4.5).

3-2 Transplantation of FL activated using Vav-iCre

i) Optimising the transplant protocols

Braun *et al* show that $Kras^{LSL\text{-}G12D}$;$Mx1Cre^{tg/+}$ mice induced in young adult life did develop a myelomoncytic leukaemia [Braun, 2004], however on transplantation of either young adult or older adult BM, previous groups have demonstrated almost universal T-cell leukaemia [Sabnis, 2009][Zhang, 2009]. Only one group have published data from transplanted FL, however these developed more of a neutrophilic leukaemia, and used a constitutive Flt3Cre model without the ability to test whether HSCs can initiate disease [Tarnawsky*, 2017].

Prior to transplantation I optimised a transplant lineage panel to assess myeloid progenitors, B-cell and T-cell output, and natural killer cells, as well as immature markers such as B220, cKit, Ter119. The final gating strategy is shown in appendix 1.4.

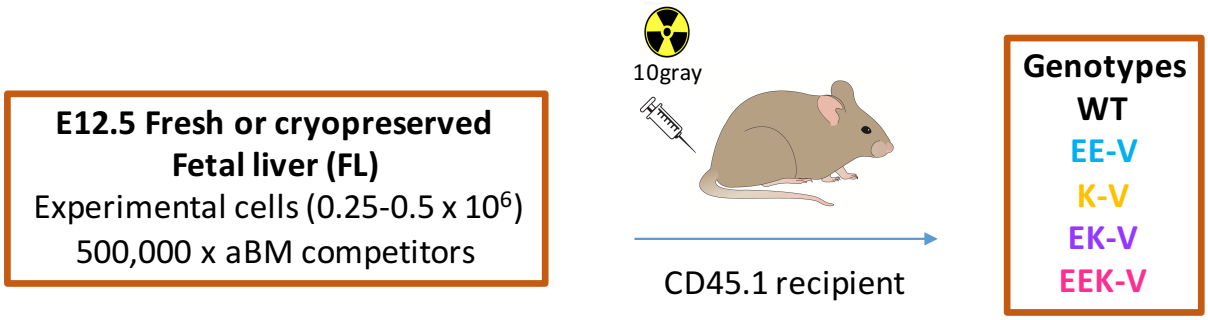


Fig 3.10: Overview of Vav-iCre FL transplantation experiments. CD45.2 E12.5 FL cells from each genotype transplanted into recipient, lethally irradiated, CD45.1 recipient mice. Mice were followed up for >16 weeks with peripheral blood monitoring (2-4 weekly) for PB count and engraftment.

Overall, my phenotypic data demonstrated a decrease in LSKs and HSCs in the FL, so to assess the leukaemia generating potential from the FL, and the ability of these *Kras* mutant cells to transmit disease I transplanted cryopreserved FL from the 5 different genotypes into recipient mice (figure 3.10). My hypothesis was that whole FL from one or more of the abnormal genotypes would cause leukaemia and, by utilising the pan-haematopoietic activation of Vav-iCre I would be able to FACS sort separate HSPCs to identify the cell of origin to study further.

Initially, I transplanted 250,000 cryopreserved CD45.2 E12.5 FL cells with 500,000 CD45.1 competitor cells into lethally irradiated mice. Overall, apart from in the WT mice, engraftment of CD45.2 cells was very poor and all the WT as well as the EE-V mice survived. By contrast, all of the K-V and EK-V mice and half of the EEK-V mice developed various forms of fatal leukaemias or leukaemia-like syndromes (see appendix 1.5 and (figure 3.11a-d), none of which closely resembled JMML.

(a)

	WT (n=3)	EE-V (n=3)	K-V (n=2)	EK-V (n=3)	EEK-V (n=4)
Survived	3	3			
T-cell leukaemia			2	1	
Probable infection					1
Failed to engraft					2
Found dead				2	1

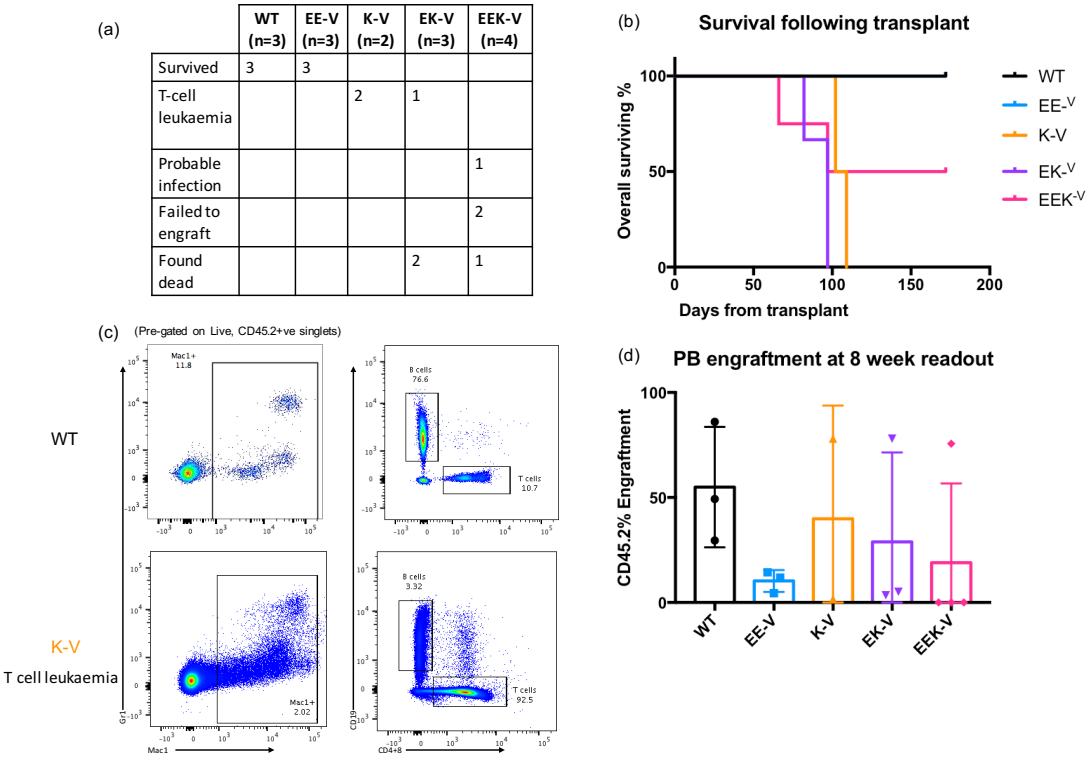


Fig 3.11: Outcome of E12.5 FL cryopreserved transplants (a) Table showing outcomes from Vav-iCre cryopreserved E12.5 FL. (b) Summary of the criteria used to determine haematopoietic disease (b) Survival of mice transplanted with 250,000 cryopreserved E12.5 FL cells in a single experiment (c) Representative PB flow cytometry plots at final readout of WT (n=3) and Kras-V (n=1) (d) PB CD45.2 percentage engraftment

Given the problems with cell recovery following cryopreservation, I repeated the experiment but instead transplanted 250,000 fresh E12.5 FL cells with 500,000 CD45.1 competitors, however there was overall very poor engraftment in EK-V and EEK-V mice (figure 3.12a) and only one mouse (K-V) developed leukaemia, again of T-cell immunophenotype (figure 3.12b-c).

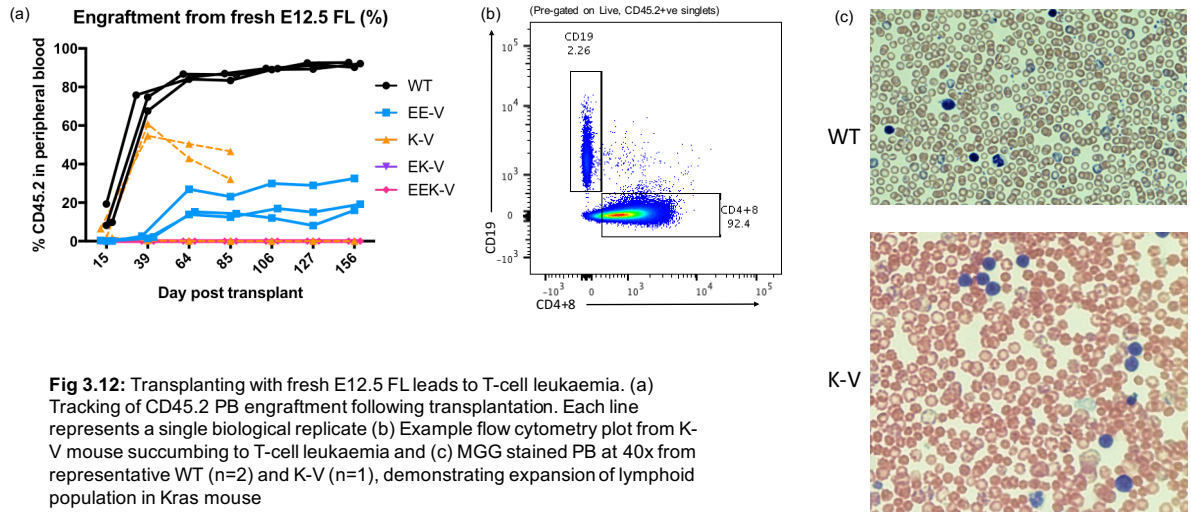


Fig 3.12: Transplanting with fresh E12.5 FL leads to T-cell leukaemia. (a) Tracking of CD45.2 PB engraftment following transplantation. Each line represents a single biological replicate (b) Example flow cytometry plot from K-V mouse succumbing to T-cell leukaemia and (c) MGG stained PB at 40x from representative WT (n=2) and K-V (n=1), demonstrating expansion of lymphoid population in Kras mouse

These results suggest that poor engraftment was not due to the effect of cryopreservation of the FL cells and most likely reflected the cell dose used for the transplants. As a pilot experiment, I next transplanted 500,000 frozen FL cells WT (n=3), EK-V (n=1) and EEK-V (n=3) mice, each with 500,000 CD45.1 competitors. Although none of the EEK-V mice engrafted or developed leukaemia, the single EK-V mouse transplanted developed a myelomonocytic leukaemia resembling JMML with thrombocytopenia and an enlarged spleen (figure 3.13a-c). This experiment demonstrated proof of principle that, although there was only a single successful replicate, transplanting Vav-iCre FL could create a model for JMML. I therefore went on to further investigate higher cell doses to determine whether this would induce a more reliable JMML model.

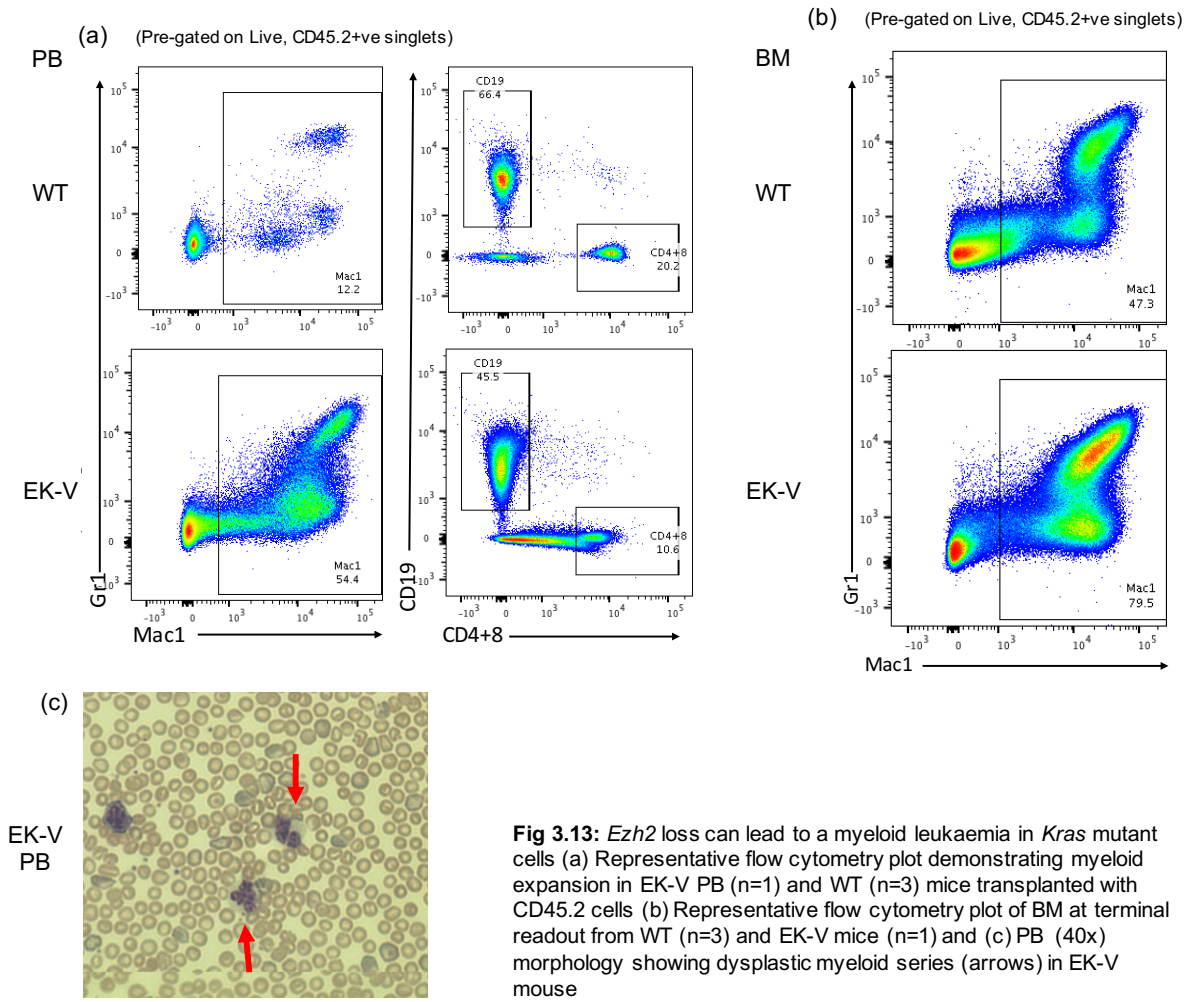


Fig 3.13: *Ezh2* loss can lead to a myeloid leukaemia in *Kras* mutant cells (a) Representative flow cytometry plot demonstrating myeloid expansion in EK-V PB (n=1) and WT (n=3) mice transplanted with CD45.2 cells (b) Representative flow cytometry plot of BM at terminal readout from WT (n=3) and EK-V mice (n=1) and (c) PB (40x) morphology showing dysplastic myeloid series (arrows) in EK-V mouse

ii) The effect of cell dosage

I next transplanted 1x10^6 CD45.2 FL cells from each genotype into CD45.1 recipients, based on a calculation from my FL phenotypic data that this should contain at least 100 HSCs. I used fresh FL to minimise cryopreservation-associated cell death and any potential functional defect (overview in figure 3.14a) in four replicate experiments. All experimental genotypes, with the exception of EEK-V, engrafted well with this approach (figure 3.17b-c). Mice transplanted with K-V or EK-V FL almost universally succumbed to disease, but with no significant difference between the two genotypes (figure 3.14b). Mice from both genotypes developed a myelomonocytic leukaemia, with a frequency of ~10-20% (figure 3.14c). This is in keeping with previous data, suggesting that induction prior to transplantation with Mx1Cre$^{tg/+}$;Kras^{LSL-}

$^{G12D/+}$ gave a myelomonocytic phenotype in ~8% of mice, whereas with induction after transplantation mice universally developed T-cell leukaemia [Sabnis, 2009][Zhang, 2009].

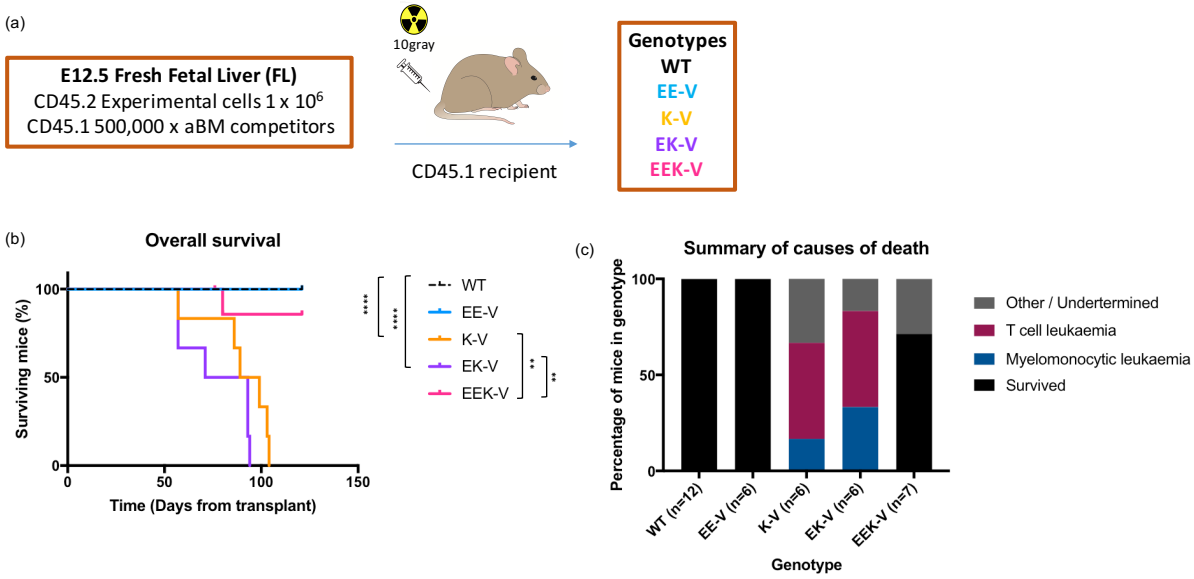


Fig 3.14: Vav-iCre FL transplants using a million experimental cells. **(a)** Overview of Vav-iCre transplantation experiments (n=4) (b) Survival curve of mice transplanted with Vav-iCre E12.5 FL and respective gentoypes (c) Summary of the outcome of mice transplanted with E12.5 FL. One mouse from EK-V was excluded due to non-engraftment following a failed injection of cells, and once mouse was censored from EEK-V as she developed a leg wound which required her to be culled early -- but on analysis of the PB and BM there were no clear suggestions of leukaemia. Statistical significance determined by Chi-squared test. ** p<0.01 **** p<0.0001

Mice succumbing to leukaemia were almost uniformly thrombocytopenic and anaemic (figure 3.15a) with splenomegaly (figure 3.15b). PB counts were similar in WT and EEK-V mice, further reinforcing the lack of disease and engraftment in these mice (figure 3.15a). Mice whose final diagnosis was T cell leukaemia had a significantly higher white cell count than those with a myelomonocytic leukaemia (figure 3.15c).

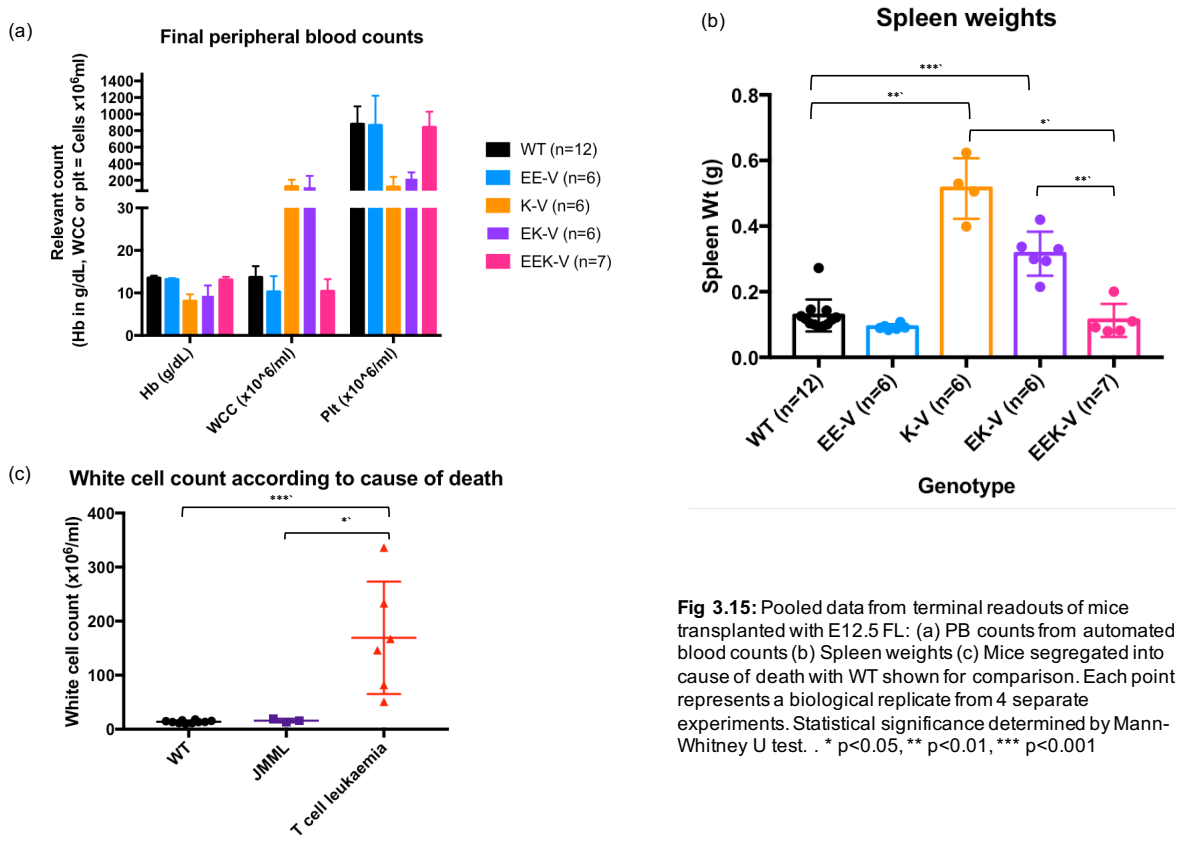


Fig 3.15: Pooled data from terminal readouts of mice transplanted with E12.5 FL: (a) PB counts from automated blood counts (b) Spleen weights (c) Mice segregated into cause of death with WT shown for comparison. Each point represents a biological replicate from 4 separate experiments. Statistical significance determined by Mann-Whitney U test. . * p<0.05, ** p<0.01, *** p<0.001

Immunophenotyping of PB and BM from the leukaemic mice suggested a clonal transplanted population (figure 3.16a-b) although I did not prove this at a molecular level, and PB films showed morphology in keeping with the immunophenotyping results (T-cell leukaemia or myelomonocytic leukaemia) (figure 3.16c-d). Mice found dead or with indeterminate phenotype but other evidence of leukaemia (splenomegaly or abnormal blood counts) were included in the survival analysis. Overall engraftment within the EEK-V group was poor as shown in all of the PB analyses (figure 3.17a) and at terminal PB and BM readout (3.17b) with almost universal failure of engraftment.

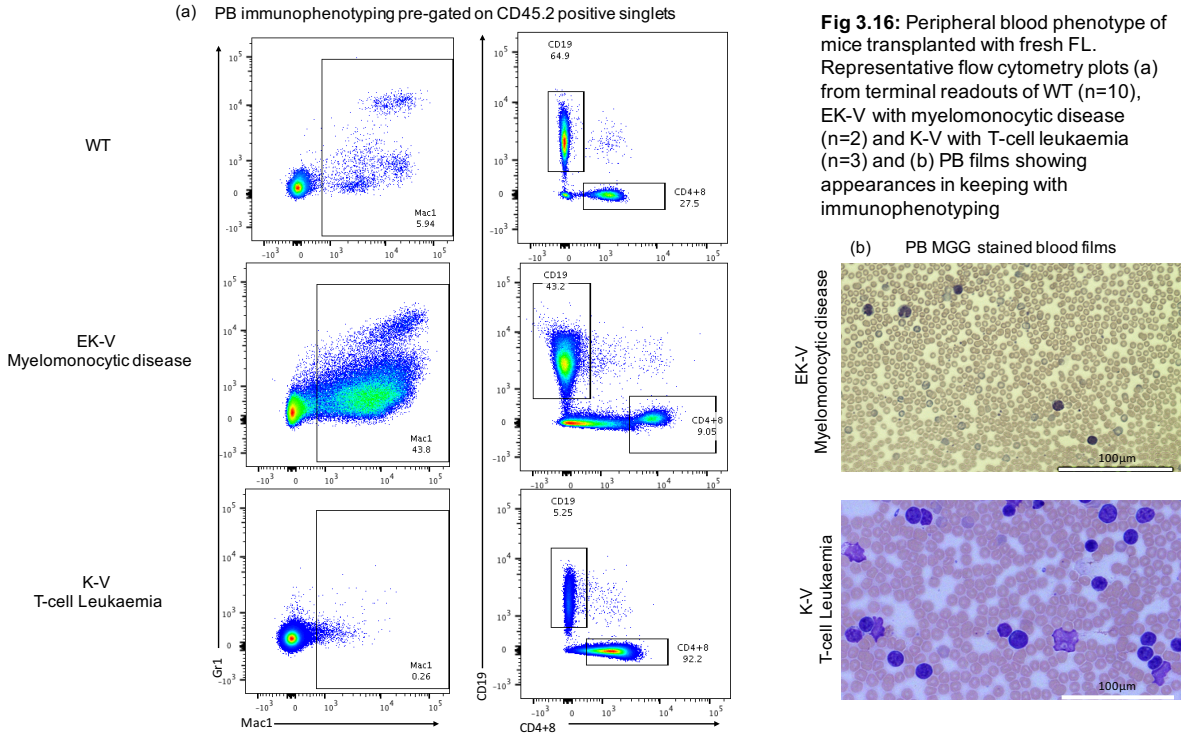


Fig 3.16: Peripheral blood phenotype of mice transplanted with fresh FL. Representative flow cytometry plots (a) from terminal readouts of WT (n=10), EK-V with myelomonocytic disease (n=2) and K-V with T-cell leukaemia (n=3) and (b) PB films showing appearances in keeping with immunophenotyping

The cause of this total failure of engraftment is not clear. Although EE-V mice have lower engraftment overall (figure 3.17a-b), this is expected as they have a B and T cell block [Su, 2003][Su, 2005], thus PB B and T cell engraftment is non-existent (figure 3.17c). Myeloid engraftment in these mice is unaffected (figure 3.17d) and at WT levels. Possible reasons for the overall poor engraftment of the EEK-V mice include an intrinsic defect in HSC function due to the double mutation or a homing defect, eg deficiency of CXCR4, a cell surface protein important in migration and HSC engraftment [Brenner, 2004][Zhang, 2009].

Overall, the data from these experiments show a clear combinatorial effect between *Kras*^{G12D} and *Ezh2*-KO, in that this combination, with Vav-iCre induction, appears to deplete fetal HSPC transplantability. However, using Vav-iCre to further study this would be difficult due to the functional problems with engraftment. Vav-iCre induction with the mutations is fetally lethal, so I would be unable to study my hypothesis that there is a difference between fetal and adult gain of oncogenic mutations and I therefore went on to explore alternative models. However,

this model served as proof of principle that a fetal Kras mutant HSPC can induce a JMML-like phenotype.

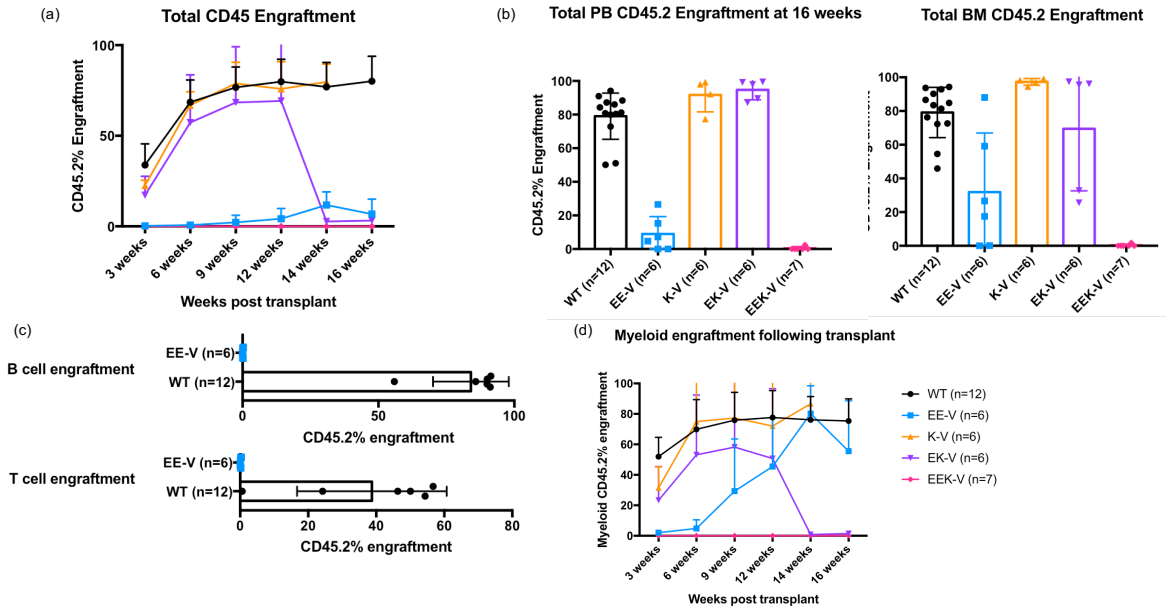


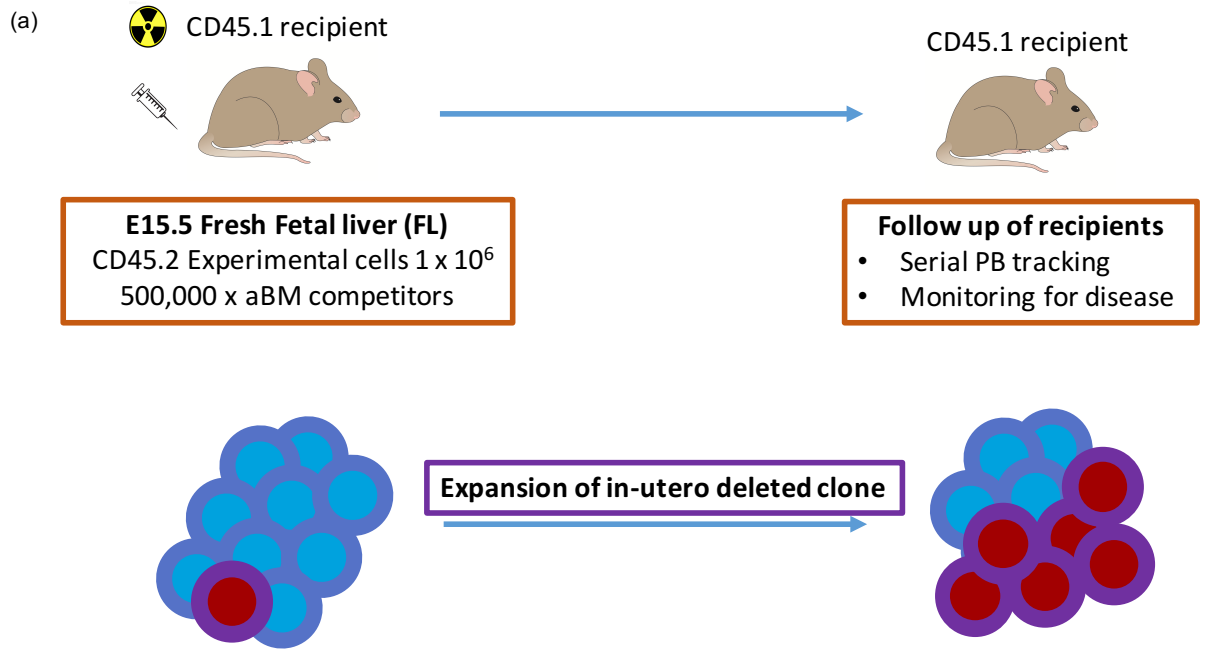
Fig 3.17: Total engraftment from Vav-iCre FL fresh experiments is reduced in *Ezh2*-KO mice (a) Total CD45.2 engraftment following transplant of Vav-iCre CD45.2+ E12.5 FL and (b) final PB and BM CD45.2 engraftment (c) Lymphoid engraftment of EE-V genotypes with WT comparators (d) Total tracking myeloid CD45.2 engraftment demonstrating no significant difference between WT and EE-V. One EEK-V mouse was found dead, with no clear cause, and another was found unwell so was terminated and analysed early. This mouse however showed no significant cytopenias and very poor PB and BM engraftment of CD45.2 cells, so was censored from analysis

3-3 Using Mx1Cre to activate mutations in a small number of FL cells

i) A transplantation based model of leukaemia derived from FL HSPCs

In order to develop a more faithful model of human disease I decided to move away from the pan-haematopoietic activation of Vav-iCre and devised a model to study FL-derived cells with mutation in a small percentage of cells. To do this I utilised Mx1Cre, which has been demonstrated to have spontaneous activation [Sabnis, 2009]. Mx1Cre is an interferon pathway Cre line and is traditionally induced with polyinosinic:polycytidylic acid (PolyI:C), which leads to conditional mutation through the interferon pathway [Booth, 2018][Di Genua, 2019]. With the aim of developing a model which would allow a better study of clonal expansion under the single leukaemic stem cell hypothesis [Jordan, 2007], I used a novel approach which involved transplanting $1x10^6$ FL cells, as in the Vav-iCre model, with 500,000 competitor cells,

but then not delivering PolyI:C and allowing clonal growth from the spontaneous activation of Mx1Cre (figure 3.18a). This is in contrast to previous studies using *Kras*^{G12D} which have only been able to study widespread activation using either constitutive or inducible Cre lines [Sabnis, 2009][Zhang, 2009][Tarnawsky*, 2017].



(b)

		Genotypes – Mx1Cre
WT	(n=13)	– Ezh2$^{+/+}$, Kras$^{+/+}$, dtomato$^{fl/+}$, *Mx1Cre$^{tg/+}$, or Mx1Cre+/+*
EE-M	(n=10)	– Ezh2$^{fl/fl}$, Kras$^{+/+}$, dtomato$^{fl/+}$, *Mx1Cre$^{tg/+}$*
K-M	(n=12)	– Ezh2$^{+/+}$, Kras$^{LoxP/+}$, dtomato$^{fl/+}$, *Mx1Cre$^{tg/+}$*
EK-M	(n=11)	– Ezh2$^{fl/+}$, Kras$^{LoxP/+}$, dtomato$^{fl/+}$, *Mx1Cre$^{tg/+}$*
EEK-M	(n=13)	– Ezh2$^{fl/fl}$, Kras$^{LoxP/+}$, dtomato$^{fl/+}$, *Mx1Cre$^{tg/+}$*

Fig 3.18: Overview of Mx1Cre transplantation experiments (a) Summary of transplantations and proposed model for clonal expansion (b) Summary of genotypes and number of transplanted mice per genotype

Using this model system, I transplanted, across six separate experiments, fresh E15.5 FL into replicate CD45.1 mice (figure 3.18b). In contrast to the Vav-iCre experiments all of the genotypes of mice, including the EEK-M mice, engrafted. Although this is not surprising given that the majority of the FL would not be recombined, lineage tracking with a reporter (dTomato, figure 3.19a) did show recombined cells across all genotypes. None of the control (WT or EE-

M) mice succumbed to disease, however using this model, mice from EEK-M did develop leukaemia over a 6 month follow-up period. Eleven out of 12 mice from the K-M genotype developed disease, universally T-cell leukaemia, and although the majority of mice from EK-M and EEK-M developed T-cell leukaemia, 2/10 mice and 2/13 mice respectively developed a myelomonocytic leukaemia (figure 3.19b).

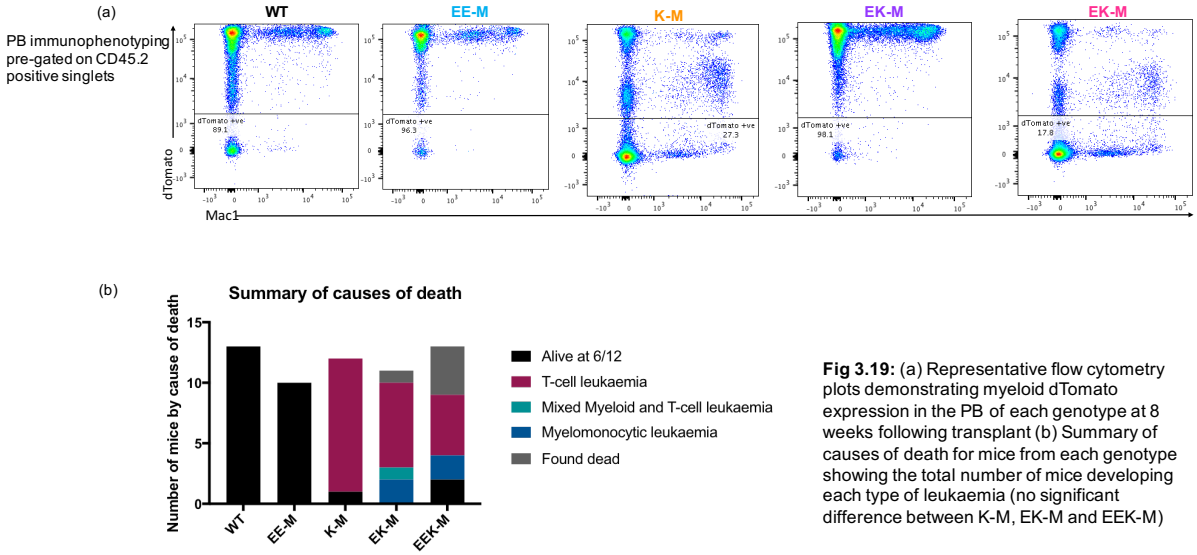


Fig 3.19: (a) Representative flow cytometry plots demonstrating myeloid dTomato expression in the PB of each genotype at 8 weeks following transplant (b) Summary of causes of death for mice from each genotype showing the total number of mice developing each type of leukaemia (no significant difference between K-M, EK-M and EEK-M)

The PB morphology and PB FACS phenotype of diseased mice is shown in figure 3.20a-b. This shows expansion of either a Mac1+Gr1- monocytic population, or a T-cell leukaemia population by flow cytometry and morphology. BM, where analysed, was similar to the PB (figure 3.20c). Interestingly, a single mouse from EK-M developed apparent mixed disease with both T-cells and monocytes in the PB and a large monocytic population in the BM (figure 3.21a-b). In addition, a number of mice had a population of CD45.2+ cells in either the PB or BM had expansion of a haematopoietic population which was negative for all the lineage markers tested (appendix 2.1). Subsequent analysis identified the cells as early T-cell leukaemias (appendix 2.1), with CD44 positivity but CD4+8 negative staining, and morphology of the PB or BM was consistent with this (appendix 2.2).

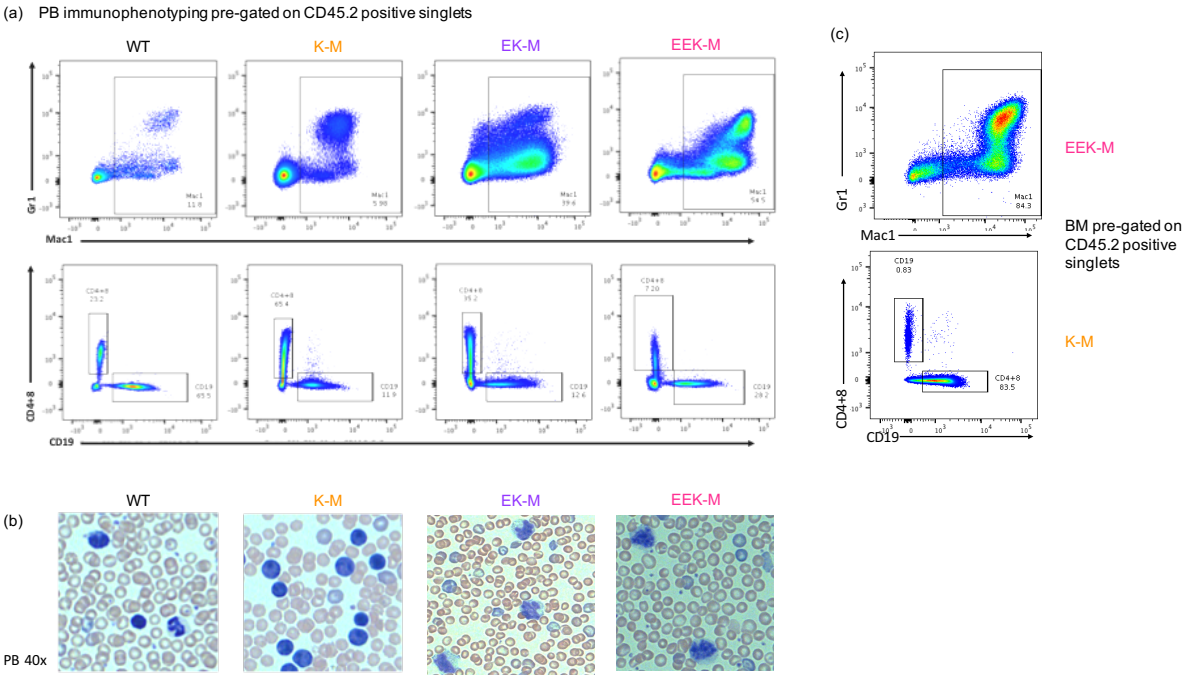


Fig 3.20: Haematological phenotype of Mx1Cre FL transplanted mice. (a) Representative flow cytometry plots demonstrating demonstrating final PB phenotype of diseased mice with WT comparison. K-M demonstrating T cell leukaemia (representative of 6/11 mice). EK-M and EEK-M demonstrating myelomonocytic leukaemia in 2 mice each (b) PB morphology of PB where flow cytometry shown in (a). (c) Representative bone marrow flow cytometry of mice reciprocating PB findings in BM.

Previous data suggest that mice transplanted with $Kras^{G12D/+}$; $Mx1Cre^{tg/+}$ develop a range of T-cell leukaemias [Sabnis, 2009][Zhang, 2009] with some mice developing double negative, thymic disease, as likely demonstrated in my model described above. Of note, as suggested from the Vav-iCre transplants, the mice succumbing to T-cell leukaemia had a significantly higher WCC than those with a myelomonocytic leukaemia (mean 39.6 v 190 $x10^9$/L), figure 3.22a.

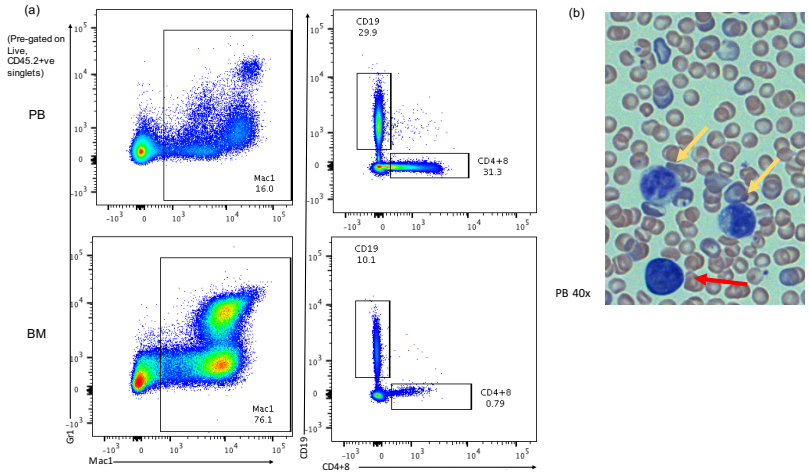


Fig 3.21: Mixed phenotype disease following transplant. (a) FACS phenotype of PB and BM from mouse demonstrating expanded myeloid population in BM, but not in the PB. (b) PB film demonstrates monocytes (yellow arrows), T cell blasts (red arrow)

Although there was a significant difference between the control and *Kras* mutant mice in survival, the addition of *Ezh2*-KO made no difference to survival (figure 3.22b). PB analysis, where feasible, showed mild anaemia, with profound thrombocytopenia and leucocytosis (figure 3.22c). Mice transplanted with EK-M FL developed significantly larger spleens all other genotypes, and were significantly more anaemic than K-M mice (figure 3.22d). This is an interesting finding in the context of JMML, where heterozygous *EZH2* LOF is common due to monosomy 7, and splenomegaly is a presenting sign.

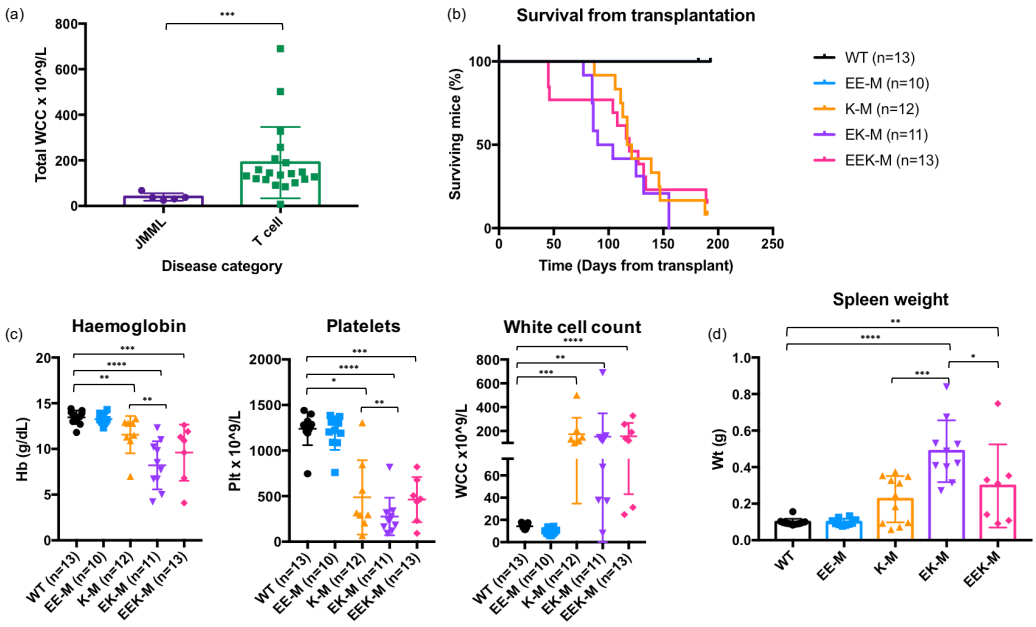


Fig 3.22: Summary of terminal readouts from FL Mx1Cre transplants. (a) White cell counts in mice developing T-cell leukaemia and myelomonocytic leukaemia (b) Survival of mice from transplantation (c) PB cell counts (d) Spleen weights. Each point represents a biological replicate Statistical significance determined by Mann-Whitney U-test. * p<0.5. ** p<0.01, *** p<0.001 **** p<0.0001

Total BM cellularity was significantly elevated in K-M and EK-M mice (figure 3.23a), but on analysis of HSPC compartments, there was a significant decrease in LSKs and HSCs in K-M and EEK-M compared to WT (figure 3.23b-c). *Ezh2* heterozygous loss rescued the *Kras* mutant LSK loss, and also elevated MPPs (appendix 2.3). This functional effect of *Ezh2* heterozygous loss may be important, especially in the context of JMML, however the majority of diseased mice using this model developed T-cell leukaemia. It is known that *Ezh2* mutations occur in T-cell leukaemia [Ntziachristos, 2012], and this model would also be consistent with the cooperation of mutations in T-cell malignancies.

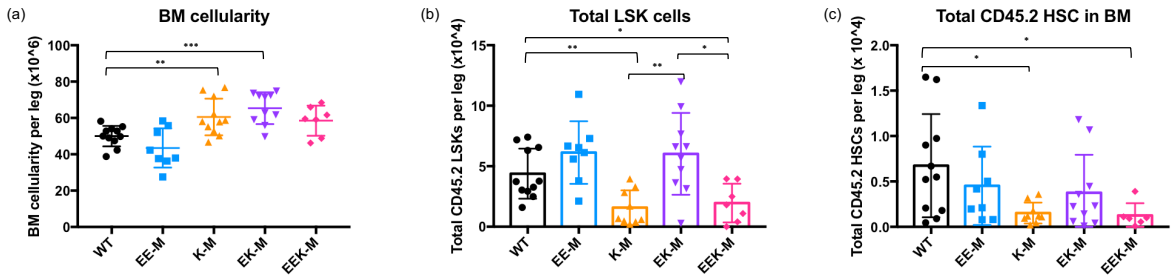


Fig 3.23: Summary of BM terminal readouts from FL Mx1Cre transplants. (a) BM cellularity per leg at the terminal readout (b) Total LSK cells per leg and (c) Total phenotypic HSCs per leg. Each point represents a biological replicate Statistical significance determined by Mann-Whitney U-test. * p<0.5. ** p<0.01, *** p<0.001

In summary, these experiments clearly show cooperation between the $Kras^{G12D}$ mutation and *Ezh2* loss. Whereas no mice of the K-M genotype developed a myelomonocytic leukaemia, 2 mice of each genotype with either heterozygous or homozygous *Ezh2* loss developed a myelomonocytic leukaemia. The mechanism is not clear from these data, but may, at least in part, be due to an increased myeloid drive with *Ezh2* loss, which has been previously suggested in models of other haematopoietic diseases [Booth, 2018].

3-4. Limitations of using Mx1Cre to study the development of leukaemia at different stages of ontogeny

Despite the successful achievement of a JMML-like disease in some of the mice using the approach of spontaneous recombination of Mx1Cre, the disadvantage of this is that it allows little control over the timing or intensity of deletion. One possibility is that transgenes (either $Kras^{G12D}$ or $Ezh2^{fl/fl}$) recombined in this model but not together -- potentially with *Ezh2* recombination occurring only heterozygously where homozygous mutation would be expected by genotype -- thereby affecting my results. I therefore analysed whole tissues on a selection of leukaemic mice to assess *Ezh2* and *Kras* recombination. This demonstrated recombination of both transgenes, in keeping with the expected genotype (appendix 2.3).

In order to demonstrate deletion within the FL, I performed bulk deletion PCRs on FL from transplanted embryos to assess recombination of the transgenes. This demonstrated *Ezh2* recombination (figure 3.24a), but *Kras* recombination was less effectively assayed. By diluting *Kras* and *Ezh2* recombined DNA with WT DNA I developed a semi-quantitative PCR. This shows that the *Kras* deletion PCR can only detect recombination effectively where recombination is ~ >50%, whereas the *Ezh2* PCR is more sensitive, with bands down to 10% (figure 3.24b). This may account for the lack of *Kras* deletion on the PCR, where *Ezh2* recombination is seen at low levels in figure 3.24.

However, when using uninduced FL, a major limitation to assess fetal *Kras/Ezh2* deletion is the lack of control over timing of mutations. Spontaneous recombination may occur at any point from fetal life or post-transplant. To definitively assess whether deletion genuinely occurred *in-utero* is difficult in any given cell, so I undertook a series of optimisation experiments to assess whether it would be possible to select deleted cells for transplant.

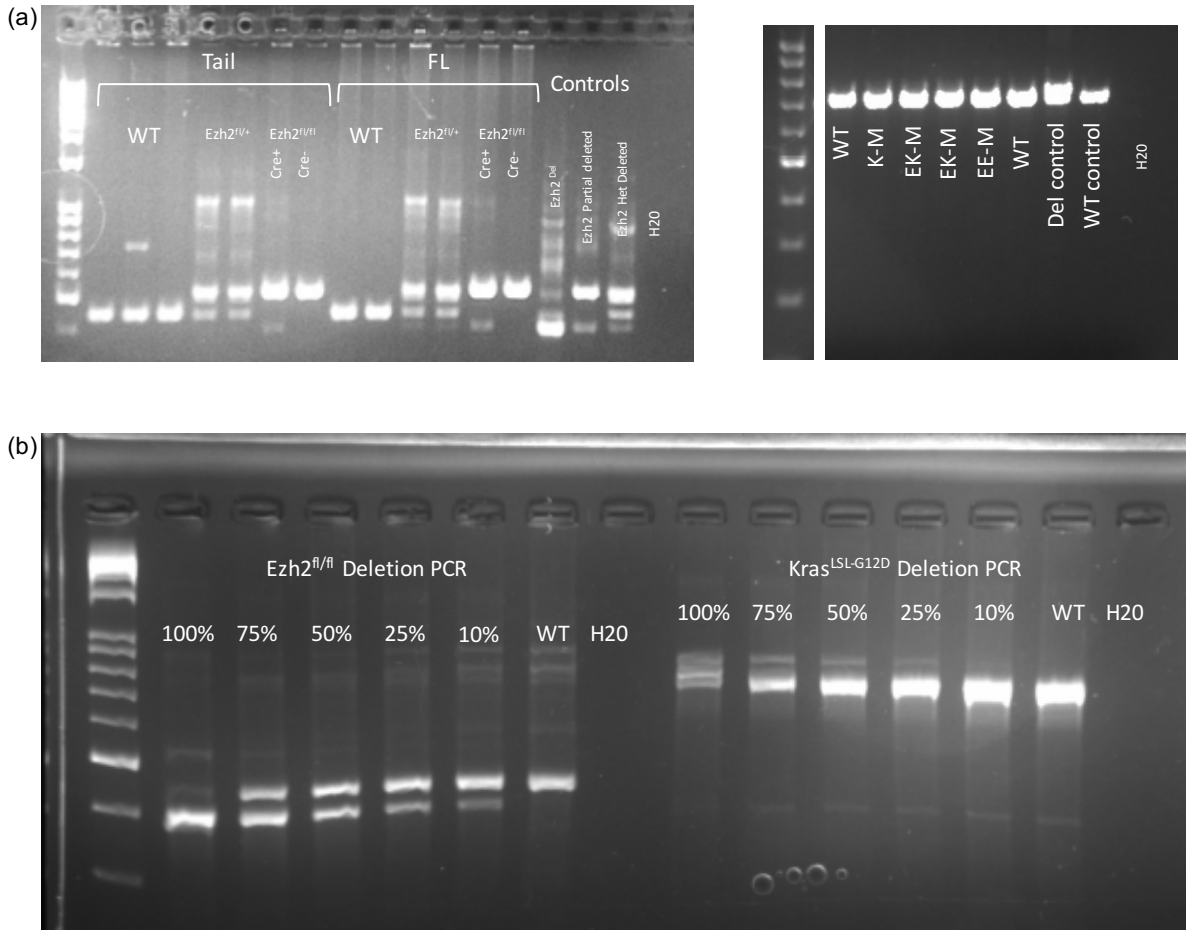


Fig 3.24 Deletion on Ezh2 and Kras FL (a) Deletion PCRs from tail and FL from embryos transplanted in Mx1Cre experiments. Top demonstrating Ezh2 deletion PCR followed on right by a gel demonstrating Kras PCR. Kras gel showing only FL and split to show ladder. (b) Optimised Ezh2 and Kras deletion PCRs with percentage of deleted DNA shown.

i) Quantifying fetal *Kras/Ezh2* deletion

In order to quantify the extent of deletion in FL, I initially sorted E15.5 FL LSK cells (figure 3.25a) and grew colonies in Methocult media (M3434 GF). Bulk FL from these E15.5 embryos was used for the transplantation experiments, described in 3-3. After 7 days I plucked 96 single colonies per biological replicate and DNA from whole colonies was analysed for deletion PCR (appendix 2.4). This showed that some, but not all cells within the FL were deleted but the level of deletion detectable was variable between genotypes and genes, but there were a high number of dropouts, and I therefore sought another method to quantify deletion in the FL.

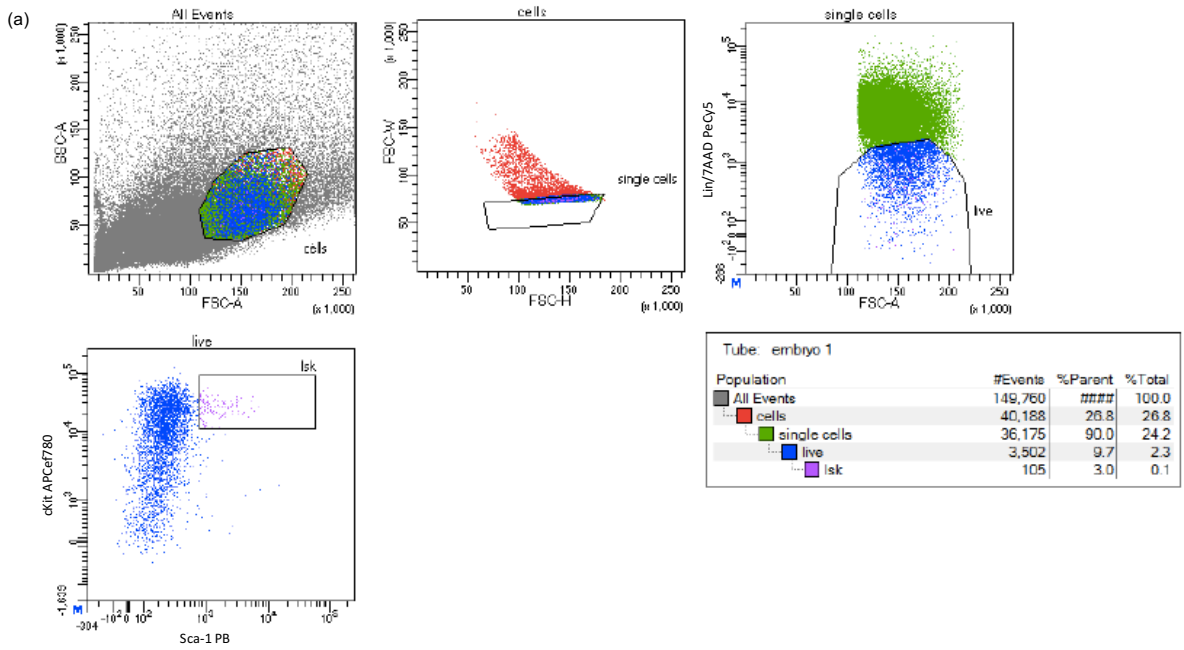


Fig 3.25 Sort gates to investigate LSK *Ezh2* deletion (a) Representative sort gates from two separate experiments and 10 biological replicates. Cells sorted from LSK gate.

I used a *dTomato*$^{fl/fl}$ reporter to examine Mx1Cre$^{tg/+}$, *dTomato*$^{fl/fl}$ E15.5 FL LSKs by flow cytometry (figure 3.26a). In two separate experiments, I demonstrated a clear Mx1Cre-mediated deletion in the FL with a mean of ~20% dTomato positive cells (figure 3.26b). There was a wide variation in results, however, with a range from no spontaneous deletion to over 90%. This again emphasises the difficulty in controlling the transplantation experiments, with some FL LSKs being >30% recombined and some FL having minimal spontaneous recombination. Although flow cytometry assessment prior to transplant could be used to select recombined embryos, this would still not allow me to prove that the cells where recombination had occurred in the FL are the leukaemogenic cells in the post-transplant setting.

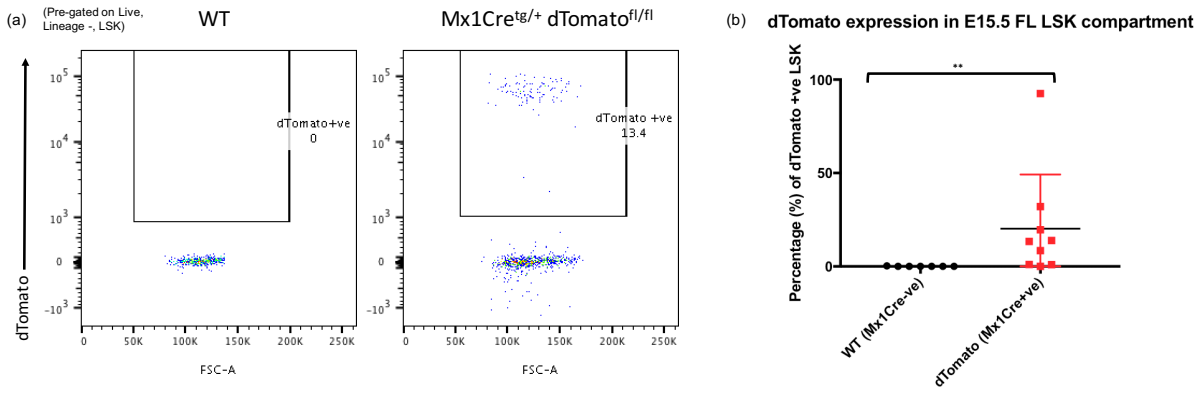


Fig 3.26 Mx1Cre spontaneous expression in E15.5 FL (a) Representative flow cytometry plots from 3 replicate experiments showing Mx1Cre negative (n=7) and Mx1Cre positive embryos with dTomato floxed expression (b) Spontaneous dtomato expression in the E15.5 FL. Each point represents a biological replicate from 3 separate experiments. ** p<0.01

ii) Is dTomato an accurate marker of recombination of other transgenes?

To determine whether cells expressing a fluorescent reporter, such as dTomato, was an accurate reflection of recombination of *Ezh2* I used Taqman based qPCR to determine whether E15.5 EE-M FL with a *dTomato*$^{fl/fl}$ reporter cells that were dTomato expressing, were also Ezh2 deleted (figure 3.27a). Whilst the positive control showed loss of *Ezh2* expression, consistent with complete recombination, the other embryos demonstrated similar levels of *Ezh2* mRNA whether from dTomato+ve or dTomato-ve cells (figure 3.27b). This demonstrates that using dTomato as a reporter may be representative of Cre activity, and perhaps provide an estimate of Cre-mediated recombination, but does not indicate specific recombination of other transgenes, and therefore would not be possible to use as a reporter for transplantation.

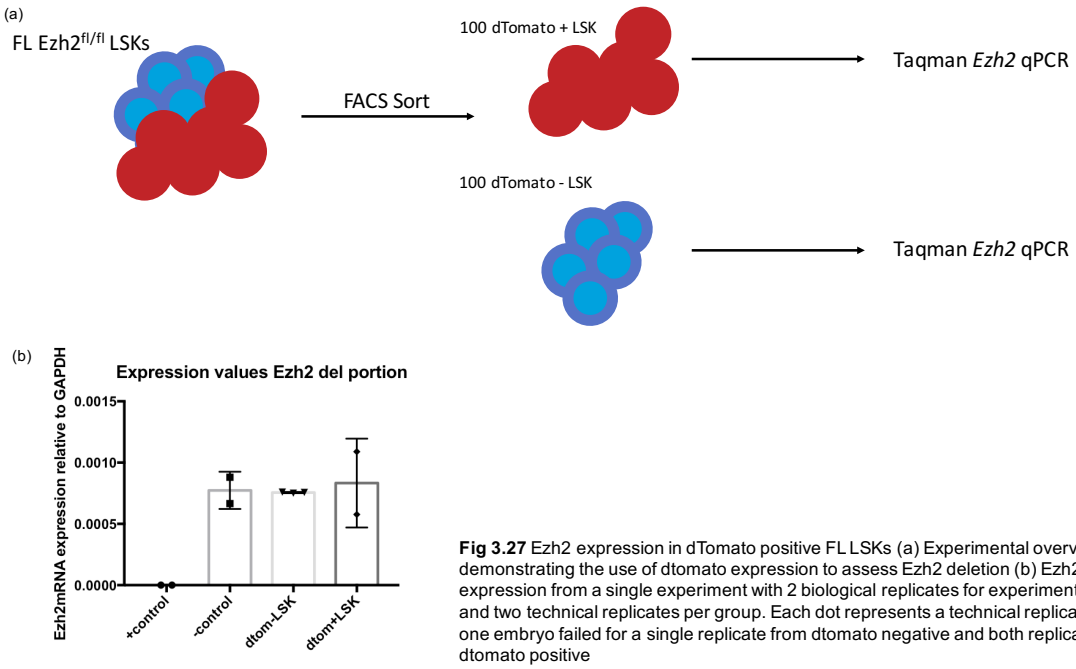


Fig 3.27 Ezh2 expression in dTomato positive FL LSKs (a) Experimental overview demonstrating the use of dtomato expression to assess Ezh2 deletion (b) Ezh2mRNA expression from a single experiment with 2 biological replicates for experimental subgroups and two technical replicates per group. Each dot represents a technical replicate, however one embryo failed for a single replicate from dtomato negative and both replicates from dtomato positive

iii) Limitations of Mx1Cre and transplantation based model systems

Overall, my Mx1Cre data so far demonstrate that FL-derived cells can give rise to a myelomonocytic leukaemia, in addition to a potential cooperation between *Ezh2*-KO and leukaemogenic *Kras* mutation, in that *Ezh2* loss appears to allow development of a myeloid leukaemia. Nevertheless there are some problems with the model: firstly, there is a very low frequency of myeloid leukaemia, which is expected from these transgenes when using a transplantation model [Sabnis, 2009][Zhang, 2009]. The preponderance of T-cell leukaemia appears to be related to the transplantation process, either through transplantation of mutant T-cells which seed recipient tissues, or through rapid immune reconstitution with mutant cells. The former of these is unlikely to be the sole reason, as transplantation models with FACS purified HSCs also develop T-cell leukaemia. Finally, there may well be a significant role of the microenvironment. Dong *et al* demonstrated that Mx1Cre transgenic, *Ptpn11* mutant recipients could drive a myelomonocytic leukaemia from donor derived WT cells, suggesting that the BM niche plays an important role in disease propagation [Dong, 2016]. Thus, it may

be that disease initiation and growth within the FL is important, rather than removing HSPCs from their native niche, and transplantation models may not accurately reflect this.

Secondly, it may simply be that the JMML initiating cell does not transplant well, and other models should be sought -- this is however, in contrast to the human xenograft models, although it should be noted that these were transplanted with established leukaemia [Louka, 2019][Caye, 2020]. Finally, using the Mx1Cre system there is no way of ascertaining whether the leukaemia-initiating cell(s) gained mutations in the FL or post-transplant and, in particular, there is no way of selecting mutant cells, even using a reporter gene, with a known mutation in the FL. I therefore concluded that these models are not suitable for testing my hypothesis that there is a difference between gain of mutations in FL versus adult life.

3-5 The potential to use primary mice: pilot experiments using Mx1Cre induced mice

As proof of principle that ontogenic timing of mutations alter the disease phenotype I utilised Mx1Cre mice and induced them with PolyI:C either in neonatal life or adult life. Neonatal mice were selected because our Home Office licence does not permit pregnant mice to be injected with polyI:C. Although Mx1Cre spontaneous recombination could occur at any time in this model -- and therefore the adult mice could have fetal/neonatal previous recombination -- it can be used to demonstrate the principle as to whether or there is a difference in the nature of the leukaemia depending on the ontogenic stage of induction. It is worth noting that, left uninduced, Mx1Cre mice carrying $Kras^{LSL\text{-}G12D}$ do succumb to leukaemia (appendix 2.5).

i) Neonatal mice

Initially, to study the induction of mutations in neonatal mice I used $Mx1Cre^{tg/+}$; $dTomato^{fl/fl}$ mice to optimise the induction in FL. Mice were selected for timed matings, and injected during

the neonatal period with IP PolyI:C for either two or three days. Recombination was assayed at 3 weeks (figure 3.28a) and 6 weeks using flow cytometry (figure 3.28-b). This demonstrated adequate dTomato expression with either 2 doses or 3 doses of PolyI:C and so I went on to use the minimum number of injections - 2 injections at days 3 and 7. There was no unexpected loss of mice following injection (figure 3.28c).

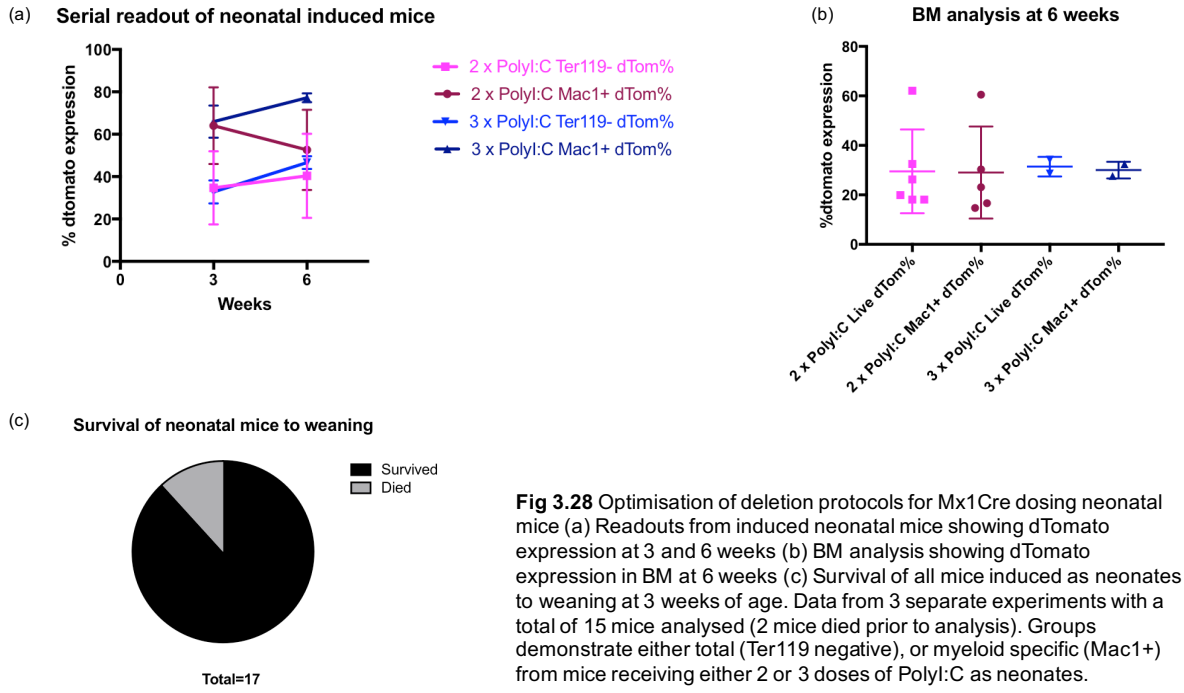


Fig 3.28 Optimisation of deletion protocols for Mx1Cre dosing neonatal mice (a) Readouts from induced neonatal mice showing dTomato expression at 3 and 6 weeks (b) BM analysis showing dTomato expression in BM at 6 weeks (c) Survival of all mice induced as neonates to weaning at 3 weeks of age. Data from 3 separate experiments with a total of 15 mice analysed (2 mice died prior to analysis). Groups demonstrate either total (Ter119 negative), or myeloid specific (Mac1+) from mice receiving either 2 or 3 doses of PolyI:C as neonates.

However, unexpectedly, all *Kras*^{G12D} mutant mice developed skin lesions, around mucous membranes and exposed skin such as mouth, anus and ear canals, requiring them to be terminated (figure 3.29a). No WT mice developed skin lesions (figure 3.29b), but no further experiments were permitted as the development of skin lesions was not an expected side effect on the Home Office licence. These skin lesions were associated with leukaemia in ~50% of the mice (figure 3.29c-d). Other mutant *Kras* mice (both K-M and EEK-M) had a raised WCC and/or splenomegaly and all of these mice developed thrombocytopenia (figure 3.29e-f).

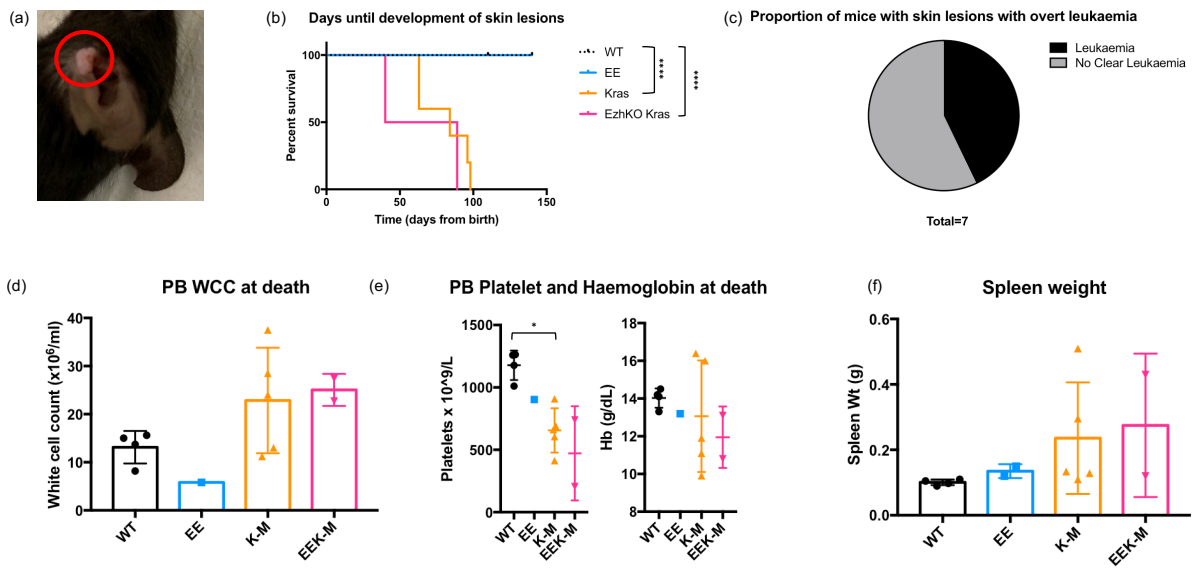


Fig 3.29: Summary of neonatal Mx1Cre transgenic mice (a) Skin lesion on ear of mouse circled in red (n=1 representative picture (b) Survival of mice until death (synonymous with the development of skin lesions) (c) Pie chart including all mice who developed skin lesions, all Kras mutant, split between the presence or absence of leukaemia (d) PB WCC at death and (e) Platelet and Hb counts at death (f) Spleen weight at death. Each point represents a biological replicate in 5 separate experiments. *p<0.05, **** p<0.0001

Expansion of the Mac1+ population was seen in all mice with leukaemia, with some mice developing a PB monocytic population (figure 3.30a). On analysis of the skin lesions themselves, flow cytometry demonstrated a population of CD45+, Mac1+ monocytes (figure 3.30b) and on histological examination there appeared to be monocytoid cells infiltrating the skin (3.30c). These data suggest that induction of leukaemogenic *Kras* within the neonatal period could lead to a myeloid expansion. The skin lesions were not described in the initial paper with 3-4week old K-M mice [Braun, 2003], thus suggesting that neonatal induction may lead to a different phenotype.

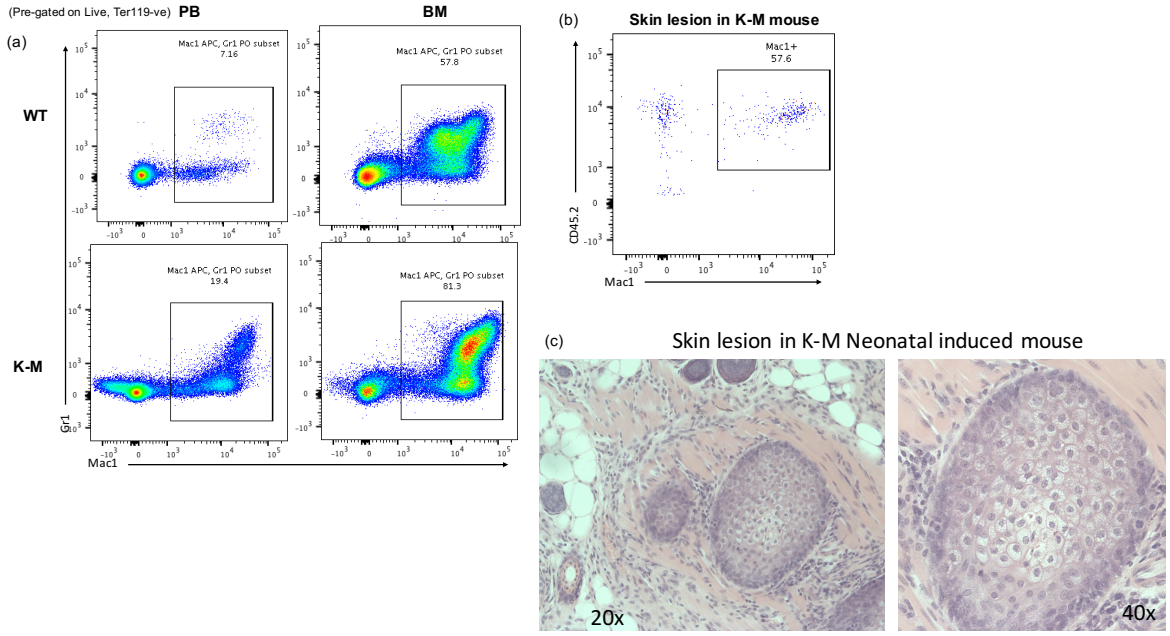


Fig 3.30: Tissue analysis of neonatal induced mice (a) PB and BM from representative sample of WT mice (n=3) and K-M (n=3 with leukaemia) showing myeloid precursors and (b) flow cytometry of skin lesion in K-M mouse (representatve n=2 skin lesions) showing CD45.2 Mac1+ cells and (c) monocytic cells in the skin on H+E stain of parrafin fixed tissue (n=2).

ii) Adult mice

Adult mice were induced at 6-8 weeks with three doses of PolyI:C, as standard protocol in our laboratory [Booth, 2018]. All experimental mice had to be terminated due to disease, with a median survival of 11 weeks (figure 3.31a), and large spleens (figure 3.31b). In contrast to the transplantation experiments, all of the mice developed myeloid leukaemias with no T-cell leukaemia (figure 3.31c). The peripheral blood counts (figure 3.31d), showed an elevation but not significant change of the WCC in *Kras* mutant experimental groups and lowering of the platelets. The majority of experimental mice showed an expansion of a myeloid population in the PB flow cytometry and blood films morphology (appendix 2.6). In contrast to the neonatal-induced mice, where 100% of the mutant *Kras* mice developed skin lesions, only 50% of the adult-induced mice developed skin lesions, although these were similar in macroscopic appearance to the neonatal skin lesions as well as by flow cytometry, where tested (see figure 3.29a and 3.30b). Of note, all mice (3/3) with EK-M genotype developed skin lesions, compared to only 1/5 mice with other genotypes. Although in this experiment there is not

enough data to support firm conclusions from this, it does suggest that the presence of heterozygous *Ezh2*-KO together with mutant *Kras* collaborate to promote myeloid leukaemia in this model which is of particular interest given the high incidence of monosomy 7 in JMML.

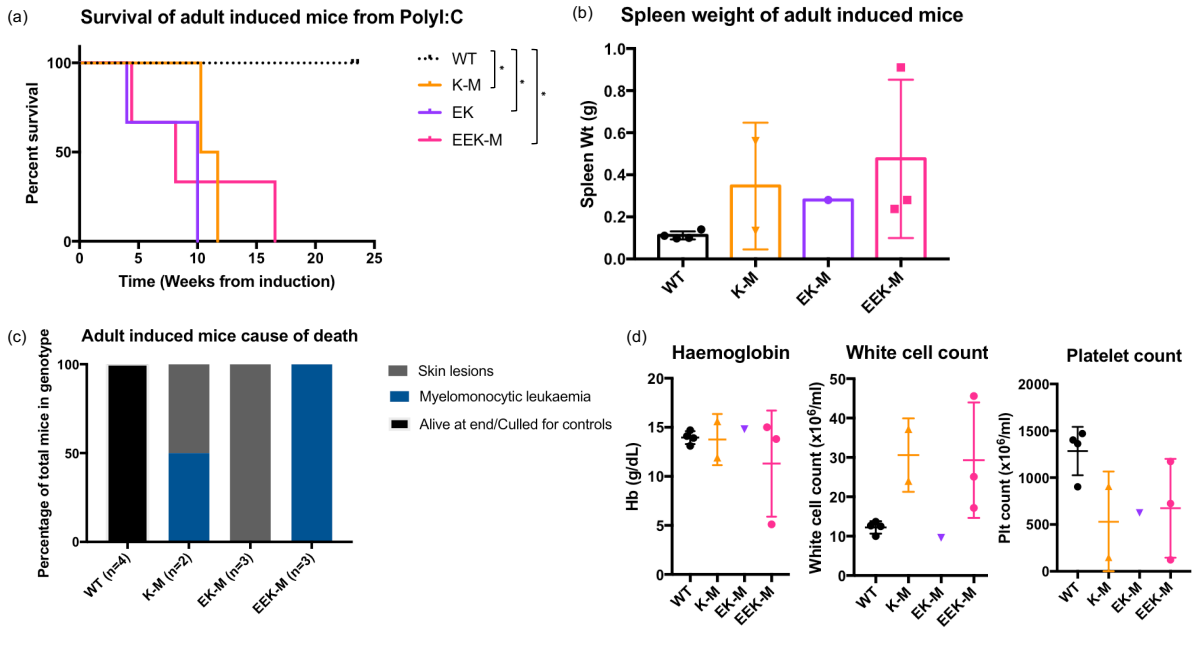


Fig 3.31: Summary of adult Mx1Cre induced primary mice (a) Survival from induction with PolyI:C shown in weeks (b) Spleen weight at death and (c) Percentage of mice per genotype per cause of death. (d) PB counts at terminal readouts, showing haemoglobin, white cell count and platelet count. Survival analysis by Mantel-Cox analysis *p<0.05

These experiments show two important findings. Firstly, there appears to be some difference, despite the limitations discussed above of using Mx1Cre, in the timing of acquisition of mutations with all neonatal mice developing skin lesions compared to a proportion of adult mice. Unfortunately, I did not have the EK-M genotype for the neonatal cohorts, and the experiments had to be discontinued due to the skin lesions (which were not an expected adverse event on the licence), and the alteration in phenotype for this group would have been interesting. These experiments could be expanded, with particular interest for the neonatal model, as human neonatal leukaemias are often associated with skin lesions [Roberts, 2018], but also a focus on whether *Ezh2* loss affects the disease, and therefore allow potential insights into the biology and function of *EZH2* in the neonatal period.

The second major finding is that by using induced primary mice, an increased percentage of mice develop myeloid leukaemia, and this appears to abrogate the T-cell leukaemia shown before. This finding is perhaps not unexpected, given previous data [Sabnis, 2009][Zhang, 2009], but reinforced my decision to use a model based on primary mice to further study my hypotheses.

3-6 Optimisation of an Fgd5CreERT2 based model

Fgd5 has been shown to highly enrich for the stem cell compartment [Gazit, 2014], with a tamoxifen inducible Cre-cassette added to allow effective induction of mutations within HSCs alone with no clear effect on cellular function [Gazit 2014]. Tamoxifen inducible Cre lines from our laboratory (CreERT2, Flt3CreERT2) historically show very little spontaneous expression, and so I crossed *Fgd5*-CreERT2 with *Kras*$^{LSL\text{-}G12D}$, *Ezh2*$^{fl/fl}$, and *dTomato*$^{fl/fl}$ to create the mouse models shown in figure 3.32. The aim of these experiments was to create a model which had no spontaneous recombination, thus abrogating the problems assessing ontogenic timing of mutations with the Mx1Cre model.

Genotypes – Fgd5CreERT2				
WT	– Ezh2$^{+/+}$,	Kras$^{+/+}$,	dtomato$^{fl/+}$,	*Fgd5CreERT2$^{tg/+}$ or Fgd5CreERT2$^{+/+}$*
EE-F	– Ezh2$^{fl/fl}$,	Kras$^{+/+}$,	dtomato$^{fl/+}$,	*Fgd5CreERT2$^{tg/+}$*
K-F	– Ezh2$^{+/+}$,	Kras$^{LoxP/+}$,	dtomato$^{fl/+}$,	*Fgd5CreERT2$^{tg/+}$*
EK-F	– Ezh2$^{fl/+}$,	Kras$^{LoxP/+}$,	dtomato$^{fl/+}$,	*Fgd5CreERT2$^{tg/+}$*
EEK-F	– Ezh2$^{fl/fl}$,	Kras$^{LoxP/+}$,	dtomato$^{fl/+}$,	*Fgd5CreERT2$^{tg/+}$*

Fig 3.32: Summary of genotypes and nomenclatures used for Fgd5CreERT2 phenotyping, transplantation and primary mice

i) Leakiness in FL and aBM

As the major limitation in using Mx1Cre is spontaneous activation, I first checked that there was no spontaneous initiation of Fgd5-CreERT2 within the FL or BM. As the HSCs in this mouse model expressed ZsGreen, a fluorescent cassette within the *Fgd5* transgene, I used ZsGreen expression by flow cytometry to evaluate the pattern of Fgd5 expression (figure 3.33a-b). This showed that ZsGreen expression was largely restricted to HSCs, with very limited expression in other cell populations, including MPPs (figure 3.33c) although FL expression generally had a higher mean fluorescence intensity (MFI) than in adult BM.

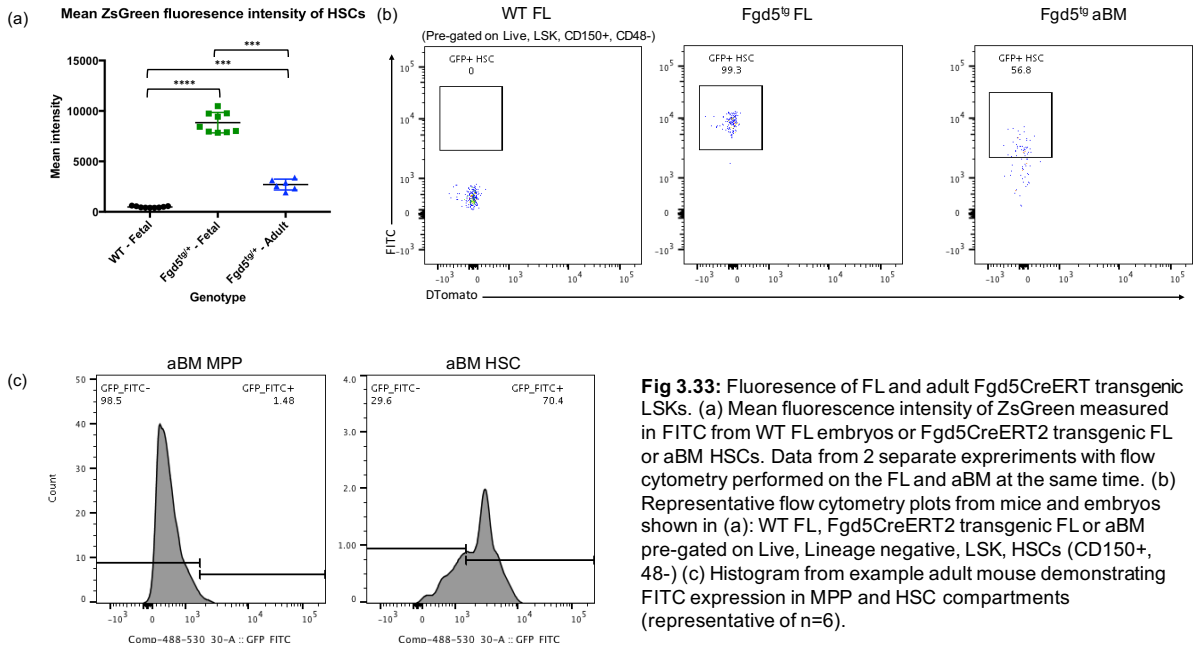


Fig 3.33: Fluoresence of FL and adult Fgd5CreERT transgenic LSKs. (a) Mean fluorescence intensity of ZsGreen measured in FITC from WT FL embryos or Fgd5CreERT2 transgenic FL or aBM HSCs. Data from 2 separate expreriments with flow cytometry performed on the FL and aBM at the same time. (b) Representative flow cytometry plots from mice and embryos shown in (a): WT FL, Fgd5CreERT2 transgenic FL or aBM pre-gated on Live, Lineage negative, LSK, HSCs (CD150+, 48-) (c) Histogram from example adult mouse demonstrating FITC expression in MPP and HSC compartments (representative of n=6).

Using the *dTomato* reporter gene I used previously, I assessed the spontaneous deletion in both the FL and aBM. This showed no dTomato expression and therefore no evidence of spontaneous recombination in FL HSCs or aBM HSCs. I also checked that there was no difference between male and female mice given that this is a tamoxifen-driven system (figure 3.34a-c). To confirm the reliability of this system, adult mice with a *Kras*$^{LSL\text{-}G12D}$ transgene and

Fgd5CreERT2$^{tg/+}$ (K-F) were kept for >8 months. None of these mice died of leukaemia, and analysis of their PB showed no spontaneous deletion at 8 months of age (figure 3.34d). Further, mice used for breeding included K-F, EK-F and EEK-F genotypes, and many of these survived to a year of age, with no excess deaths in contrast to the Mx1Cre data shown above where mice with a mutant *Kras* allele and with spontaneous deletion would develop leukaemia.

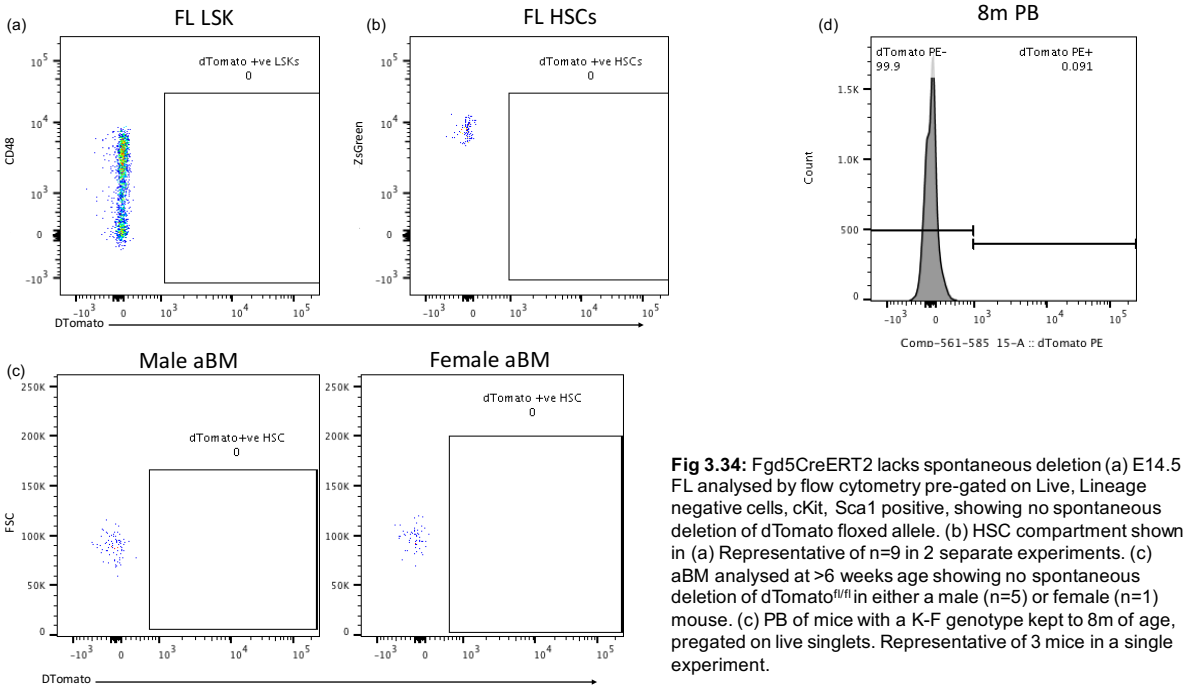


Fig 3.34: Fgd5CreERT2 lacks spontaneous deletion (a) E14.5 FL analysed by flow cytometry pre-gated on Live, Lineage negative cells, cKit, Sca1 positive, showing no spontaneous deletion of dTomato floxed allele. (b) HSC compartment shown in (a) Representative of n=9 in 2 separate experiments. (c) aBM analysed at >6 weeks age showing no spontaneous deletion of dTomato$^{fl/fl}$ in either a male (n=5) or female (n=1) mouse. (c) PB of mice with a K-F genotype kept to 8m of age, pregated on live singlets. Representative of 3 mice in a single experiment.

Overall, these data indicate that, both in the FL and aBM, Fgd5CreERT2 demonstrates no spontaneous deletion.

ii) Induction of mutations using tamoxifen in FL and adult BM (aBM)

Tamoxifen is a partial oestrogen agonist, and administration to Fgd5CreERT2 transgenic mice induces the endoplasmic reticulum-bound Cre to be translocated into the nucleus and become active [Schwenk, 1998]. However, although tamoxifen administration can induce *in-utero* recombination of mutations there are significant potential risks. Firstly, there is a risk of miscarriage, and severe bleeding, resulting in the need to sacrifice the pregnant dam -- commonly around E14-15.5 if given in the first trimester [Ved, 2019]. Secondly, tamoxifen, as an oestrogen agonist, can interfere with the natural parturition of mice, leading to obstructed labour, particularly if given late in gestation [Lizen, 2015]. To overcome these complications, progesterone is often used, particularly at the extremes of gestation [Lizen, 2015][Ved, 2019][Lord, 2017].

I therefore used a time in mid-gestation, to assess the biological impact on HSCs within the FL (but not the YS) to minimise complications to the dams. The dosage chosen is in keeping with previous protocols which suggested adequate deletion using this method [Lord, 2017]. Female *dTomato*$^{fl/+}$ mice were used in a timed mating with *Fgd5CreERT2*$^{tg/+}$ males and tamoxifen (4mg) was administered at E12.5 and E13.5 by oral gavage to the dams. I harvested embryos at E14.5 to assess deletion in the FL with a dTomato reporter, and although only one embryo was transgenic for both *dTomato* and *Fgd5CreERT2*, this did show deletion in the LSK, including MPP and HSCs (figure 3.35a).

Our laboratory already had a standard operating procedure in place for induction in adult mice using 4mg of tamoxifen by oral gavage for 5 days. Using this technique on mice aged 6-8 weeks I demonstrated, in my hands, variable but adequate recombination in BM LSKs (figure 3.35b). One experiment was excluded: in a single cage of two mice, one mouse was dosed and

one mouse followed up for spontaneous deletion. On analysis, the mouse supposedly dosed with tamoxifen showed no deletion, but the mouse with no tamoxifen demonstrated deletion in keeping with other experiments. It is likely that either the wrong mouse received the drug, or that at analysis the tissues were accidentally switched. However, following this, I made one important modification; mice are coprophagic, and it is conceivable that mice not expected to be dosed with tamoxifen receive some in the faeces. Therefore, although the tamoxifen in faeces may not be enough to lead to deletion, I separated any future mice receiving tamoxifen.

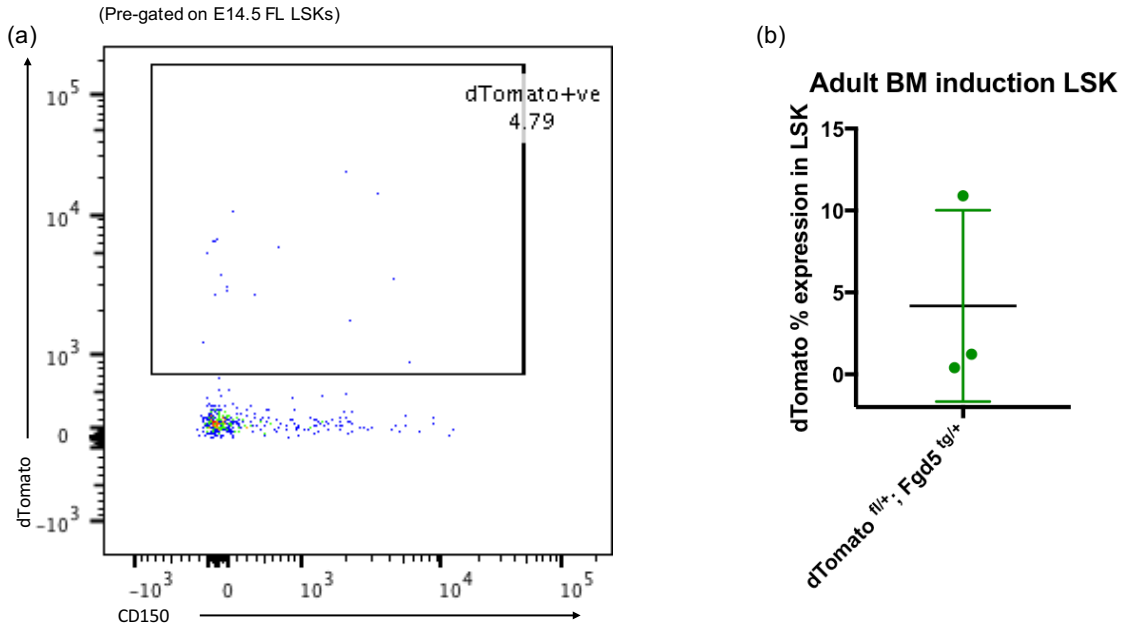


Fig 3.35: Proof of principle that tamoxifen can be used for dual stage deletions (a) Deletion efficiency in the LSK compartment of the E14.5 FL following 4mg tamoxifen at E12.5 and E13.5 to the dam. Single mouse from one experiment. (b) Adult BM deletion within the LSK compartment following 4mg tamoxifen by oral gavage for 5 days and harvested 10 days after final dose. 3 mice from a single experiment.

iii) Transplantation of HSPCs induced in FL or aBM

To confirm that the FL or aBM induction methods led to sufficient recombination to permit leukaemogenesis without impairing cellular function, I transplanted all the genotypes cryopreserved aBM and FL cells induced with the methods above (figure 3.36). This

demonstrated that both induced FL and aBM could engraft, with no deleterious effect from the tamoxifen (figure 3.37a). Some animals from both FL-induced and aBM-induced transplants from all of the genotypes including mutant *Kras* developed leukaemia. In the mice receiving FL-induced cells, all of the leukaemias were T lineage (figure 3.37b). Two mice (both transplanted with mutant *Kras* aBM-induced cells) developing a myelomonocytic leukaemia (figure 3.37b and appendix 3.1). The high frequencies of transplantation-associated T cell leukaemia match my previous data in the other models described earlier in this chapter.

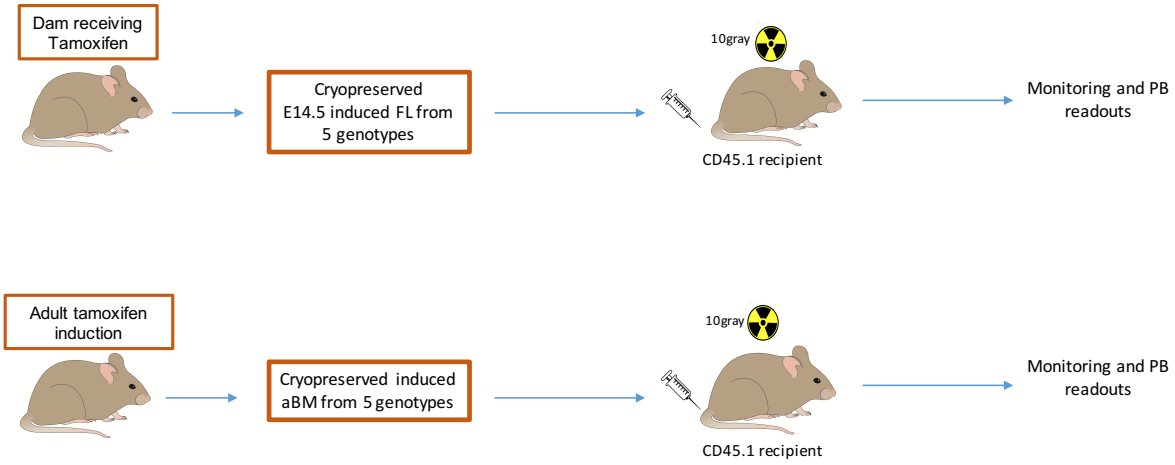


Fig 3.36: Overview of tandem transplantation experiments using Fgd5CreERT2 induction in FL

Unfortunately, some the results were compounded by technical difficulties which led to only ½ - ¾ of the planned cell dose being injected into 4 of the 24 fetally-induced cohort. These 4 mice engrafted but did not develop disease and so it is possible that either the induction efficiency was poor in these embryos, or that the reduced cell dose was insufficient to cause disease. Although the induction efficiency appears the same between FL and aBM, the function of the FL cells or the survival of mutant induced cells in fetal life may be altered and impact on the frequency of leukaemogenesis. However, my data did allow me to confirm the absence of spontaneous deletion in this model as mice with low cell doses engrafted with similar proportions to other FL mice, but did not develop disease (appendix 3.2).

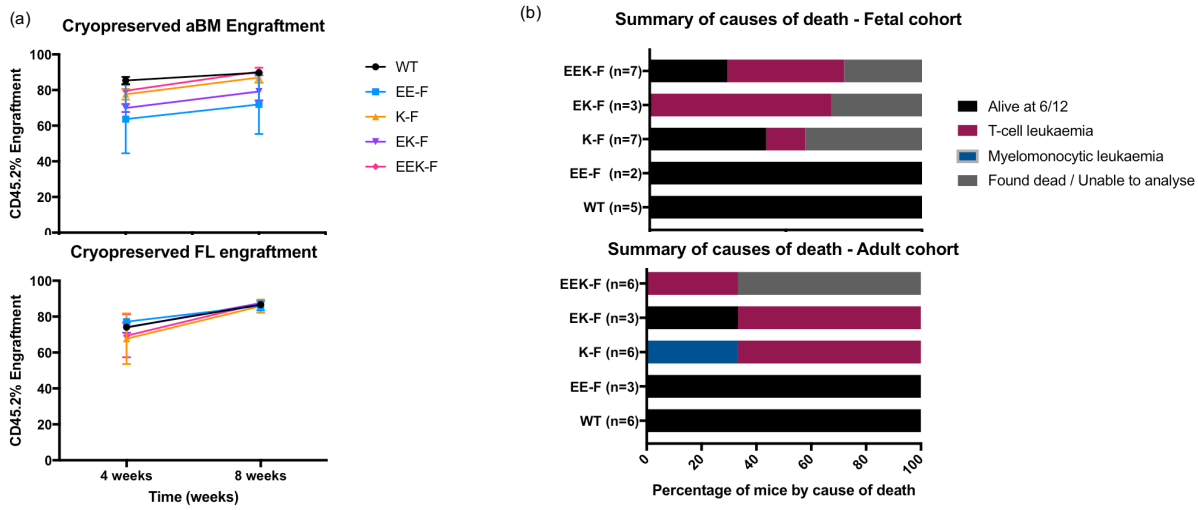


Fig 3.37: Fgd5CreERT2 transplanted FL and adult induced mice (a) Engraftment at 4 and 8 weeks of CD45.2 myeloid cells in both aBM (top) and FL (bottom) transplanted mice (b) Summary of causes of death shown as a percentage of total mice per genotype. Data from 2 separate experiments with biological replicate mice shown in figure (b). 2 biological FL or aBM replicates used in each genotype except for EE-F and EK-F, where only a single was used.

iv) The effect of expansion within the FL microenvironment

A potential explanation for the inconsistent results of the transplant experiments so far, is that the microenvironment may play a larger role. Therefore, to assess whether a prolonged exposure to the fetal microenvironment allows enhanced leukaemogenesis, K-F embryos were induced with 4mg tamoxifen at E12.5 and E13.5 but FL was not transplanted until E19.5. This approach resulted in the development of myelomonocytic leukaemia (figure 3.38a), with moderately raised WCC, thrombocytopenia and splenomegaly (figure 3.38b-c) in 4/4 mice. This suggests that *Kras* mutant cells induced within a fetal environment can cause a JMML-like disease, as long as these cells are allowed to expand within a fetal liver microenvironment -- although the cell dose used was higher (2 million experimental cells) and all of the transplants were performed with fresh rather than cryopreserved FL cells, and it is plausible that mutant T-cells leave the FL between E14.5 and 19.5. Nevertheless, despite these potential biases, this experiment does reinforce that FL induced primary mice may be vital for my model system.

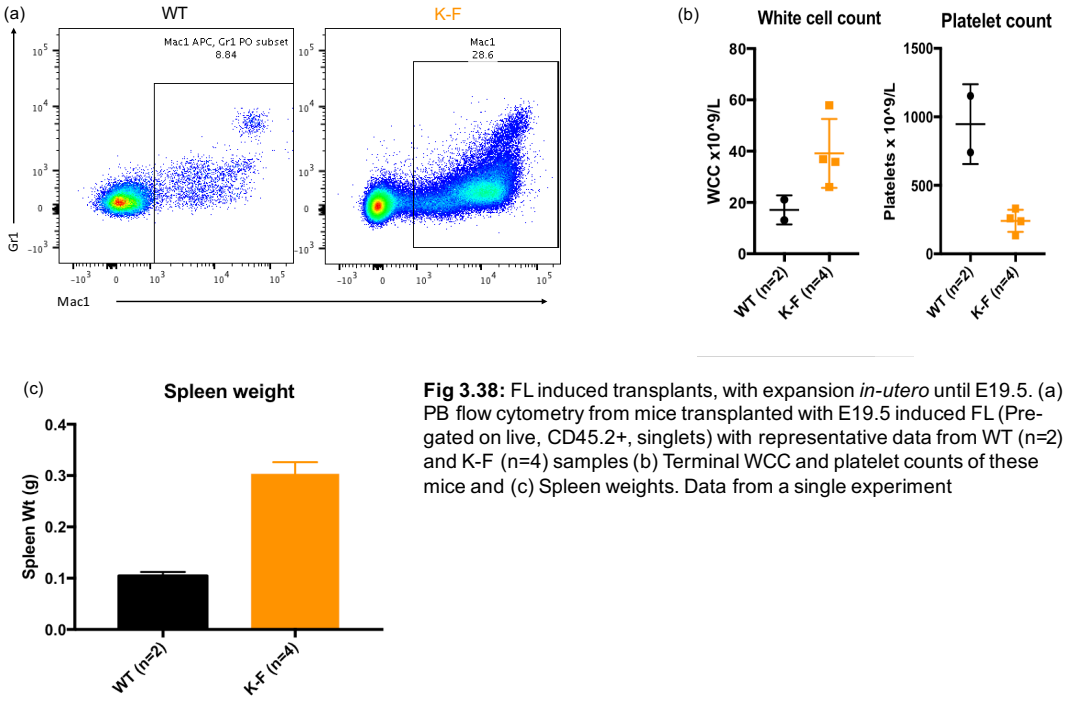


Fig 3.38: FL induced transplants, with expansion *in-utero* until E19.5. (a) PB flow cytometry from mice transplanted with E19.5 induced FL (Pre-gated on live, CD45.2+, singlets) with representative data from WT (n=2) and K-F (n=4) samples (b) Terminal WCC and platelet counts of these mice and (c) Spleen weights. Data from a single experiment

v) Identifying the correct dosage for FL induction to allow pups to survive fostering

I next went on to optimise the protocol for fetal induction and delivery to allow induction at the FL stage of gestation. Initially dams were induced with 4mg tamoxifen by oral gavage at E12.5 and E13.5, as described above. Due to the potential for tamoxifen to interfere with the natural parturition process, a terminal caesarean section (CS) was performed at E18.5, as described in published protocols [Yamada, 2008][Boland, 2009] and neonatal pups were cross-fostered to females at postnatal day (PND) 0-1. Unfortunately, after three experiments with a total of 22 successfully resuscitated pups, no pups survived longer than PND2.

As these results indicated that either the tamoxifen was toxic *in-utero*, or that delivery at E18.5 was too early, I next investigated delivering the pups at E19.5. Eight procedures were performed, with all dams mated with a potential to have pups with K-F, EK-F or EEK-F genotype (figure 3.39a). Although a total of 52 pups were fostered, of which 21 survived to

genotyping, none of these pups were Kras$^{tg/+}$ with Fgd5CreERT2$^{tg/+}$ (figure 3.39b). The reasons for this were not clear as it cannot be ascertained whether these pups were cannabilised due to illness with leukaemia, maternal stress during the fostering process, or other reasons. It is unlikely to be purely caused by tamoxifen, however, given 21 surviving WT pups had no ill effects.

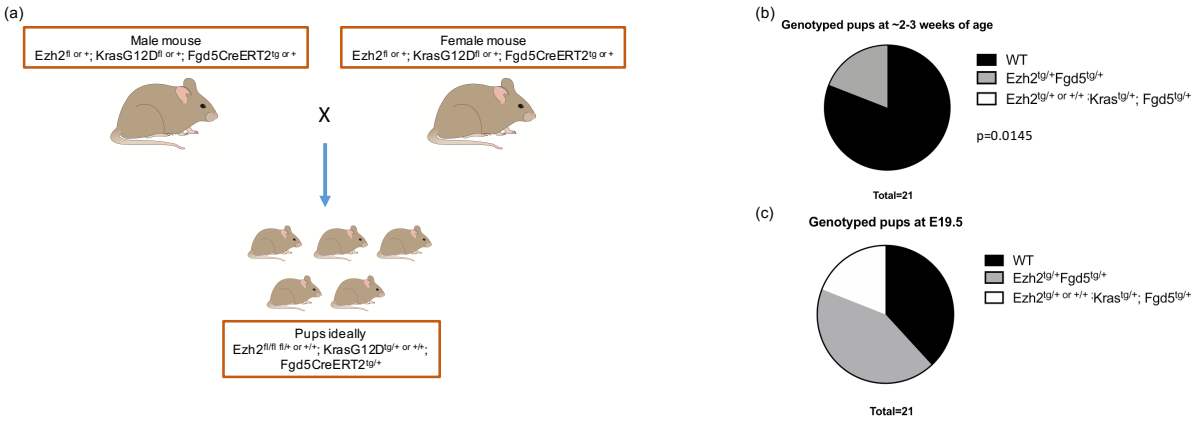


Fig 3.39: Optimising fetal induced mice (a) Mating strategy demonstrating timed mating techniques to achieve all five experimental genotypes (b) Pie chart showing genotype of pups alive at >2 weeks from dams receiving 4mg doses of tamoxifen at E12.5 and E13.5 from 3 separate litters. p-value between observed and expected genotypes by Chi-sqaured and (c) Genotypes of pups alive at E19.5 from the same dosing strategy from 3 separate litters

Therefore, to determine whether or not mutant *Kras* pups induced in this way were surviving to term, three females were mated and induced at E12.5 and E13.5 with 4mg tamoxifen, and culled at E19.5. Embryos were genotyped, and showed an expected proportion of *Kras* mutant embryos (figure 3.39c). However, on analysis of the FL and BM of these E19.5 pups by flow cytometry, there was no clear expansion of any leukaemic population (figure 3.40a, appendix 3.3), despite the presence of dTomato expression in both WT and K-F genotypes suggesting a degree of induction (figure 3.40b).

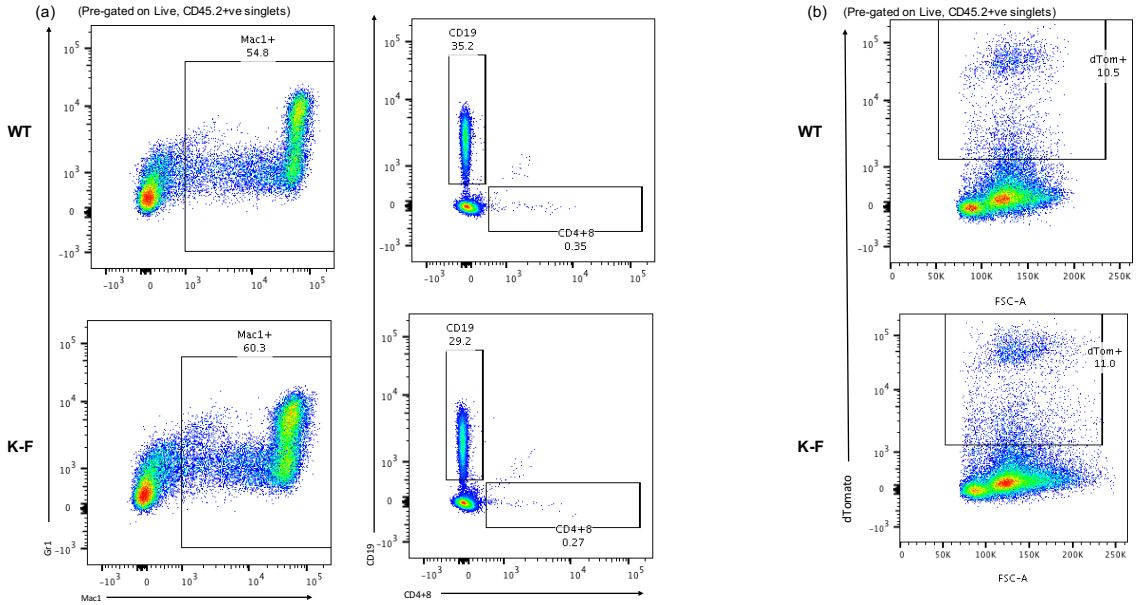


Fig 3.40: FL induced at E12.5 and E13.5 with 4mg tamoxifen. Representative flow cytometry plots of WT (n=6) and K-F (n=2) from 2 separate experiments on FL using a lineage panel with (a) Myeloid and lymphoid cells and (b) expression of dTomato in CD45.2 positive cells.

Taken together, my data suggest that the tamoxifen regimen used in this model is not lethal as the WT pups survived. The reason for the differential effects on the mutant Kras mice is unclear, as all fostered mice appeared macroscopically normal. It is possible that there was a rapid leukaemic expansion in these mice prior to weaning, leading to early death. However, there is no direct evidence for this as all the 'missing' mice were cannibalised before PND3, and flow cytometry did not show a definite leukaemia. Other possible explanations would be that the *Kras* mutant pups are too unwell to feed normally, or that the foster parents can identify 'defective' pups and remove these early. PB sampling from these pups was attempted, but accurate counts could not be obtained.

Given the problems with the fostering process, for further optimisation experiments I next used only *Ezh2* WT mice to negate any potential confounding or accelerated phenotype from EK-F or EEK-F genotypes. Using 4mg at E14.5 and removing all foster pups from the cage, survival improved slightly (~50% compared to 40%) there were still no $Kras^{tg/+}$ mice at weaning (figure

3.41a). Finally, I investigated the use of a lower dose of tamoxifen (single dose of 2mg at E14.5). This approach yielded a survival of 16/17 fostered pups to genotyping at ~ 10 days of age, of which 3 pups were K-F genotype, 2 of which survived to weaning (figure 3.41b). To ensure that this dose of tamoxifen did induce mutation in HSCs, *dTomato*$^{fl/fl}$ mice were plugged with *Fgd5CreERT2*$^{tg/+}$ males and dams were given 2mg tamoxifen at E14.5 and E19.5 FL was assessed for deletion by flow cytometry. This demonstrated deletion in both the FL HSCs and downstream progenitors (figure 3.41c-d).

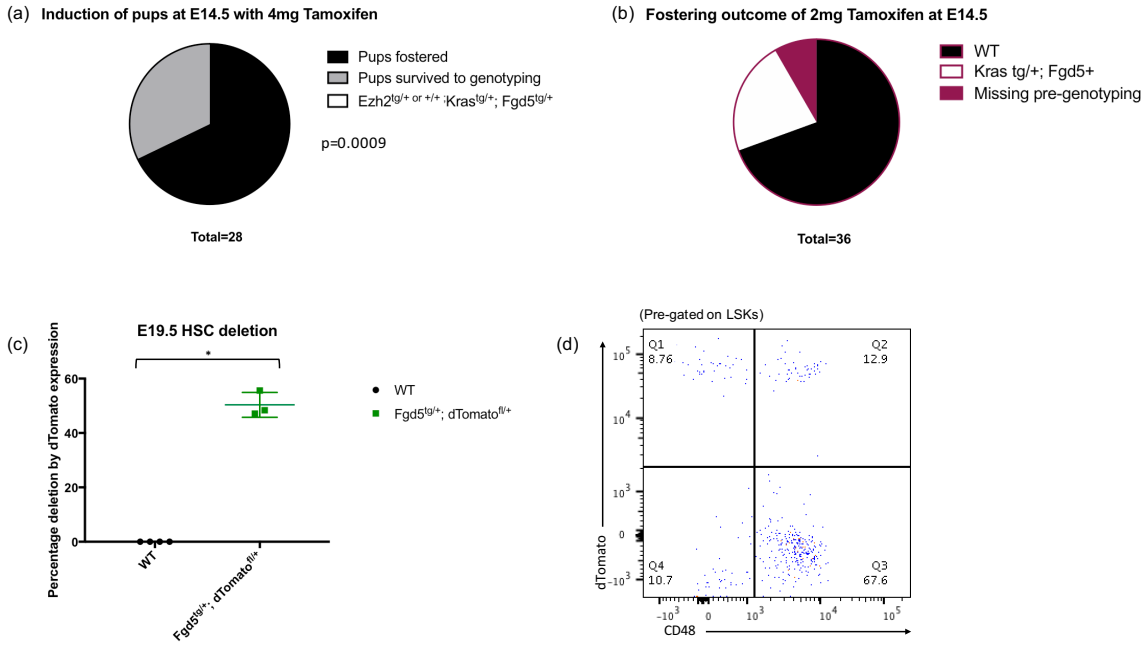


Fig 3.41: Fetal deletion and weaning using a single dose of tamoxifen at E14.5 (a) Genotypes at weaning of pups induced with 4mg tamoxifen at E14.5 from 3 separate experiments. p-value using Chi-squared analysis of observed v expected genotypes. (b) Fostering outcomes following 2mg tamoxifen at E14.5 of genotyped pups and (c) HSC deletion at E19.5 following a single dose of tamoxifen at E14.5 of 2mg and (d) LSKs gated on CD48 and dTomato showing quartile based deletion and lineage tracking of deletion in CD48+ve (downstream progenitors). (c) and (d) from a single experiment. *p <0.05

Therefore, this method could be used to induce adult and fetal mice with tamoxifen and achieve induction of mutations at differing stages of ontogeny -- thereby allowing study of my hypothesis that there is a differing effect in the gain of leukaemogenic mutations in fetal life compared to adult life.

3-7 Summary and Discussion

Overall, the data in this chapter show that there are both phenotypic and functional consequences of *Ezh2* loss in conjunction with $Kras^{G12D}$ *in-utero.* Whilst not conclusive, this is consistent with a combinatorial effect between the mutations that warrants further study. In addition, the experiments described in section 3.6 demonstrate a unique optimised method for deletion *in-utero* that can be used to distinguish and compare fetal and adult initiation of potentially leukaemogenic mutations.

i) The effect of *Ezh2* in combination with mutant *Kras*

Whilst recent papers have suggested a role for a combinatorial role between *EZH2* and a mutant *RAS* pathway in human disease [De Raedt, 2014][Caye, 2015][Stieglitz, 2015][Booth, 2018], it is difficult to study the biological effect of these mutations in human disease given the comparative rarity of the conditions. Some studies have suggested a role for secondary mutations in mutant RAS pathways using mouse models [De Raedt, 2014][Di Genua, 2019] but no study as yet has been able to study these in fetal induced disease. JMML should be a useful model system to explore how mutations causing PRC2 inactivation collaborate with mutations causing constitutive activation of the RAS-pathway as a mouse model with a potential JMML-like phenotype exists [Braun, 2003] and there is a relatively high co-occurrence of these mutations in the human disease. Furthermore, there is substantial evidence for an in utero origin of the leukaemia in many cases [Matsuda, 2010][Steiglitz 2015].

Initial phenotyping data in the FL demonstrated a depletion of the phenotypic HSC compartment with mutant *Kras*, which appeared to be partially rescued on *Ezh2* loss. No study as yet has studied the phenotypic effect of *Kras* mutation in HSCs during fetal life. Although these data only just reached statistical significance, these in vitro data are supported by my

transplantation data which also demonstrated a loss of phenotypic HSCs in *Kras* mutant mice and is in keeping with published data suggesting a depletion of HSCs in adult life with *Kras* mutation [Sabnis, 2009][Di Genua, 2019]. In addition, my phenotypic data expands on the previous limited studies using Vav-iCre and *Kras* [Tang, 2013] by showing a block in erythroid differentiation with $Kras^{G12D}$ mutation, a finding that would be consistent with the defects in erythropoiesis in human JMML.

The data from the Mx1Cre transplantation models (section 3.3) showed that whereas all K-M mice developed T-cell leukaemia, additional *Ezh2* loss predisposes to a myeloid neoplasm, supporting the notion of a cooperative effect of *Ezh2* and mutant *Kras.* Interestingly, previous studies in the lab suggest that the functional stem cell depletion on transplantation of $Kras^{G12D}$ cells can be rescued by secondary mutations, such as AML1ETO [Di Genua, 2019]. However, my data are the first to suggest an alteration in phenotype, with potential myeloid drive, on *Ezh2* loss. There are well documented problems with transplanting Kras mutant fetal HSPCs, as demonstrated here: an almost universal T-cell leukaemia, either due to intrinsic or extrinsic cellular role; and spontaneous deletion not limited to fetal life which is difficult to control for or monitor. Nevertheless, my data set the scene for further studies to answer important questions about whether *Ezh2* LOF mutations have a role in JMML pathogenesis, including whether they have an ontogeny specific effect.

ii) Developing a model to study the timing of mutations using Fgd5CreERT2

Due to the limitations of transplantation experiments, I optimised the use of primary mice. Neonatal induction with Mx1Cre showed a clear alteration of phenotype compared to induction during adult life, despite the limitations of using this model system. The skin lesions are particularly interesting as neonatal leukaemias and JMML both present with leukaemia cutis

[Niemeyer, 2014][Roberts, 2018], and further study using this, or similar, models may help understand the biology of the rare neonatal leukaemias.

My data shows that there is no spontaneous deletion with Fgd5CreERT2 which has not been reported before. The phenotypic data from K-F mice induced in FL provide very preliminary evidence that this could provide a useful JMML model although further study will be required to elucidate whether $Kras^{G12D}$ induced in FL with tamoxifen can reliably cause to a myeloid leukaemia.

iii) Future work

The complete failure of engraftment with the EEK-V genotypes on transplantation of FL is interesting. Although not in the remit of my study, it would be useful to investigate the functional and molecular consequences of this, for example on HSPC homing. The work described in this chapter using Fgd5CreERT2 induction technique, though aimed in my project at comparing the effects of mutant *Kras* +/- *Ezh2* loss in fetal versus adult cells, could also be used to study other conditional mutations in FL HSCs. It would also be interesting to study further the neonatal mouse model, however this may require targeted cellular inductions such as combinations of Fgd5CreERT2, Flt3CreERT2 and either pan-haematopoietic CreERT2 or specific lineage inductions to elucidate which cells contribute to the skin lesions.

References

Böiers C, Carrelha J, Lutteropp M, et al. Lymphomyeloid contribution of an immune-restricted progenitor emerging prior to definitive hematopoietic stem cells. *Cell Stem Cell*. 2013;13(5):535-548.

Boland MJ, Hazen JL, Nazor KL, Rodriguez AR, Gifford W, Martin G, Kupriyanov S, Baldwin KK. Adult mice generated from induced pluripotent stem cells. *Nature*. 2009 Sep 3;461(7260):91-4.

Booth CAG, Barkas N, Neo WH, et al. Ezh2 and Runx1 Mutations Collaborate to Initiate Lympho-Myeloid Leukemia in Early Thymic Progenitors. *Cancer Cell*. 2018;33(2):274-291.e8.

Braun BS, Tuveson DA, Kong N, et al. Somatic activation of oncogenic Kras in hematopoietic cells initiates a rapidly fatal myeloproliferative disorder. *Proc Natl Acad Sci U S A*. 2004;101(2):597-602.

Brenner S, Whiting-Theobald N, Kawai T, et al. CXCR4-transgene expression significantly improves marrow engraftment of cultured hematopoietic stem cells. *Stem Cells*. 2004;22(7):1128-1133.

Caye A, Strullu M, Guidez F, et al. Juvenile myelomonocytic leukemia displays mutations in components of the RAS pathway and the PRC2 network. *Nat Genet*. 2015;47(11):1334-1340.

Caye A, Rouault-Pierre K, Strullu M, et al. Despite mutation acquisition in hematopoietic stem cells, JMML-propagating cells are not always restricted to this compartment [published correction appears in Leukemia. 2020 Jan 31;:]. *Leukemia*. 2020;34(6):1658-1668.

De Raedt T, Beert E, Pasmant E, et al. PRC2 loss amplifies Ras-driven transcription and confers sensitivity to BRD4-based therapies. *Nature*. 2014;514(7521):247-251.

Di Genua C, Norfo R, Rodriguez-Meira A, et al. Cell-intrinsic depletion of Aml1-ETO-expressing pre-leukemic hematopoietic stem cells by K-Ras activating mutation. *Haematologica*. 2019;104(11):2215-2224.

Dong L, Yu WM, Zheng H, et al. Leukaemogenic effects of Ptpn11 activating mutations in the stem cell microenvironment. *Nature*. 2016;539(7628):304-308.

Gan T, Jude CD, Zaffuto K, Ernst P. Developmentally induced Mll1 loss reveals defects in postnatal haematopoiesis. *Leukemia*. 2010;24(10):1732-1741.

Gazit R, Mandal PK, Ebina W, Ben-Zvi A, Nombela-Arrieta C, Silberstein LE, Rossi DJ. Fgd5 identifies hematopoietic stem cells in the murine bone marrow. *J Exp Med*. 2014 Jun 30;211(7):1315-31.

Gomez Perdiguero E, Klapproth K, Schulz C, et al. Tissue-resident macrophages originate from yolk-sac-derived erythro-myeloid progenitors. *Nature*. 2015;518(7540):547-551.

Herviou L, Cavalli G, Cartron G, Klein B, Moreaux J. EZH2 in normal hematopoiesis and hematological malignancies. *Oncotarget*. 2016;7(3):2284-2296.

Jordan CT. The leukemic stem cell. *Best Pract Res Clin Haematol.* 2007;20(1):13-18.

Khalaf WF, White H, Wenning MJ, Orazi A, Kapur R, Ingram DA. K-Ras is essential for normal fetal liver erythropoiesis. *Blood*. 2005;105(9):3538-3541.

Lizen B, Claus M, Jeannotte L, Rijli FM, Gofflot F. Perinatal induction of Cre recombination with tamoxifen. *Transgenic Res*. 2015 Dec;24(6):1065-77.

Lord A, personal communication from Karolinska Institutet. June 2017. Karolinska SOP for tamoxifen preparation 2016_10_28.

Louka E, Povinelli B, Meira AR. Heterogeneous disease-propagating stem cells in juvenile myelomonocytic leukemia. *BioRXiv.* 2019; May 07. https://doi.org/10.1101/628479.

Matsuda K, Sakashita K, Taira C, et al. Quantitative assessment of PTPN11 or RAS mutations at the neonatal period and during the clinical course in patients with juvenile myelomonocytic leukaemia. *Br J Haematol*. 2010;148(4):593-599.

McGrath KE, Frame JM, Fegan KH, et al. Distinct Sources of Hematopoietic Progenitors Emerge before HSCs and Provide Functional Blood Cells in the Mammalian Embryo. *Cell Rep*. 2015;11(12):1892-1904.

Neo WH, Booth CAG, Azzoni E, et al. Cell-extrinsic hematopoietic impact of Ezh2 inactivation in fetal liver endothelial cells. *Blood*. 2018;131(20):2223-2234.

Niemeyer CM, Kratz CP. Paediatric myelodysplastic syndromes and juvenile myelomonocytic leukaemia: molecular classification and treatment options. *Br J Haematol*. 2008;140(6):610-624.

Niemeyer CM. RAS diseases in children. *Haematologica*. 2014;99(11):1653-1662.

Ntziachristos P, Tsirigos A, Van Vlierberghe P, et al. Genetic inactivation of the polycomb repressive complex 2 in T cell acute lymphoblastic leukemia. *Nat Med*. 2012;18(2):298-301.

Oguro H, Ding L, Morrison SJ. SLAM family markers resolve functionally distinct subpopulations of hematopoietic stem cells and multipotent progenitors. *Cell Stem Cell*. 2013;13(1):102-116.

Pietras EM, Reynaud D, Kang YA, et al. Functionally Distinct Subsets of Lineage-Biased Multipotent Progenitors Control Blood Production in Normal and Regenerative Conditions. *Cell Stem Cell*. 2015;17(1):35-46.

Pronk CJ, Rossi DJ, Månsson R, et al. Elucidation of the phenotypic, functional, and molecular topography of a myeloerythroid progenitor cell hierarchy. *Cell Stem Cell*. 2007;1(4):428-442.

Roberts I, Fordham NJ, Rao A, Bain BJ. Neonatal leukaemia [published correction appears in Br J Haematol. 2019 Jul;186(1):196]. *Br J Haematol*. 2018;182(2):170-184.

Sabnis AJ, Cheung LS, Dail M, et al. Oncogenic Kras initiates leukemia in hematopoietic stem cells. *PLoS Biol*. 2009;7(3):e59.

Schwenk F, Kuhn R, Angrand PO, Rajewsky K, Stewart AF. Temporally and spatially regulated somatic mutagenesis in mice. *Nucleic Acids Res*. 1998 Mar 15;26(6):1427-32.

Stieglitz E, Taylor-Weiner AN, Chang TY, et al. The genomic landscape of juvenile myelomonocytic leukemia [published correction appears in Nat Genet. 2015 Nov;47(11):1333] [published correction appears in Nat Genet. 2016 Jan;48(1):101]. *Nat Genet*. 2015;47(11):1326-1333.

Su IH, Basavaraj A, Krutchinsky AN, et al. Ezh2 controls B cell development through histone H3 methylation and Igh rearrangement. *Nat Immunol*. 2003;4(2):124-131.

Su IH, Dobenecker MW, Dickinson E, et al. Polycomb group protein ezh2 controls actin polymerization and cell signaling. *Cell*. 2005;121(3):425-436.

Tang P, Gao C, Li A, Aster J, Sun L, Chai L. Differential roles of Kras and Pten in murine leukemogenesis. *Leukemia*. 2013;27(5):1210-1214.

Tarnawsky* SP, Kobayashi M, Chan RJ, Yoder MC. Mice expressing KrasG12D in hematopoietic multipotent progenitor cells develop neonatal myeloid leukemia. *J Clin Invest*. 2017;127(10):3652-3656.

Ved N, Curran A, Ashcroft FM, Sparrow DB. Tamoxifen administration in pregnant mice can be deleterious to both mother and embryo. *Lab Anim*. 2019;53(6):630-633.

Xie H, Xu J, Hsu JH, et al. Polycomb repressive complex 2 regulates normal hematopoietic stem cell function in a developmental-stage-specific manner. *Cell Stem Cell*. 2014;14(1):68-80.

Yamada M, Hatta T, Otani H. Mouse exo utero development system: protocol and troubleshooting. *Congenit Anom (Kyoto)*. 2008 Dec;48(4):183-7.

Yoshimi A, Balasis ME, Vedder A, et al. Robust patient-derived xenografts of MDS/MPN overlap syndromes capture the unique characteristics of CMML and JMML [published correction appears in Blood. 2017 Sep 28;130(13):1602]. *Blood*. 2017;130(4):397-407.

Zhang J, Socolovsky M, Gross AW, Lodish HF. Role of Ras signaling in erythroid differentiation of mouse fetal liver cells: functional analysis by a flow cytometry-based novel culture system. *Blood*. 2003;102(12):3938-3946.

Zhang J, Wang J, Liu Y, et al. Oncogenic Kras-induced leukemogeneis: hematopoietic stem cells as the initial target and lineage-specific progenitors as the potential targets for final leukemic transformation. *Blood*. 2009;113(6):1304-1314.

Zhang Y, Patel S, Abdelouahab H, et al. CXCR4 inhibitors selectively eliminate CXCR4-expressing human acute myeloid leukemia cells in NOG mouse model. *Cell Death Dis*. 2012;3(10):e396.

Chapter 4: The effect of leukaemogenic mutation at different stages of gestation

The data in Chapter 3 demonstrated that using FL-derived cells from *Kras* mutant, Mx1Cre transgenic mice can cause a myelomonocytic leukaemia. However, using both a transplantation model or Mx1Cre activation proved technically difficult and relatively unreliable, in addition to the inability to compare adult and fetal activation. Published data have focussed on the initiation of leukaemia in a specific setting, either fetal or adult life [Braun, 2004][Sabnis, 2009][Tarnawsky, 2017], but no study has developed a model to allow comparison of mutation acquisition between different stages of ontogeny. The use of Mx1Cre neonatal and adult mice, as demonstrated in chapter 3-5, clearly shows a differential effect between adult and neonatal leukaemia, in keeping with human disease [Roberts, 2018]. However, as I confirmed, Mx1Cre is 'leaky' and cannot be used to accurately study disease, and so Fgd5CreERT2 offers a potentially more reliable model.

The importance of a model able to compare the effects of mutation induction in fetal versus postnatal life lies in the fact that many human leukaemias, particularly JMML, have been shown to have a fetal origin [Matsuda, 2012][Stieglitz, 2015]. Nevertheless, the reasons for this are not clear and could be extremely valuable for developing new treatment strategies. The prognosis for JMML is particularly poor, with a high relapse rate of ~50% post-HSCT and a 5-year survival of 50-60% despite optimal treatment [Niemeyer, 2008][Locatelli, 2005][Locatelli, 2015]. HSCT carries significant morbidity and mortality, and alternative curative treatments for JMML would therefore be beneficial, e.g. by allowing the identification of fetal cell-specific treatment targets.

4-1 Survival and phenotypic changes associated with the timing of induction of *Kras*^{G12D} mutation

In order to compare the effect of adult or fetal gain of a leukaemogenic mutation, I set up timed matings and breedings to develop WT and K-F fetal or adult mice. Dams were then dosed according to the protocol demonstrated in chapter 3, with a single 2mg of tamoxifen by oral gavage at E14.5, and adult mice aged 6-8 weeks were induced with 4mg daily for 5 days (figure 4.1). Mice were followed up for the development of leukaemia with PB analysed 3 weekly from birth (for fetal mice) or induction (for adult mice) until 12 weeks followed by 4 weekly readouts until 20 weeks (fetal mice) or 24-26 weeks (adult mice) when mice had a final, terminal, readout. Fetal mice had a shorter follow-up as the home office licence stipulated that mice induced *in-utero* had to be terminated by 20 weeks of age.

Table 4-1 summarises the classification used to define different diseases as shown in the figures.

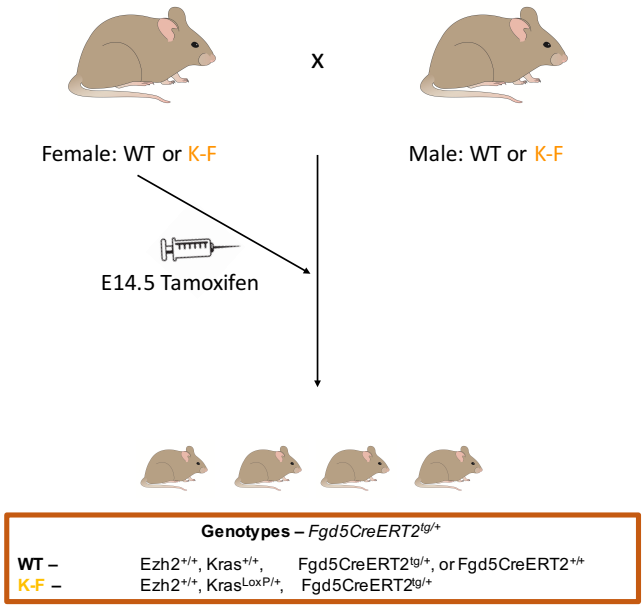


Fig 4.1: Overview of mating strategy and tamoxifen administration to achieve WT and K-F pups. Mice were mated to achieve genotypes shown, using a combination of WT and K-F males and female adult mice. Tamoxifen (2mg) was dosed at E14.5, and pups birthed through terminal caesarian section at E19.5 and fostered to a post-natal day 0-1 female mouse. Mice were monitored and PB readouts 3 weekly between 3 and 12 weeks, then 4 weekly thereafter until 6 months.

	Myeloid disease		***T cell leukaemia***	***Unrelated / No clear cause***
	Myelomonocytic disease	*MPD / AML*		
1	Leucocytosis	Leucocytosis	Leucocytosis (generally extreme >100)	Up to one lineage abnormality on FBC
2	Monocytic population on flow/morphology in PB	Gr1+ expansion on flow or neutrophilia on PB smear	T cell expansion on flow or PB smear	No expanded population on flow cytometry
3	<20% blasts in PB/BM	<20% (MPD) or >20% blasts (AML)	>20% blasts	<20% blasts
4	Splenomegaly	Splenomegaly	Splenomegaly	No splenomegaly
5	Thrombocytopenia	Thrombocytopenia or thrombocytosis	Thrombocytopenia	See '1' above

Table 4-1: Classification of diseases. Criteria used to define disease types in mice found unwell. Mice required the first 3 criteria, followed by one of the other two criteria (spleen size and platelet count). AML (acute myeloid leukaemia), BM (bone marrow), FBC (full blood count), MPD (myeloproliferative disease), PB (peripheral blood).

i) Comparison of survival of FL and aBM-induced mice

In-utero induced mice developed thrombocytopenia rapidly (17-71 post-natal days), which heralded death within the next week, so mice were culled either when they appeared unwell, or when their PB platelet count dropped below $350x10^9$/L. Following mutant *Kras* induction in-utero, mice had significantly shorter survival when compared to adult induction (median survival 51 v 97.5 days, $p<0.001$) (figure 4.2a). Of the fetally-induced mice which died, almost all (10/11 analysed; 91%) K-F mice developed a myelomonocytic leukaemia, the remaining mouse dying of no definable cause, and 3 mice were found dead but were thrombocytopenic in the preceding week. By contrast, in the adult-induced mice, 4/6 developed myeloid leukaemia (67%) and 2/6 developed lymphoid leukaemia. Considering the myeloid leukaemias alone, the FL-induced mice still demonstrated significantly shorter survival (figure 4.2b).

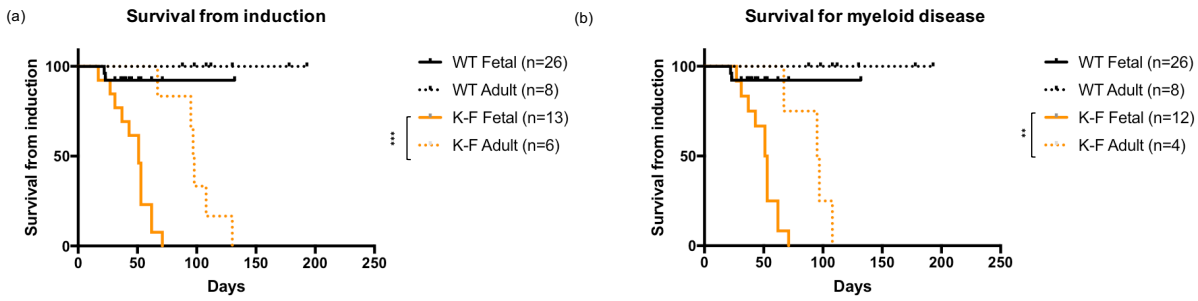


Fig 4.2: Survival of mice from induction. (a) All fetal and adult induced mice (b) Mice developing non-myeloid disease excluded. Fetal cohort measured from birth at E19.5 (5 days following induction) and adult cohort from the end of 5 days tamoxifen administration. Statistical significance determined by Chi-squared analysis. ** p<0.01, *** p<0.001

The reasons for the shorter survival of the FL-induced mice are unclear, but may be due to the rapid expansion and proliferative drive of FL cells, despite a 10-fold lower tamoxifen induction dose in fetal induction. One caveat is that, based on data from using higher doses of tamoxifen *in utero*, the fostering process permits K-F mice to be removed by the foster mothers and it is possible that the K-F mice may be preferentially removed. However, throughout the induction of dams, only small numbers of mice were lost prior to weaning, except where whole litters were cannibalised.

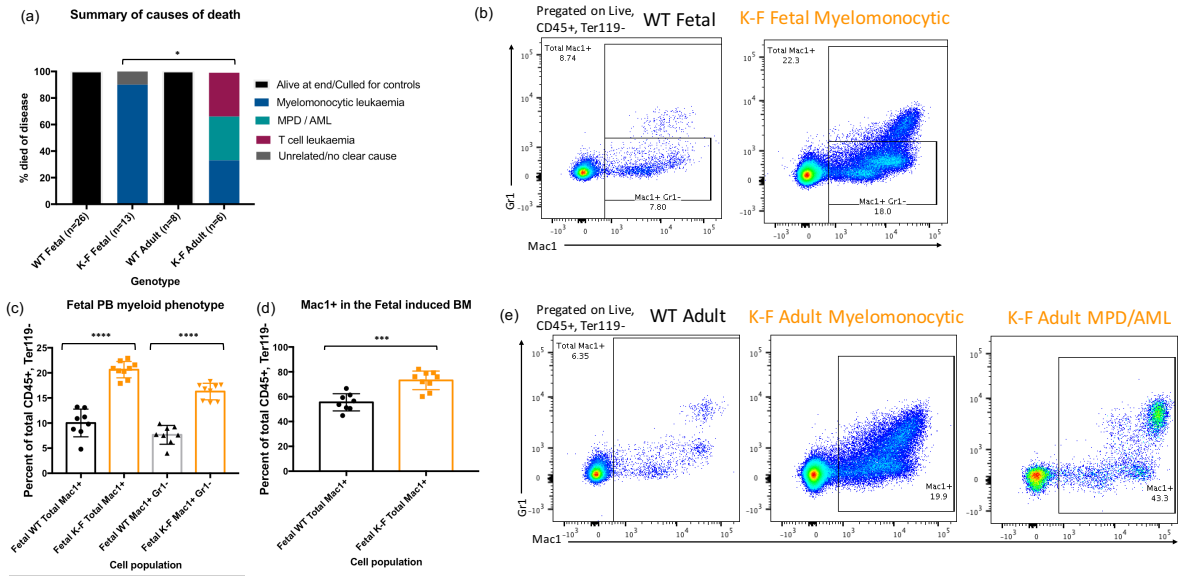


Fig 4.3: Phenotype of fetal and adult-induced mice. (a) Summary of causes of death, excluding those found dead (b) Representative flow plot of fetal K-F (n=9) and Fetal WT (n=8) PB (c) PB phenotype of myeloid cells showing total Mac1+ and total Mac1+, Gr1 negative cells of total CD45, Ter119negative cells (d) Myeloid cells in the BM from fetal induced mice. (e) Representative flow plot of PB from adult WT (n=8), myelomonocytic leukaemia (n=2) and K-F Adult with Gr1 expansion, showing a mouse from the MPD/AML group (n=2). (b-d) showing matched littermate WT controls. Each data point representative of a biological replicate. Statistical significance determined by Mann Whitney U test. * p<0.05, ** p<0.01, *** p<0.001, **** p<0.0001

ii) High frequency of myelomonocytic leukaemia in FL-induced K-F mice

There were also phenotypic differences between induction *in utero* versus adult life (figure 4.3a). Fetal K-F mice almost universally developed a myelomonocytic leukaemia with BM myeloid expansion and none of the mice developed T-cell leukaemia (figure 4.3b-d) while a single fetally-induced K-F mouse (n=1/13) developed pancytopenia with no clear cause. In contrast, adult mice developed a significantly different pattern of disease (p=0.021) with 2/6 developing T-cell leukaemia (figure 4.3a); 2/6 (33%) developing myelomonocytic leukaemia similar to the fetally-induced cases; and 2/6 developing a granulocytic myeloproliferative disease (MPD)/myeloid leukaemia (Gr1+, Mac1+) rather than monocytic (Mac1+ Gr1-), which was not seen in the fetal cohort (figure 4.3e). One of these mice had a mature neutrophilic expansion, the other morphological AML (figure 4.6c-d).

All leukaemic mice were thrombocytopenic, with enlarged spleens (figure 4.4a,c). The white cell count was significantly increased in the K-F FL-induced mice compared to WT controls ($p<0.001$) (figure 4.4d). In the adult-induced K-F mice, the mice with T cell leukaemia and 3/4 mice with myeloid disease also had a raised white cell count (figure 4.4d). Despite these phenotypic features of myeloid leukaemia in the FL-induced K-F mice and 4/6 of the adult-induced mice, there was no increase in the percentage of blasts, except in the aBM-induced mouse with frank AML (figure 4.4b). However, there was a significant increase in the numbers and percentages of monocytic cells in the FL- and aBM-induced KF mice with myelomonocytic disease and almost all of these were dysplastic (figure 4.4b,e).

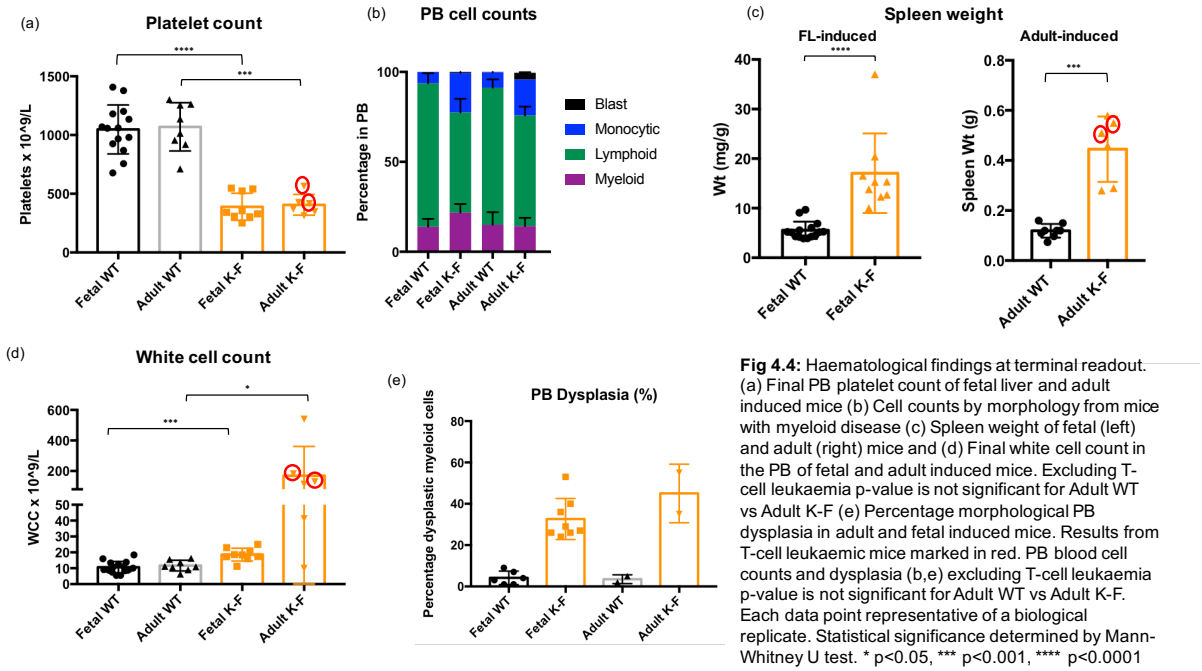


Fig 4.4: Haematological findings at terminal readout. (a) Final PB platelet count of fetal liver and adult induced mice (b) Cell counts by morphology from mice with myeloid disease (c) Spleen weight of fetal (left) and adult (right) mice and (d) Final white cell count in the PB of fetal and adult induced mice. Excluding T-cell leukaemia p-value is not significant for Adult WT vs Adult K-F (e) Percentage morphological PB dysplasia in adult and fetal induced mice. Results from T-cell leukaemic mice marked in red. PB blood cell counts and dysplasia (b,e) excluding T-cell leukaemia p-value is not significant for Adult WT vs Adult K-F. Each data point representative of a biological replicate. Statistical significance determined by Mann-Whitney U test. * p<0.05, *** p<0.001, **** p<0.0001

A surprising feature was that the haemoglobin concentration was raised in the FL-induced K-F mice compared to the WT controls and to the aBM-induced K-F mice (figure 4.5a). To determine whether the increase in haemoglobin was due to an increase in embryonic haemoglobins, isoelectric focussing (IEF) was carried out (by Dr Fisher) (figure 4.5b). However, there was no persistent fetal or embryonic haemoglobin (as evidenced by the E10.5 fetal controls) and the cause for the raised haemoglobin in the fetal cohort remains unclear, although dehydration is a possible explanation. My previous data demonstrated a marked erythroid expansion in the FL, and therefore it is also possible that mutant *Kras* induction may have led to an expansion of HSCs with an erythroid drive and the polycythaemia is an effect of activated cellular pathways. Further analysis of expression of erythroid transcription factors, such as Gata2 and Lin28B [Tsai, 1994][Basak, 2020], would be useful to investigate this further, as well as intracellular pathways including the Stat pathway.

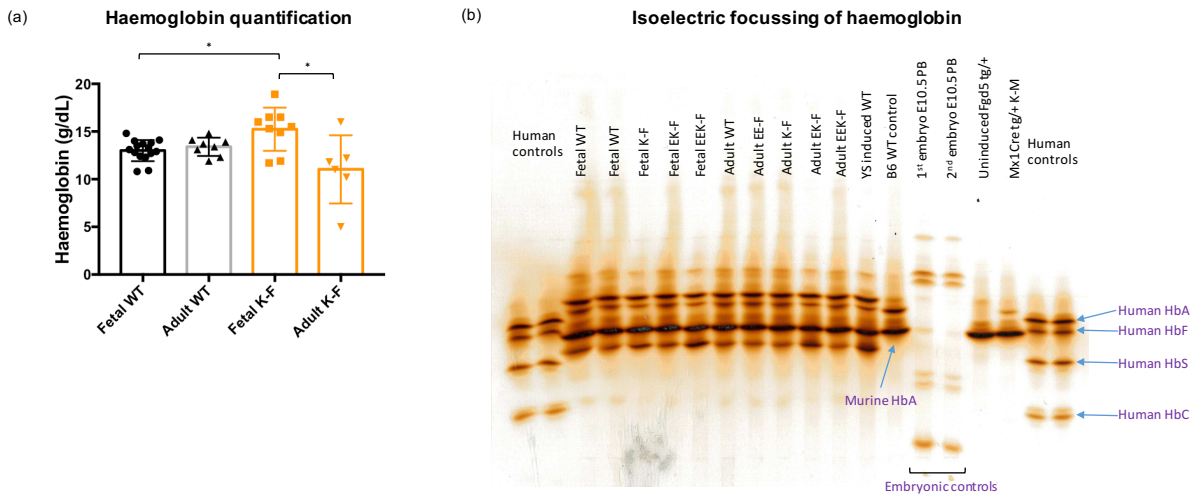


Fig 4.5: Haemoglobin analysis. (a) Haemoglobin at final readout per genotype (b) Isoelectric focussing of haemoglobin across different genotypes in the PB showing all genotypes including EK-F and EEK-F as analysed at the same time in a single experiment. Demonstrating no different haemoglobin between any fetal or adult genotypes. All individual replicates stored at -20, except for B6 and embryo controls, which were fresh. Statistical analysis by Mann-Whitney U test, *p<0.05.

PB morphology demonstrated a significant dysplastic population within the myeloid compartment in fetal mice (figure 4.6a), but no significant increase in morphological blast cells. Mice with T-cell leukaemia and AML or granulocytic expansion were easily identified on the PB smear prior to flow cytometry analysis (figure 4.6b-d). Adult mice with a myelomonocytic leukaemia also demonstrated dysplasia (figures 4.4e, 4.6a).

A single mouse, from the adult K-F cohort had to be excluded retrospectively. Deletion PCR from secondary transplantations showed a heterozygous germline deletion of *Ezh2*, which was confirmed on analysis of BM from the terminal readout of that mouse (appendix 4.1). Analysis of the siblings from the same cohort and other experimental mice showed no other mice with germline deletion (appendix 4.1). Three K-F adult mice were excluded from analysis as following induction they were culled at ~9 weeks of age due to the COVID-19 pandemic and restrictions within the WIMM and analysis. These mice demonstrated a slightly raised WCC, but no other abnormalities on their FBC and did not have an expanded T-cell population.

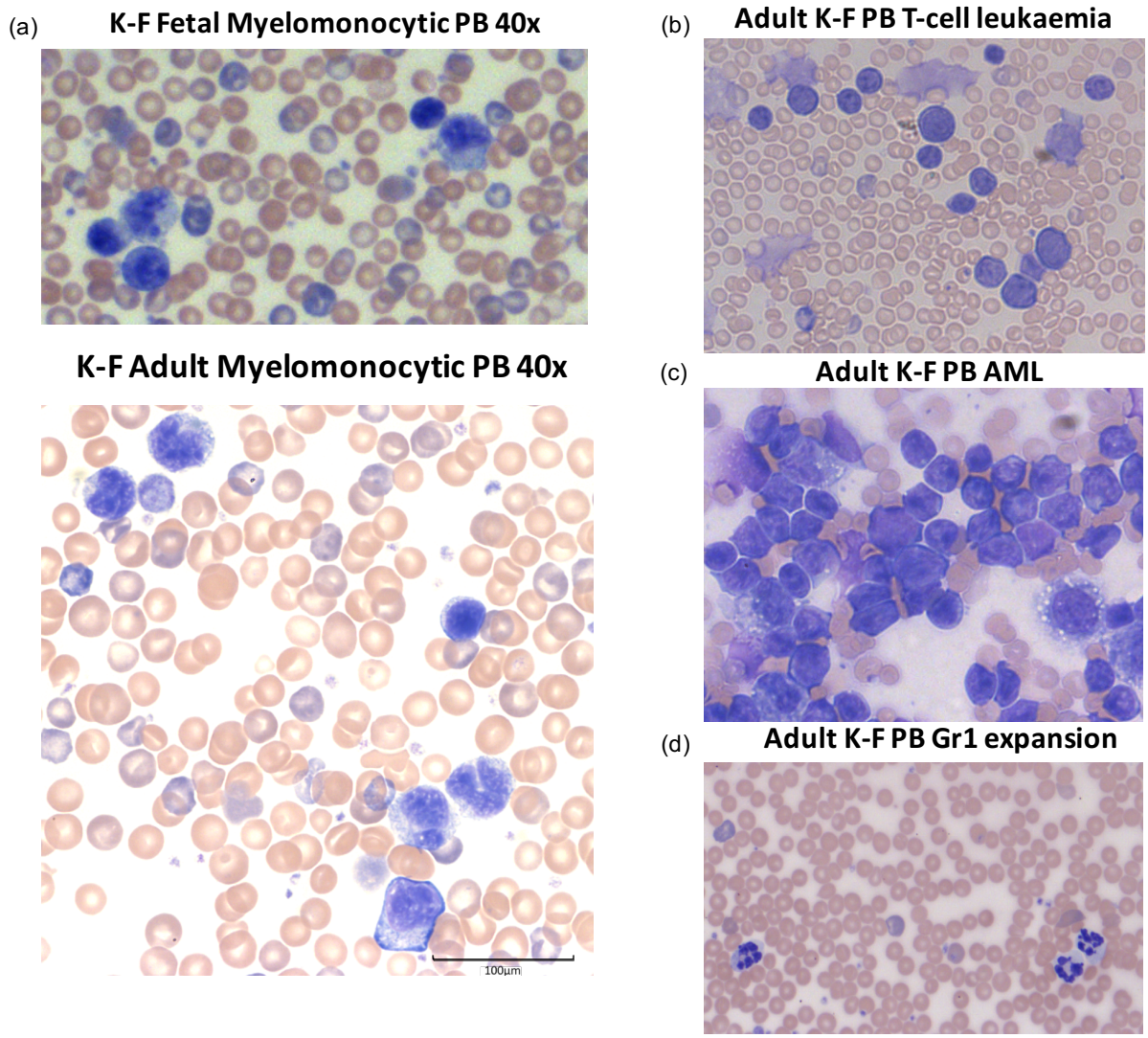


Fig 4.6: PB morphology of primary mice. (a) PB morphology of fetal (top, n=8) or adult (bottom, n=2), mice with myelomonocytic leukaemia. (b-d) Examples of adult mice with other diseases (b) T cell leukaemia, (n=2), (c) AML (n=1), (d) Gr1 expansion (n=1)

iii) Histological changes in tissues from FL- and aBM-induced K-F mice

Fetal- and adult-induced mice had altered bone marrow architecture on histology, including increased monocytes (figure 4.7) and decreased megakaryocytes in keeping with the thrombocytopenia. Adult K-F mice were visibly unwell at the time of death, however, although fetal K-F mice appeared slightly smaller than their peers (appendix 4.2), there were no other signs of impending death. Of note, despite marked thrombocytopenia, there was no obvious bleeding.

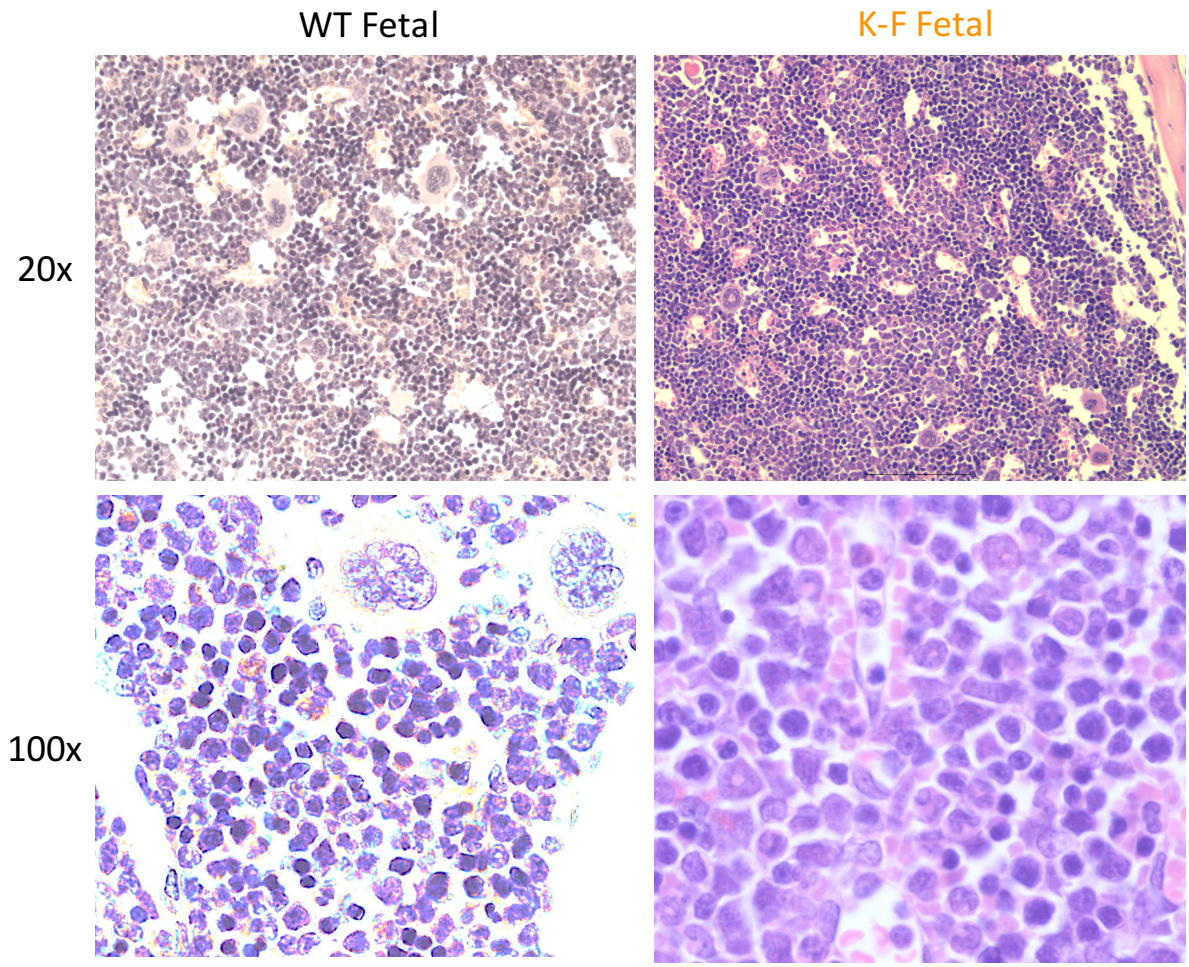


Fig 4.7: Histopathology of BM from K-F fetal mice. (a) H+E stained sections of Fetal K-F BM at 20x and 100x. Representative of 2 biological samples per genotype

Next, as lung infiltrates are well described in JMML [Kimura, 2010][Gustafsson, 2011], and may be a cause of rapid onset of disease and subsequent death, I investigated whether there were any abnormalities of lung histology in the FL-induced mice. Haemotoxylin and eosin staining clearly demonstrates a pathological lung infiltrate of monocytoid cells (figure 4.8) not present in WT mice. Thus, lung infiltration may explain the cause of sudden death in the K-F mice. To further investigate this, more replicates are needed for each genotype (see section 5-3.i) but I could also use immunohistochemical stains to demonstrate co-expression of CD45 and myeloid markers, such as Mac1, thereby confirming a myeloid lung infiltrate.

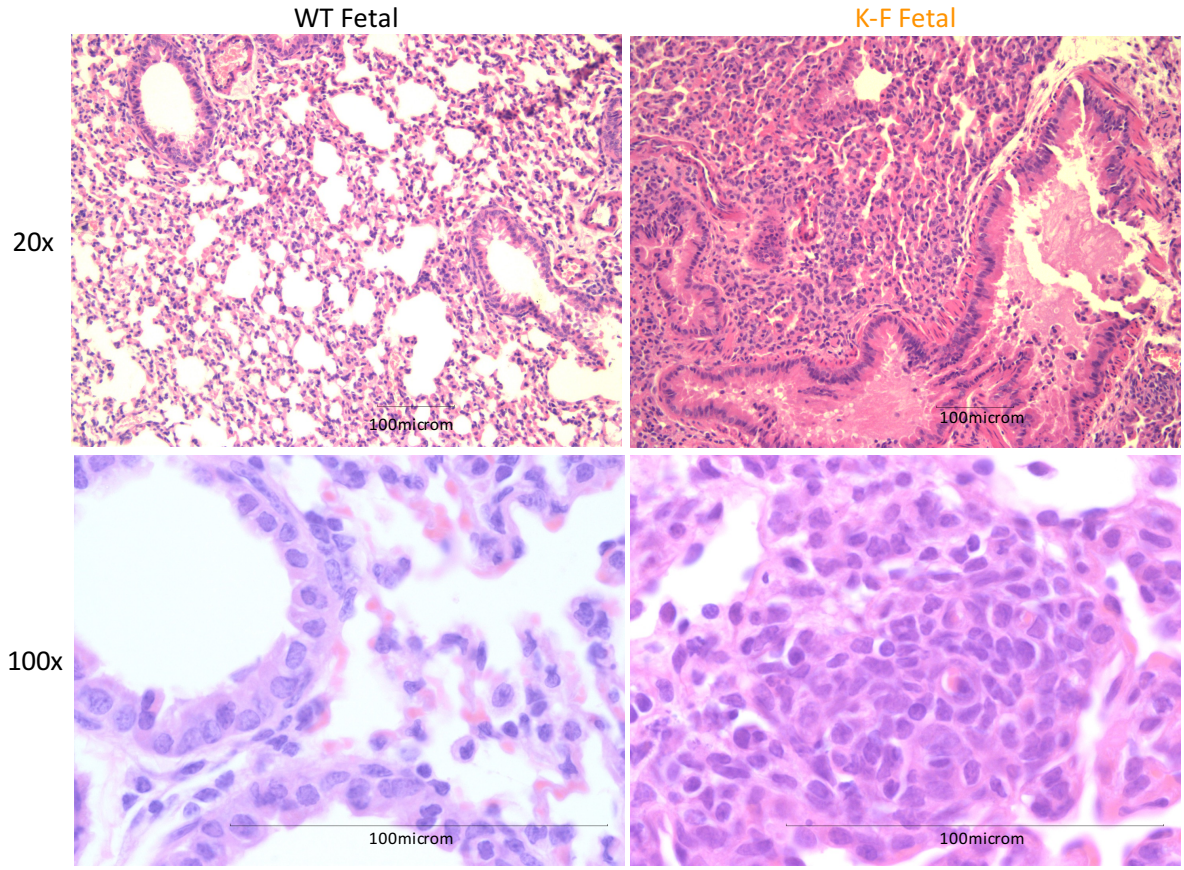


Fig 4.8: Histopathology of lungs. 20x and 100x H+E stains of fixed lung tissues. Representative of n=1 per genotype

iv) Alterations in the HSPC compartments

As there were no significant differences in overall BM cellularity between *Kras* mutant mice and WT mice (figure 4.9a), I went on to analyse the HPSC compartments in detail. There were no significant differences in the total LSK or MPP compartments (figure 4.9b). However, there was a striking difference between FL- versus aBM-induction in the total number of HSCs in leukaemic mice (figure 4.9c). The number of HSCs was significantly reduced in adult-induced K-F mice compared both to their WT controls but also to the FL-induced K-F mice. Whilst the loss of phenotypic HSCs in adult-induced K-F mice would be consistent with my transplant

data and with previous data from our lab [Neo, 2018], the preservation of HSCs in the fetally-induced mice was unexpected. This suggests that the aberrant program leading to proliferation and loss of quiescence in adult HSPCs [Di Genua, 2019] is not present when *Kras* mutation is gained in a fetal HSC, and allowed to expand in a fetal environment. The fetal program may protect the HSCs, allowing proliferation but without loss of their surface phenotype.

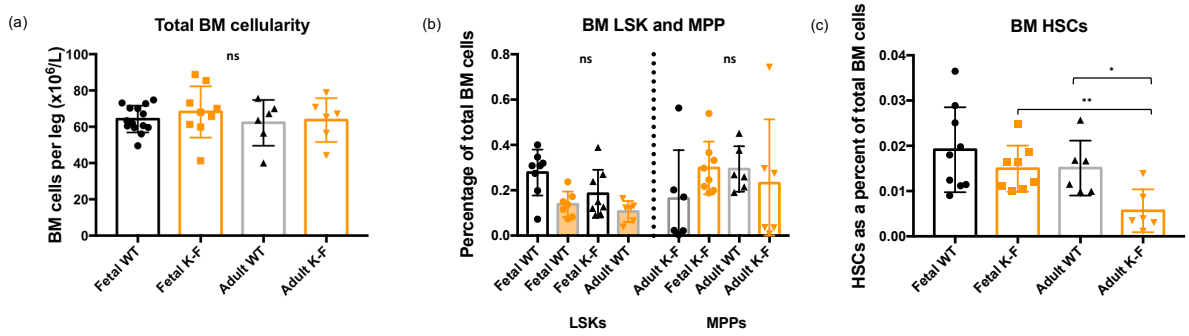


Fig 4.9: Bone marrow LSKs in K-F mice. (a) Total BM cellularity of fetal and adult induced mice and (b) Percent of LSKs and MPPs as a percentage of total cells and (c) HSCs as a percentage of total cells. Each point represents a biological replicate. Statistical significance determined by Mann-Whitney U test. * p<0.05, ** p<0.01

To evaluate the effects on megakaryocyte (MK) and erythroid progenitors I used the Bryder panel [Pronk, 2007] when sufficient cells were available. Both fetal-induced and adult-induced K-F mice had lower MkPs, although this was only statistically significant for the fetally-induced mice (figure 4.10c). The frequency of early erythroid progenitors (pre-CFUe) was also reduced in K-F mice but this reached statistical significance in the adult-induced mice where these progenitors were almost undetectable (figure 4.10b). Although, the overall frequency of LK cells (and to some extent the GMPs) was lower in the adult-induced K-F mice, it is important to note that the analysed mice all had T-cell leukaemia or granulocytic MPD, and no adult K-F mice shown had myelomonocytic leukaemia (figure 4.10a,d).

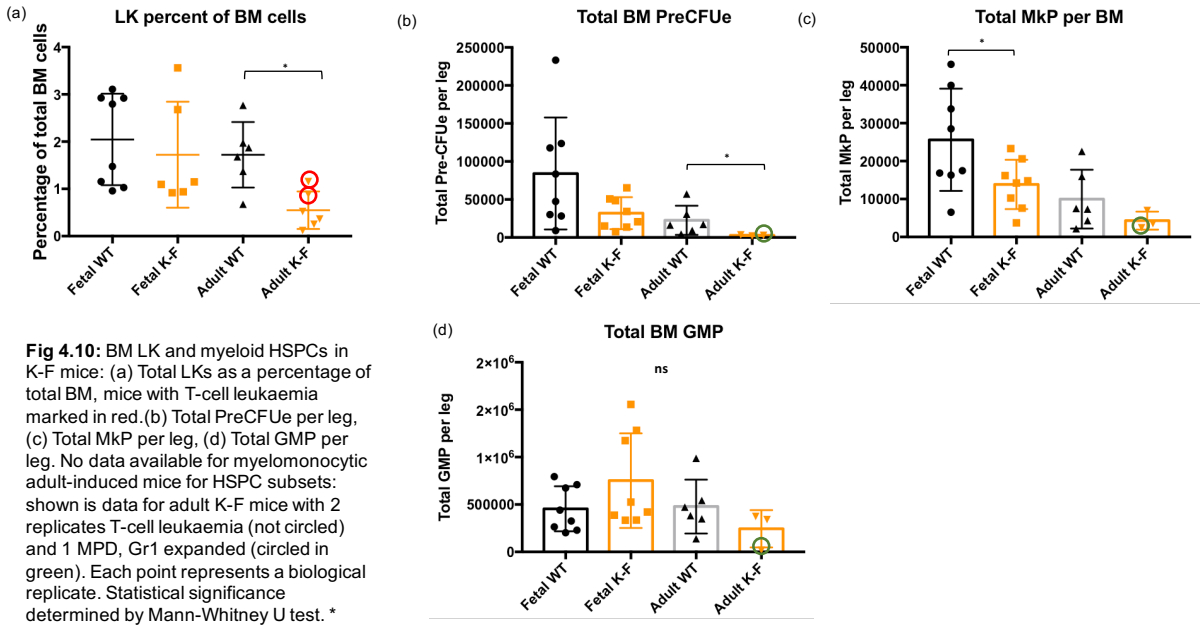


Fig 4.10: BM LK and myeloid HSPCs in K-F mice: (a) Total LKs as a percentage of total BM, mice with T-cell leukaemia marked in red.(b) Total PreCFUe per leg, (c) Total MkP per leg, (d) Total GMP per leg. No data available for myelomonocytic adult-induced mice for HSPC subsets: shown is data for adult K-F mice with 2 replicates T-cell leukaemia (not circled) and 1 MPD, Gr1 expanded (circled in green). Each point represents a biological replicate. Statistical significance determined by Mann-Whitney U test. * $p<0.05$

v) Deletion efficiency using a reporter and molecular methods

To assess the level of recombination in the FL and aBM-induced mice, I assessed dTomato expression by flow cytometry, particularly to ensure that the rapid onset leukaemia deaths in the fetal K-F mice were not attributable to enhanced induction. For the mice in which I had used a dTomato reporter, both WT and K-F aBM-induced mice demonstrated an increase in induction compared to the FL-induced mice (figure 4.11a-b). Both cohorts had no significant dTomato expression compared to their WT comparators. The increased induction frequency by reporter in the aBM-induced mice may simply be reflective of the dose of tamoxifen used (10x higher in adults), or the amount of time to develop leukaemia in this model: in the adult cohort, mice are alive >9 weeks, whereas all fetal mice have succumbed to disease by this time point and thus may not have such strong reporter expression. Despite this, the fetal cohort succumb more rapidly to disease, further suggesting that the dTomato reporter is not representative of deletion at other transgenes.

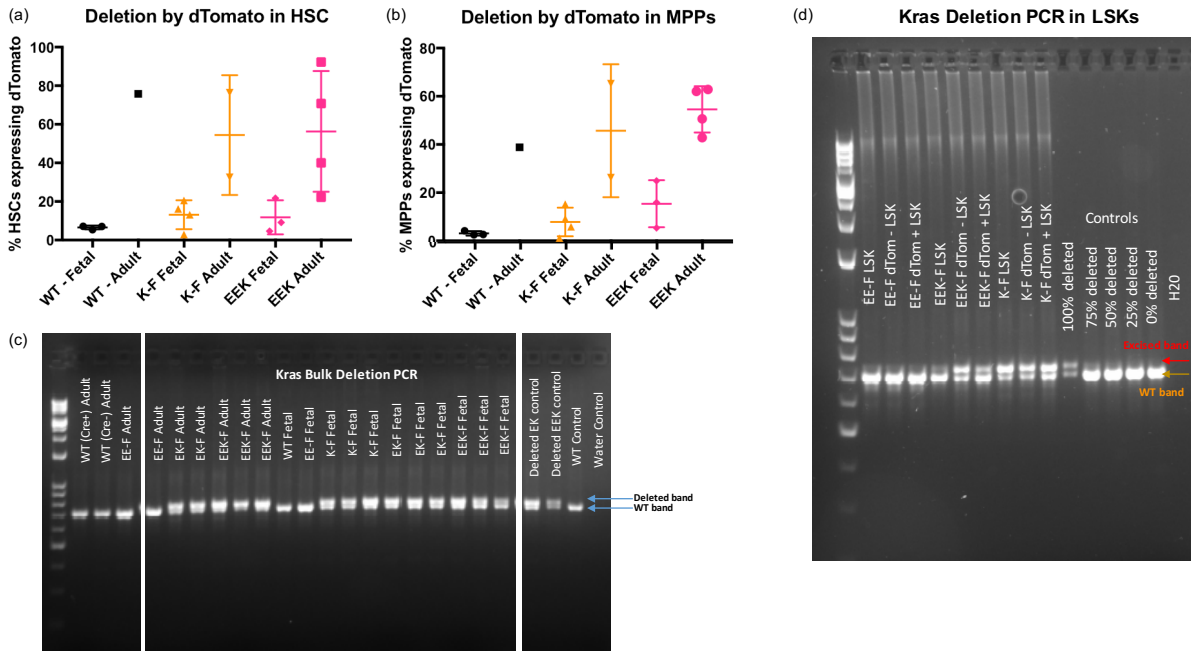


Fig 4.11: Deletion in the LSK compartment in FL- and aBM-induced mutant Kras and Ezh2 deficient mice. Deletion by flow cytometry of dTomato in fetal and adult HSCs (a) and MPPs (b). (c) Kras deletion PCR in bulk spleen of mice at terminal readout. Genotypes shown in figure and bands marked. Gel split to show relevant data.(d) Kras deletion PCR of FACS sorted, genome amplified, FL LSKs across the dTomato+ and negative compartments. Each point represents a biological replicate. Ladders at 100bp

My previous data with Mx1Cre demonstrated that dTomato is representative of some recombination, but is not necessarily representative of recombination of other transgenes. DNA extracted from bulk splenic cells showed clear $Kras^{LSL\text{-}G12D}$ recombination in both fetal and adult induced mice (figure 4.11c). Prior to secondary transplantations, and as a pilot experiment to assess whether HSPCs are significantly $Kras^{G12D}$ recombined I sorted 100 phenotypic LSKs from diseased and WT mice, whole genome amplified extracted DNA, and did a deletion PCR on the resultant material. This demonstrated, by using the previously designed, semi-quantitative PCR, that there was at least 50% recombination in the FL-induced mice LSKs (figure 4.11d). I also analysed Ezh2 recombination in adult and FL induced mice using the same methods, which demonstrated that both have Ezh2 recombination, although it is less prominent in the FL induced cohort (Appendix 4.2a-b). This is further discussed in chapter 5, but suggests that in the FL, *Ezh2*-KO is somehow detrimental, either alone or in combination

with $Kras^{G12D}$ mutation, which is in keeping with my previous Vav-iCre transplantation data (chapter 3).

4-2 The functional consequence of *Kras* mutation in fetal HSPC

My data from the Fgd5CreERT2 model suggests a depletion of the phenotypic HSC compartment when induced in adult life, compared with FL. To assess any functional differences between FL and aBM induction I utilised two methods. Firstly, I used secondary and tertiary transplantations to assess *in-vivo* leukaemic stem cell potential. Secondly, I utilised the *in-vitro* method of serial replating, but in tandem assessed whether the activating Kras mutation led to increased GM-CSF hypersensitivity, as previously shown in mouse models and JMML patient samples [Araki, 2004][Braun, 2004][Niemeyer, 2008].

i) Serial transplantability of mutant *Kras* HSPC

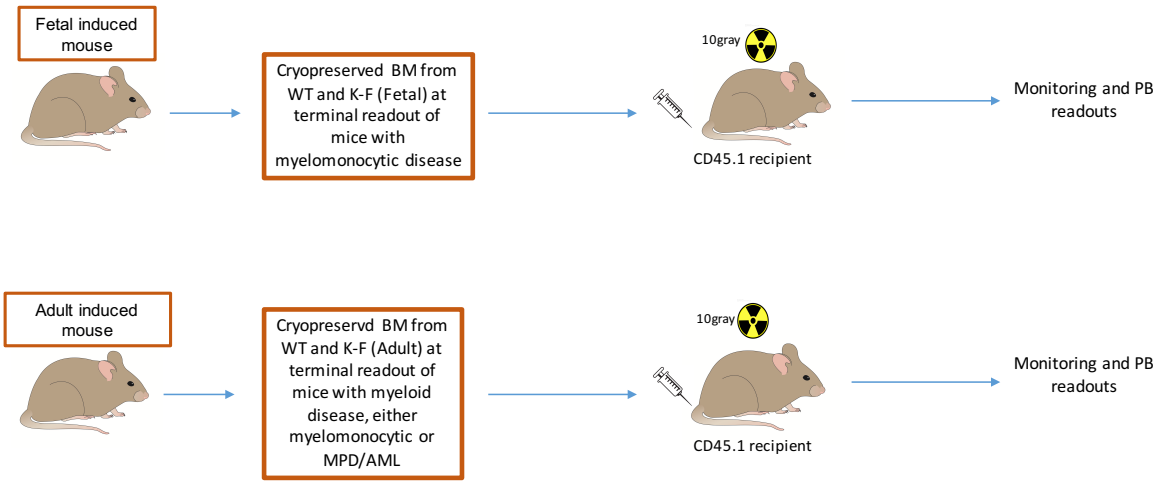


Fig 4.12: Overview of transplantation experiments using cryopreserved BM from primary induced mice. Mice transplanted with BM from myeloid disease (either myelomonocytic disease or MPD/AML). PB taken at 2 weekly intervals until 8 weeks followed by 4 weekly for monitoring engraftment and leukaemia development.

To assess any differences between the stem cell capacity of fetal-induced versus adult-induced myelomonocytic leukaemias, secondary transplantation of BM from sick primary mice was performed (figure 4.12). A total of 8 biological replicates for FL-induced K-F and 6 replicates

for aBM-induced K-F as well as their corresponding WT counterparts were transplanted. Two adult cohort mice from an initial 8 were excluded after a primary mouse demonstrated germline deletion (see chapter 4.1.ii and appendix 4.1). All 4 of the 4 FL-induced K-F mice and 2/3 of the aBM-induced mice had myelomonocytic leukaemia -- the remainder had a myeloproliferative disease -- at the time that the cells were harvested from the first transplant and BM cells from these mice were then used for transplantation with equivalent numbers of WT cells as controls. Unfortunately, 6 K-F and 5 WT mice had to be culled early (at ~8 weeks) because of the closure of our institute due to the Covid-19 pandemic and the risk that the mice would become sick during that time. Therefore, data are available from 5 of the FL-induced and 3 of the aBM-induced secondary transplants. Three of the 5 FL-induced K-F mice again developed myelomonocytic leukaemia but 1/5 developed T cell leukaemia despite being transplanted with mainly myelomonocytic leukaemia cells and one was found dead and could not be analysed (figure 4.13a). By contrast 1/3 aBM-induced K-F secondary transplants developed myelomonocytic leukaemia while 2/3 developed T cell leukaemia (figure 4.13a). Survival of both FL-induced and aBM-induced secondary transplanted mice was reduced compared to their WT controls (figure 4.13b).

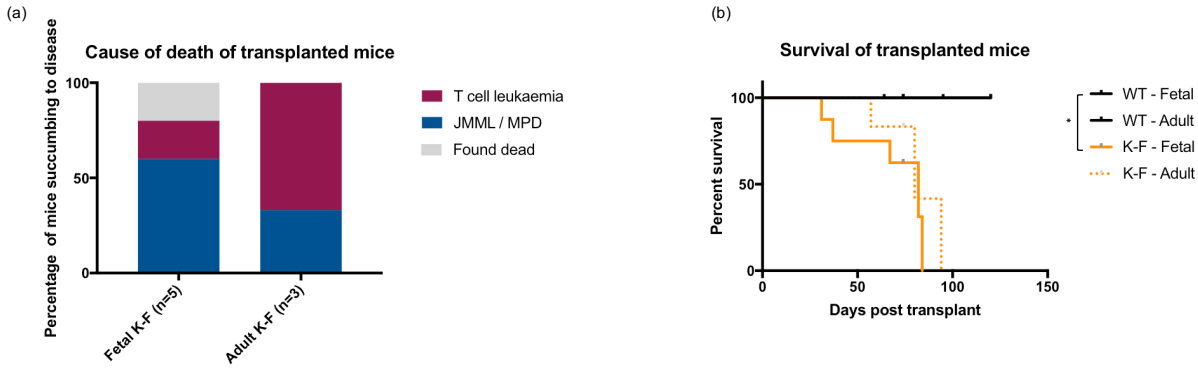


Fig 4.13: Despite the findings in primary mice, T cell leukaemia is still prevalant in the transplantation setting. (a) Summary of causes of death of transplanted mice from Adult and Fetal K-F cryopreserved BM. 3/8 (Fetal) and 3/6 (Adult) K-F mice culled at ~8 weeks due to COVID-19 closure of the facility, impacting on the wellbeing and ability to analyse the animals. (b) Surivival of mice transplanted from either Fetal WT (n=3), K-F (n=5) or Adult WT (n=3), K-F (n=3) cryopreserved BM. Excluding mice culled early due to COVID-19. Statistics by log-rank analysis. * $p<0.05$

These results indicate that the myelomonocytic leukaemias derived from both fetal- and adult-induced K-F mice can be transplanted (figure 4.14a-c), consistent with the presence of leukaemia stem cell activity in the primary transplanted mice. Nevertheless, it demonstrates further that the leukaemic cell population of murine *Kras*^{G12D} mutant myeloid leukaemias are propagated in secondary transplants in only ~50% of cases (4/8 assessable mice). Further, a significant proportion of these mice develop T-cell leukaemia. There may be a number of reasons for this. First my protocol involved transplanting whole BM, including T-cells; second, the need to rapidly reconstitute the host immunity in this transplantation setting and doing so with mutant T-cells; or third, the longevity of T-cells may allow residual mutant T-cells to self-renew and cause T-cell leukaemia even where an earlier myelomonocytic leukaemia has arisen. The T-cell leukaemia incidence at transplantation makes it impossible to assess myeloid disease transplantability and latency in serial transplants.

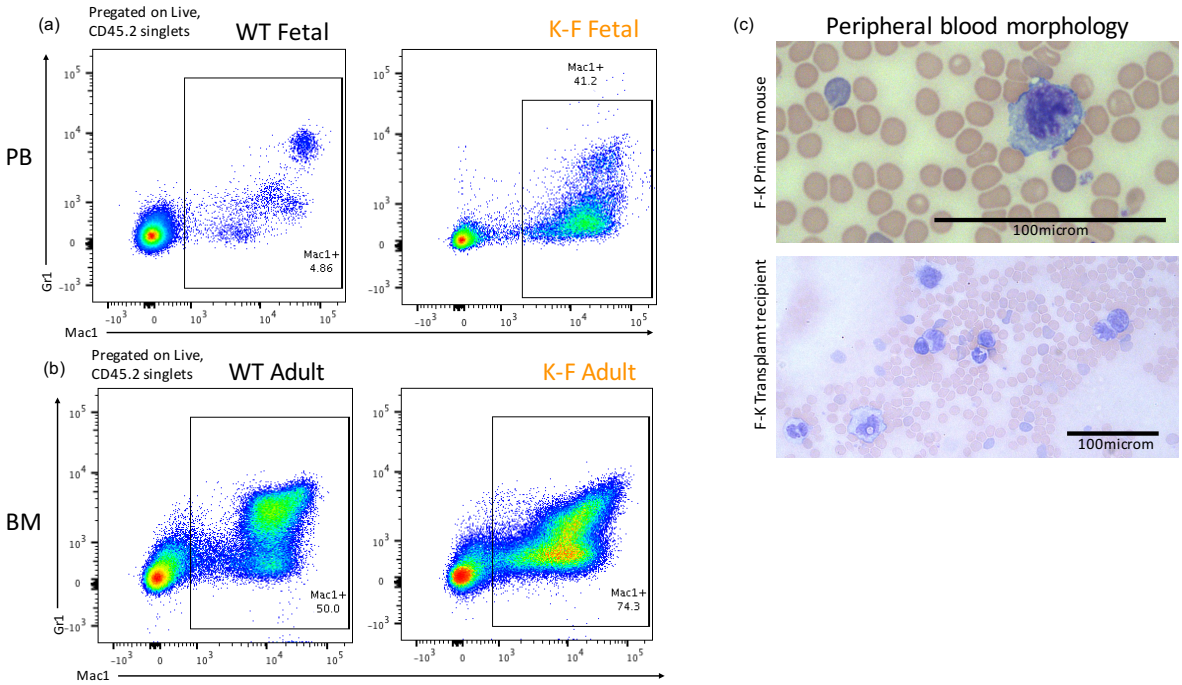


Fig 4.14: Myelomonocytic leukaemia can be transplanted from both adult and fetal and adult induced K-F mice (a) Flow cytometric PB phenotype of mice transplanted from fetal WT (n=3) or K-F (n=3) primary mice, pregated on live, CD45.2 singlets. (b) FACS BM phenotype of mice transplanted from adult WT (n=3) and K-F (n=2) primary mice. (c) PB morphology of blood film showing monocytes of primary FL induced K-F mouse and transplanted recipient. Representative of 3 transplanted recipients.

Finally, I attempted to transplant the myeloid leukaemia from the secondary transplants into tertiary recipient mice (figure 4.15a), to assess if on serial transplantation *Kras* mutant leukaemia cells lost the capacity to repopulate, as previously described [Di Genua, 2019]. This demonstrated engraftment in both fetal-induced KF tertiary transplants (n=4) and aBM-induced KF tertiary transplants (n=5) (figure 4.15b) but by 8 weeks, the level of PB myeloid cell engraftment had started to fall and no mice had developed leukaemia by 8 weeks when these experiments also had to be terminated because of the Covid-19 pandemic.

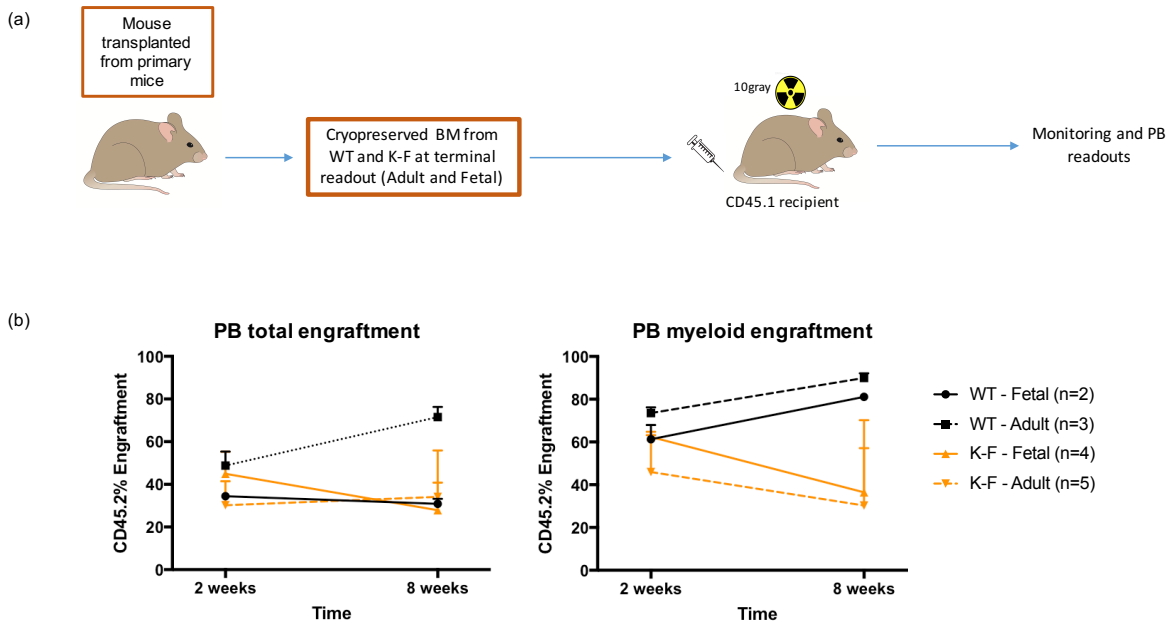


Fig 4.15: Transplantation of secondary transplanted mice into tertiary transplant recipients. (a) Experiment overview (b) Total PB and Myeloid engraftment in PB at serial readouts. Mice culled due to COVID restrictions shortly after 8 weeks. WT-Fetal (n=2), WT-Adult (n-3), K-F Fetal (n=4), K-F Adult (n=5).

ii) *In-vitro* studies: re-plating and GM-CSF hypersensitivity of fetally-induced K-F LSKs

To further investigate stem cell function in mutant *Kras* cells I also performed in vitro replating assays. FACS-sorted LSKs (100/plate) were grown in Methocult M3434 and colony growth assessed after 7 days. At that time individual single cell-derived colonies were replated in

individual wells of Methocult and serial replating was further performed at 7 day intervals until <5 colonies were grown (figure 4.16).

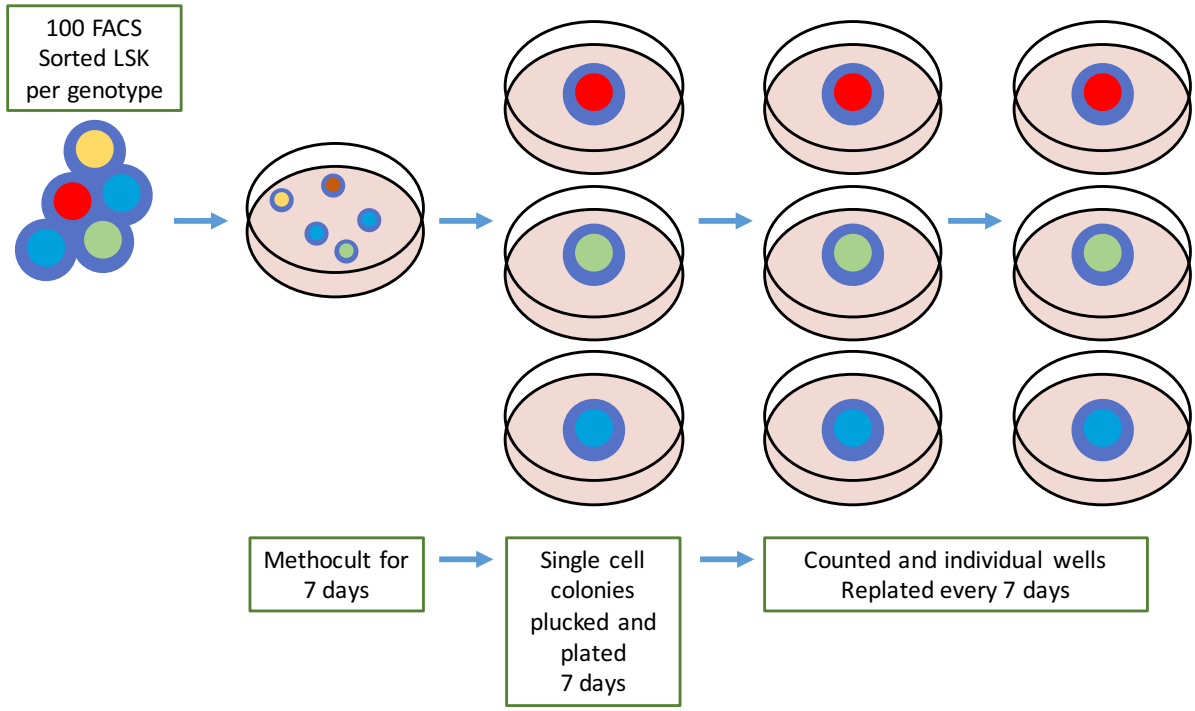


Fig 4.16: Experimental overview of re-plating assays

Overall, there was a small, but significant, increase in the total number of colonies on first plating K-F LSKs compared to their WT control LSK (p=0.026) and on the second replating (p=0.01). There was a similar increase in adult-induced K-F cells but this failed to reach statistical significance (figure 4.17a). LSKs from both K-F and WT genotypes, fetal as well as adult, were able to undergo at least 5 rounds of serial replating although the proportion of both K-F and WT colonies fell progressively and there were no significant difference between them (figure 4.17b).

The increased proliferative ability of fetally-induced K-F LSKs, albeit modest, suggests that fetal-like functionality may persist postnatally when cells gain a *Kras* mutation in fetal life.

Fetal cells are known to be more proliferative, as discussed in chapter 1-1.2 [Morrison. 1995][Busch, 2015].

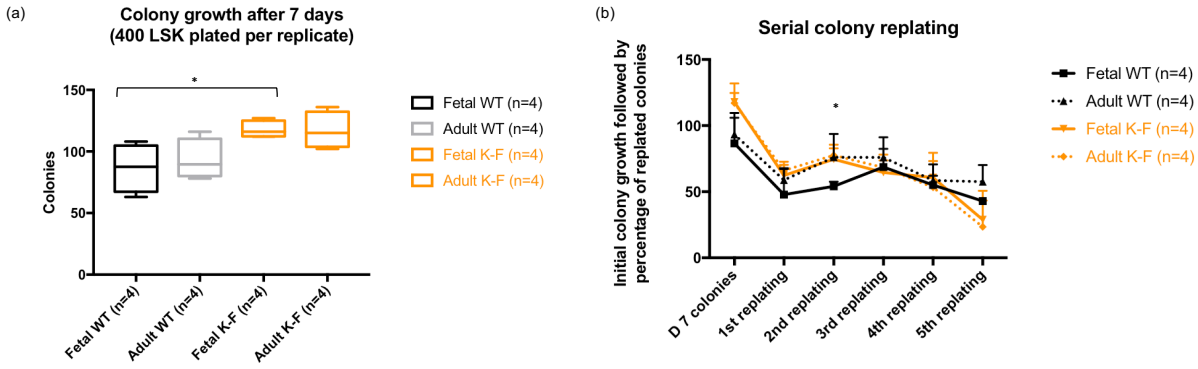


Fig 4.17: Colony replating assays. (a) Box and whisker plots showing min-max and mean from initial colony growth (400 cells per replicate, 4 biological replicates per genotype) and (b) Serial replating every 7 days showing initial colony growth followed by percentage of colonies sucessfully replating over 5 replatings. Statistics by multivariant t-test. *p<0.05

As many mouse models with Ras activation demonstrate GM-CSF hypersensitivity, [Araki, 2004][Braun, 2004], I next assessed this in my mouse model by culturing 100 LSK cells from 4 biological replicates from the four genotypes (fetal and adult WT and K-F) in Methocult M3134 culture in the presence and absence of a range of concentrations of GM-CSF. This showed a significantly greater growth of cells at low levels of GM-CSF in fetally-induced K-F cells compared to WT cells, but no difference between fetal and adult induction (figure 4.18a-b).

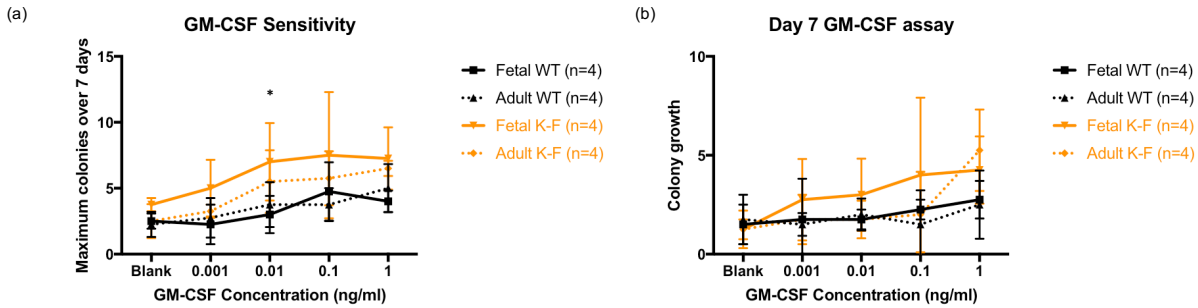


Fig 4.18: Fetal induction leads to borderline GM-CSF hypersensitivity (a) showing maximal colony growth over 7 days with assessment at Days 3,5,7. (b) D7 colony growth. Statistics by Multiivariate t-test. *p<0.05

This would be consistent with a functional effect of an active Ras pathway in these cells, although overall the total growth of these cells in vitro was relatively poor. This likely reflects the culture conditions as, to rigorously test GM-CSF sensitivity, I omitted other exogenous cytokines and utilised a previously published protocol [Tarnawsky, 2018]. This led to a poor overall growth, with generally only clusters of cells, rather than large colonies, suggesting the addition of other cytokines, such as stem cell factor, thrombopoietin, or IL-6 might be needed to facilitate cell growth and survival.

4-3 Cellular origins of fetal induced myelomonocytic leukaemia

i) Identifying leukaemia-propagating cells by transplantation of purified HSPC populations

In order to identify a propagating cell of origin for JMML in my mouse model, I designed an experiment to FACS sort specific HSPC populations (figure 4.19a). I used the phenotypic data from WT BM (figure 4.9) to assess how many of each HSPC population would be found, based on the numbers of HSC, MPP and LKs in WT BM as shown in figure 4.19b. This experiment was particularly difficult because of the low HSPC numbers in *Kras* mutant mice. Example FACS sorting gates are show in figure 4.19c.

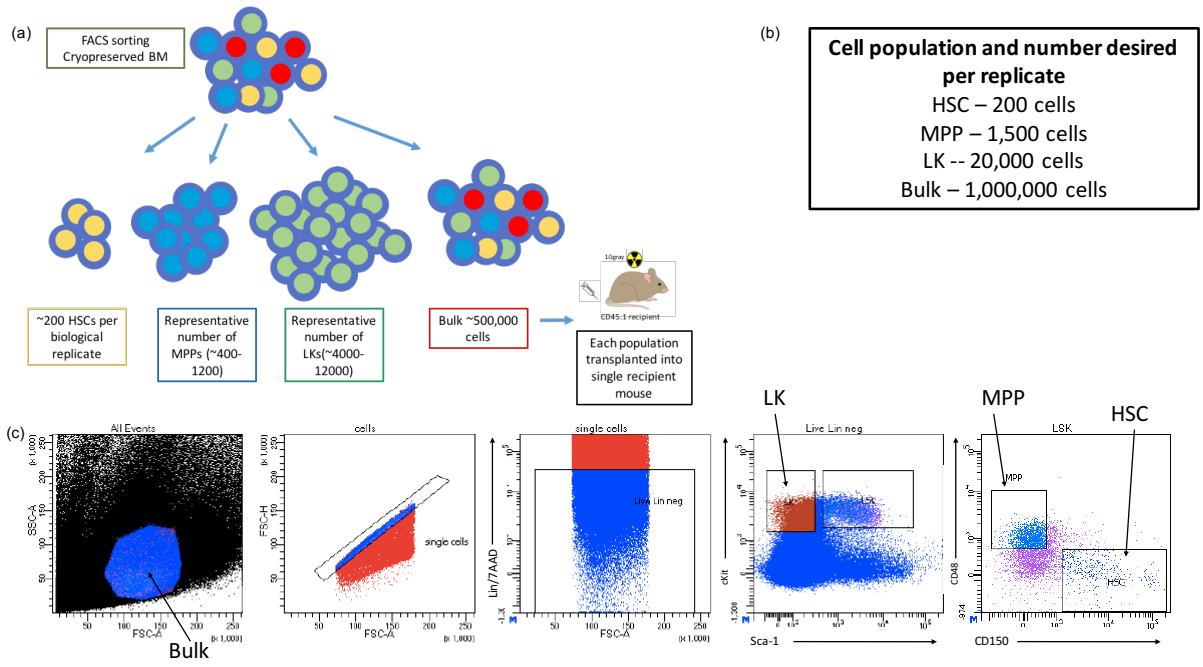


Fig 4.19: FACS sorting of cell populations (a) Overview of transplantation experiment of specific FACS sorted HSPC populations from K-F mice (b) desired numbers of each sorted population and (c) example gating strategy from WT fetal mouse BM

Two readouts, at 4 and 8 weeks were obtained, showed no engraftment of LK cells, but good engraftment of both fetal and adult HSCs (figure 4.20a-b). Engraftment of MPPs was lower overall and was higher in the K-F mice though this was variable and not statistically significant (figure 4.20c). Unfortunately, as a result of the Covid-19 pandemic, further PB monitoring could not be completed and although mice were monitored and the experiment terminated when the mice became ill or died, no analyses to determine the cause of death were feasible.

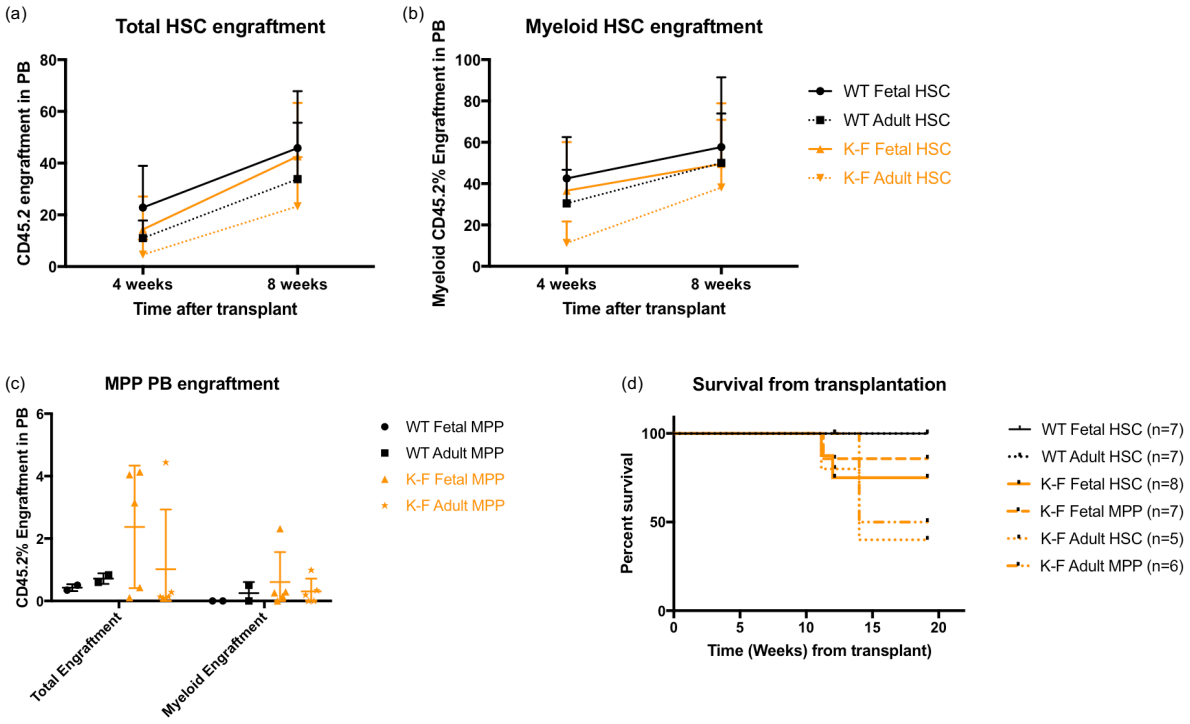


Fig 4.20: Engraftment of HSPC populations from fetally-induced and adult-induced K-F and WT mice. HSC engraftment showing (a) Total and (b) Myeloid specific PB engraftment of mice transplanted with HSCs from fetal or adult WT (n=3 each), Fetal K-F (n=5), Adult K-F (n=3). (c) Total and myeloid engraftment of MPPs from fetal and adult WT or K-F mice at 8 weeks following transplant. (a-c) data from single experiment, 2 primary mice used per genotype. (d) Survival of mice from transplantation. Data from 2 separate experiments. Unable to analyse 2nd experiment for PB reconstitution due to COVID restrictions. Each point represents a transplanted mouse.

Although no WT mice died, 2/5 mice transplanted with fetally-induced K-F HSCs and 1/7 transplanted with fetal MPPs died while 1/3 transplanted with adult-induced K-F HSCs died (figure 4.20d). In addition, 3/5 mice transplanted with whole sorted BM from K-F but not WT HSPC died. Overall these data suggest that transplanted fetally-induced and adult-induced KF HSCs engraft and potentially transmit leukaemia, whereas cells outside the LSK compartment do not. The latency of the disease from HSCs and MPPs is in keeping with the T-cell leukaemia seen in previous transplantation experiments, however given the inability to analyse cause of death it is impossible to further assess whether the myeloid disease is propagated by HSCs or MPPs. To further assess this, and avoiding transplant based models, inducible models using both Fgd5CreERT2 (HSC induced) or Flt3CreERT2 (MPP induced) would be required.

Unfortunately, a repeat experiment also had minimal follow-up and had to be terminated due to the Covid-19 restrictions, but again demonstrated engraftment within all groups.

4-4 Molecular changes associated with induction of $Kras^{G12D}$ in fetal or adult life

RNA sequencing of engrafted HSPCs from K-F versus WT mice was planned but cancelled twice due to the COVID-19 pandemic both due to lockdown and a shortage of the necessary reagents required in COVID-19 testing in March 2020 and November 2020. I had also planned to perform RNA sequencing of HSCs and total LSKs from my Fgd5CreERT2 K-F model, which is induced on HSCs [Gazit, 2014], as this showed almost 100% penetrance of myelomonocytic leukaemia when induced in the FL, but much more heterogeneous disease in the aBM-induced cells, with only ~30% myelomonocytic leukaemia. My aim was to confirm that my mouse model matched human JMML, ie that the leukaemia-propagating cell lies within the LSK/HSC compartment [Caye, 2020][Louka, 2019] and, specifically, to test the hypothesis that a persistent fetal gene expression profile was present in the fetally-induced but not the adult-induced K-F HSPCs. Unfortunately these experiments could not be performed due to the COVID-19 pandemic.

4-5 Don't forget the yolk sac (YS)!

My data so far focusses on induction within the FL. Haematopoiesis, as discussed in Chapter 1-1, begins earlier in the mouse at ~E7.5 within the YS blood islands. Very few studies have addressed this question due to the technical difficulties involved although, interestingly, one study in a *Ptpn11* mutant mouse model showed that although mutant EMPs did demonstrate active RAS pathway signalling, this did not cause disease in a transplantation model [Tarnawsky, 2017]. This may, in part, reflect the problems with transplanting EMPs and YS cells: many papers have tried with variable success to successfully engraft YS derived HSPCs,

but no paper as yet has shown YS-derived leukaemia [Yoder, 1997] [Cumano 2001] [Yoshimoto, 2011] [McGrath, 2015].

Given that JMML patients have a monocytosis with a myeloid leukaemia and erythroid changes in the form of raised fetal haemoglobin, EMPs or early fetal progenitors are a potential target cell of origin. To investigate this, I designed transplantation experiments to assess whether JMML could be derived from *Kras* mutant cells within the YS. In order to assess whether the role of *Ezh2* could be assessed using these techniques, I also used EK-V and EEK-V genotypes for these experiments.

i) Proof of principle: YS derived leukaemia from Vav-iCre transplantation

Initially to assess feasibility, 3 or 4 pooled E10.5 CD45.2 YS from timed matings were transplanted into 3 CD45.1 recipients. This showed an initial wave of myeloid engraftment at ~ 2 weeks (figure 4.21a) with low level persistent engraftment of CD45.2 cells at 10 weeks post-transplant (figure 4.21b). The engrafted cells were not phenotypic HSCs (figure 4.21c), but there were also no cKit positive progenitors, and the majority of remaining cells were Sca-1 lymphoid progenitors (figure 4.21c). These preliminary data show that YS derived precursors can lead to persistence of precursors, in the absence of flow cytometry detectable haematopoietic progenitors. These data are based on analysis of 2 CD45.1 recipient mice as 1 mouse died during injection.

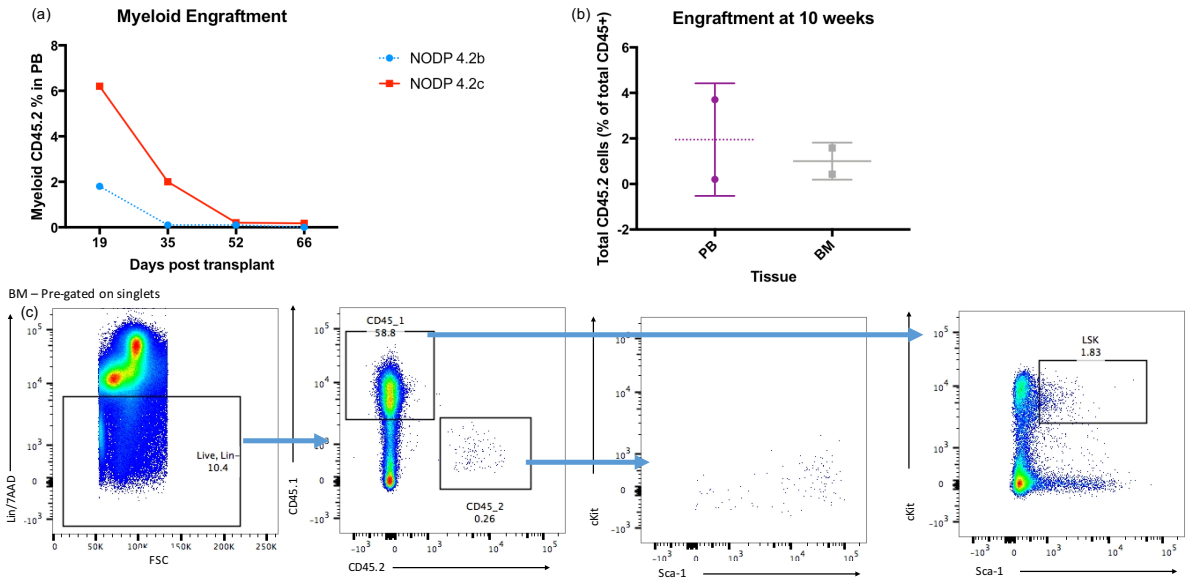
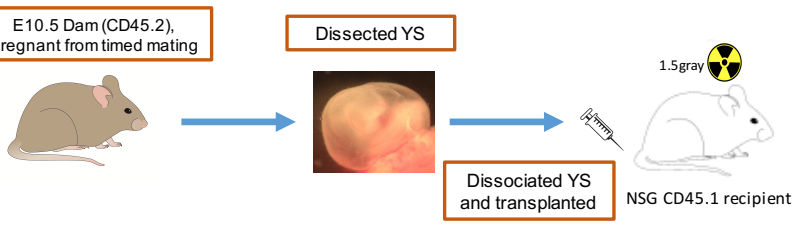


Fig 4.21: Optimisation of yolk sac HSPC transplantation in NSG mice. Engraftment of CD45.2 cells from transplantation of whole, pooled YS into sublethally irradiated CD45.1 NSGs shown as serial myeloid PB engraftment in 2 recipients (a) and total PB and BM engraftment at 10 weeks. (c) Example of BM flow cytometry plots at 10 weeks, showing HSC panel. Representative of 1/2 mice.

To assess further the ability of a single YS to cause leukaemia, in a series of twelve experiments, sublethally irradiated NSG mice were transplanted with single, fresh, dissociated E10.5 YS from timed matings (figure 4.22a) using both Vav-iCre and Tie2-Cre conditional induction (Tie2 data not shown). The number of transplanted embryos per genotype is shown in figure 4.22b.

(a)



(b)

Genotype	Replicate number	Time (weeks) followed up
WT	7	4 >16 weeks, 3 ~12 weeks
EE-V	9	3 >16 weeks, 3 ~12 weeks, 2 died with infection at 2-3 weeks
K-V	3	Kept >12 weeks
EK-V	9	5 kept for >16 weeks, 4 ~12 weeks
EEK-V	4	3 >16 weeks, 1 ~12 weeks

Fig 4.22: Summary of single Vav-iCre YS experiments. (a) overview of experiments and (b) number and genotypes of transplanted mice

These showed early, but variable, engraftment (figure 4.23a), initially with myeloid cells (data not shown) but with evidence of long-term lymphoid engraftment in some mice (figure 4.23b).

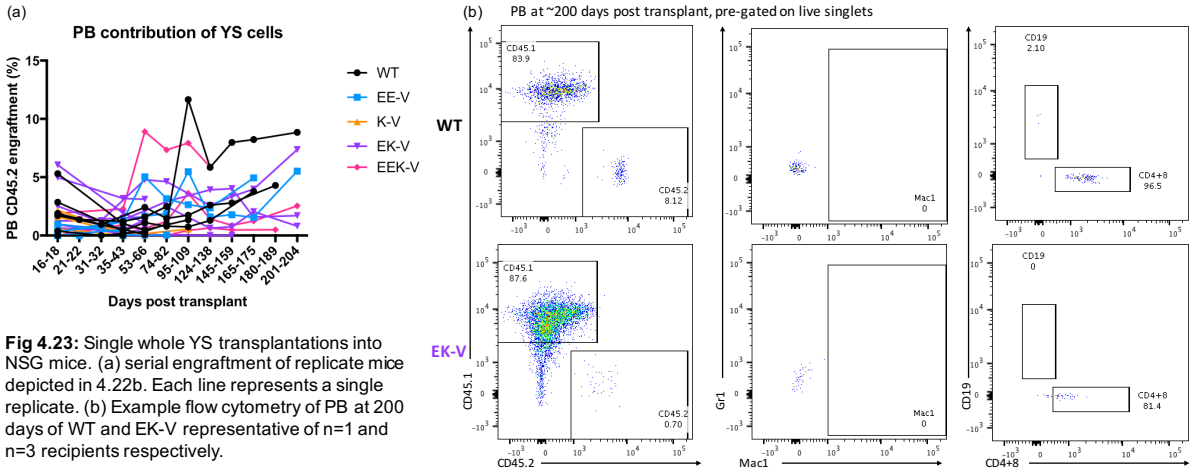
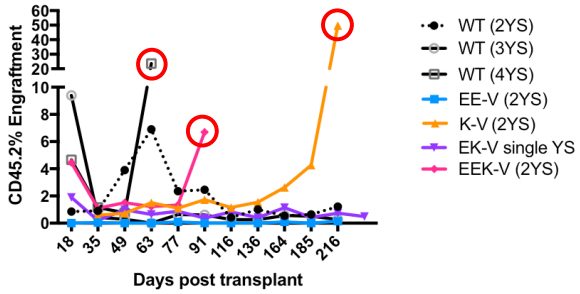


Fig 4.23: Single whole YS transplantations into NSG mice. (a) serial engraftment of replicate mice depicted in 4.22b. Each line represents a single replicate. (b) Example flow cytometry of PB at 200 days of WT and EK-V representative of n=1 and n=3 recipients respectively.

No Vav or Tie2 Cre -transplanted mice developed leukaemia from single YS transplantation experiments, however 3 mice transplanted with 2 pooled YS in a separate Vav-iCre transplant experiment needed to be culled due to disease (figure 4.24a-b). The WT mouse showed donor CD45.2 T-cell expansion, and appeared to have bled within its abdomen, possibly due to infection or graft-versus host disease (figure 4.24b, appendix 4.3). The expansion of CD45.2 donor cells demonstrates the potential for long-term engraftment of YS cells, despite minimal detectable PB contribution during monitoring. It is possible that the YS EMPs migrate to other areas, such as the liver or skin, rather than the BM to repopulate in times of stress, which could be investigated through lineage tracing using inducible models.

The other two mice who died, one from K-V and one EEK-V genotype, each developed leukaemia after transplantation with 2 pooled YS of the same genotype, this higher cell dose potentially being important to ensure long-term engraftment and hence leukaemogenic

(a) **PB Engraftment of pooled transplanted YS**



(b)

	WT (2YS) Survived	WT (4YS) Died	K-V	EEK-V
Hb (g/dL)	12.3	7.2	9.8	5.8
WCC (x10^9/L)	3.2	3.7	6.9	20.5
Plt (x10^9/L)	867	1413	403	527
Spleen wt (g)	0.047	0.16	0.981	5.17

Fig 4.24: Data from pooled YS transplants. In a single experiment two YS with the same genotypes were pooled and transplanted into CD45.1 NSG mice. (a) Serial PB CD45.2 engraftment from mice transplanted with pooled YS of the same genotype. Mice dying early or from disease circled in red. Each line represents a single mouse (b) PB counts and spleen weight of WT (2YS) mouse and the 3 mice that died.

potential. The K-V mouse developed leucocytosis and anaemia ~200 days after transplantation and flow cytometric analysis of the PB and BM showed expansion of CD45.2 donor cells with a B-cell phenotype (figure 4.25a-b) together with a lymphoid infiltrate on histological examination of the BM and spleen (figure 4.25c). The EEK-V mouse developed moderate anaemia and thrombocytopenia (figure 4.24b). Further analysis showed a CD45 negative infiltrate in PB, BM and spleen (figure 4.26a-b), with a massive spleen (figure 4.24b, 4.26c). These cells also expressed cKit and CD71, an erythroid marker (figure 4.26a-b), and morphology of spleen showed effacement by blasts with erythroid morphology (figure 4.26d). To demonstrate that these CD45negative cells were donor-derived, I performed deletion PCR on whole BM and spleen which showed recombination of both *Kras* and *Ezh2* alleles and Vav-iCre expression (figure 4.26e-f).

Mice were kept for between 16 and 52 weeks, and these were the only two leukaemias. A decision was made to terminate the remaining mice, as although the YS leukaemias were extremely interesting, they did not yield a myelomonocytic leukaemia. Terminated mice were analysed, and demonstrated LT engraftment in all genotypes in BM and spleen (appendix 4.4). Four other mice died during the course of the experiment, however these demonstrated minimal

CD45.2 or negative engraftment, with no splenomegaly and an expansion of CD45.1

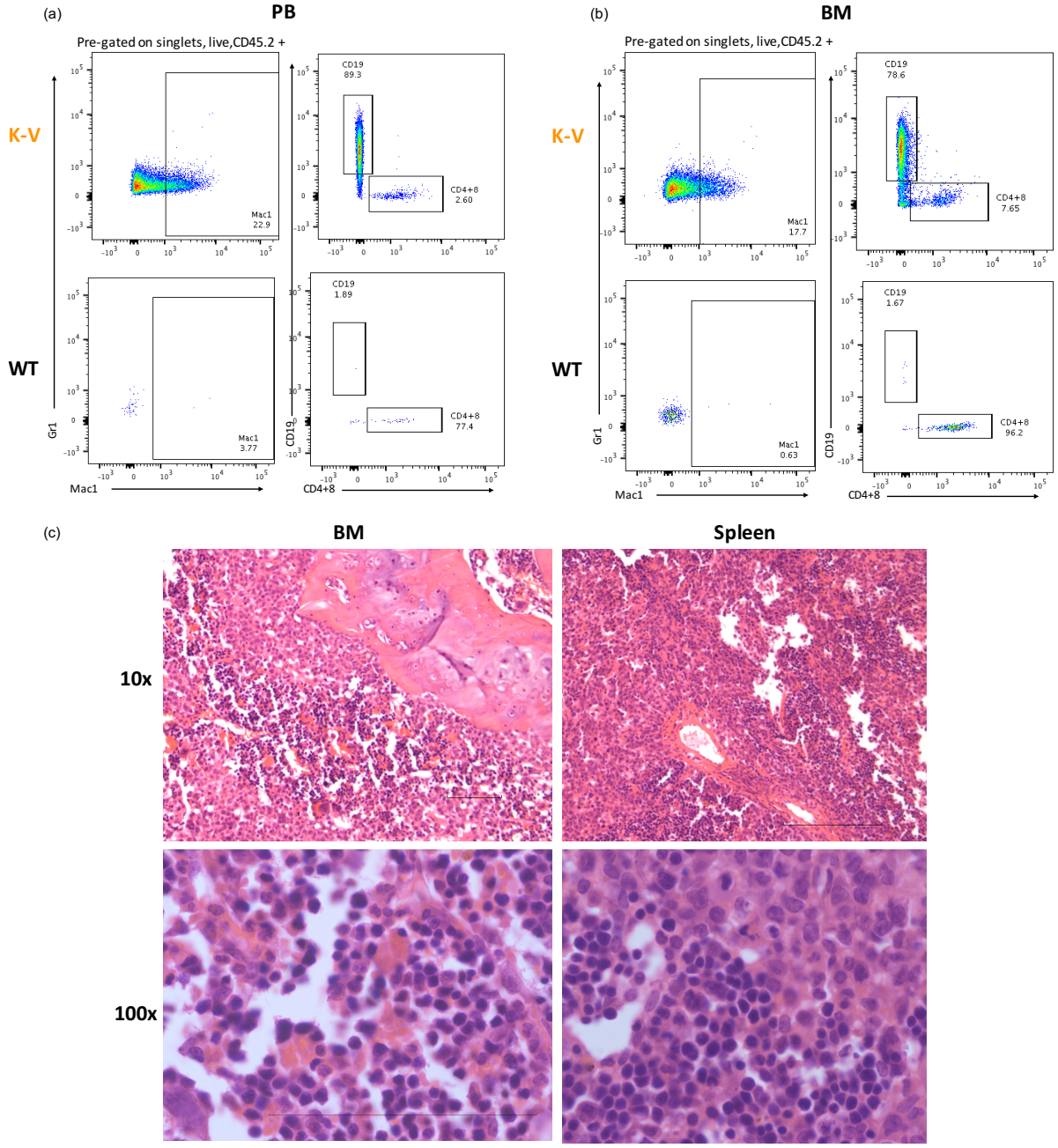


Fig 4.25: Analysis of PB, BM and spleen from the YS-derived K-F leukaemia. K-V YS sick transplanted mouse FACS plots. (a) K-V and WT transplanted mice FACS of PB cells and (b) BM cells. Pre-gated on CD45.2+, live singlets. (c) Histology of BM and Spleen from K-V YS transplanted mouse. Stained with MGG, images taken at 10x and 100x magnification. Showing infiltrates of lymphoid cells in both BM and spleen.

myeloid cells, suggestive of infection. This is not unexpected in the NSG cohort, due to the lack of adaptive immunity.

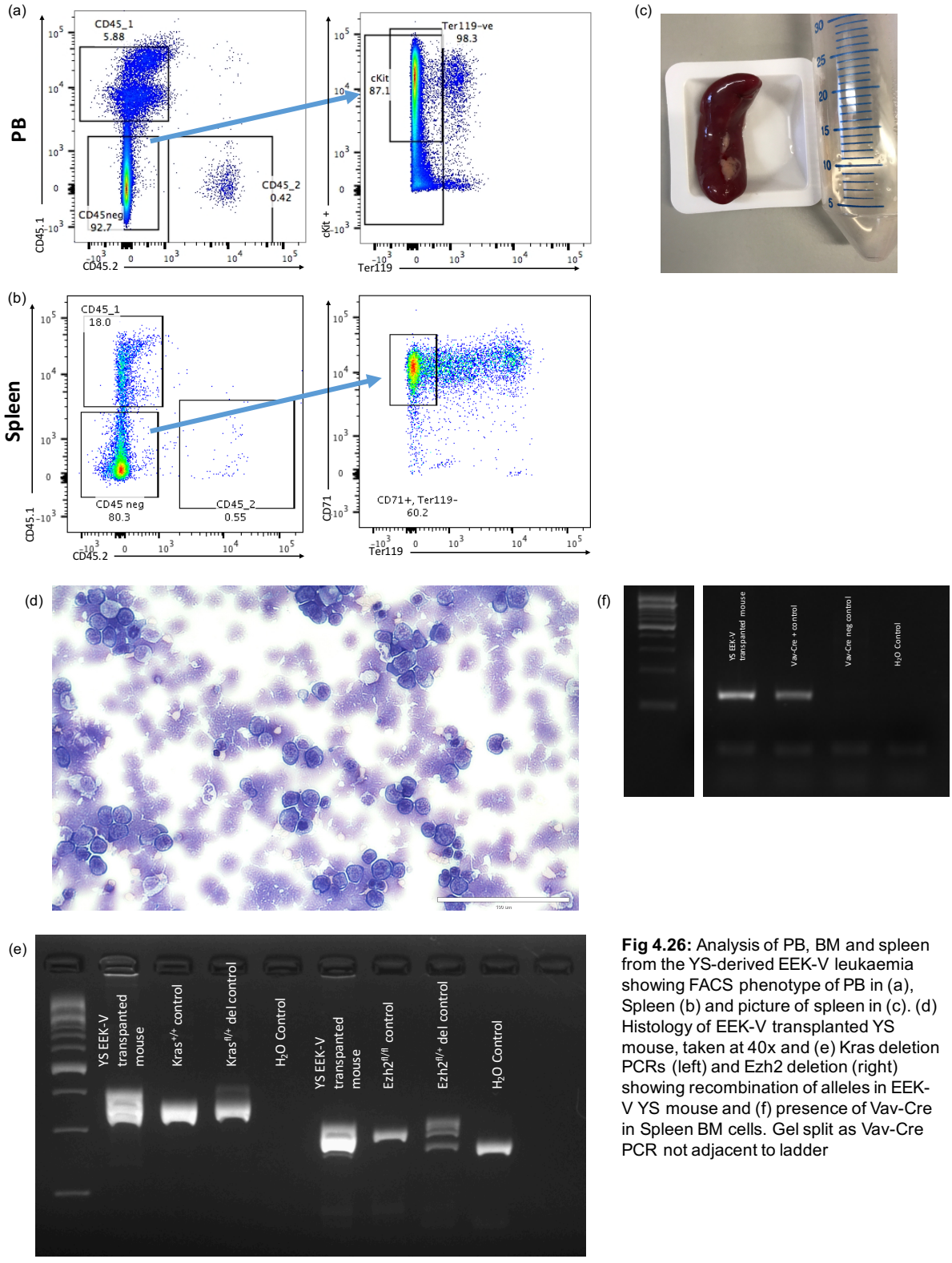


Fig 4.26: Analysis of PB, BM and spleen from the YS-derived EEK-V leukaemia showing FACS phenotype of PB in (a), Spleen (b) and picture of spleen in (c). (d) Histology of EEK-V transplanted YS mouse, taken at 40x and (e) Kras deletion PCRs (left) and Ezh2 deletion (right) showing recombination of alleles in EEK-V YS mouse and (f) presence of Vav-Cre in Spleen BM cells. Gel split as Vav-Cre PCR not adjacent to ladder

Finally, cryopreserved BM from the two mice with leukaemia and a WT control with long-term engraftment of YS-derived cells were transplanted into secondary CD45.1 C57Bl/6

recipients. None of these mice subsequently showed long-term secondary engraftment. One mouse showed temporary B-cells engraftment in the PB (1/3 mice transplanted with leukaemic primary BM engrafted with K-F YS-derived cells) (appendix 4.5), but these were not persistent and all mice survived to 16 weeks. As it is possible that YS derived leukaemia does not transplant well, and requires a more tolerant environment to develop, secondary transplantation into NSG mice may have produced different results.

In summary, these data are the first to demonstrate the YS potential for leukaemia. However, as none of these leukaemias were myelomonocytic or resembled JMML, I was unable to pursue these interesting results further. Otherwise, it would have been potentially interesting to evaluate YS engraftment and leukaemogenesis with different Ras pathway mutations, as well as cell sorting the different populations within the YS. In addition, evaluation with lineage tracing, and potentially bioluminescent analysis, could be undertaken to assess where the YS cells engraft, given their apparent potential for long-term engraftment despite the apparent lack of PB contribution, demonstrated by the ability to expand in times of stress and persistence of lymphoid precursors.

ii) YS Erythro-myeloid progenitors (EMPs) have surface expression of Fgd5, which is inducible

Whilst my data proves the principle that the YS cells can undergo leukaemic transformation following expression of certain oncogenes such as mutant *Kras*, to specifically assess the transformability of EMP would require large numbers of embryos, particularly since it is known that engraftment of WT EMP is poor [McGrath, 2015]. Therefore, to assess whether YS derived EMPs can cause leukaemia I designed a novel *in-vivo* model.

Using Fgd5CreERT2, which carries a ZsGreen fluorescent cassette within the transgene, I used flow cytometry to assess the E9.5 and E10.5 YS, which demonstrated that EMPs have cell surface expression of Fgd5 (figure 4.27a-b). Further phenotypic assessment could be undertaken by whole mounting embryos to assess where the fluorescent cells sit, or through molecular methods to ensure that the Fgd5 gene is expressed, however I investigated whether this surface expression translated into a functional capacity to induce mutation through the CreERT2 transgene.

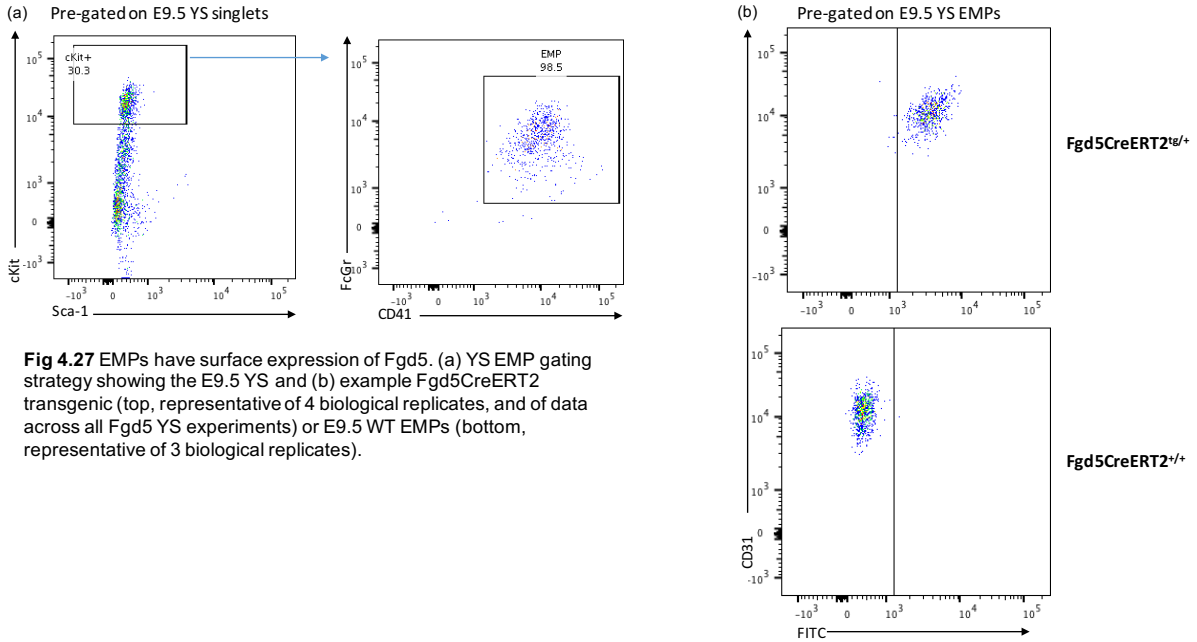


Fig 4.27 EMPs have surface expression of Fgd5. (a) YS EMP gating strategy showing the E9.5 YS and (b) example Fgd5CreERT2 transgenic (top, representative of 4 biological replicates, and of data across all Fgd5 YS experiments) or E9.5 WT EMPs (bottom, representative of 3 biological replicates).

Timed matings were set with *dTomato*$^{fl/fl}$ reporter mice, and *Fgd5CreERT2*$^{tg/+}$ males. Females were given 4mg tamoxifen by oral gavage at E8.5 and E9.5, and YS EMPs assessed by flow cytometry at E10 and E11 respectively. This demonstrated significantly better induction at E8.5 (figure 4.28a-b). The earlier induction may be better for many reasons. First, because induction at E9.5 means assessing induction at E11, by which time EMPs have begun migrating. Secondly, as HSC emergence begins at E10.5 [Medvinsky, 1996][de Bruijn, 2000], earlier induction is beneficial to avoid AGM/FL HSC induction.

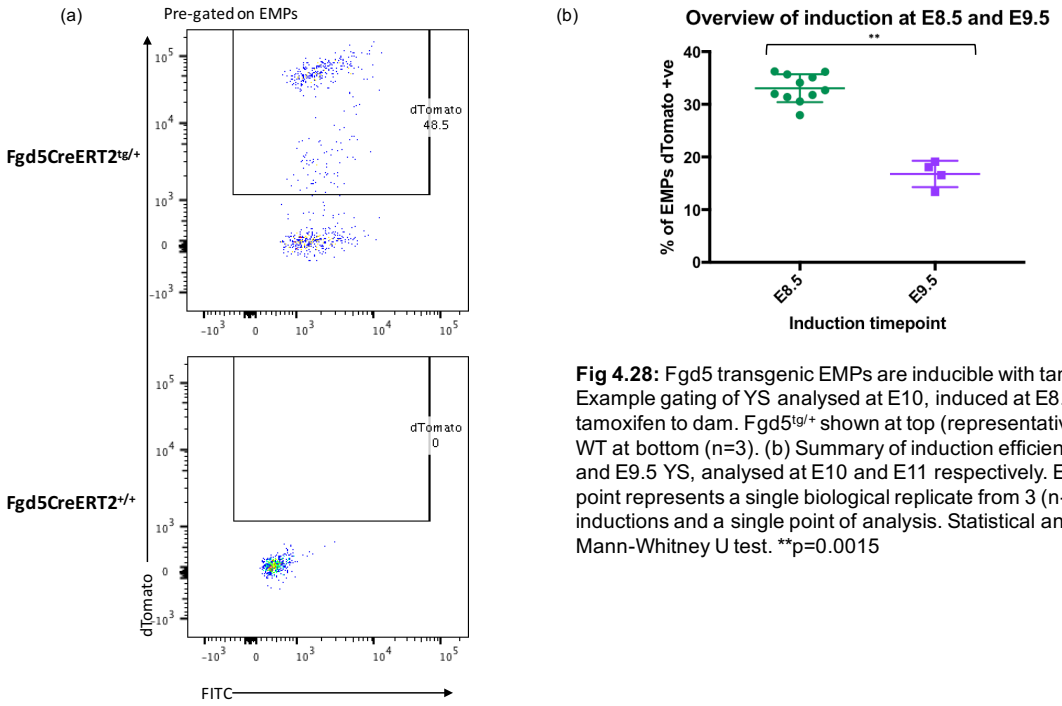


Fig 4.28: Fgd5 transgenic EMPs are inducible with tamoxifen. (a) Example gating of YS analysed at E10, induced at E8.5 with 4mg tamoxifen to dam. Fgd5$^{tg/+}$ shown at top (representative of n=11), WT at bottom (n=3). (b) Summary of induction efficiency in E8.5 and E9.5 YS, analysed at E10 and E11 respectively. Each data point represents a single biological replicate from 3 (n-2 for E8.5) inductions and a single point of analysis. Statistical analysis by Mann-Whitney U test. **p=0.0015

iii) Optimising the induction of EMPs

In order to assess YS and EMP leukaemic potential, I optimised a recombination strategy to delivery adequate YS induction of leukaemogenic mutations, but without inducing HSCs. Using 2mg tamoxifen at E7.5 and E8.5 demonstrated good recombination in EMPs (figure 4.29b). However, as there was still dTomato expression within the LSK compartment in the E16.5 FL using E8.5 induction (figure 4.29a), I decided to induce only at E7.5.

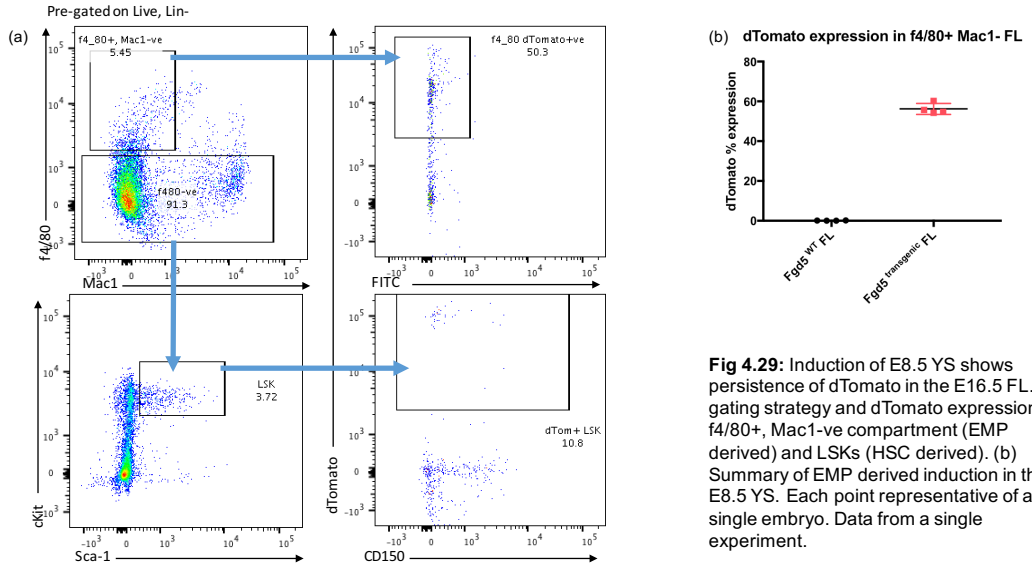


Fig 4.29: Induction of E8.5 YS shows persistence of dTomato in the E16.5 FL. (a) gating strategy and dTomato expression in f4/80+, Mac1-ve compartment (EMP derived) and LSKs (HSC derived). (b) Summary of EMP derived induction in the E8.5 YS. Each point representative of a single embryo. Data from a single experiment.

Using 2.5mg tamoxifen with progesterone 1.25mg (to prevent miscarriages, as per Gomez-Perdiguero et al, 2015) at E7.5 delivered good induction within the EMP derived progenitors, but with very little LSK and HSC compartment induction at E16.5 (figure 4.30a), and so this dose was used to induce EMPs and generate primary mice. Unfortunately, after 5 further attempts to give this dose to dams at E7.5 all resulted in miscarriage, with no mice carrying past E14.5. This is a known problem with oestrogens in pregnancy in mice, particularly in early or late gestation, and so I decreased the tamoxifen dose from 2.5mg to 2mg. Unfortunately, this was unsuccessful as the dams miscarried. Finally, however, using 1.5mg tamoxifen with 0.75mg progesterone allowed the dams to carry to term and I could demonstrate induction of EMPs at E10.5 (figure 4.30b-c).

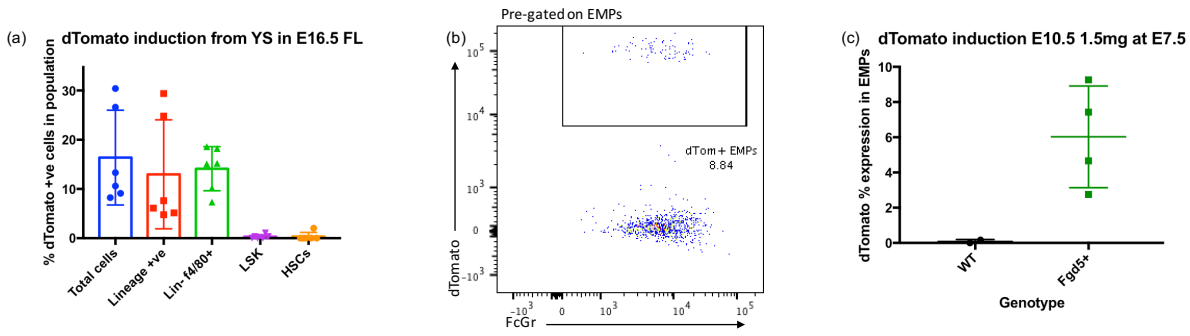


Fig 4.30: Optimisation of tamoxifen dosing. (a) Fgd5 transgenic, dtomato fl/fl FL at E16.5 following induction with 2.5mg tamoxifen at E7.5. Each data point represents a biological replicate (n=6) from 3 separate experiments. (b) Representative induction by using 1.5mg tamoxifen at E7.5 and analysis at E9.5. Representative of 4 separate replicates from a single experiment. (c) Summary data showing EMP dtomato induction from 1.5mg tamoxifen at E7.5. From a single experiment.

iv) Preliminary data from primary YS induced mice: could JMML arise earlier in ontogeny than the FL?

Dams from three separate timed matings received tamoxifen 1.5mg and 0.75mg progesterone at E7.5. This led to the birth of 15 mice, of which 13 survived to genotyping and 3 mice had a *Kras* mutation (figure 3.31a). PB readouts at 3 weeks showed minimal but persistent dTomato positive cells in the mutant mice, but not in the WT mice (figure 3.31b). All WT mice survived until ~19 weeks when the experiments had to be terminated according to the

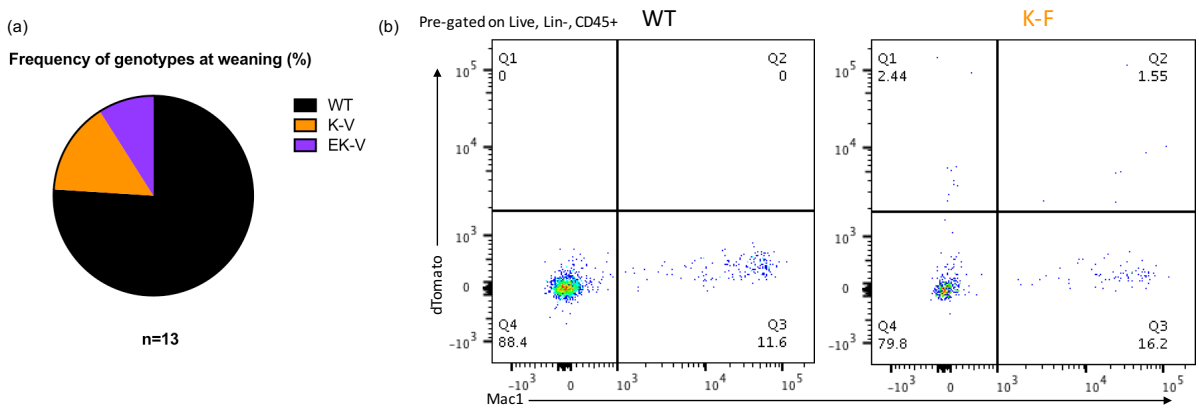


Fig 4.31: Induction of Kras mutant embryos at E7.5 with 1.5mg Tamoxifen. (a) Frequency of genotypes at weaning from 15 mice born in 3 litters. (b) summary of PB FACS phenotyping at 3 weeks showing representative WT (n=3) and K-F (n=1). The other Kras and WT embryos were lacking the dTomato floxed reporter gene

terms of the Home Office licence. Although all three *Kras* mutant mice were culled prior to the end of the experiment, none of these had a YS derived leukaemia. The EK-F mouse was found to be thrombocytopenic at PB readout, and had a similar myelomonocytic leukaemia to the FL induced mice (figure 3.32a-b). However, on analysis of the BM, there was HSC induction by dTomato, suggesting that this disease was not YS derived (figure 3.32c). Of the other two mice, one was found sick, but did not have splenomegaly, cytopenias or abnormal leucocyte populations in the PB or BM compared to WT mice and likely died due to an infection. The other was profoundly pancytopenic on a routine readout, so was culled, however on terminal analysis of the PB count there were no cytopenias or splenomegaly, so it is likely that this mouse had a spurious PB count.

After these 3 successful inductions using 1.5mg tamoxifen, subsequent experiments with this dose failed due to miscarriages at ~E13-15.5. On discussion with the veterinary team, the dose of tamoxifen was reduced first to 1mg and subsequently to 0.5mg together with 0.25mg progesterone, which allowed some, low level dTomato induction (figure 3.33a). Of 7 litters, two gave birth spontaneously at E19.5, despite the tamoxifen, possibly due to the very low doses of tamoxifen used early in pregnancy. The frequency of genotypes at weaning (figure

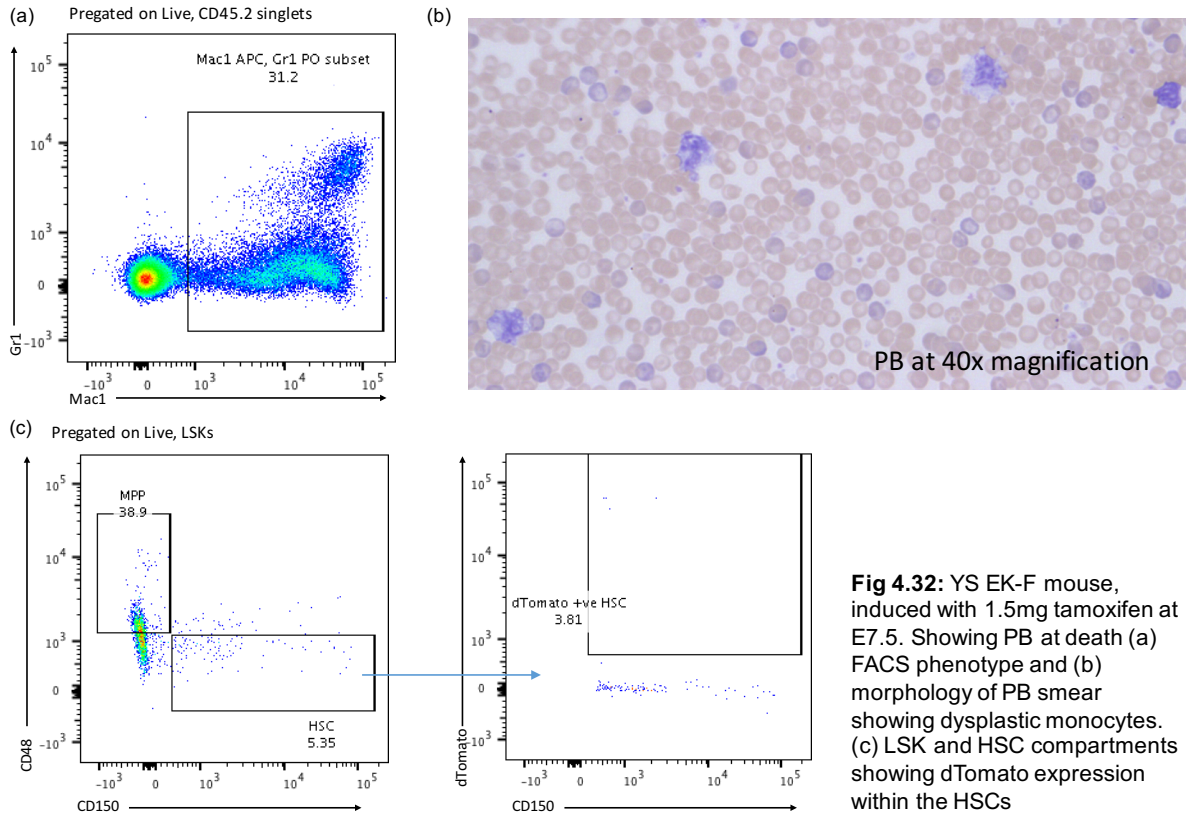


Fig 4.32: YS EK-F mouse, induced with 1.5mg tamoxifen at E7.5. Showing PB at death (a) FACS phenotype and (b) morphology of PB smear showing dysplastic monocytes. (c) LSK and HSC compartments showing dTomato expression within the HSCs

4.33b) differed from the expected frequency (figure 4.33c) in that no K-V or EEK-V mice survived to weaning suggesting that there may have been preferential loss of *Kras* mutant embryos. In addition, at 19 weeks of age, when the mice were terminated according to the Home Office licence, none of the mice showed signs of leukaemia.

The lack of leukaemia in these experiments cannot be taken as proof that the YS cannot give rise to a myelomonocytic leukaemia, but it appears that YS cells are much less susceptible to transformation than FL. However, there are some interesting findings from these experiments. First, the K-F mouse did have persistent dTomato expression at 3 weeks of age, whereas the WT mice did not. It is therefore possible that secondary mutations could be gained at or before this point, leading to leukaemia in post-natal life. Second, it is surprising that none of the *Kras* mutant mice induced with 1.5mg tamoxifen survived and that even with 0.5mg there were very few mice born with a K-F, EK-F or EEK-F genotype, despite an overall expected frequency of

~25%. This could be stochastic, or as mentioned above, there may be a preferential selection, either biologically or by the mothers due to subclinical signs of ill health.

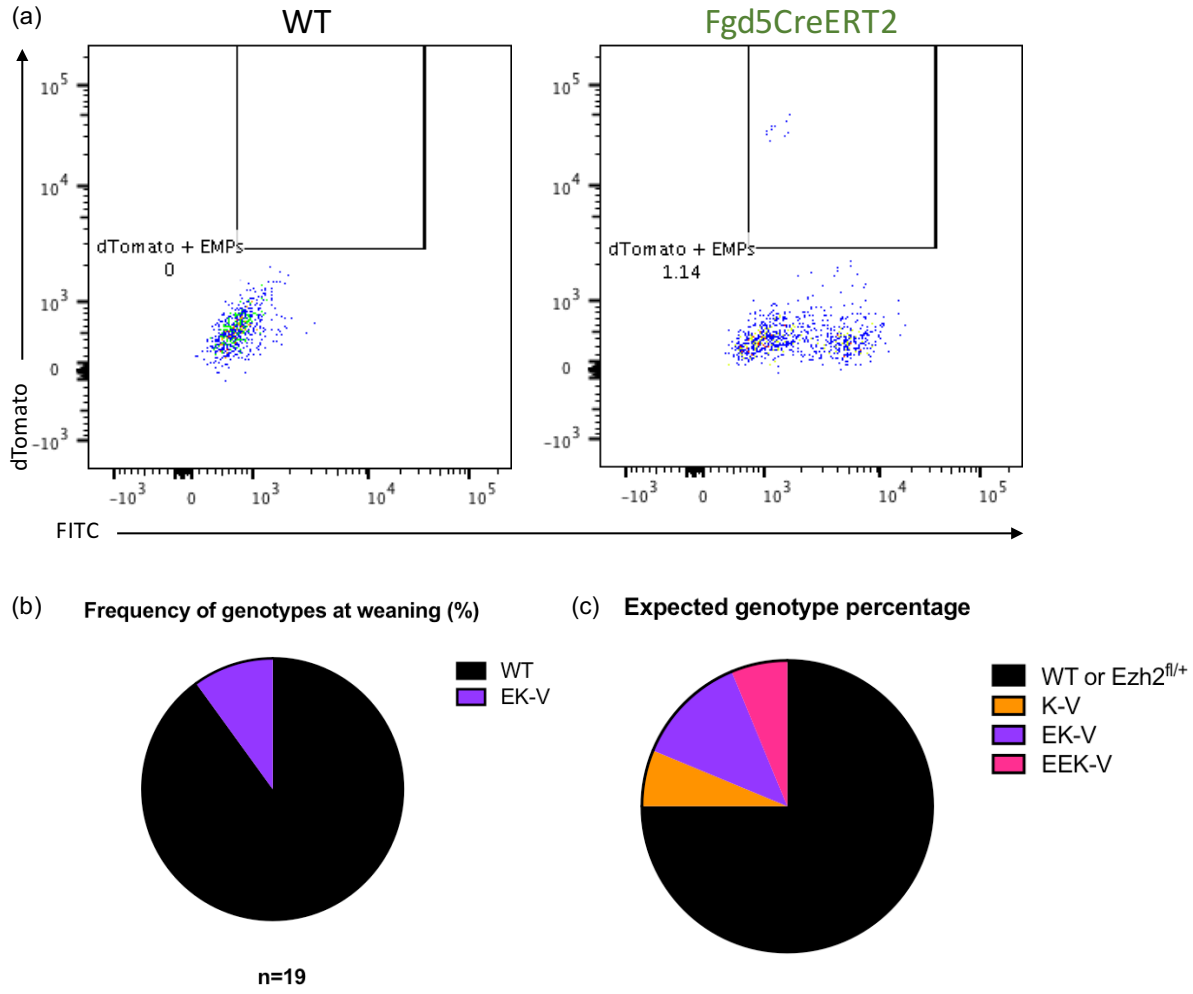


Fig 4.33: Induction of mutant *Kras* and *Ezh2* deletion at E7.5 with 0.5mg tamoxifen. (a) analysis of EMPs at E10.5 with representative flow cytometry of WT (n=4) and FgdfCreERT2 transgenic (n=3) mice. (b) observed and (c) expected genotype frequency from four surviving litters, totalling 19 mice

4-6 Summary and Discussion

In summary, using Fgd5CreERT2 allowed the development of a model of myelomonocytic leukaemia. In addition, I have demonstrated clear phenotypic differences between FL- versus aBM-induction of mutant *Kras* in HSCs with Fgd5CreERT, thereby developing a novel model which can be used to investigate the differences between fetally- and adult-induced mutations for other oncogenes.

i) Phenotypic differences between adult and fetal induction methods

Induction of HSCs with *Kras*^{G12D} in the FL, lead to markedly decreased leukaemia-free survival compared to adult induction, despite no decrease in induction in the adult mice. This may be due to the proliferative, cycling, nature of fetal HSPCs [Morrison, 1995] [Busch, 2015], although this does not explain the different types of leukaemia resulting from fetal vs adult induction. Although fetal HSPCs have a strong erythroid drive, with high GATA2 expression which may explain the higher haemoglobins in the FL-induced mice [Mikkola, 2006], this in itself is interesting as it suggests persistent expression of a fetal transcriptome, despite a median age of death at ~7 weeks postnatally. Most importantly, FL-induced mice had an almost universal penetrance of myelomonocytic expansion, thrombocytopenia and splenomegaly, as in patients with JMML [Niemeyer, 2008]. By contrast, with aBM induction ~33% of the mice developed myelomonocytic leukaemia, 33% developed other forms of myeloid disease and 33% developed T-cell leukaemia which was not seen at all in the FL-induced mice. The reasons for this are not yet clear and may be due to the differences in latency, with the longer time required to develop mutant T-cells from HSCs. Indeed, FL-induced mice developed a much more aggressive disease and all mice of the FL-induced K-F mice had to be culled due to thrombocytopenia.

Despite these major differences in the survival and phenotype of FL- and aBM-induced mice, differences in the HSPC compartment were modest. Although the aBM-induced mice demonstrated persistent depletion of HSCs in keeping with the data in Chapter 3, there was a difference in the HSC compartment when induced in the FL with no decrease in phenotypic HSCs. Whilst this may suggest that FL acquisition is important to leukaemic HSC survival, this may be due to experimental considerations. For example, while the extent of induction as

measured by dTomato expression appeared to be higher in adult-induced cells, potentially explaining why *Kras* mutant HSCs are more depleted, assessment of deletion in FL LSKs by molecular methods in fact showed a high level of deletion in these cells. Thus, the higher induction by dTomato expression in adult life may therefore not represent molecular changes in other transgenes, as is the case with my Mx1cre model (chapter 3-4).

ii) The effect of ontogeny on function of malignant HSPCs

To assess the functional effects of *Kras* mutation on HSPCs I used both transplantation and *in-vitro* methods. These experiments showed that in both fetally-induced and adult-induced *Kras* mutant mice, the myelomonocytic leukaemia was transplantable into secondary recipients, although not as penetrant as in the primary mice. Unfortunately, the transplantation experiments were again confounded by the high frequency of T-cell leukaemias, potentially due to transplantation of mutant T-cells within the secondary transplants or possibly due to cell-extrinsic effects.

Replating experiments were used to investigate functional differences in the fetally- and adult-induced K-F mice and showed that fetal K-F LSK cells are slightly more proliferative. This is interesting as these cells are from the BM at time of death (~5-7 weeks of age), which is beyond age (3 weeks) when these cells are expected to have acquired adult characteristics [Morrison, 1995]. This suggests that leukaemogenic FL cells maintain at least some FL characteristics for longer than expected. This is demonstrated by a difference between both the FL K-F and adult K-F, as well as the FL WT and K-F cells. These data were supported by a slight increase in colony growth at the second replating on serial replating assays and the increased sensitivity to low dose GM-CSF in hypersensitivity assays. Together these findings suggest that there are

functional differences of acquiring the same mutation depending on whether or not the mutation occurs in a fetal versus an adult cell.

iii) The leukemic potential of YS HSPC

My data are the first to show that YS cells can have leukaemic potential. One previous study demonstrated a neurodegenerative model following induction of a BRAF mutation in the YS, due to glial cells [Mass, 2017], however no model has been able to show leukaemia. I utilised an optimised transplant method, with minimal irradiation as demonstrated in McGrath *et al*, 2015. This may have allowed engraftment of functionally 'fragile' cells, which otherwise may not have engrafted.

Using Fgd5CreERT2 proved difficult for induction in the YS, mainly due to problems with the oestrogen agonist activity of tamoxifen. However, using very low doses early in gestation, these mice did not need fostering, as has been suggested in other studies [Gomez-Perdiguero, 2015][Mass, 2017], and so for future work this could help simplify experiments. Alternatively, it may be useful to use 4-hydroxytamoxifen, the active metabolite of tamoxifen, which has a much shorter half-life, and thus may solve the problems with HSC induction and allow doses closer to E8.5. Induction of YS EMPs was possible, nevertheless, and did show persistent dTomato expression on PB analysis at 3 weeks postnatally, despite no mice developing leukaemia.

iv) Future work

As a significant part of the work in this chapter was interrupted by the Covid-19 pandemic, a major question which I hope to be able to answer, is the nature of the molecular changes that underpin the differences between FL- and aBM induction through RNA sequencing of BM

LSKs and HSCs. In particular, this would determine whether there is persistent fetal gene expression in the leukaemias in FL-induced cells.

A second important question that remains to be addressed is whether the disease is initiated through HSCs or MPPs. This could be done using a Flt3CreERT2, which is an inducible mouse model allowing induction in any cell expressing Flt3 -- i.e. MPPs and downstream -- and would thereby allow differentiation between HSC induction with Fgd5CreERT2 which only induces in HSCs.

Thirdly, it would be very interesting to further investigate the potential of YS cells as leukaemia initiating cells either using a transplantation model or the Fgd5CreERT2 model, as described above. Although there was no leukaemia through this method, there were significant experimental considerations which could be altered, such as using 4-hydroxytamoxifen, to develop a model which allows the study of gain of mutation at any stage of ontogeny, from the YS, FL and aBM and could help to identify important factors in both leukaemogenesis but also fetal haematopoietic biology.

References

Araki T, Mohi MG, Ismat FA, et al. Mouse model of Noonan syndrome reveals cell type- and gene dosage-dependent effects of Ptpn11 mutation. *Nat Med*. 2004;10(8):849-85.

Basak A, Munschauer M, Lareau CA, et al. Control of human hemoglobin switching by LIN28B-mediated regulation of BCL11A translation. *Nat Genet*. 2020;52(2):138-145.

Braun BS, Tuveson DA, Kong N, et al. Somatic activation of oncogenic Kras in hematopoietic cells initiates a rapidly fatal myeloproliferative disorder. *Proc Natl Acad Sci U S A*. 2004;101(2):597-602.

Busch K, Klapproth K, Barile M, et al. Fundamental properties of unperturbed haematopoiesis from stem cells in vivo. *Nature*. 2015;518(7540):542-546.

Caye A, Rouault-Pierre K, Strullu M, et al. Despite mutation acquisition in hematopoietic stem cells, JMML-propagating cells are not always restricted to this compartment [published correction appears in Leukemia. 2020 Jan 31;:]. *Leukemia*. 2020;34(6):1658-1668.

Cumano A, Ferraz JC, Klaine M, Di Santo JP, Godin I. Intraembryonic, but not yolk sac hematopoietic precursors, isolated before circulation, provide long-term multilineage reconstitution. *Immunity*. 2001;15(3):477-485.

de Bruijn MF, Speck NA, Peeters MC, Dzierzak E. Definitive hematopoietic stem cells first develop within the major arterial regions of the mouse embryo. *EMBO J.* 2000;19(11):2465-2474.

Di Genua C, Norfo R, Rodriguez-Meira A, et al. Cell-intrinsic depletion of Aml1-ETO-expressing pre-leukemic hematopoietic stem cells by K-Ras activating mutation. *Haematologica*. 2019;104(11):2215-2224.

Gazit R, Mandal PK, Ebina W, et al. Fgd5 identifies hematopoietic stem cells in the murine bone marrow. *J Exp Med*. 2014;211(7):1315-1331.

Gomez Perdiguero E, Klapproth K, Schulz C, et al. Tissue-resident macrophages originate from yolk-sac-derived erythro-myeloid progenitors. *Nature*. 2015;518(7540):547-551.

Gustafsson B, Hellebostad M, Ifversen M, Sander B, Hasle H. Acute respiratory failure in 3 children with juvenile myelomonocytic leukemia. *J Pediatr Hematol* Oncol. 2011 Dec;33(8):e363-7.

Kimura Y, Sugita Y, Seki R, Inada H, Arakawa F, Kiyasu J, Takeuchi M, Hashikawa K, Aoki R, Niino D, Ohshima K. Infant juvenile myelomonocytic leukemia (JMML) with rapid infiltration of multiple organs. *Pathol Int*. 2010 Apr;60(4):333-5.

Locatelli F, Nöllke P, Zecca M, et al. Hematopoietic stem cell transplantation (HSCT) in children with juvenile myelomonocytic leukemia (JMML): results of the EWOG-MDS/EBMT trial. *Blood*. 2005;105(1):410-419.

Locatelli F, Niemeyer CM. How I treat juvenile myelomonocytic leukemia. *Blood*. 2015;125(7):1083-1090.

Louka E, Povinelli B, Meira AR. Heterogeneous disease-propagating stem cells in juvenile myelomonocytic leukemia. *BioRXiv*. 2019; May 07. https://doi.org/10.1101/628479.

Mass E, Jacome-Galarza CE, Blank T, Lazarov T, Durham BH, Ozkaya N, Pastore A, Schwabenland M, Chung YR, Rosenblum MK, Prinz M, Abdel-Wahab O, Geissmann F. A somatic mutation in erythro-myeloid progenitors causes neurodegenerative disease. Nature. 2017 Sep 21;549(7672):389-393.

Matsuda K, Sakashita K, Taira C, et al. Quantitative assessment of PTPN11 or RAS mutations at the neonatal period and during the clinical course in patients with juvenile myelomonocytic leukaemia. *Br J Haematol*. 2010;148(4):593-599.

McGrath KE, Frame JM, Fegan KH, et al. Distinct Sources of Hematopoietic Progenitors Emerge before HSCs and Provide Functional Blood Cells in the Mammalian Embryo. *Cell Rep*. 2015;11(12):1892-1904.

Medvinsky A, Dzierzak E. Definitive hematopoiesis is autonomously initiated by the AGM region. *Cell*. 1996;86(6):897-906.

Mikkola HK, Orkin SH. The journey of developing hematopoietic stem cells. *Development*. 2006;133(19):3733-3744.

Morrison SJ, Hemmati HD, Wandycz AM, Weissman IL. The purification and characterization of fetal liver hematopoietic stem cells. *Proc Natl Acad Sci U S A*. 1995;92(22):10302-10306.

Neo WH, Booth CAG, Azzoni E, et al. Cell-extrinsic hematopoietic impact of Ezh2 inactivation in fetal liver endothelial cells. *Blood*. 2018;131(20):2223-2234.

Niemeyer CM, Kratz CP. Paediatric myelodysplastic syndromes and juvenile myelomonocytic leukaemia: molecular classification and treatment options. *Br J Haematol*. 2008;140(6):610-624.

Roberts I, Fordham NJ, Rao A, Bain BJ. Neonatal leukaemia [published correction appears in Br J Haematol. 2019 Jul;186(1):196]. *Br J Haematol*. 2018;182(2):170-184.

Sabnis AJ, Cheung LS, Dail M, et al. Oncogenic Kras initiates leukemia in hematopoietic stem cells. *PLoS Biol*. 2009;7(3):e59.

Stieglitz E, Taylor-Weiner AN, Chang TY, et al. The genomic landscape of juvenile myelomonocytic leukemia [published correction appears in Nat Genet. 2015 Nov;47(11):1333] [published correction appears in Nat Genet. 2016 Jan;48(1):101]. *Nat Genet*. 2015;47(11):1326-1333.

Tarnawsky SP, Yoshimoto M, Deng L, Chan RJ, Yoder MC. Yolk sac erythromyeloid progenitors expressing gain of function PTPN11 have functional features of JMML but are not sufficient to cause disease in mice. Dev Dyn. 2017 Dec;246(12):1001-1014.

Tarnawsky* SP, Kobayashi M, Chan RJ, Yoder MC. Mice expressing KrasG12D in hematopoietic multipotent progenitor cells develop neonatal myeloid leukemia. *J Clin Invest*. 2017;127(10):3652-3656.

Tarnawsky SP, Yu WM, Qu CK, Chan RJ, Yoder MC. Hematopoietic-restricted Ptpn11E76K reveals indolent MPN progression in mice. *Oncotarget*. 2018;9(31):21831-21843.

Tsai FY, Keller G, Kuo FC, Weiss M, Chen J, Rosenblatt M, Alt FW, Orkin SH. An early haematopoietic defect in mice lacking the transcription factor GATA-2. *Nature*. 1994;371:221–226.

Yoder MC, Hiatt K. Engraftment of Embryonic Hematopoietic Cells in Conditioned Newborn Recipients. *Blood* 1997; 89 (6): 2176–2183.

Yoshimoto M, Montecino-Rodriguez E, Ferkowicz MJ, et al. Embryonic day 9 yolk sac and intra-embryonic hemogenic endothelium independently generate a B-1 and marginal zone progenitor lacking B-2 potential. *Proc Natl Acad Sci U S A*. 2011;108(4):1468-1473.

Chapter 5: The effect of *Ezh2* knock-out on a mouse model of JMML

Having created a mouse model that allows robust initiation and comparison of mutations either in fetal life or adult life, I next used the model to test my final hypothesis, that *Ezh2* alters $Kras^{G12D}$ driven leukaemogenesis. In JMML, LOF of *Ezh2* occurs in ~30% of cases [Caye, 2015], either through LOF mutations or loss of all or part of chromosome 7 where *Ezh2* is found in both mouse and humans [Caye, 2015] [Stieglitz, 2015]. Whilst any secondary mutations lead to a poorer prognosis [Caye, 2015] [Stieglitz, 2015], the specific role of *EZH2* loss has not been studied.

Ezh2 expression is increased in FL LT-HSCs compared to adult BM HSCs [Xie, 2014], and there appears to be a differential role for *Ezh2* and the PRC2 during ontogeny with changes in HSPC phenotype and function depending on the stage of loss [Neo, 2018][Vo, 2018]. Previous data suggest that *Ezh2* has a role in fetal stem cell survival [Mochizuki-Kashio, 2011], and therefore may help to rescue fetal stem cell loss in the models studied above. Further, *Ezh2*-KO in other cancer models, such as malignant peripheral nerve sheath tumours, show increased RAS signalling and aggressive disease [De Raedt, 2014]. Similarly, models of lymphomyeloid leukaemia [Booth, 2018] and T-ALL [Ntziachristos, 2012] show a more aggressive disease with *Ezh2* loss, which in the case of lymphomyeloid leukaemia can be modified by bromodomain inhibition [Booth, 2018]. Taken together, these data, the clinical data and my data so far, support a potential combinatorial effect in a range of cell types.

5-1 Using the Mx1Cre model to assess serial transplantability of mutant *Kras* with or without *Ezh2* loss

i) The phenotypic consequence of *Ezh2* KO in a $Kras^{G12D}$ mouse model

My data from Chapter 3 shows that on transplantation of *Kras* mutant HSPCs with Mx1Cre induction, *Ezh2* loss drives a myeloid phenotype in a small proportion of mice. In addition, phenotypic data from these mice and the Vav-iCre FL shown in Chapter 3.1 suggest that *Ezh2* loss rescues the phenotypic HSC loss.

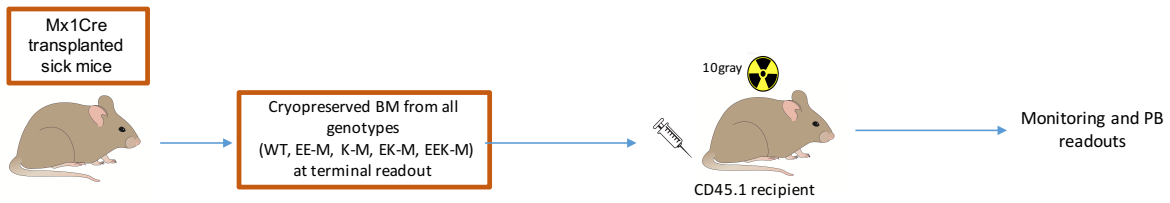


Fig 5.1: Overview of transplantation experiments of mutant *Kras* with or without *Ezh2* loss using cryopreserved BM from mice transplanted with Mx1Cre induced FL. Mice were monitored for signs of ill health, and PB taken for monitoring at 2 weekly intervals until 8 weeks followed by 4 weekly intervals until 16 weeks.

In order to assess the combined effect of *Ezh2* loss on the transplantability of $Kras^{G12D}$- driven leukaemias in my mouse model, I transplanted cryopreserved BM from leukaemic primary transplanted mice (see figures 3.19-3.20) into secondary recipients (figure 5.1). All of the K-M mice died of T cell leukaemia (figure 5.2a-d), as in the primary transplants. By contrast, the only genotype where the primary myeloid leukaemia (from EK-M and EEK-M replicates, as all primary K-M mice had T-cell leukaemia) was maintained on secondary transplantation was EEK-M, where 4/6 mice developed fatal myeloid leukaemia (figure 5.2c-d; figure 5.3a-b). Interestingly, 3/4 of these mice had expansion of dysplastic Gr1+ cells rather than monocytic cells (figure 5.3a-b). Interestingly, all of the EK-M mice developed T-cell leukaemia despite the fact that the transplanted primary cells were from 3 mice with a primary myeloid leukaemia and 3 mice with a T-cell leukaemia (figure 5.3c-d).

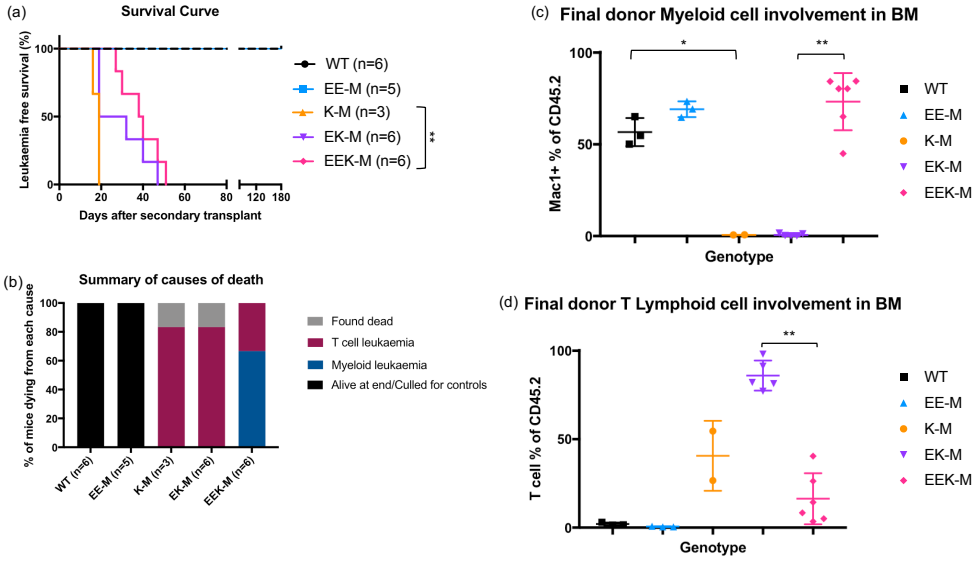


Fig 5.2: Ezh2-KO permits the transplantation of myeloid leukaemia. (a) Survival of mice from time of transplant (b) Summary of each cause of death (c) Myeloid cells and (d) T-cells. Each data point representative of a single replicate in two separate transplant experiments. WT and EE-M replicates only assessed in single experiment. Statistical analysis with Mantel-Cox test for survival curve and Mann-Whitney U test otherwise. *p<0.05, **p<0.01

Overall these data support the hypothesis that *Ezh2* and mutant *Kras* have a combinatorial effect. The data also suggest that *Ezh2* loss leads to a myeloid drive, as evidenced by EEK-M being the only genotype allowing both the development and propagation of myeloid disease. In addition, it appears that even a few mutant T-cells in the transplanted BM can lead to a rapid proliferation and death due to T-cell leukaemia.

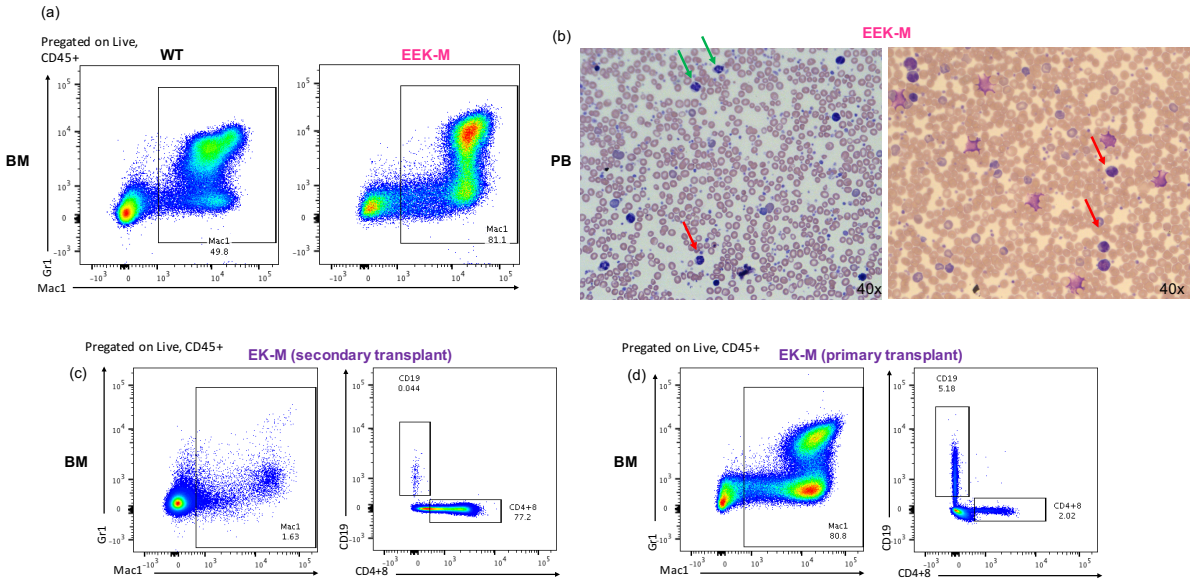


Fig 5.3: Phenotypic switching on serial transplantation of BM cells from myeloid primary mice. (a) Representative example of FACS analysis of BM at termination of WT (n=3) and EEK-M (n=3). (b) PB of EEK-M at termination from two separate biological samples, taken at 40x magnification, with dysplastic monocytes (red arrows) and neutrophils (green arrows) (c) Representative FACS plots from BM of EK-M (n=5) at terminal readout and (d) FACS of BM at termination of primary transplant, transplanted into mouse shown in (a).

ii) Does *Ezh2* loss in a fetal cell enhance self-renewal?

In previous experiments, mice developing T-cell leukaemia did so with a longer latency, and therefore, by using mice for secondary transplants after a prolonged period in primary transplants this would allow time for development of mutant T-cells. To avoid T-cell leukaemia confounding my aim to investigate the cooperation between mutant *Kras* and *Ezh2* loss on myeloid leukaemia development, I developed a model, based on a previous strategy in the lab [Di Genua, 2019]. FL HSPCs were induced with PolyI:C immediately after transplantation in order to induce as close to fetal life as possible, and then rapid sequential serial transplantations were performed within 8 weeks of the previous transplant (figure 5.4).

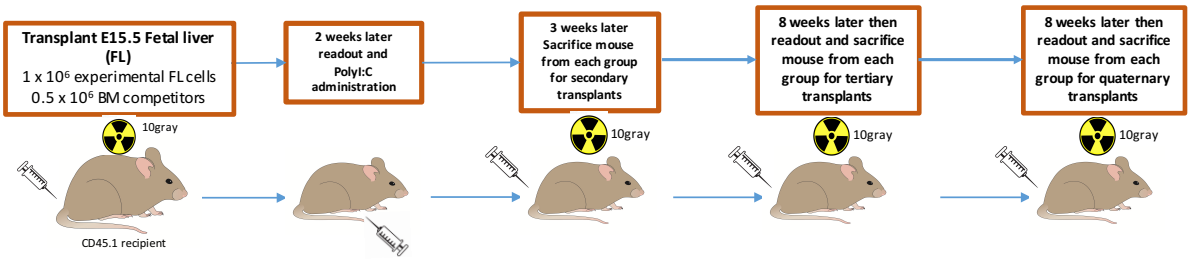


Fig 5.4: Overview of serial, rapid, sequential transplantation experiments. Testing serial engraftment of HSPCs whilst attempting to minimize T-cell leukaemia. BM from transplanted mice transplanted into further CD45.1 recipient mice up to quaternary transplants. First secondary transplant performed earlier than planned as primary transplanted mice developed weight loss soon after polyI:C administration

Overall engraftment: As expected, engraftment diminished with each sequential transplant, across each genotype (figure5.5a-d). Overall engraftment of mice with homozygous loss of *Ezh2* (EE-M) mice, was significantly reduced after primary and secondary transplantation (figure 5.5a,b) but, interestingly, EE-M mice were the only genotype to demonstrate sustained engraftment after quaternary transplantation (figure 5.5d). Engraftment of *Kras* mutant mice was maintained until tertiary transplantation but was lost thereafter, consistent with previous data in *Kras* mutant mice where secondary mutations were necessary to restore stem cell function [Di Genua et al, 2019]. However, evidence of co-operativity of mutant *Kras* with *Ezh2* loss was again observed as engraftment was sustained into quaternary transplants in EEK-

M and EK-M mice, particularly in the mice with homozygous *Ezh2* loss (EEK-M) (figure 5.5d).

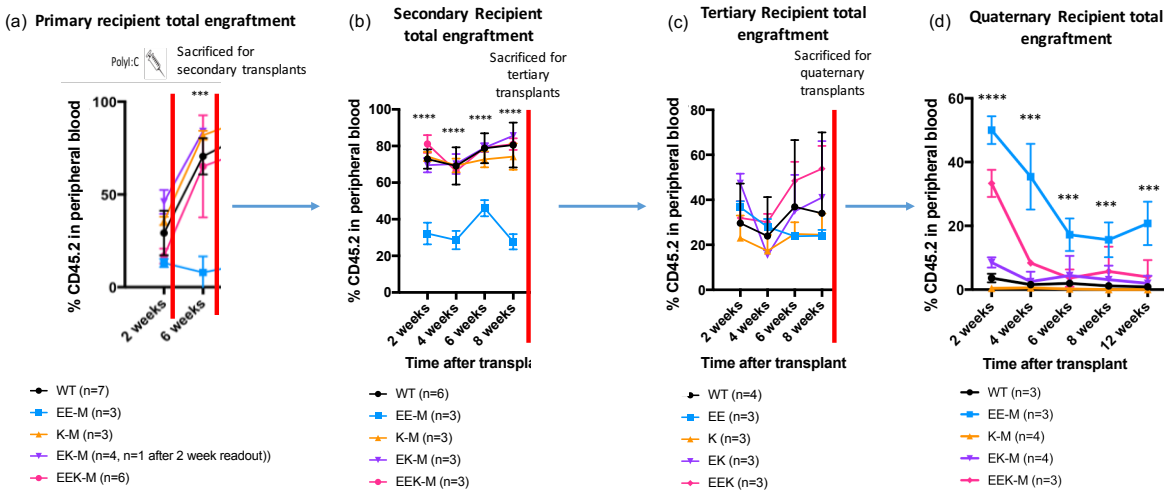


Fig 5.5: Ezh2-KO alone permits serial transplantability. CD45.2% engraftment shown across primary transplants (a) and sequential transplants secondary (b), tertiary (c), quaternery (d). Each single experiment, but primary and secondary in two separate experiments for different genotypes. Replicates per experiment shown in legend for each graph. Statistics by ANOVA. **p<0.01, ***p<0.001, ****p<0.0001.

Myeloid and T-cell engraftment: Serial transplantability of EE-M cells was due to sustained engraftment of Mac1+ myeloid cells in the absence of any T-cell engraftment of these cells after primary transplantation (figure 5.6a-e). These results suggest that *Ezh2* loss alone may increase self-renewal of fetal myeloid cells, but it is known that *Ezh2*-KO mice do not produce PB T-cells [Su, 2005]. By contrast, K-M mice lost myeloid engraftment more quickly than the other genotypes and T-cell engraftment, with or without leukaemia, predominated on serial transplantation (figure 5.6a-c).

Leukaemia: Replicate mice which were not transplanted were kept for each genotype for 16 weeks as controls to monitor the expected frequency of leukaemia. T-cell leukaemia did develop in 1/7 K-M, 3/7 EK-M and 1/7 EEK-M but in none of the WT or EE-M mice and no

myeloid leukaemias developed (figure 5.7a-b). As the serial transplantation approach into

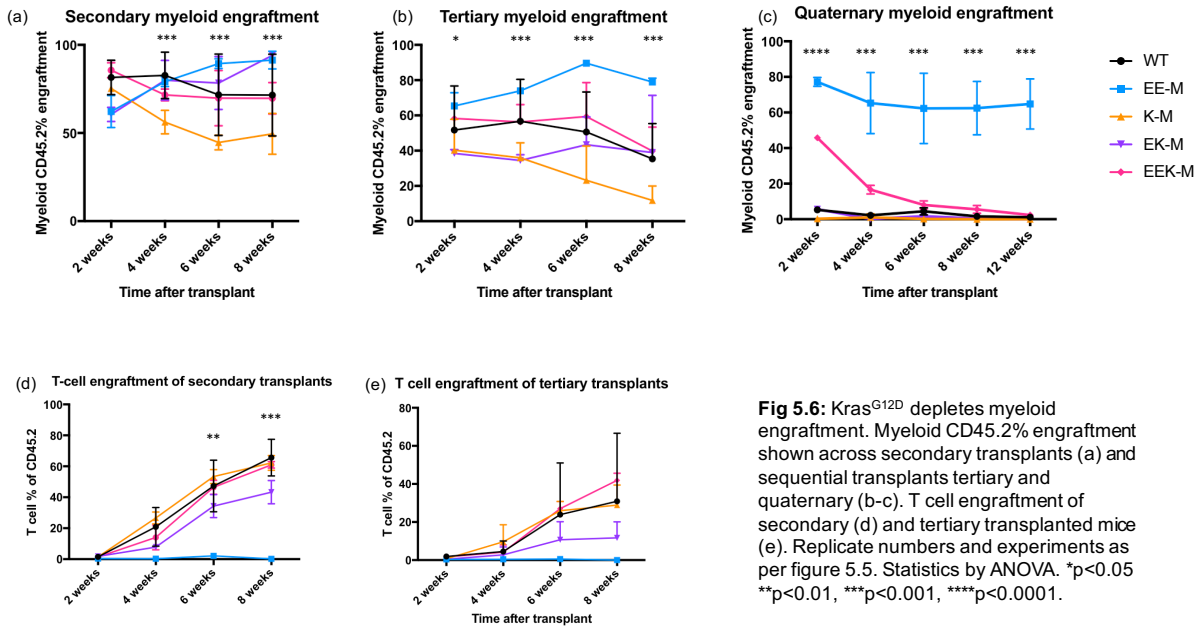


Fig 5.6: Kras^{G12D} depletes myeloid engraftment. Myeloid CD45.2% engraftment shown across secondary transplants (a) and sequential transplants tertiary and quaternary (b-c). T cell engraftment of secondary (d) and tertiary transplanted mice (e). Replicate numbers and experiments as per figure 5.5. Statistics by ANOVA. *p<0.05 **p<0.01, ***p<0.001, ****p<0.0001.

lethally irradiated mice still allowed T cell leukaemia to develop in the *Kras* mutant mice, with or without *Ezh2* loss, I also performed serial transplants into sublethally irradiated mice (figure 5.8a). Previous reports suggested that transplanting BM from mice with T-cell leukaemia into sublethally irradiated mice entirely removed the T-cell leukaemic potential [Sabnis, 2009].

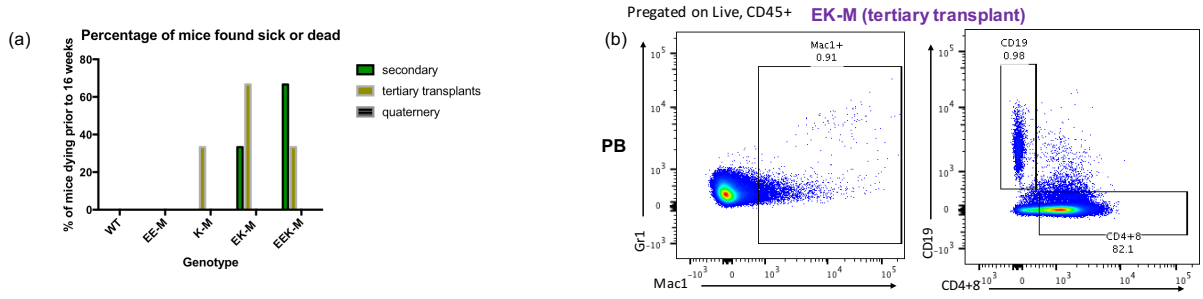


Fig 5.7: Serial transplantation diminishes but does not abolish T cell leukaemia (a) Percentage of mice found sick or dead in sequential transplants from total replicate number in each experiment. All mice able to be analysed had T cell leukaemia (1/7 K-M, 3/7 EK-M,1/7 EEK-M) (b) Example gating strategy of EK-M mouse at terminal readout from tertiary transplants (representative of n=2).

My data showed similar engraftment trends to the lethal irradiation experiments in the secondary transplants (figure 5.8b), but with overall lower engraftment, and by tertiary transplantation there was loss of engraftment in all genotypes (figure 5.8c-d). Two mice

developed T-cell leukaemia in all sublethal transplants (1/6 K-F, and 1/7 EK-F), and no mice developed myeloid leukaemia.

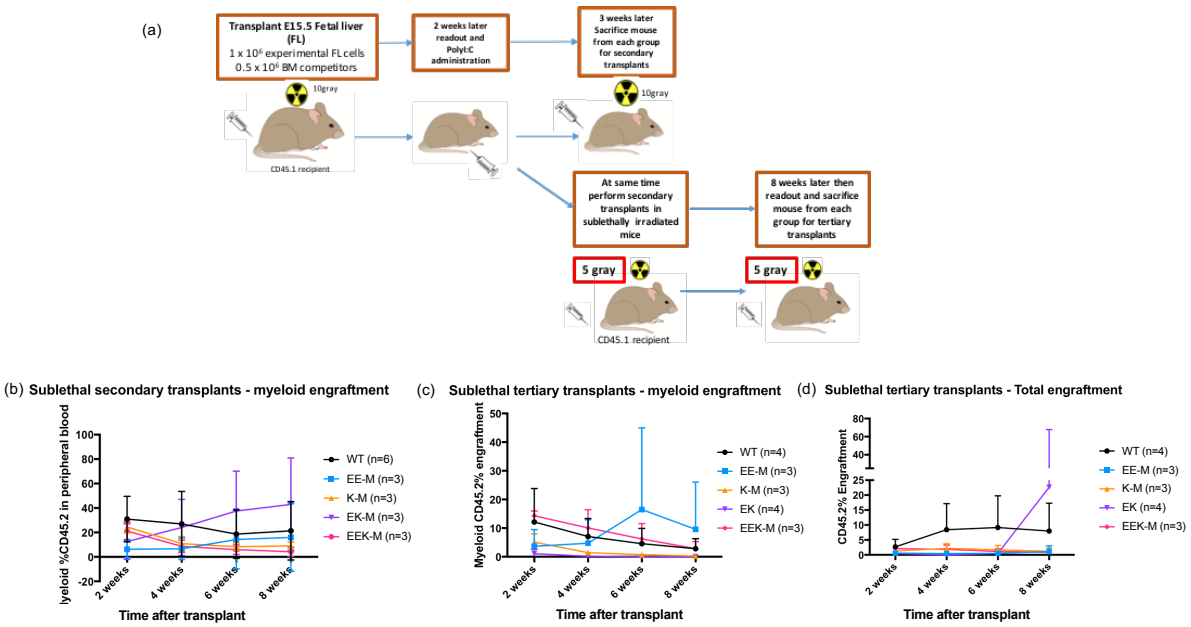


Fig 5.8: Using a sublethal irradiation protocol to investigate the interaction between mutant Kras and Ezh2 loss in leukaemogenesis (a) Overview of sublethal transplantation experiment to avoid T-cell leukaemia. Sequential myeloid engraftment of myeloid cells in secondary transplants (b) and tertiary transplants (c). (d) Summary of tertiary total engraftment. Summary of single experiments.

Overall, these experiments confirm the reduced serial transplantability of mutant *Kras* HSPCs and rescue of the mutant HSPCs to some extent by secondary mutations [Di Genua, 2019], in this case Ezh2 loss. These results suggest that the effect of *Ezh2* on self-renewal of fetal cells is sustained to some extent even in the presence of *Kras* mutation. However, the leukaemias that developed were of T-cell lineage and the JMML propagating cells appear to transplant poorly. Further, whilst fetal-derived HSPCs were used in these experiments, and the induction was performed within a few weeks of transplant, induction of the mutation still occurs post-transplantation in the adult setting. Therefore, to investigate the interaction and phenotypic effect of *Ezh2* loss on a *Kras* mutant myeloid leukaemia, I used my primary mouse model, as described in chapter 4.

5-2. Does *Ezh2* knock-out in adult life alter the phenotype in a JMML model?

In other models of myeloproliferative diseases, PRC2-KO leads to a reactivation of fetal pathway genes [Shimizu, 2016][Yang, 2016]. It is clear that *Ezh2* has a role in ontogeny, with control of many fetal pathways [Oshima 2016][Sashida, 2016], however the effect of reactivation of these fetal genes in myeloid diseases is unclear. Mouse models have shown that *Ezh2*-KO as a secondary mutation generally leads to a more aggressive phenotype [Muto, 2013][Shimizu, 2016][Yang, 2016]. In JMML patients, secondary mutations also lead to more aggressive disease [Stieglitz, 2015], but the effect of these mutations at the functional and molecular level has not been studied. Although studies have demonstrated *EZH2* and other PRC2 mutations to be secondary in nature to the RAS mutations, the timing of PRC2 mutations is not clear, where the RAS mutations occur in fetal life [Caye, 2015][Stieglitz, 2015].

An attractive hypothesis is that *Ezh2*-KO in *Kras* mutant cells permits a more 'fetal' like disease with increased proliferation of the mutant cells. To test this hypothesis, I next investigated whether the timing of *Ezh2*-KO induction would affect the nature of the resulting leukaemias. To do this, I induced Fgd5CreERT2 transgenic primary mice in fetal life or in adult life with both *Kras* mutation and *Ezh2*-KO. Heterozygous *Ezh2* loss was also used to model if there was an important role for monosomy 7.

i) Leukaemia from primary mice induced to express mutant *Kras*, with or without *Ezh2* loss, in adult life

Primary mice where mutant *Kras* was induced in adult life (at 6-8 weeks of age) all developed leukaemia, as defined in table 4-1 (chapter 4 and figure 5.9a-b). Leukaemia-free

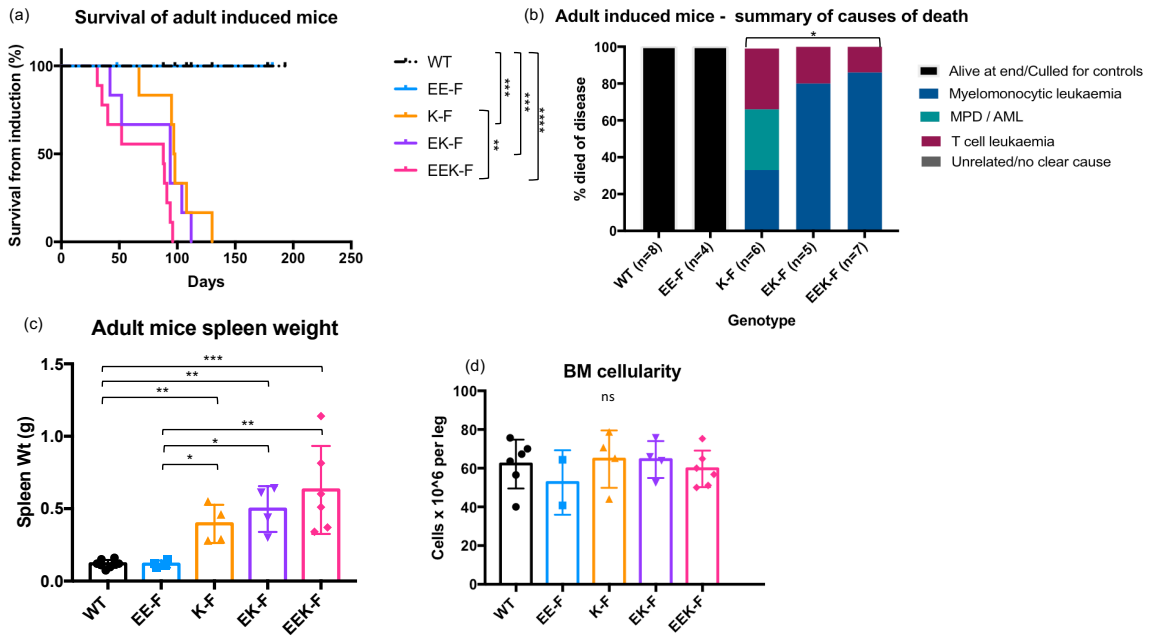


Fig 5.9: Ezh2 loss in Kras^{G12D} mutant mice accelerates disease and alters the phenotype. (a) Survival following induction (b) Percentage of mice succumbing to each disease, excluding those found dead. Replicate numbers able to be analysed shown in (b). (c) Spleen weight (g) of mice at terminal readout (d) BM cellularity of a single leg at terminal readout. T cell leukaemic mice excluded in (c) and (d). Each data point represents a single biological replicate. Statistical analysis of survival with Mantel-Cox test, of summary death ANOVA, of (c), (d) Mann-Whitney U test. *p<0.05 **p<0.01, ***p<0.001, ****p<0.0001, ns=not significant

survival was significantly shorter in *Kras* mutant mice with homozygous *Ezh2* loss (EEK-F) compared to mutant *Kras* alone (K-F; p=0.0055), and slightly, but not significantly shorter with heterozygous *Ezh2* loss and mutant *Kras* (EK-V) (figure 5.9a). The spectrum of mutant *Kras*-driven leukaemia depended on whether or not there was also heterozygous or homozygous *Ezh2* (figure 5.9b) consistent with the hypothesis that this interaction is important. When mutant *Kras* alone (K-F) was induced in adult mice, 2/6 mice developed T-cell leukaemia, 2/6 developed myelomonocytic leukaemia and 2/6 developed a fatal Gr+ myeloproliferative disorder, as shown in chapter 4-1 (shown again in figure 5.9b). By contrast, all but one of the EEK-F or EK-F mice (6/7 and 4/5 respectively) developed a myelomonocytic leukaemia with the remaining mouse in each of the EEK-F and EK-F groups developing T-cell leukaemia. Of note, no mice with *Ezh2*-KO developed either with an expanded Gr1 population, as the K-F mice did (see chapter 4-1).

All of the mutant Kras mice had splenomegaly compared to WT and EE-F mice but there was no significant difference between the mutant Kras mice with or without Ezh2 loss (figure 5.9c), There was no significant difference in BM cellularity between any of the groups of mice (figure 5.9d). All of the mutant *Kras* mice were thrombocytopenic and *Ezh2* loss had no additional effect (Table 5.1). In addition, all of the mutant *Kras* mice were slightly anaemic, apart from a single K-F replicate with JMML and polycythaemia (Table 5.1). The white cell count was increased in all of the mutant Kras mice and, again, was not significantly different in the presence or absence of Ezh2 loss (Table 5.1).

	WT	EE-F	K-F	EK-F	EEK-F
Haemoglobin (g/dL)	13.4 (n=8, 11.9-14.8)	13.4 (n=4, 13-13.7)	11.3 (n=4, 5-16)	11.5 (n=4, 8-12.5)	10.5 (n=6, 8-12.5)
White cell count ($x10^9$/L)	11.7 (6.3-16.2)	12.8 (8.3-19.7)	176.3 (10-539.8)	28.2 (18.6-34.2)	29.12 (12.1-50.2)
Platelet count ($x10^9$/L)	1070 (712-1302)	983 (872-1179)	398 (312-564)	429 (287-616)	575 (252-1471)

Table 5-1: Blood parameters at terminal readouts of adult-induced mice. Mean and range from mice with myelomonocytic leukaemia or MPD, T-cell leukaemic mice excluded. WT (n=8), EE-F (n=4), K-F (n=4), EK-F (n=4), EEK-F (n=6).

Overall, the immunophenotypic and morphological characteristics of the myelomonocytic leukaemia were similar in the 3 different genotypes of *Kras* mutant mice. However, when compared to K-F mice with myeloid disease, there was a significant expansion of the monocytic (Mac1+Gr1-) compartments in EEK-F mice (figure 5.10a-c). This myeloid expansion was also clearly visible on histology of the BM (figure 5.11).

To assess any differences in the stem cell compartment I used flow cytometry and excluded the mice with T-cell leukaemia from these analyses. To further the results in chapter 4-1 (figure 4-9), this showed, where K-F mice had a depletion of the LSK and HSC compartment

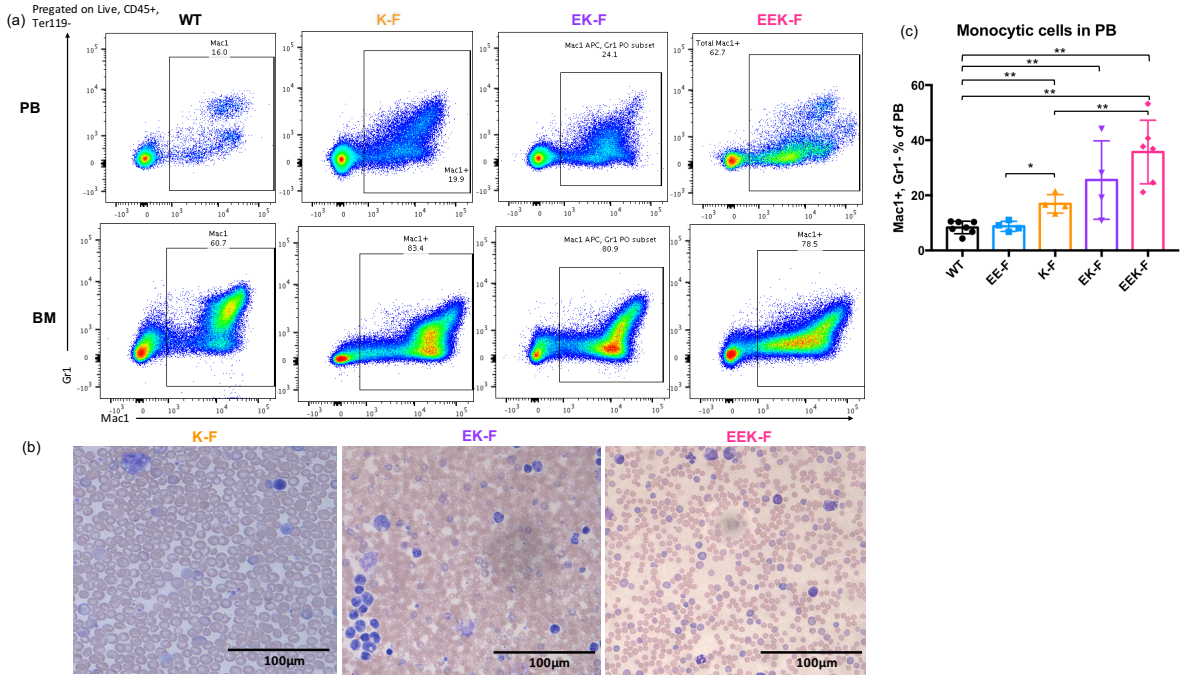


Fig 5.10: Adult mice with Kras induced leukaemia develop a myeloid leukaemia with loss of Ezh2. (a) Representative flow cytometry plots of WT (n=7), K-F (n=2), EK-F (n=4), and EEK-F (n=6), pre-gated on live CD45+Ter119- cells. (b) Representative PB films of mice with myelomonocytic leukaemia from K-F (n=2), EK-F (n=2), EEK-F (n=4). Images taken at 40x magnification. These show blast cells and abnormal monocytoid cells, with an increased number also of abnormal granulocytic cells in the EEK-F mice consistent with the flow cytometric results. (c) Total PB monocytic cells defined as Gr1-ve Mac1+ve CD45.2+, Ter119-ve, live singlets. Each data point represents a biological replicate. Statistical analysis by Mann-Whitney U test. *p<0.05 **p<0.01

there was rescue of this depletion by *Ezh2* loss (figure 5.12a-d); this rescue was statistically significant ($p<0.01$) for the EEK-F mice where there were 5 mice but not significant for the EK-F mice where there were only 3 mice. A similar pattern was seen for MPP and LK populations (figure 5.12c-f). No significant changes were found in any of the other HSPC 'Bryder' panel compartments between K-F and EK-F or EEK-F genotypes (appendix 4.6).

As overall BM cellularity is the same in all of the *Kras* mutant mice and WT mice, these findings suggest that while Kras leads to proliferation of more mature cells concomitant with depletion of HSPCs, loss of Ezh2 rescues this imbalance albeit that these are leukaemic rather than normal HSPC populations.

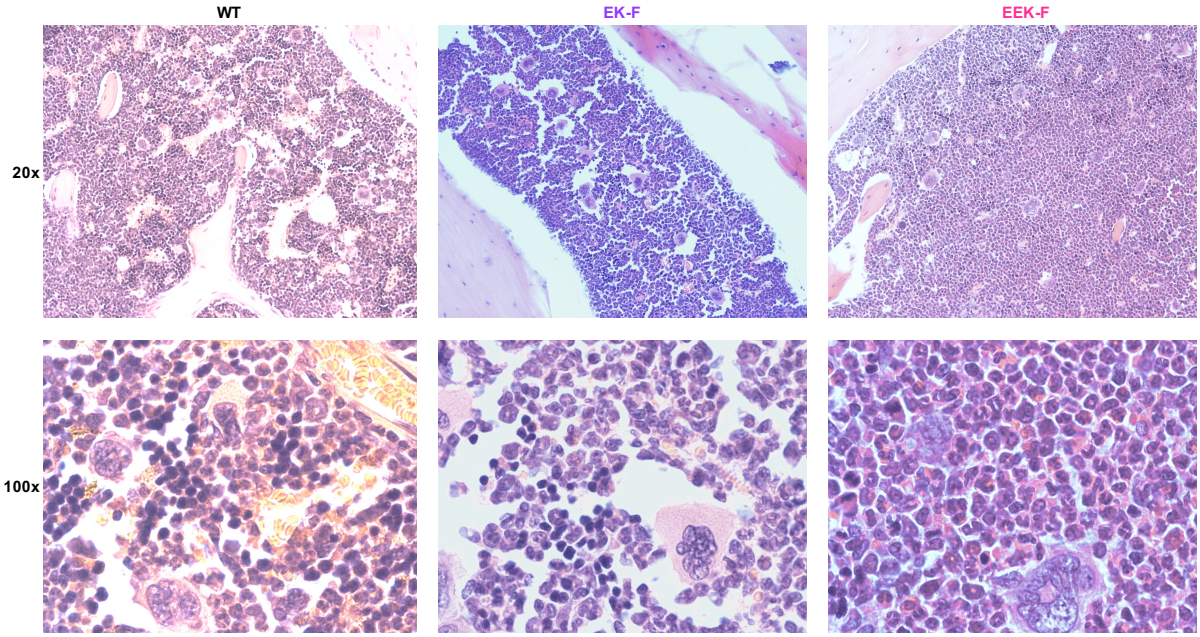


Fig 5.11: BM histology of adult induced mice consistent with flow cytometry. Expansion of myeloid cells, both monocytic and neutrophilic in all Kras mutant genotypes available with depletion of megakaryocytes. H+E stained sections of BM from WT (n=2), EK-F (n=2) and EEK-F (n=2). No K-F mice available for analysis.

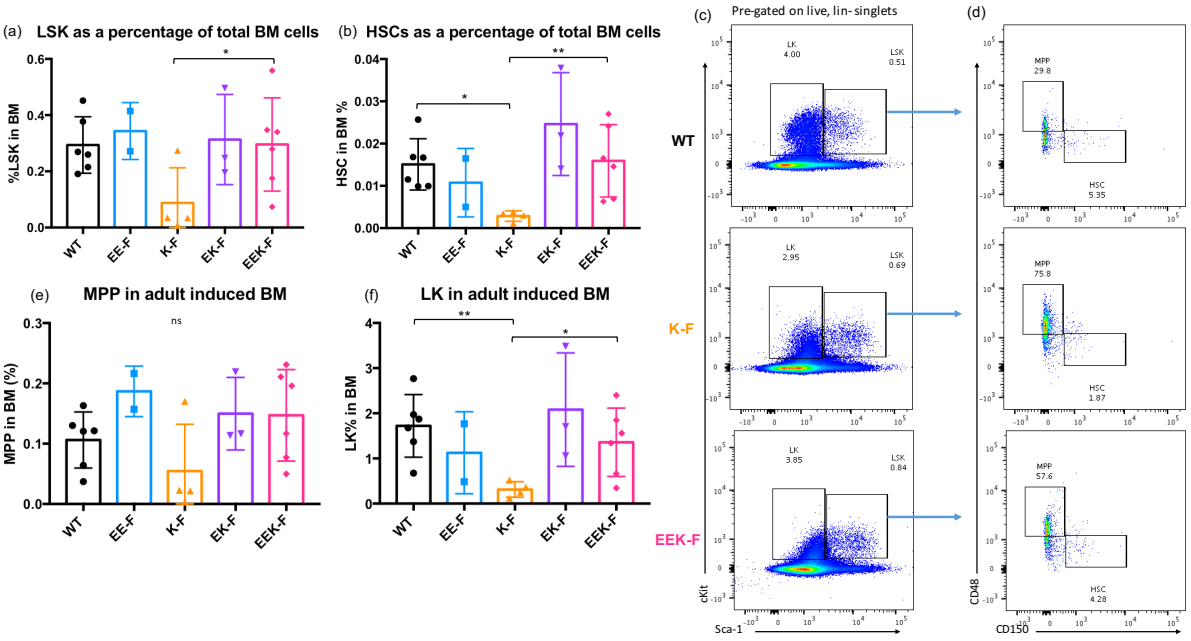


Fig 5.12: *Ezh2* loss rescues the stem cell depletion of K-F mice. (a) Lin-, Sca-1+, cKit+ cells shown as a percentage of total BM cells (b) HSCs (LSKs, CD150+,CD48-) shown as a percentage of total BM cells. Each point represents a biological replicate. (c) Representative LSK gating from WT (n=6) or mice with myelomonocytic leukaemia from K-F (n=2), EEK-F (n=6) and (d) HSC gating from these mice. (e) MPPs (LSKs, CD150-, CD48+) as a percentage of total BM and (f) LK cells. T cell leukaemic mice excluded. Each data point represents a single biological replicateT-cell leukaemic mice excluded from LSK, HSC, MPP and LK graphs. Statistical analysis by Mann-Whitney U test. *p<0.05 **p<0.01, ns = not significant.

ii) Does *Ezh2* loss permit transplantation of a leukaemia derived from adult cells

Next, to assess whether EK-F or EEK-F rescued the stem cell function as well as HSC phenotype, I performed secondary transplants into CD45.1 mice using BM from CD45.2 adult mice originally transplanted with EK-F and EEK-F cells as well as EE-F and WT controls. This showed PB engraftment of myeloid and B and T lineage cells in all of the mice 4 and 8 weeks after transplant (figures 5.13a-d). Unfortunately, as a result of the COVID-19 restrictions, the 12-week readout could not be conducted and all remaining mice were culled at ~16 weeks. However, prior to this T cell leukaemia developed in 2/7 EK-F/EEK-F mice while a further 2/7 were found dead and presumed to have T cell leukaemia (figure 5.13e-g). This high frequency of T-cell leukaemia further emphasises the limitations of using the transplantation model for study of Kras^{G12D} -induced myeloid leukaemia.

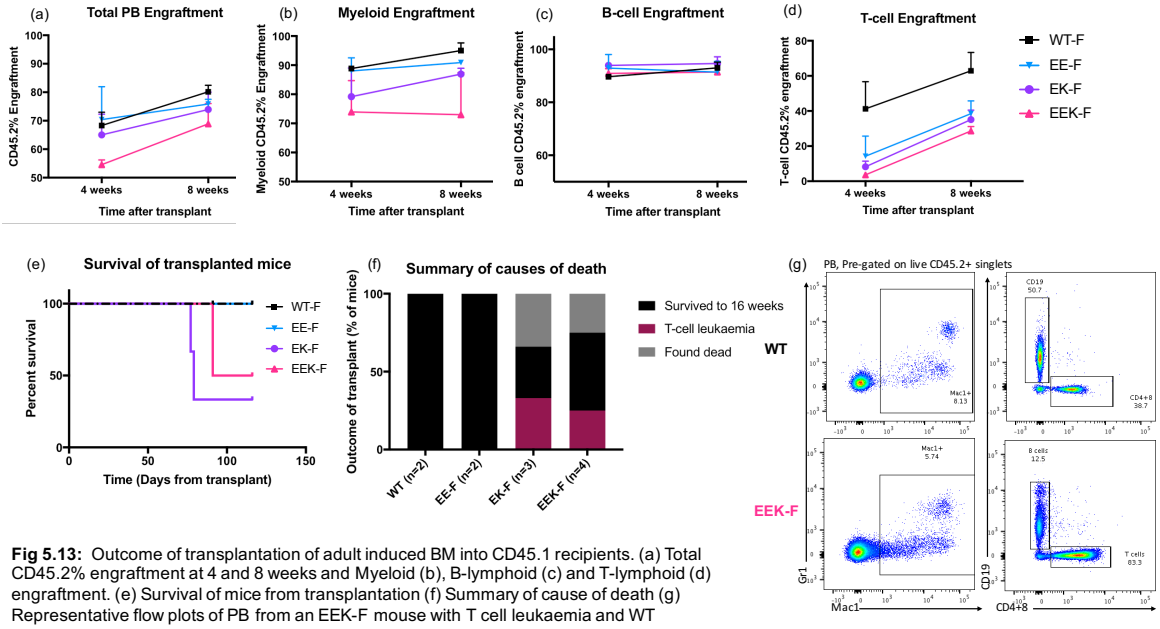
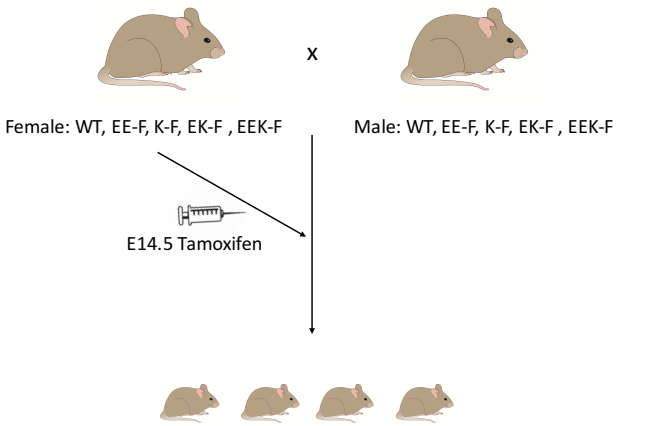


Fig 5.13: Outcome of transplantation of adult induced BM into CD45.1 recipients. (a) Total CD45.2% engraftment at 4 and 8 weeks and Myeloid (b), B-lymphoid (c) and T-lymphoid (d) engraftment. (e) Survival of mice from transplantation (f) Summary of cause of death (g) Representative flow plots of PB from an EEK-F mouse with T cell leukaemia and WT control. Results from a single experiment. Replicates: WT (n=2), EE-F (n=2), EK-F (n=3), EEK-F (n=4)

5-3. How does *Ezh2* loss in fetal life affect the $Kras^{G12D}$ model of leukaemia

Overall, my data from the adult-induced primary mice suggests that *Ezh2*-KO does alter Kras mutant leukaemogenesis. Specifically, taken together with the transplanted Mx1Cre model, my data suggest that *Ezh2-KO* drives a myeloid phenotype and that perhaps even heterozygous loss of *Ezh2* diminishes the T-cell leukaemia potential. The reasons for this are not clear, but it is known that *Ezh2* loss depletes the ability for T-cells to mature [Su, 2005].

As JMML is likely to arise in fetal cells and certainly well before adulthood, since this disease is never seen in adults, the most useful insight into the ways in which mutant *Kras* and *Ezh2* loss combine to cause this aggressive leukaemia is likely to require experiments in in fetal cells. Therefore, to investigate the effect of *Ezh2* loss on a mutant fetal cell, I induced pregnant dams with tamoxifen at E14.5, which had been mated with male mice and were expected to bear litters with EK-F or EEK-F genotypes (figure 5.14). After birth, the mice were followed up to determine the timing and phenotype of any leukaemias developing.



Genotypes – Fgd5CreERT2				
WT	– $Ezh2^{+/+}$,	$Kras^{+/+}$,	$dtomato^{fl/+}$,	*Fgd5CreERT2$^{tg/+}$ or Fgd5CreERT2$^{+/+}$*
EE-F	– $Ezh2^{fl/fl}$,	$Kras^{+/+}$,	$dtomato^{fl/+}$,	*Fgd5CreERT2$^{tg/+}$*
K-F	– $Ezh2^{+/+}$,	$Kras^{LoxP/+}$,	$dtomato^{fl/+}$,	*Fgd5CreERT2$^{tg/+}$*
EK-F	– $Ezh2^{fl/+}$,	$Kras^{LoxP/+}$,	$dtomato^{fl/+}$,	*Fgd5CreERT2$^{tg/+}$*
EEK-F	– $Ezh2^{fl/fl}$,	$Kras^{LoxP/+}$,	$dtomato^{fl/+}$,	*Fgd5CreERT2$^{tg/+}$*

Fig 5.14: Design of experiments to investigate the impact of Ezh2 loss on mutant Kras-driven leukaemia by induction in fetal cells

i) Impact of Ezh2 on the phenotype of mutant Kras driven disease in fetal cells

Timing and nature of leukaemia: All mice with mutant Kras, with or without *Ezh2* loss died of leukaemia within 70 days of life (figure 5.15a). However, both heterozygous or homozygous *Ezh2*-KO accelerated the onset of disease, although this reached statistical significance only for the mice with heterozygous *Ezh2* loss (EK-F) (figure 5.15a). The acceleration of leukaemia with Ezh2 loss is similar to the adult-induced mice, however the nature of the disease was distinctly different in the fetally-induced mice. All fetally-induced Kras mutant mice developed fatal myelomonocytic disease resembling JMML but with variable expansion of Mac1+Gr1+ cells (figure 5.15b-c). Interestingly, for 4/6 of the EK-F mice and 3/7 of the EEK-F mice the Mac1+ population was largely Gr1+ (figure 5.15b-c) and

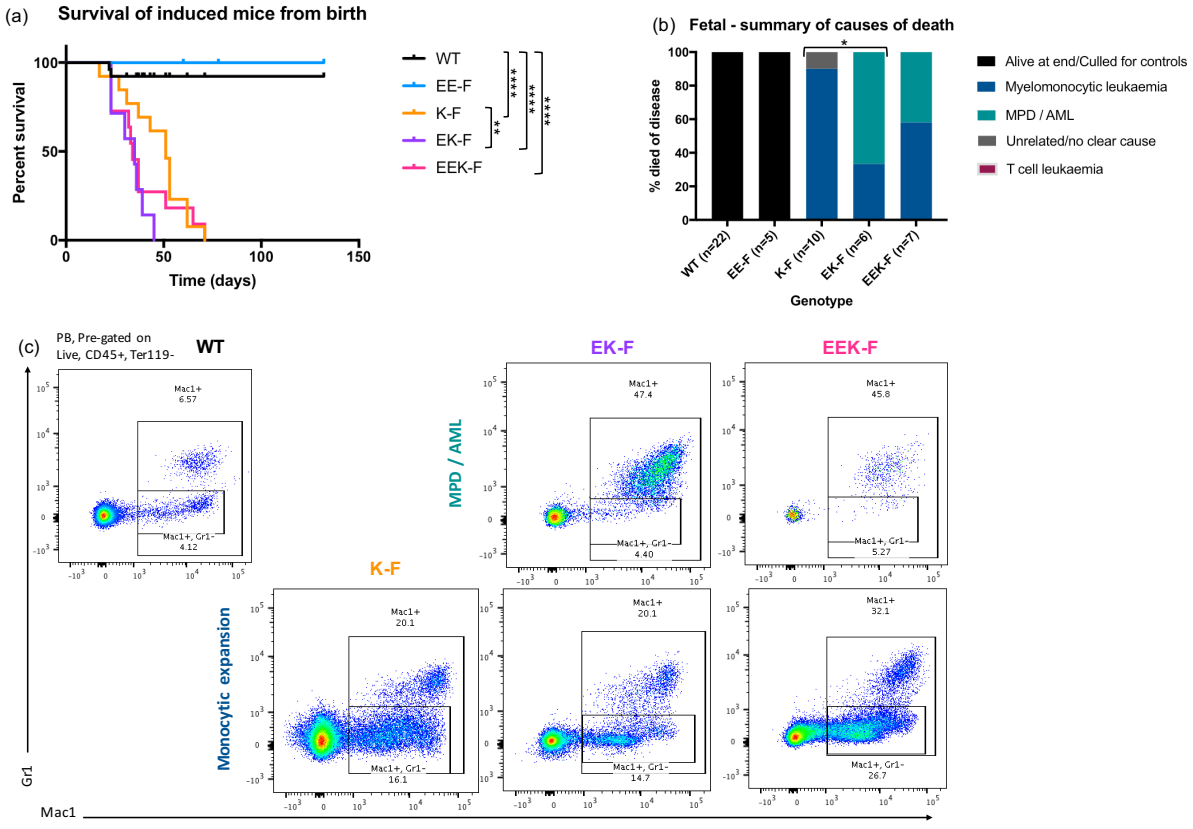


Fig 5.15: Ezh2 loss in fetal induced Kras^{G12D} mutant mice accelerates disease and alters the phenotype. (a) Survival following induction. Median survival was reduced in both EK-F mice (35 days) and EEK-F mice (34 days) compared to K-F mice (51 days). (b) Percentage of mice succumbing to each disease, excluding those found dead. (c) Example FACS plots from representative WT (n=22), or EK-F (n=4) or EEK-F (n=2) mice with MPD/AML and K-F (n=9), EK-F (n=2) or EEK-F (n=4) with myelomonocytic leukaemia. Replicate numbers able to be analysed shown in (b). Statistical analysis of survival with Mantel-Cox test, of summary death ANOVA. *p<0.05 **p<0.01, ***p<0.001, ****p<0.0001

I designated these MPD/AML as these also had other evidence of increased numbers of mature and immature neutrophils on PB films (figure 5.17c) and BM (figure 5.18a) histology, and the flow cytometry resembled the adult phenotype seen with K-F mice (figure 4.3, table 4-1). This may be similar to the pattern seen in some patients with JMML where the PB/BM may show prominent changes in the granulocytic cells and their precursors as well as abnormal monocytes. However, this phenotype was seen only in the fetally-induced mutant Kras mice with Ezh2 loss suggesting that this difference is driven by the loss of Ezh2.

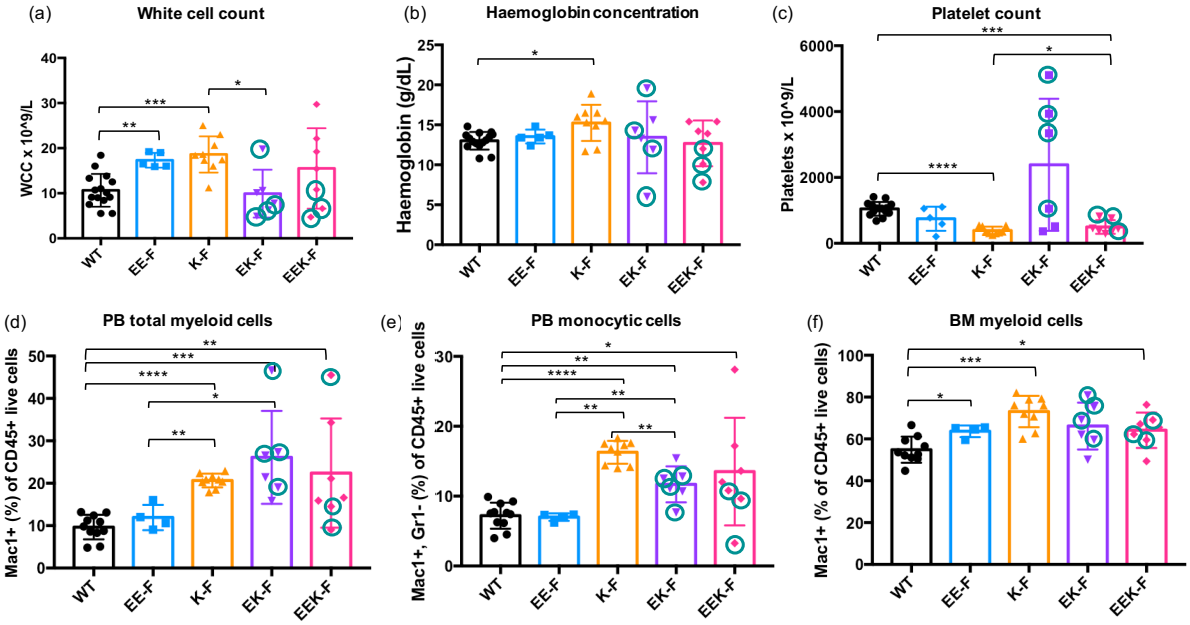


Fig 5.16: Ezh2 loss changes the PB phenotypic findings in fetal induced mice. (a) Final white cell count (x10^9/L) (b) Haemoglobin concentration at final readout (g/dL) and (c) Final platelet count (x10^9/L). (d) Myeloid series by FACS differentiation of Total Mac1+ in PB (e) Mac1+, Gr1-, monocytic cells and (f) total Mac1+ve cells in BM. MPD/AML mice marked with circles in each graph. Data at terminal readout, each data point represents a biological replicate. Statistical analysis with Mann-Whitney U test. *p<0.05, **p<0.01 ***p<0.001, ****p<0.0001

Blood counts and blood films: Analysis of blood counts from the fetally-induced mutant Kras mice showed a significant increase in white cell count in the K-F and EE-F mice compared to WT mice but, unexpectedly, this seemed to be ameliorated in mutant Kras mice with *Ezh2* loss (figure 5.16a). None of the mice developed anaemia; indeed the haemoglobin in the K-F mice

was slightly higher than the WT mice (figure 5.16b). However, apart from 3 EK-F mice,

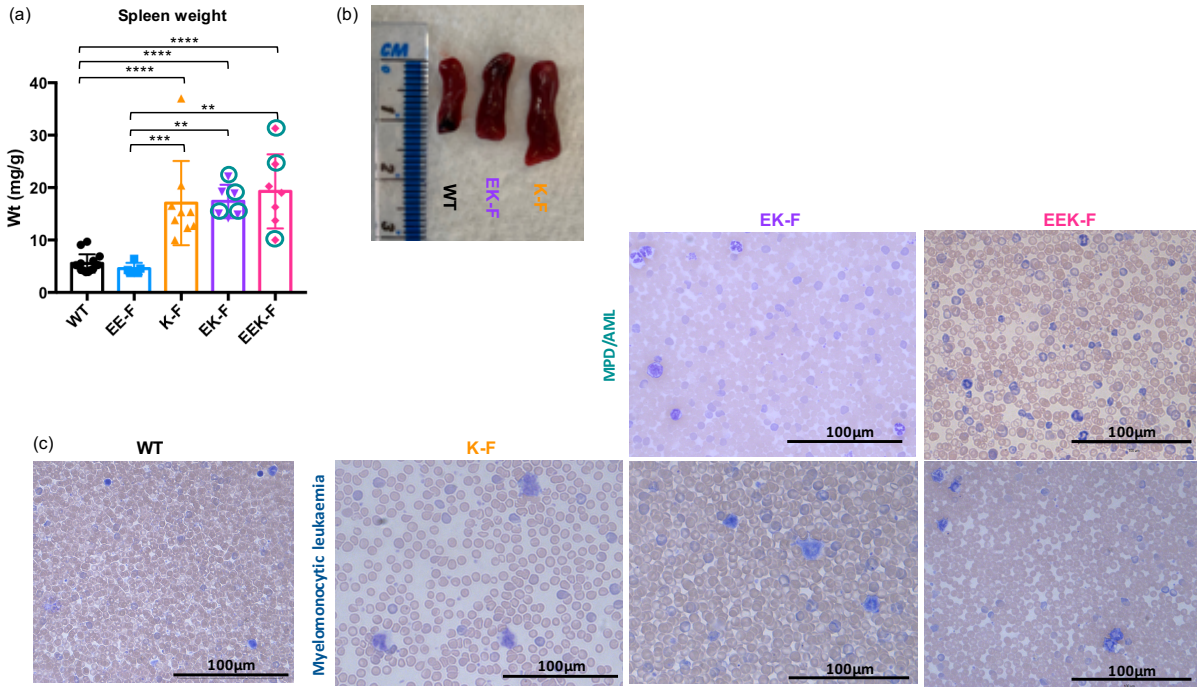


Fig 5.17: Fetal Ezh2 loss affects the morphology of Kras mutated leukaemia. (a) Spleen weights (mg/g) in fetal induced mice with MPD/AML mice marked with circles and (b) example size of spleens (n=1 representative image) (c) Representative PB films from fetal WT (n=6), K-F mice with myelomonocytic leukaemia (n=8) and either EK-F with MPD/AML expansion (n=2) or myelomonocytic disease (n=2) or EEK-F mice with MPD/AML(n=1) or myelomonocytic leukaemia (n=3) . This shows expansion of monocytes in the myelomonocytic leukaemias, or neutrophils in the MPD/AML cohort. Statistical analysis with Mann-Whitney U test. **p<0.01, ***p<0.001, ****p<0.0001

all of the mutant Kras mice developed thrombocytopenia (figure 5.16c). These 3 EK-F mice had very marked thrombocytosis (platelet counts 3,000-5,000 x 10^9/L). The reasons for this are unclear although these mice also had MPD/AML rather than myelomonocytic leukaemia. The overall percentage of Mac1+ cells in PB was increased in the mutant Kras mice and this was not significantly affected by Ezh2 loss (figure 5.16d). However, the proportions of Mac1+Gr- and Mac1+Gr+ cells in PB, though increased in all of the Kras genotypes was affected by Ezh2 loss (figure 5.16e), with a significant decrease in the PB Mac1+Gr1- compartment in EK-F mice compared with K-F mice, and a decrease of the mean in EEK-F mice. There was also non-significant decrease with *Ezh2* loss in myeloid cells in the BM when compared to K-F mice (figure 5.16f). These results were supported by manual differential counts and morphological assessment of the white blood cells on PB films (figure 5.17c, 5.20c).

Tissue involvement: All of the mutant *Kras* fetally-induced mice developed splenomegaly consistent with the presence of JMML-like disease and there was no difference between spleen size in the presence of absence of *Ezh2* loss (figure 5.17a-b). As well as splenic infiltration, mutant *Kras* mice showed myelomonocytic infiltration of the BM (figure 5.18a), and lungs (5.18b).

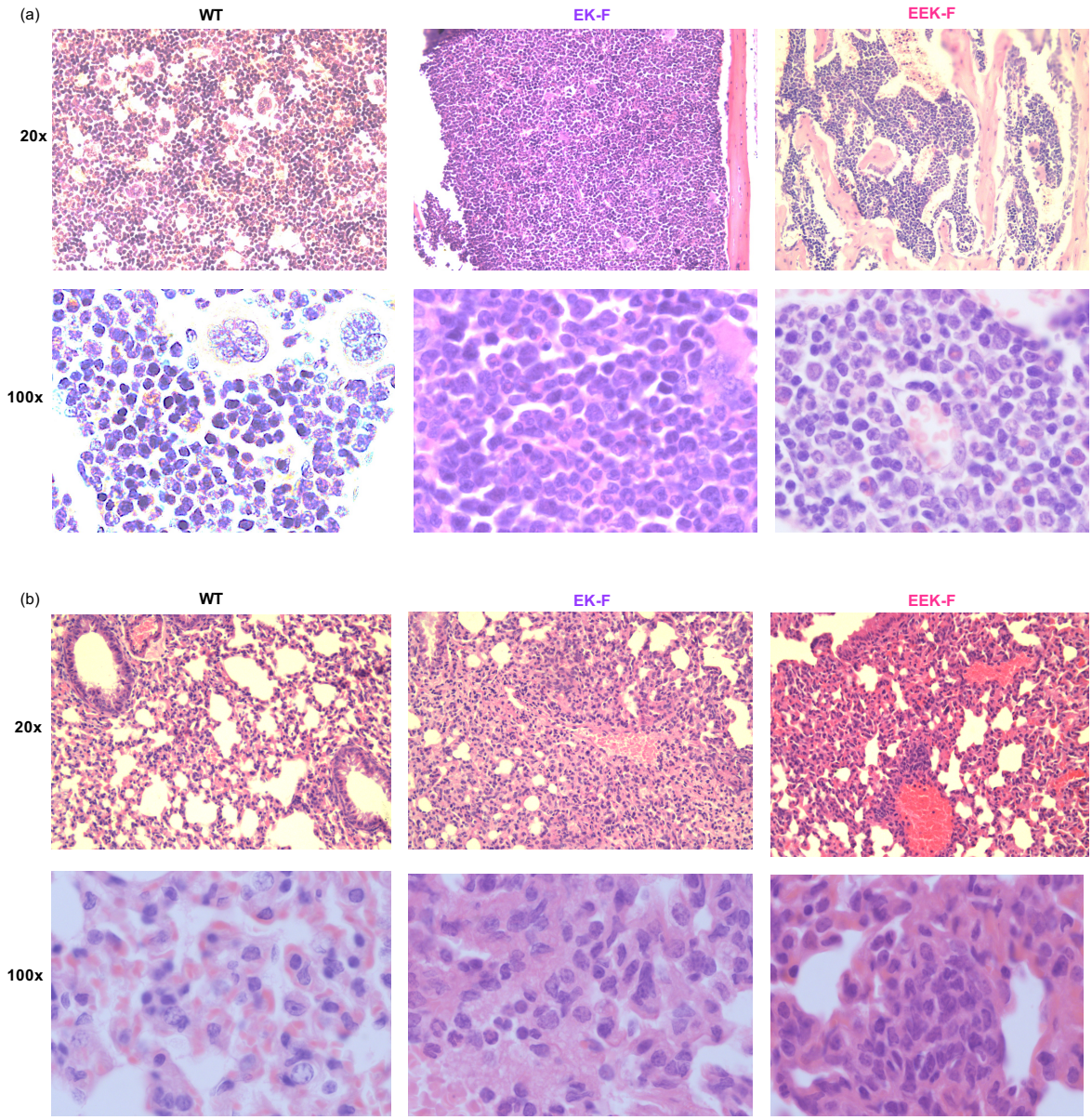


Fig 5.18: Tissue infiltration in BM and Lungs of myelo-monocytic cells. (a) BM infiltration of myeloid cells in fetal induced EK-F and EEK-F mice. H+E stained sections of BM from WT (n=1), EK-F (n=2) and EEK-F (n=2) with myelomonocytic leukaemia. (b) Lung infiltration of myeloid cells in fetal induced Kras leukaemic mice. H+E stained sections of lungs from WT (n=1), EK-F (n=2) and EEK-F (n=1). EK-F mice lung histology from mouse with MPD/AML. Images taken at 20x and 100x magnification.

Immunophenotypic analysis of the HSC and LSK compartments: BM cellularity was similar to WT in Kras mutant mice but was slightly reduced in the presence of Ezh2 loss, particularly with heterozygous Ezh2 loss (figure 5.19a). While LSK, HSC and MPP frequency was preserved in the K-F mice compared to WT mice, *Ezh2* loss caused a significant loss of LSK, HSC and MPP (figure 5.19b-c). Of note, HSC loss was most profound in the EE-F mice without *Kras* mutation (figure 5.19c).

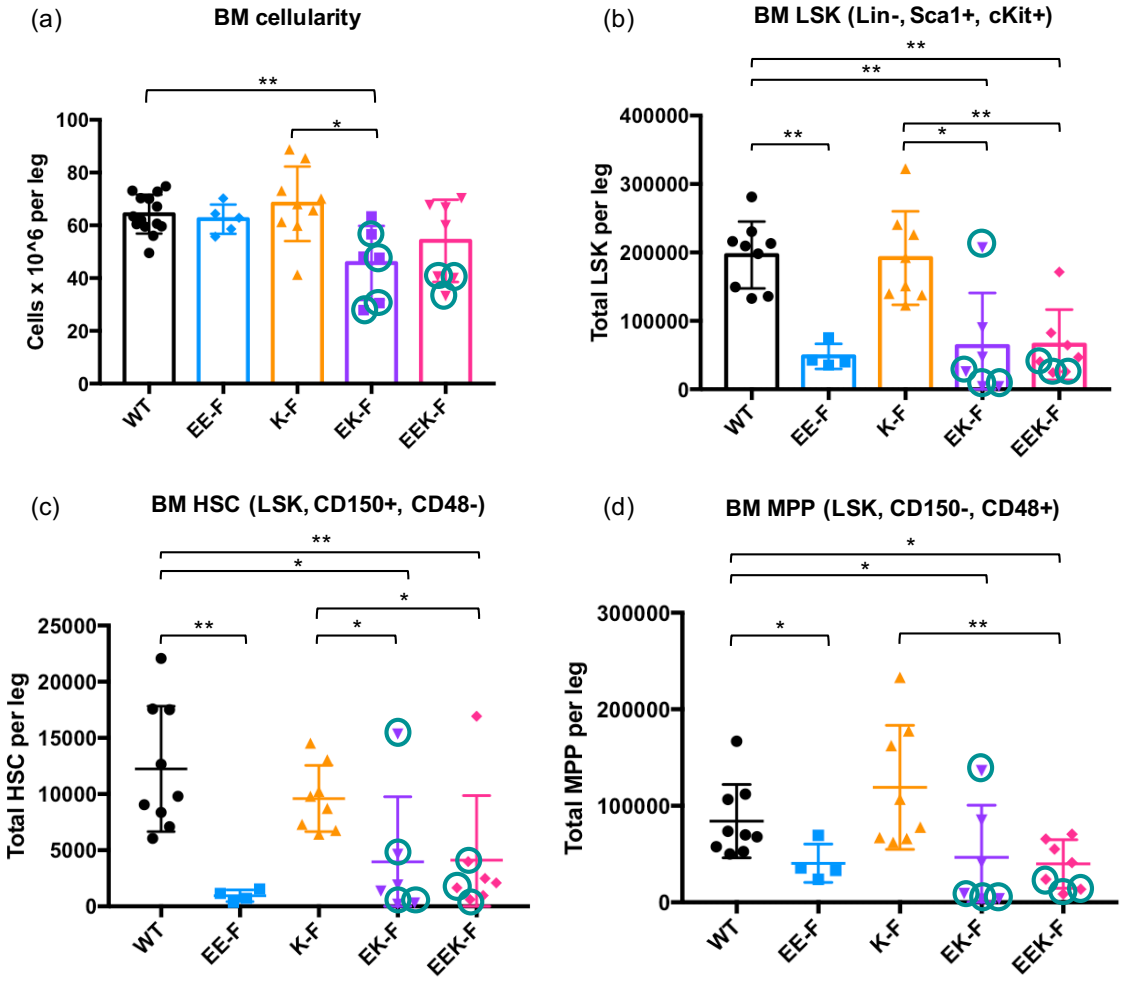


Fig 5.19: Ezh2 loss depletes the LSK and HSC compartments. (a) Total BM cellularity at terminal readout of fetal induced mice (b) LSKs shown as total LSK cells per leg and (c) HSCs, (d) MPPs. MPD/AML mice marked with a circle. Each data point represents a biological replicate. Statistical analysis with Mann-Whitney U test. *p<0.05, **p<0.01

This was surprising, given that in all other situations Ezh2-KO appears to enhance stem cell function, but this is the first time in my studies which I had successfully induced the LOF in a fetal cell. Ezh2 loss alone appeared to replicate this loss of phenotypic LSKs, suggesting an important role for *Ezh2* in fetal cells (figure 5.19b-c). Further replicates, particularly of EE-F, are required to assess these phenotypes further, especially as the published data using other Cre lines to induce in fetal life suggests an expansion of HSCs during fetal life with *Ezh2*-KO [Neo, 2018]. However, it is in keeping with my phenotypic data using Vav-Cre in chapter 3 demonstrating a slight depletion of LK and LSKs, particularly MPPs, in the E12.5 FL. Further, given that *Ezh2*-KO in these other models is fetally lethal, my *Fgd5* induced model is the first to allow study of the transition between fetal and adult HSC activity.

This loss of phenotypic LSKs and HSCs may represent an important role of *Ezh2* in the fetal-adult transition and to study this further, the functional effect of *Ezh2* induced in FL, adult life, or allowed to transition, could be assessed through tandem transplantation experiments. Importantly however, *Ezh2* loss alone appears to exert subtle effects on HSC function, as EE-F mice survived without developing leukaemia and with only borderline leucocytosis and mild increase in total BM myeloid cells. This relative proliferation may explain the depletion in other compartments.

ii) Does *Ezh2* loss alter the function of Kras mutated leukaemia?

Given the findings that *Ezh2* loss modified the leukaemia phenotype in fetally-induced K-F mice, I next performed transplantation experiments using BM from the mice with JMML-like myelomonocytic disease. Unfortunately, as with my previous transplantation experiments, the only leukaemias which developed were of T-lineage (figures 5.20a-b). Further functional assays could be undertaken by assessing serial replating in vitro, however this would not assess

in-vivo function. If time had allowed, an alternative approach would have been to transplant fetal- or adult-induced cells *in*-utero to assess if the fetal liver microenvironment plays an important role in disease development.

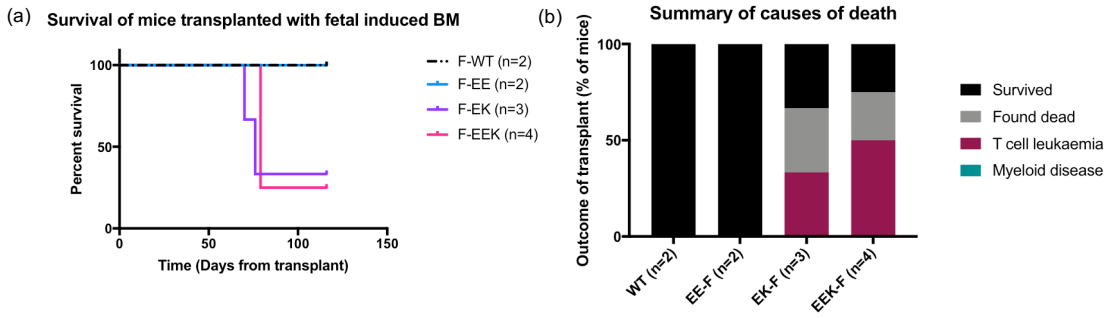


Fig 5.20: Transplantation of BM from fetal induced mice with myelomonocytic leukaemia into CD45.1 recipients. (a) Survival of mice transplanted with leukaemic BM from primary fetal induced mice and (b) summary of the outcome of these mice. Replicate number shown in figure (a). Results from a single experiment.

iii) Does *Ezh2* loss have differential effects in fetal and adult leukaemic mice?

Finally, I compared the impact of Ezh2 loss with Kras mutation according to whether induction was performed in fetal or adult life. This comparison revealed several important differences. First, whilst *Ezh2* loss appears to accelerate the disease in either setting, all fetal genotypes had significantly shorter survival (figure 5.21a). Second, while T-cell leukaemia occurred in a proportion of all mutant Kras adult-induced mice, no fetal mice developed T-cell leukaemia (figure 5.21b). Thirdly, Ezh2 loss led to an increase in the proportion of MPD/AML in fetally-induced compared to a diminished proportion in adult-induced mutant Kras mice (figure 5.21b).

In fetal K-F mice, the monocytic expansion was similar, whereas in adult mice with EK-F or EEK-F genotypes there was a clear expanded monocytic population (T-cell leukaemia excluded), and although present in fetal induced mice, this was less marked (figure 5.21c,

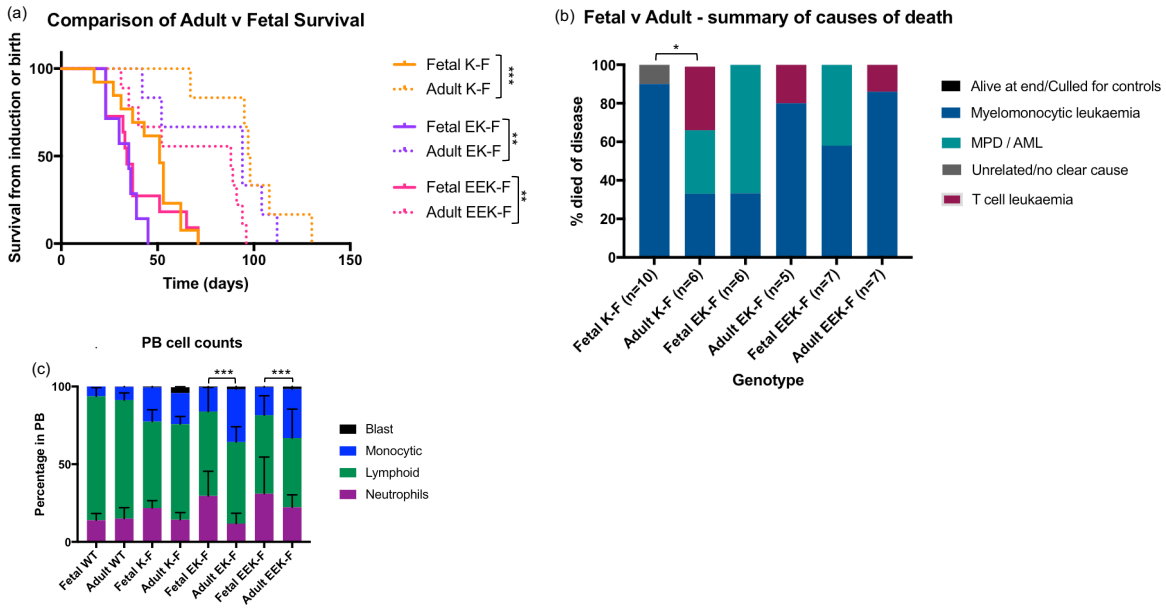


Fig 5.21: The effects of Ezh2 loss alter depending when in ontogeny the loss occurs. (a) Survival comparison of fetal and adult mice from the end of induction or birth (5 days after first exposure to tamoxifen. Median survival fetal K-F (51 days), EK-F (35 days), EEK-F (34 days) and adult K-F (97.5 days), EK-F (94 days), EEK-F (88 days). (b) Summary of causes of death, showing adult and fetal induced mice with mutant Kras +/- Ezh2 loss. (c) Manual PB differential cell counts (200 cell counts) of mice with myelomonocytic leukaemia or MPD/AML. Statistical analysis of survival with Mantel-Cox test, of summary death and cell counts ANOVA. *p<0.05, **p<0.01, ***p<0.001

5.22a). Further the alterations in the HSPC compartments are surprising. With Ezh2-KO in adult life there is a rescue of the phenotypic HSCs and LSKs, whereas induction in fetal life appears to lead to a depletion (figure 5.22b-d). This may be an effect of *Ezh2*-KO alone, where although the replicate numbers are small there is a marked depletion with fetal induction (figure 5.22d). This suggests an important role of *Ezh2 in* stem cell evolution throughout ontogeny, and possibly importance in the transition between fetal and adult stem cell function.

5-4. Molecular alterations associated with *Ezh2* loss in $Kras^{G12D}$ mutated HSPCs

In order to investigate the molecular changes which *Ezh2* leads to in Kras mutant HSPCs I planned to undertake RNA sequencing of all the genotypes in both the adult and fetal-induced mice. This would study the hypothesis that *Ezh2* loss in adult leukaemic HSPCs

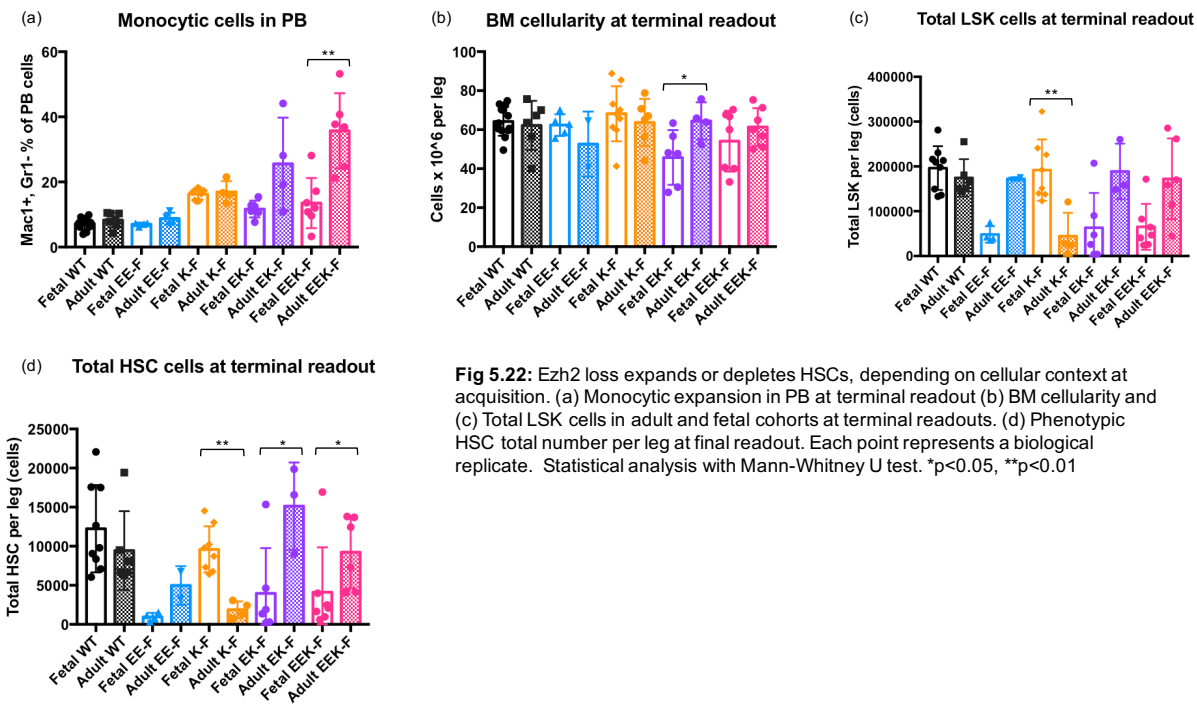


Fig 5.22: Ezh2 loss expands or depletes HSCs, depending on cellular context at acquisition. (a) Monocytic expansion in PB at terminal readout (b) BM cellularity and (c) Total LSK cells in adult and fetal cohorts at terminal readouts. (d) Phenotypic HSC total number per leg at final readout. Each point represents a biological replicate. Statistical analysis with Mann-Whitney U test. *p<0.05, **p<0.01

leads to a 'fetal' like program, whereas loss in fetal life dysregulates haematopoiesis and alters the fate of the leukaemic stem cell. This experiment would help to support the hypothesis that in the human disease, *EZH2* loss is acquired postnatally, but may also provide insight into the role of *Ezh2* in stem cell biology, particularly the switch between fetal and adult stem cells. Another reason for sequencing would be to identify a potential therapeutic target, ideally a fetal-specific target, which could then be validated using mechanistic experiments.

Unfortunately, due to the COVID-19 pandemic and recurrent lockdowns in combination with clinical commitments, as discussed in chapter 4, this experiment has been postponed until it is logistically feasible. The experiment would be as described in chapter 4, targeting either LSKs or HSCs to assess the impact of *Ezh2* loss in combination with $Kras^{G12D}$ throughout ontogeny.

5-5. Summary and Discussion

These experiments show a differential effect of *Ezh2* on *Kras* mutant leukaemogenesis throughout ontogeny. Xie *et al* [Xie, 2014], demonstrated that *Ezh2* is sequentially downregulated from fetal life through to neonatal and adult life, thus suggesting that *Ezh2* is important for the switch from a functional fetal HSC to an adult HSC. My data support this finding and suggests an important role for *Ezh2* in leukaemogenesis, as well as in developmental stem cell function.

The experiments in this chapter also show the development of a new murine model of JMML that mimics the human disease more closely than existing models. Furthermore, it uses primary fetal cells and circumvents many of the problems associated with transplantation models. By using either alternative CreERT2 transgenic models or alternative conditionally mutated genes this method could be used to study the biology of other genes throughout ontogeny, or other fetally derived leukaemias, such as MLL-AF4 infant leukaemia.

i) Does *Ezh2* loss alter the $Kras^{G12D}$ driven leukaemia?

The data shown above suggests that *Ezh2-KO* alters the phenotype of both adult and fetal leukaemia. Whereas only a third of adult K-F mice develop JMML, *Ezh2* loss of any sort increases that to proportion to ~5/6. Further, where ~$1/3^{rd}$ of adult mice developed T-cell leukaemia, *Ezh2-KO* reduced that by 50% to $1/6^{th}$. This increasing proportion of myeloid disease is accompanied by increased myeloid cells in the BM and a rescue of the $Kras^{G12D}$ associated HSC depletion.

Induction of the mutations in fetal life also demonstrates the impact of *Ezh2* loss in that setting. Whilst these mice did not develop T-cell leukaemia, there was a decrease in HSCs with *Ezh2*

loss. *Ezh2*-KO alone in the FL also depleted the HSC compartment. Given that with pan-haematopoietic KO with VavCre, there is an increase in HSC numbers throughout fetal life [Neo, 2018], and with an increased expression of *Ezh2* mRNA in fetal life compared to adult life [Xie, 2014], this data suggesting that *Ezh2* is vital for the fetal to adult switch. This appears not to alter function, as although transplantation experiments are flawed for the leukaemia model, all EE-F and EE-M mice engrafted myeloid cells to similar proportion to WT mice. The occurrence of thrombocytosis in half of the fetally-induced EK-F mice, in contrast to the thrombocytopenia and raised haemoglobin in fetally-induced K-F mice also suggests the potential importance of *Ezh2* balance in determining haematopoietic cell fate decisions.

ii) Is there a differential effect between adult and fetal *Ezh2* loss?

The reason for the phenotypic differences between fetal and adult life is not clear from the data, however, it is possible that *Ezh2* in adult life drives a more fetal, or myeloid, phenotype. *Ezh2*-KO is known to increase the proportion of myeloid cells, partly through depleting the B- and T-cell potential [Su, 2003][Su, 2005]. The reason for the depletion of HSCs and myelomonocytic leukaemia in fetal life is not clear, and needs further investigation, but can most logically be explained by an important role of *Ezh2* at a vital point of leukaemia development. There are also some similarities between adult and fetal *Ezh2* loss, the main one being that heterozygous and homozygous *Ezh2* loss appeared to shorten the latency of disease which is perhaps not surprising since *Ezh2* loss is a feature of both childhood and adult leukaemias.

Nevertheless, there are some clear differences between adult and fetal *Ezh2* loss. *Ezh2* differentially rescued and depleted the HSC compartment in the Kras mutant adult or fetal HSCs respectively. Functionally, this would be important to address, however transplantation

experiments are fraught with T-cell leukaemia development. No fetal primary mice developed T-cell leukaemia, however still ~1/6th of adult mice did, even with Ezh2-KO.

Given that EE-F appears to share many of the findings of EK-F and EEK-F in fetal induced mice, it may be that these effects are primarily due to *Ezh2*-loss rather than the effect of *Ezh2* in mutant cells. There are suggestions that this is not entirely the case, as evidenced by the accelerated disease and slight but persistent alterations in phenotype with *Ezh2* loss in fetal life. However, it may be that *Ezh2* plays a major role in the ontogenic development of normal stem cell function, as evidenced by the change of expression over time from fetal through to adult life [Xie, 2014]. Given the clear change in phenotype observed and the reversion to a more 'fetal' phenotype with *Ezh2* loss in adult mice, as well as the alteration of the myelomonocytic phenotype observed in fetal life, it is possible to use this to hypothesise that *Ezh2* mutations occur postnatally, where the RAS pathway mutations generally occur *in-utero* in JMML.

It is possible, given these findings in the EEK-F mice that *Ezh2* loss may deplete HSC activity, that the initial model using Vav-Cre was representative, given EEK-V FL did not engraft at all. It might also be interesting to study the transcriptome of the EEK-V FL HSPCs to assess whether they share any dysregulated genes with EEK-F mutant HSPCs.

iii) Future work

Unfortunately, COVID-19 restrictions precluded the planned transcriptomic studies needed to investigate the molecular basis for the phenotypic and functional differences I have observed in mutant Kras induced leukaemogenesis, both in the presence and absebce of Ezh2 loss, and in fetal versus adult onset disease.

Studying the effect of *Ezh2* loss throughout ontogeny is difficult without the ability to use transplantation experiments. With the possibility to transplant cells, it would be of use to study the effect of transplantations at different stages of development to assess the role of *Ezh2* in leukaemogenesis. Whilst this may be possible for Ezh2-KO alone, this would not be fruitful for mutant cells given the problems with T-cell leukaemia. However, given the alteration in phenotype seen on induction of neonatal mice in the Mx1Cre experiments, a series of inductions of primary mice at sequential stages of ontogeny (early FL, late FL, neonatal, 3weeks old and adult) could help to elucidate any differences.

An alternative would be to assess *in-vitro* the functional effect of *Ezh2*-KO, either through pharmaceutical means (eg UNC-1999, an *Ezh* inhibitor) or inducible knockdown, however the lack of major difference on *in-vitro* assessment between adult and fetal K-F cells (see chapter 4) suggests it may be difficult to discern a difference. Transplantation experiments between the different environments (fetal to adult transplants, or adult to fetal transplants) could be attempted but may carry similar problems as described frequently above. The definitive, but difficult, experiment to show this effect would be sequential induction, either using a Dre-rox method or an inducible knockdown, to assess the role of secondary mutation of *Ezh2* in Kras mutant cells. This would also help solve a flaw in many mouse models that mutations in haematopoietic disease are sequential, rather than acquired together.

References

Booth CAG, Barkas N, Neo WH, et al. Ezh2 and Runx1 Mutations Collaborate to Initiate Lympho-Myeloid Leukemia in Early Thymic Progenitors. *Cancer Cell*. 2018;33(2):274-291.e8.

Caye A, Strullu M, Guidez F, et al. Juvenile myelomonocytic leukemia displays mutations in components of the RAS pathway and the PRC2 network. *Nat Genet*. 2015;47(11):1334-1340.

De Raedt T, Beert E, Pasmant E, et al. PRC2 loss amplifies Ras-driven transcription and confers sensitivity to BRD4-based therapies. *Nature*. 2014;514(7521):247-251.

Di Genua C, Norfo R, Rodriguez-Meira A, et al. Cell-intrinsic depletion of Aml1-ETO-expressing pre-leukemic hematopoietic stem cells by K-Ras activating mutation. *Haematologica*. 2019;104(11):2215-2224.

Neo WH, Booth CAG, Azzoni E, et al. Cell-extrinsic hematopoietic impact of Ezh2 inactivation in fetal liver endothelial cells. *Blood*. 2018;131(20):2223-2234.

Mochizuki-Kashio M, Mishima Y, Miyagi S, et al. Dependency on the polycomb gene Ezh2 distinguishes fetal from adult hematopoietic stem cells [published correction appears in *Blood*. 2012 Jul 26;120(4):924]. *Blood*. 2011;118(25):6553-6561.

Muto T, Sashida G, Oshima M, et al. Concurrent loss of Ezh2 and Tet2 cooperates in the pathogenesis of myelodysplastic disorders. *J Exp Med*. 2013;210(12):2627-2639.

Ntziachristos P, Tsirigos A, Van Vlierberghe P, et al. Genetic inactivation of the polycomb repressive complex 2 in T cell acute lymphoblastic leukemia. *Nat Med*. 2012;18(2):298-301.

Oshima M, Hasegawa N, Mochizuki-Kashio M, et al. Ezh2 regulates the Lin28/let-7 pathway to restrict activation of fetal gene signature in adult hematopoietic stem cells. *Exp Hematol*. 2016;44(4):282-96.e3.

Sabnis AJ, Cheung LS, Dail M, et al. Oncogenic Kras initiates leukemia in hematopoietic stem cells. *PLoS Biol*. 2009;7(3):e59.

Sashida G, Wang C, Tomioka T, et al. The loss of Ezh2 drives the pathogenesis of myelofibrosis and sensitizes tumor-initiating cells to bromodomain inhibition. *J Exp Med*. 2016;213(8):1459-1477.

Shimizu T, Kubovcakova L, Nienhold R, et al. Loss of Ezh2 synergizes with JAK2-V617F in initiating myeloproliferative neoplasms and promoting myelofibrosis. *J Exp Med*. 2016;213(8):1479-1496.

Stieglitz E, Taylor-Weiner AN, Chang TY, et al. The genomic landscape of juvenile myelomonocytic leukemia [published correction appears in Nat Genet. 2015 Nov;47(11):1333] [published correction appears in *Nat Genet*. 2016 Jan;48(1):101]. *Nat Genet*. 2015;47(11):1326-1333.

Su IH, Dobenecker MW, Dickinson E, et al. Polycomb group protein ezh2 controls actin polymerization and cell signaling. *Cell*. 2005;121(3):425-436.

Xie H, Xu J, Hsu JH, et al. Polycomb repressive complex 2 regulates normal hematopoietic stem cell function in a developmental-stage-specific manner. *Cell Stem Cell*. 2014;14(1):68-80.

Vo LT, Kinney MA, Liu X, et al. Regulation of embryonic haematopoietic multipotency by EZH1. *Nature*. 2018;553(7689):506-510.

Yang Y, Akada H, Nath D, Hutchison RE, Mohi G. Loss of Ezh2 cooperates with Jak2V617F in the development of myelofibrosis in a mouse model of myeloproliferative neoplasm. *Blood*. 2016;127(26):3410-3423.

Discussion

As discussed in this thesis, whilst the initiating mutation in JMML is known to occur *in-utero* at least in some cases [Matsuda, 2010][Stieglitz, 2015], there is no current model which adequately reflects JMML and arises from a fetal cell (see Table 1.2). The closest model [Tarnawsky*, 2017], does develop a myeloproliferative disease but the main characteristic is neutrophilia, rather than monocytosis. Furthermore, investigations into the impact of the timing of mutation acquisition is not possible as this model utilises a constitutive conditional activation in Flt3Cre. Although it is known that additional mutations confer a worse prognosis [Caye, 2015][Stieglitz, 2015], these are suspected to occur postnatally and there is no clear evidence on the timing of these in patients. Novel models allowing comparison of fetal and adult mutational gain would therefore be very useful.

Fetal HSCs are more proliferative than their adult counterparts [Morrison, 1995][Busch, 2015] and also have distinct trancriptional programs [Tsai, 1994][Warren, 1994][North, 2002] Copley 2013. For example, *Ezh2* appears to be dispensible for normal fetal HSC maintenance [Xie, 2014][Mochizuki-Kashio, 2011][Neo, 2018]. This may be due to *Ezh1* compensation [Mochizuki-Kashio, 2011], but cell context also seems to be important as reflected by differential effects on repopulating ability of HSPCs when activated at different stages of ontogeny [Mochizuki-Kashio, 2011][Neo, 2018][Vo, 2018]. Intriguingly, *Ezh2* loss in malignant cells, almost universally accelerates disease [Muto, 2013][Yang, 2016][Sashida, 2016][Shimizu, 2016] and does so in tandem with reactivation of fetal gene expression [Shimizu, 2016][Yang, 2016] making this a relevant model to study in the context of JMML. To date, the role of *Ezh2* in $Kras^{G12D}$ leukaemias has not been studied, and although studies suggest a synergistic effect of Ras activation and PRC2 LOF in both haematopoietic and non-

haematopoietic malignancies [de Raedt, 2014][Booth, 2018], it would be important to use a robust fetal model to investigate the effect of *Ezh2* LOF in the context of JMML.

6-1 The development of a mouse model to investigate the fetal origins of leukaemia

i) The advantages and disadvantages of the different models used

A summary of current mouse models of JMML can be seen in Table 1.2. Only one of the published models demonstrates a fetal origin for JMML, and the majority are transplantation models. My initial transplantation data (chapter 3-2 and 3-3) reinforces that using a $Kras^{G12D}$ model provides a T-cell leukaemia model rather than a JMML model. Although it would be possible to use an alternative RAS activating mutation to try to avoid this scenario I chose not to do this for two reasons. Firstly, *KRAS* mutations in JMML are particularly associated with *EZH2* loss [Stieglitz, 2015], and secondly, *KRAS* mutant patients present at an earlier age than those with other *RAS* mutations [Louka, 2019], further suggesting a potential important interaction of these mutations. My data reinforced this interaction (chapter 3-3) as I observed a myeloid drive with *Ezh2* loss and *Kras* mutant mice compared to *Kras* mutant mice without *Ezh2* loss.

Unfortunately, using Mx1Cre primary mice is not possible, both due to restrictions on fetal Cre activation in our licence, but also as my data (chapter 3-4) demonstrates that Mx1Cre spontaneous activation is present even in fetal life, and therefore unsuitable for studies involving ontogenic activation in adult life. Despite these caveats, pilot studies in neonatal and adult mice (chapter 3-5) did demonstrate age-related disease differences with myelomonocytic leukaemia and an increase in skin lesions, as seen in JMML, in neonatal mice. This indicates that using a robust Cre-activating system in primary mice should create a novel and useful model to study both the ontogenic timing of mutations in JMML but also the interaction

between *Ezh2* and leukaemogenic *Kras*. Using the *Fgd5CreERT2* system appeared to offer an ideal approach as *Fgd5* is exclusively expressed in HSCs [Gazit, 2014], which are the candidate cell of origin in JMML [Louka, 2019][Caye, 2020].

ii) Future directions and possibilities of the Fgd5CreERT2 model

My data in chapter 3-6 did indeed demonstrate that Fgd5CreERT2 is a robust Cre with no spontaneous activation in either fetal life or adult life. Uninduced mice with $Kras^{G12D}$ in combination with Fgd5CreERT2 did not develop disease and when analysed at >8 months of age demonstrated no detectable reporter gene or alterations in blood parameters when compared to WT mice. Using the optimised, fetal induction with $Kras^{G12D}$ did allow me to create a novel model for JMML, discussed below in section 6-2. This is also the first study to develop an *in-vivo* mouse model to compare the effect of oncogenic mutations gained in adult or fetal life. Furthermore, the ability to cleanly induce fetal or adult HSCs without significant neonatal loss despite fostering (chapter 3-6) could also be used to study the differential impact of genes involved in fetal and adult haematopoiesis, such as *Ezh2* or *Soz17* [Kim, 2007][Neo, 2018], but without resorting to transplantations, different mechanisms of induction, or Cre lines, between fetal and adult life.

6-2 Does the timing of acquisition of mutations matter?

My primary aim was to create a model to investigate the fetal origins of JMML, then to use this to investigate the effect of $Kras^{G12D}$ acquisition in fetal life compared with adult life. Using the Kras model I was able to demonstrate the proof of principle that $Kras^{G12D}$ mutation in E14.5 fetal liver cells can lead to JMML (chapter 4-1). This, compared to the published studies in Table 2.1, is the most faithful model of JMML with splenomegaly, monocytosis and thrombocytopenia, derived from a fetal origin without the requirement for transplantation.

Comparison of the YS, FL and aBM induction of leukaemia: My initial YS studies with Vav-iCre transplantation (chapter 4-5) demonstrate the proof of principle that YS cells can cause leukaemia. This was a novel and unexpected finding as whilst other papers have induced *Braf* mutations in the YS and caused a neurodegenerative disease through somatic mutation in EMPs [Mass, 2017], no study has demonstrated the ability for YS derived HSPCs to cause leukaemia. This is partly due to experimental considerations, such as the small number of cells, poor viability *ex-vivo*, and difficult engraftment into recipient mice [McGrath, 2015]. Interestingly, the YS leukaemias were erythroid and B-cell lineage and while this would have been tempting to investigate further, it was clear that this approach did not model JMML. Indeed, using both transplantation methods, and also *in-vivo* mutation with Fgd5CreERT2 induction, I was unable to demonstrate that YS EMPs can be the origin for JMML. This may be because of the optimisation problems, and the difficulties dosing dams with tamoxifen for induction early in pregnancy, without causing miscarriage. Further study could be to use 4-OH-tamoxifen, the active metabolite, which has a much shorter half-life and so may minimise HSC induction whilst inducing early in pregnancy. Nevertheless, using this approach, it appears that YS EMPs are not a readily accessible source of study for the cell of origin in JMML. This is in keeping with data from patients, where the initiating cell appears to sit within the CD34+, CD38- stem cell compartment [Louka, 2019][Caye, 2020]. Whilst the immunophenotype of EMPs in humans has yet to be defined, and may reside within the CD34+ compartment, the most recent studies demonstrate the ability of the phenotypic HSCs and MPPs to recapitulate the disease in recipient mice [Louka, 2019][Caye, 2020], thereby suggesting that JMML is driven from the HSC compartment. Finally, however, murine fetal haematopoiesis is different to that of the human, for example the lack of fetal haemoglobin [Sankaran, 2010] and therefore the murine model may not be ideal to answer questions about the putative EMP origins of JMML.

Fetal liver and adult BM induction, by contrast, demonstrated the ability of induced HSCs to cause a JMML-like disease, with myelomonocytic expansion in K-F mice from both conditions (chapter 4-1). Notably, survival of fetal liver-induced mice was shorter (chapter 4-1), which may reflect the proliferative nature of fetal cells [Morrison, 1995]. More striking was the alteration of phenotype with an almost fully penetrant myelomonocytic leukaemia from fetal liver-induced mice, with thrombocytopenia, splenomegaly and tissue infiltration with monocytic cells. In comparison, whilst ~33% of adult-induced mice developed a similar disease, the majority demonstrated a different phenotype, either T-cell leukaemia, or a different MPN with either neutrophil expansion or AML. This is further evidence, that whilst an activating *Kras* mutation in adult life can cause a myelomonocytic leukaemia, mutation induction in a fetal environment causes profoundly different patterns of disease. It is possible, that this explains the difference between my model, using Fgd5CreERT2 and the Mx1Cre model: which demonstrates a fully penetrant myelomonocytic leukaemia [Braun, 2004]. Whilst the Mx1Cre is not ostensibly fetal in origin these mice are induced as young mice (~3 weeks), compared to the adult mice in my study (~7 weeks). The transplantation data suggests further that the origin of induction is vital. Induction followed by rapid transplantation delivers a uniform T-cell leukaemia with either Mx1Cre [Sabnis, 2009][Zhang, 2009], or Fgd5CreERT2 (chapter 4-2, 4-3). However, induction in FL and expansion to E19.5 before transplantation allows a more penetrant myelomonocytic disease (4/5 mice, chapter 4-2). This hypothesis is in keeping with published data, with a clear suggestion that the microenvironment plays a role in murine models of JMML [Dong, 2016]. The caveat to this is that it is known that the HSC dose is important for the development of myelomonocytic leukaemia in these mice [Sabnis, 2009], and in my E19.5 experiments, more cells were transplanted. It may be that the murine cell of

origin is just not functional on transplantation experiments, hence the better performance in primary mice.

In-vitro assays demonstrated very minor differences functionally between fetal and adult BM LSKs, and validated the model with the GM-CSF hypersensitivity assays usually seen in these published models with Ras activation (chapter 4-2). However, the single cell population, and bulk transplantation experiments (chapter 4-2, 4-3), were unhelpful both due to the problems with transplantation with the *Kras* mouse model, discussed throughout my thesis, and as they had to be terminated early due to the COVID-19 pandemic. Investigations into the molecular basis of my findings, unfortunately, have had to be postponed to beyond the end of my project because of the COVID-19 pandemic but cells from these mouse models have been cryopreserved and RNAseq will be undertaken by another DPhil student. These will hopefully help to elucidate any differences between fetal and adult induction, particularly if fetal K-F HSCs maintain a fetal stem cell signature, when compared the adult K-F induced BM HSCs. This could be vital for both the biological understanding of JMML, and potentially lead to novel therapeutic targeting.

6-3 The effect of *Ezh2* knock-out on a mouse model of JMML

Whilst it is known that *Ezh2* loss in mouse models of myeloproliferative disorders, such as *Jak2* mutant myelofibrosis, leads to reactivation of fetal programs [Shimizu, 2016][Yang, 2016], and that *Ezh2* is known to control many fetal programs [Lund, 2014][Herviou, 2016], the role of *Ezh2* loss in fetal-derived leukaemia has not been studied. An important question for JMML is whether *Ezh2* loss alters the *Ras* driven leukaemia and prevents exhaustion of the leukaemic stem cell pool. Secondary mutations in JMML are known to worsen the prognosis [Stieglitz, 2015], and secondary AML1-ETO mutation when combined with $Kras^{G12D}$ mutation

allows stem cells to survive serial transplantation [Di Genua, 2019]. It is not clear in JMML when these secondary mutations occur, but the importance of *Ezh2* in fetal HSCs is controversial due to the potential compensation by *Ezh1* [Mochizuki-Kashio, 2011][Hidalgo, 2012], and my model comparing fetal and adult induction could be used to help answer these questions.

i) Does *Ezh2* loss alter the phenotype of the mouse model?

Even early transplantation experiments using Mx1Cre E15.5 FL in chapter 3-3, there was a suggestion that *Ezh2* loss combined with *Kras* mutation altered the phenotype of leukaemia, with only *Ezh2* mutant mice developing myeloid disease. However, the aforementioned probems with both the transplantation and Mx1Cre models does not permit a study of when these mutations occur. It is clear however, from my data in chapter 5-1, and elsewhere [Neo, 2018], that on transplantation *Ezh2* loss alone prevents stem cell exhaustion with repopulation of myeloid cells even in quaternary transplantations. This did not appear to be enough to rescue the *Kras* mutant cells (see chapter 5-1).

To study the effect of *Ezh2* loss in a JMML model, I induced FL and adult mice across the genotypes (EE-F, EK-F, EEK-F), as shown in chapter 5-2 and 5-3, thus allowing comparison with the K-F model. Where adult K-F mice had a range of different phenotypes (1/3 each T-cell leukaemia, myelomonocytic leukaemia and MPD/AML), either heterozygous or homozygous *Ezh2* loss altered this, with no mice developing MPD/AML, the vast majority of mice developing myelomonocytic leukaemia (EK-F 4/5, EEK-F 6/7) and abrogation of T-cell leukaemia (EK-F 1/5, EEK-F 1/7). In contrast, when induced in fetal life EK-F and EEK-F mice lost the high penetrance of myelomonocytic leukaemia and developed alternative MPDs in ~50% of mice. In both settings, however, *Ezh2* loss accelerated the disease with a shortened

median survival, and fetal mice retained a significantly shorter survival than adult counterparts. This acceleration of disease is in keeping with both human data [Caye, 2015][Stieglitz, 2015], as well as mouse models combining Polycomb loss with leukaemogenic mutations [Shimizu, 2016][Yang, 2016][Booth, 2018][Di Genua, 2019]. However, the differential effects of *Ezh2* in fetal life and adult life are novel and not previously described; the potential explanation and further evaluation is discussed further in section 6-3.ii, below.

On analysis of the HSPC compartment, adult K-F mice had a significant depletion of HSCs, which was not seen in EK-F or EEK-F mice. In FL induced mice, K-F mice did not lose phenotypic HSCs, but strikingly EK-F and EEK-F mice had HSC depletion both compared to the WT mice and K-F mice. This was accompanied by a moderate depletion in BM cellularity. The fact that secondary mutations can rescue the stem cell phenotype in the *Kras* mutant adult mice is in keeping with published data [Di Genua, 2019], as is the addition of *Ezh2* to other stem cell-depleting mutations [Shimizu, 2016][Yang, 2016]. However, this effect has not been described with *Ezh2* and *Kras* previously and the most surprising finding from my experiments was the opposite effect exerted by *Ezh2* in FL-derived compared to adult cells, i.e. when induced in fetal life, the combination of *Ezh2* with $Kras^{G12D}$ depleted phenotypic HSCs, in addition to the phenotypic changes described above. To investigate this further, ideally transplant experiments would be undertaken to assess stem cell function. Unfortunately however these were not helpful, as discussed in chapter 5-3 and the reason for these phenotypic changes is not clear at present. My model is the first to allow the transition from fetal life to adult life, and these changes were similar to the HSC phenotype in EE-F mice alone. It may be, therefore, that this effect is due to *Ezh2* loss in fetal life rather than the combination of *Ezh2* and mutant *Kras.* The role of *Ezh2* in this transition period has not been studied, but from other studies it is clear that the role of PRC2 is highly dependent on cellular context, and therefore

this differential effect may not be that surprising [Hidalgo, 2012][Neo, 2018][Vo, 2018]. To further investigate this, serial inductions of YS, early FL, late FL, neonatal life through to early adult and later adult induction may be useful. My model system would allow this, and combined with RNA-seq, may help to understand the evolving role of *Ezh2* from fetal to adult life in the future.

ii) Does the Fgd5CreERT2 model inform us about the timing of acquisition of *Ezh2* loss?

My Fgd5CreERT2 model demonstrates a difference in phenotype between induction of leukaemogenic *Kras* mutation in fetal or adult life. Further, there is a clear differential role for *Ezh2*, with an alteration of phenotypes in both settings despite an acceleration of disease. Where there is good evidence for *in-utero* RAS mutation in JMML [Matsuda, 2010][Stieglitz, 2015], the timing of *Ezh2* loss is not clear. One hypothesis (see figure 1-3) is that *Ezh2* loss is postnatal and prevents exhaustion of the FL-derived leukaemia. My data is certainly supportive that *Ezh2* loss is a postnatal event, with abrogation of the other leukaemias when induced in adult life but loss of penetrance in the fetal cohort. To fully examine this, however, sequential induction would be useful either through an inducible knockdown of *Ezh2* or by using an alternative to the Lox-Cre system, such as Dre-Rox [Anastassiadis, 2009]. An alternative would be to use an *in-vitro* system, with chemical or inducible knockdown, but would lack the refinement of an *in-vivo* model, which as demonstrated by my model the environment or stage at which mutations are gained can be important.

One other hypothesis is that the leukaemic cell of origin is different between FL and adult BM. My model is the first mouse model to derive a JMML model from fetal HSCs. However, the granulocytic expansion of predominantly neutrophils (such as the MPD/AML mice) appears

similar to the MPP induced model in fetal life Tarnawsky *et al* [Tarnawsky*, 2017]. It may be that from the FL either HSCs or MPPs can lead to JMML, however in adult life, only HSCs with secondary mutations can survive. Transplant experiments of HSCs and MPPs between environments could be used, but may not help, given the high frequency of T-cell leukaemias in the *Kras* mouse model. Alternatively, to investigate the different timings it would be possible to use an inducible Cre line, such as *Flt3CreERT2,* to induce mutations from MPPs. This would then answer whether the disease is different in the cohorts of adult or FL-induced HSCs or MPPs. A combination of these two theories would be that *Ezh2* loss occurs in a postnatal cell but downstream of the initiating HSC. This would be tricky to investigate, but Dre-Rox using an MPP specific Dre might be a useful approach [Anastassiadis, 2009], allowing induction of *Ezh2-KO* as a secondary mutation in MPPs with the initial *Fgd5CreERT2* induced *Kras* mutation in HSCs.

iii) The implications of *Ezh2* loss for patient care and potential therapeutic targets

As a clinician, my foremost desire is to help patients. However, to help find therapeutic targets, would certainly require transcriptomic data as a starting point, e.g. to determine whether K-F mice retain a fetal program when induced in the FL, or whether *Ezh2* loss in adult life drives reactivation of this fetal program. If a fetal-specific program is initiated then targeting therapy towards genes which are not expressed in normal post-natal cells may be a powerful approach.

6-4 Limitations of the work in this project

Probably the most important limitation of all of the models that I developed, in keeping with the majority of other models studying cooperation of mutations, was that they did not investigate the effect of sequential mutations. Whilst this does allow investigation of cooperating effects, the impact on clonal expansion of secondary mutations cannot be shown.

Further, whilst there is a depletion of phenotypic HSCs in fetal life with EK-F and EEK-F mice, it is not clear if this is an effect of *Ezh2* loss in combination with mutant *Kras* or simply due to *Ezh2* loss in fetal life. The loss of *Ezh2* sequentially in postnatal life would be important to elucidate both the sequential effect but the timing of *Ezh2* mutation.

A second major problem with the transplantation models I used was the high frequency of T-cell leukaemia, as previously published [Sabnis, 2009][Zhang, 2009]. Other limitations were that although induced cells are fetal-derived, once transplanted the cell is in an adult environment.

Thirdly, the different induction models are all associated with specific technical limitations. There are often problems with individual Cre lines, such as Mx1Cre, not being robust. Even when using primary Fgd5CreERT2 mice to initiate disease it appears that the disease is not readily transplantable (chapter 4-3). This is not in keeping with the human disease where xenografts demonstrate that JMML is transplantable [Louka, 2019][Caye, 2020], with the caveat that the human disease is a fully transformed leukaemia. The reasons for this are otherwise not clear, but may reflect the fact that the mouse model lacks the heterogenous range of secondary mutations or epigenetic alterations seen in human disease, as well as the capacity to faithfully recapitulate the human disease. When using the Fgd5CreERT2 model, it is difficult to avoid the fact that the induction methods, efficiency and doses are different between fetal and adult life. Whilst this is necessary due to the early problems with fetal loss and fostering with higher doses of tamoxifen, it may be that with more significant fetal induction the disease phenotypes are much more aggressive, which could explain the early fetal loss. This difference can be seen in figure 4.11, where the adult deletion efficiency is markedly increased when dTomato expression is compared to FL induction. This could be that dTomato is not reflective

of other transgene expression, or that FL induction cannot be as efficient as otherwise these mice are lost as pups. Overall, however, for matched induction I could try using a model -- such as the PTPN11 mutant models Ptpn11$^{E76K \text{ and } D61G}$ -- with a more gentle disease and extremely long latency. This would also help to answer if mutations in other Ras pathway genes can recreate similar diseases (see chapter 6-5).

Fourthly, my experiments have not been able to definitively say that the disease is not YS derived. Whilst transplant experiments with Vav-iCre developed leukaemia, these were B lineage or erythroid, not JMML. The induction from Fgd5CreERT2 did not yield any myelomonocytic leukaemia, but again due to the problems with EMP induction and avoiding HSC induction, the efficiency using <1mg tamoxifen at E7.5 is very poor. Further optimisation and experimentation using the rapid acting 4-OH-tamoxifen may be able to overcome some of these difficulties.

Finally, the role of *Ezh2* is not clear in this setting. Whilst molecular studies should provide important additional insight, it is known that in a malignant setting, *EZH2* functions in both a canonical and non-canonical method [Score, 2012][Herviou, 2016]. It is likely, that due to mutations in other PRC2 genes in JMML, that canonical PRC2 is important [Caye, 2015][Stieglitz, 2015], however it may be that in JMML the epigenome is altered such that *Ezh2* loss allows alterations both dependent and independent of polycomb. To study this, knock-out of an alternative PRC2 gene, such as *Eed,* which completely removes PRC2 function [Xie, 2014], would be important. It may be, as in human disease monosomy 7 is the most common mechanism of *EZH2* loss, that other chromosome 7 genes are also important, particularly those on 7q [Caye, 2015][Stieglitz, 2015]. This, however, does not detract from

the fact that using this model system there is a difference in phenotype between *Ezh2* loss in fetal life and adult life in the setting of a *Ras* mutant JMML model.

6-5 Future work

As mentioned above, RNAsequencing of HSCs from FL-induced and adult-induced models is expected to be performed shortly. The importance of key molecular differences could then be determined using using knockdown or correction studies and/or drug testing in vitro and in vivo. Further validation in human JMML samples, including xenografts, would also be important [Louka, 2019]. In addition, it would be useful to study the effect of an alternative Ras mutation. The obvious choice would be $Ptpn11^{E76K}$, as this model is well established, with a relatively short latency compared to the other Ras mutations, and is a relatively faithful JMML model [Dong, 2016]. However, an NF1 mutant model may be useful, to study the effect of primarily a mutation acquired in the germline rather than the primarily somatic KRAS mutations [Zhang, 2001]. Already mentioned above are the options to study alternative PRC2 mutations, and these could be used to ascertain whether the other mutations seen in JMML, such as *EED, SUZ12 or ASXL1,* act through PRC2 and therefore *EZH2* loss, or whether there is an effect through an alternative pathway.

Another way to study whether the fetal environment helps to drive leukaemia, would be to transplant adult induced cells into embryos, and follow these up postnatally. This would be logistically challenging, and would not study the fetal effects of mutation gain, but would give an inclination that the extrinsic cellular effect of the environment help drive the leukaemia, rather than the intrinsic molecular aberrations. Data to support this is seen in the expansion within the FL in chapter 3-6.iii, where 4/5 mice develop a myelomonocytic leukaemia whereas experiments with limited fetal growth develop T-cell leukaemia. Further, the studies by Dong

et al [Dong, 2016], suggest that WT cells driven by a mutant niche can develop a myelomonocytic leukaemia.

I have demonstrated an importance at the stage of ontogeny at which mutations are gained. To investigate further, more detailed and better activation of YS cells are required to ensure that JMML is not YS derived, as described in section 6-4. However, other stages would be interesting to study, such as late FL (~E17-E19), neonatal life (up to PND7) -- particularly given that the Mx1Cre mice developed skin lesions with neonatal induction -- and pre-adult mice (<3 weeks postnatal). The comparison, particularly in the molecular changes, would be interesting for the furthering of our understanding of congential and fetally-derived leukaemia.

A final but important experiment, described above, would be to sequentially induce *Ezh2* mutation in a *Kras* mutant cell. This could be done by inducible knockdown, but given the median survival of fetal mice may need to be done early in postnatal life. Other methods would include the use of drug treatment to deplete Ezh2 postnatally, or alternative conditional induction, such as Dre-Rox.

6-6 Conclusions

In keeping with my aims, I have created a faithful model for JMML, showing a fetal derived leukaemia, initiated in HSCs, with mice developing monocytosis, splenomegaly and thrombocytopenia. It is the most faithful model of JMML described so far in the literature.

My data further demonstrates that there is a differential effect on the induction of mutations at different stages of ontogeny, which is in keeping with my second aim, and suggests that my second hypothesis -- that the acquisition of leukaemogenic mutations at differing stages of ontogeny alters phenotypic, functional, and/or molecular properties of leukaemia -- can be

accepted. Further data is required to investigate the exact functional and molecular changes, however this effect of ontogeny is visible in the data shown. Finally, I have also shown that *Ezh2* loss alters the phenotype of leukaemia, in keeping with my third hypothesis being correct, but interestingly that *Ezh2* loss is also affected by the stage of ontogeny at induction. Further studies, such as RNAseq, will help to delineate these differences further.

References

An W, Mohapatra BC, Zutshi N, et al. VAV1-Cre mediated hematopoietic deletion of CBL and CBL-B leads to JMML-like aggressive early-neonatal myeloproliferative disease. *Oncotarget*. 2016;7(37):59006-59016.

Anastassiadis K, Fu J, Patsch C, Hu S, Weidlich S, Duerschke K, Buchholz F, Edenhofer F, Stewart AF. Dre recombinase, like Cre, is a highly efficient site-specific recombinase in E. coli, mammalian cells and mice. Dis Model Mech. 2009 Sep-Oct;2(9-10):508-15.

Araki T, Mohi MG, Ismat FA, et al. Mouse model of Noonan syndrome reveals cell type- and gene dosage-dependent effects of Ptpn11 mutation. *Nat Med*. 2004;10(8):849-85.

Booth CAG, Barkas N, Neo WH, et al. Ezh2 and Runx1 Mutations Collaborate to Initiate Lympho-Myeloid Leukemia in Early Thymic Progenitors. *Cancer Cell*. 2018;33(2):274-291.e8.

Braun BS, Tuveson DA, Kong N, et al. Somatic activation of oncogenic Kras in hematopoietic cells initiates a rapidly fatal myeloproliferative disorder. *Proc Natl Acad Sci U S A*. 2004;101(2):597-602.

Busch K, Klapproth K, Barile M, et al. Fundamental properties of unperturbed haematopoiesis from stem cells in vivo. *Nature*. 2015;518(7540):542-546.

Caye A, Strullu M, Guidez F, et al. Juvenile myelomonocytic leukemia displays mutations in components of the RAS pathway and the PRC2 network. *Nat Genet*. 2015;47(11):1334-1340.

Caye A, Rouault-Pierre K, Strullu M, et al. Despite mutation acquisition in hematopoietic stem cells, JMML-propagating cells are not always restricted to this compartment [published correction appears in Leukemia. 2020 Jan 31;:]. *Leukemia*. 2020;34(6):1658-1668.

De Raedt T, Beert E, Pasmant E, et al. PRC2 loss amplifies Ras-driven transcription and confers sensitivity to BRD4-based therapies. *Nature*. 2014;514(7521):247-251.

Di Genua C, Norfo R, Rodriguez-Meira A, et al. Cell-intrinsic depletion of Aml1-ETO-expressing pre-leukemic hematopoietic stem cells by K-Ras activating mutation. *Haematologica*. 2019;104(11):2215-2224.

Dong L, Yu WM, Zheng H, et al. Leukaemogenic effects of Ptpn11 activating mutations in the stem cell microenvironment. *Nature*. 2016;539(7628):304-308.

Gazit R, Mandal PK, Ebina W, et al. Fgd5 identifies hematopoietic stem cells in the murine bone marrow. *J Exp Med*. 2014;211(7):1315-1331.

Helsmoortel HH, Bresolin S, Lammens T, et al. LIN28B overexpression defines a novel fetal-like subgroup of juvenile myelomonocytic leukemia. *Blood*. 2016;127(9):1163-1172.

Hidalgo I, Herrera-Merchan A, Ligos JM, et al. Ezh1 is required for hematopoietic stem cell maintenance and prevents senescence-like cell cycle arrest. *Cell Stem Cell*. 2012;11(5):649-662.

Kim I, Saunders TL, Morrison SJ. Sox17 dependence distinguishes the transcriptional regulation of fetal from adult hematopoietic stem cells. *Cell*. 2007;130(3):470-483.

Li Q, Haigis KM, McDaniel A, et al. Hematopoiesis and leukemogenesis in mice expressing oncogenic NrasG12D from the endogenous locus. *Blood*. 2011;117(6):2022-2032.

Louka E, Povinelli B, Meira AR. Heterogeneous disease-propagating stem cells in juvenile myelomonocytic leukemia. *BioRXiv*. 2019; May 07. https://doi.org/10.1101/628479.

Mass E, Jacome-Galarza CE, Blank T, Lazarov T, Durham BH, Ozkaya N, Pastore A, Schwabenland M, Chung YR, Rosenblum MK, Prinz M, Abdel-Wahab O, Geissmann F. A somatic mutation in erythro-myeloid progenitors causes neurodegenerative disease. Nature. 2017 Sep 21;549(7672):389-393.

Matsuda K, Sakashita K, Taira C, et al. Quantitative assessment of PTPN11 or RAS mutations at the neonatal period and during the clinical course in patients with juvenile myelomonocytic leukaemia. *Br J Haematol*. 2010;148(4):593-599.

McGrath KE, Frame JM, Fegan KH, et al. Distinct Sources of Hematopoietic Progenitors Emerge before HSCs and Provide Functional Blood Cells in the Mammalian Embryo. *Cell Rep*. 2015;11(12):1892-1904.

Mochizuki-Kashio M, Mishima Y, Miyagi S, et al. Dependency on the polycomb gene Ezh2 distinguishes fetal from adult hematopoietic stem cells [published correction appears in *Blood*. 2012 Jul 26;120(4):924]. *Blood*. 2011;118(25):6553-6561.

Mohi MG, Williams IR, Dearolf CR, et al. Prognostic, therapeutic, and mechanistic implications of a mouse model of leukemia evoked by Shp2 (PTPN11) mutations. *Cancer Cell*. 2005;7(2):179-191.

Morrison SJ, Hemmati HD, Wandycz AM, Weissman IL. The purification and characterization of fetal liver hematopoietic stem cells. *Proc Natl Acad Sci U S A*. 1995;92(22):10302-10306.

Muto T, Sashida G, Oshima M, et al. Concurrent loss of Ezh2 and Tet2 cooperates in the pathogenesis of myelodysplastic disorders. *J Exp Med*. 2013;210(12):2627-2639.

Neo WH, Booth CAG, Azzoni E, et al. Cell-extrinsic hematopoietic impact of Ezh2 inactivation in fetal liver endothelial cells. *Blood*. 2018;131(20):2223-2234.

Niemeyer CM. RAS diseases in children. *Haematologica*. 2014;99(11):1653-1662

North TE, de Bruijn MF, Stacy T, et al. Runx1 expression marks long-term repopulating hematopoietic stem cells in the midgestation mouse embryo. *Immunity*. 2002;16(5):661-672.

Oshima M, Hasegawa N, Mochizuki-Kashio M, et al. Ezh2 regulates the Lin28/let-7 pathway to restrict activation of fetal gene signature in adult hematopoietic stem cells. *Exp Hematol*. 2016;44(4):282-96.e3.

Sabnis AJ, Cheung LS, Dail M, et al. Oncogenic Kras initiates leukemia in hematopoietic stem cells. *PLoS Biol*. 2009;7(3):e59.

Sankaran VG, Xu J, Orkin SH. Advances in the understanding of haemoglobin switching. *Br J Haematol*. 2010;149(2):181-194.

Sashida G, Wang C, Tomioka T, et al. The loss of Ezh2 drives the pathogenesis of myelofibrosis and sensitizes tumor-initiating cells to bromodomain inhibition. *J Exp Med*. 2016;213(8):1459-1477.

Shimizu T, Kubovcakova L, Nienhold R, et al. Loss of Ezh2 synergizes with JAK2-V617F in initiating myeloproliferative neoplasms and promoting myelofibrosis. *J Exp Med*. 2016;213(8):1479-1496.

Stieglitz E, Taylor-Weiner AN, Chang TY, et al. The genomic landscape of juvenile myelomonocytic leukemia [published correction appears in Nat Genet. 2015 Nov;47(11):1333] [published correction appears in Nat Genet. 2016 Jan;48(1):101]. *Nat Genet*. 2015;47(11):1326-1333.

Tarnawsky SP, Yoshimoto M, Deng L, Chan RJ, Yoder MC. Yolk sac erythromyeloid progenitors expressing gain of function PTPN11 have functional features of JMML but are not sufficient to cause disease in mice. *Dev Dyn*. 2017;246(12):1001-1014.

Tarnawsky* SP, Kobayashi M, Chan RJ, Yoder MC. Mice expressing KrasG12D in hematopoietic multipotent progenitor cells develop neonatal myeloid leukemia. *J Clin Invest*. 2017;127(10):3652-3656.

Tsai FY, Keller G, Kuo FC, Weiss M, Chen J, Rosenblatt M, Alt FW, Orkin SH. An early haematopoietic defect in mice lacking the transcription factor GATA-2. *Nature*. 1994;371:221–226.

Vo LT, Kinney MA, Liu X, et al. Regulation of embryonic haematopoietic multipotency by EZH1. *Nature*. 2018;553(7689):506-510.

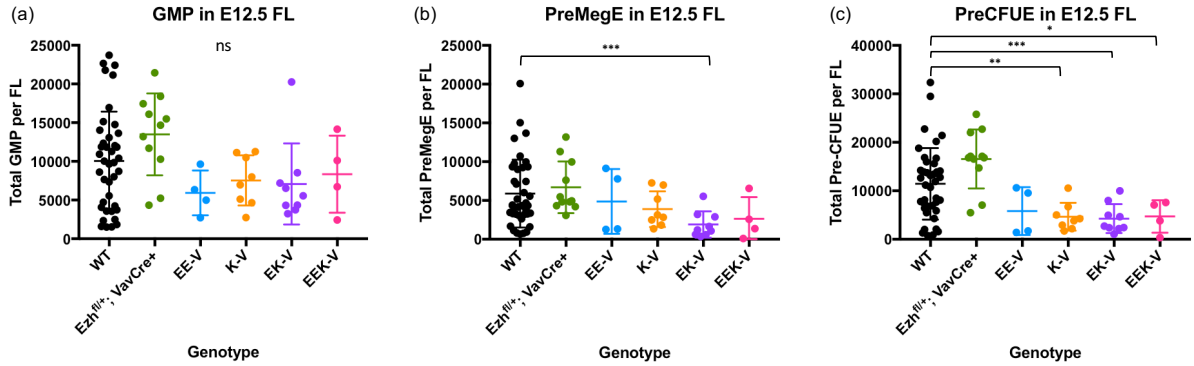
Warren AJ, Colledge WH, Carlton MB, Evans MJ, Smith AJ, Rabbitts TH. The oncogenic cysteine-rich LIM domain protein rbtn2 is essential for erythroid development. *Cell*. 1994;78(1):45-57.

Yang Y, Akada H, Nath D, Hutchison RE, Mohi G. Loss of Ezh2 cooperates with Jak2V617F in the development of myelofibrosis in a mouse model of myeloproliferative neoplasm. *Blood*. 2016;127(26):3410-3423.

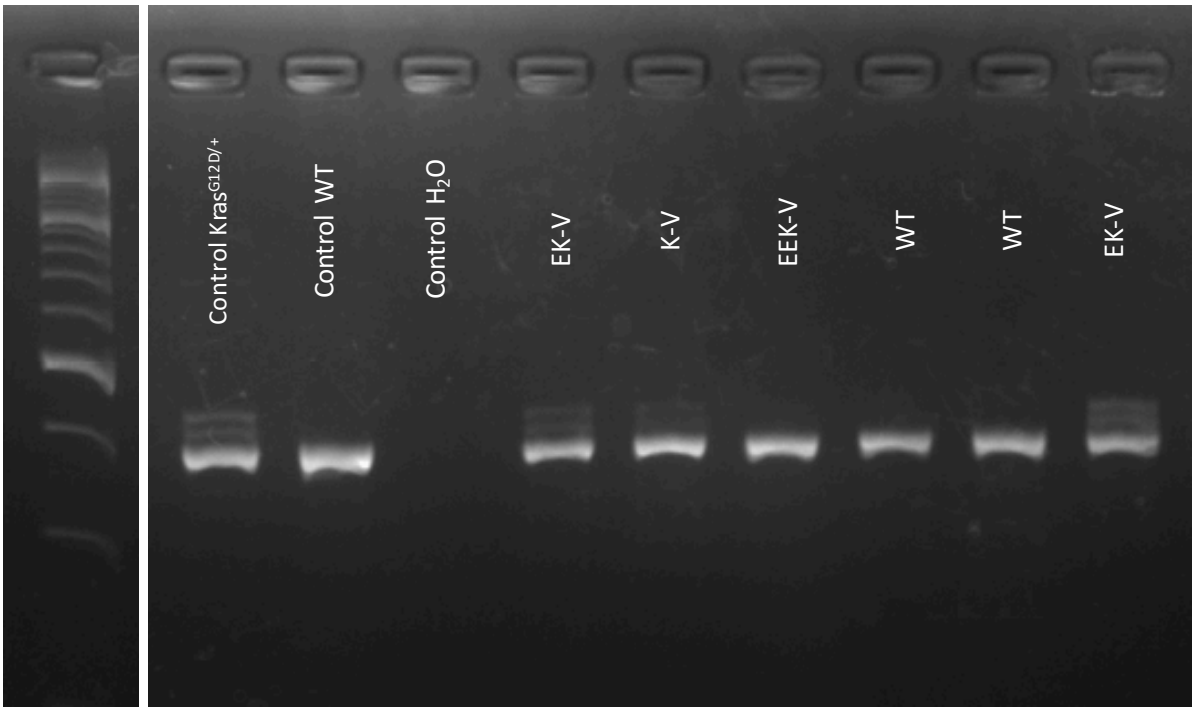
Zhang Y, Taylor BR, Shannon K, Clapp DW. Quantitative effects of Nf1 inactivation on in vivo hematopoiesis. *J Clin Invest*. 2001;108(5):709-715.

Zhang J, Wang J, Liu Y, et al. Oncogenic Kras-induced leukemogeneis: hematopoietic stem cells as the initial target and lineage-specific progenitors as the potential targets for final leukemic transformation. *Blood*. 2009;113(6):1304-1314.

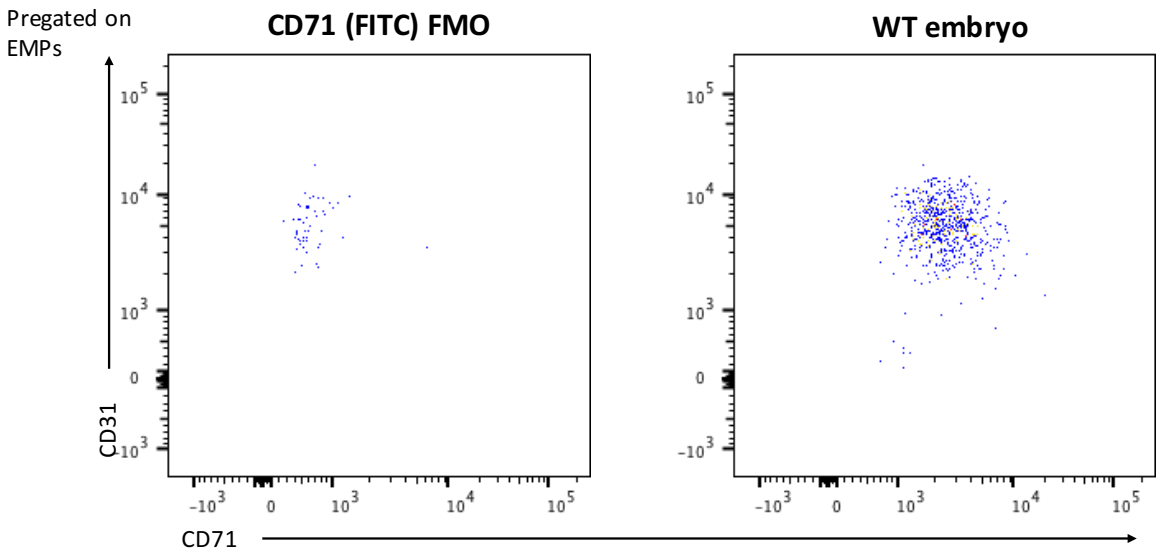
Appendix 1: Vav-iCre



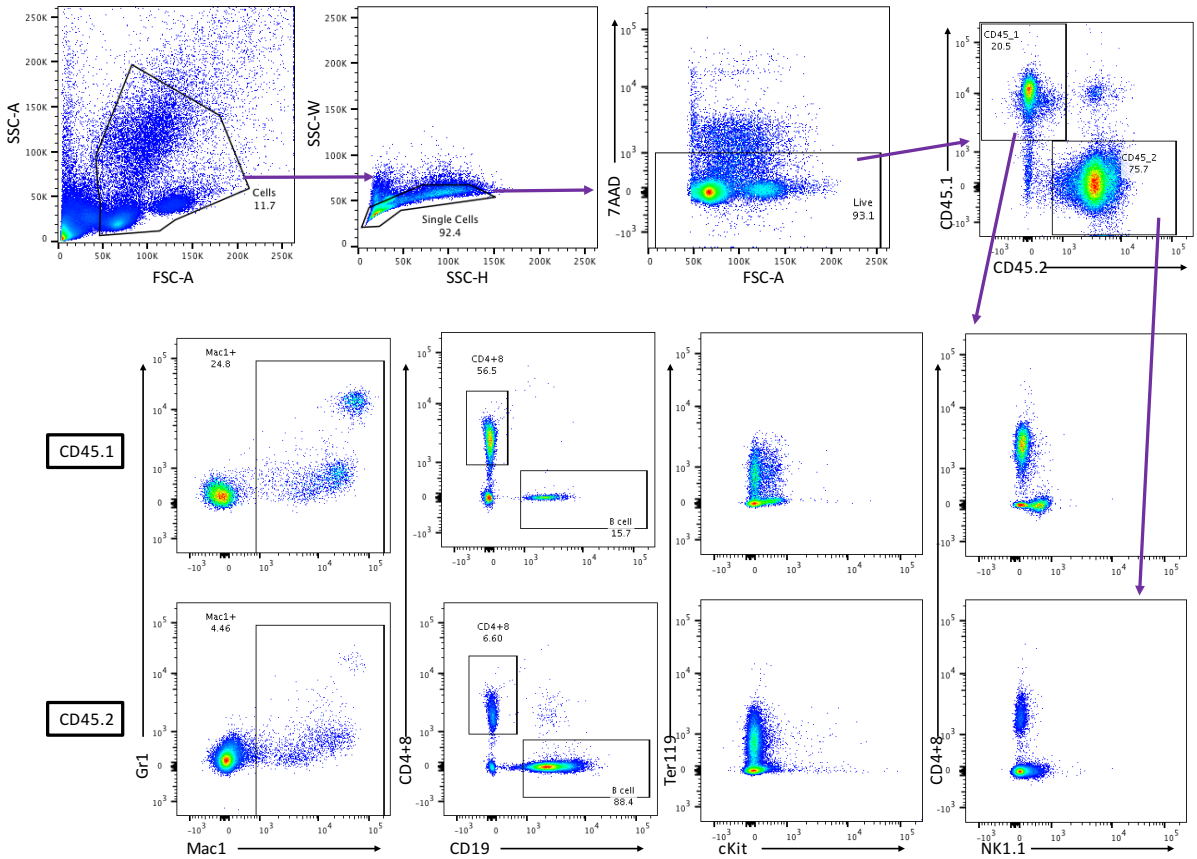
Appendix 1.1: HSPC numbers in E12.5 FL. Total numbers per E12.5 Fl of (a) Granulocyte-monocyte-progenitor (GMP; LK, CD41-,FcGR+) (b) Pre-Megakaryocyte-Erythroid progenitors (PreMegE; LK, CD41-, FcGR-, CD150+, CD105-) and (c) Pre-Colony-forming-units-erythroid (PreCFUE; LK, CD41-, FcGR-, CD150+, CD105+). Each point represents a biological replicate from 8 separate experiments. Statistical significance determined by Mann-Whitney U test. *p<0.05, **p<0.01,*** p<0.001



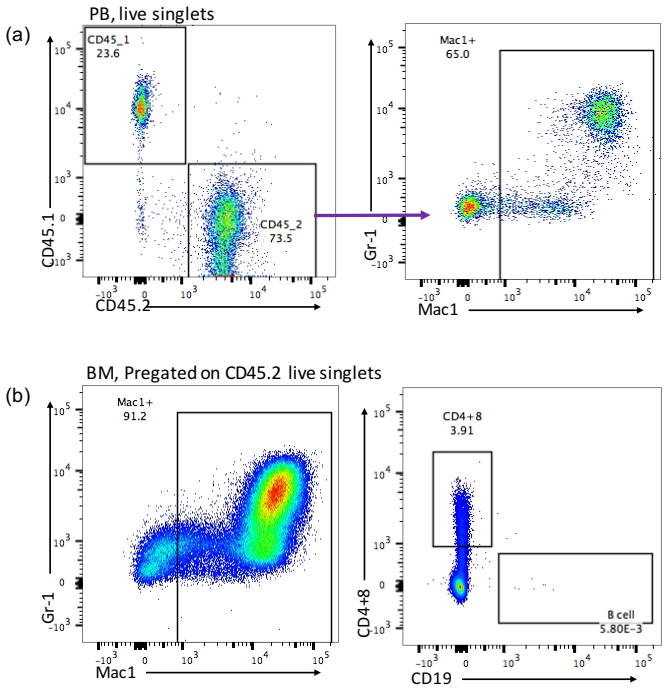
Appendix 1.2: $Kras^{LSL\text{-}G12D}$ Deletion PCR of DNA from Bulk FL. Showing controls from adult BM ($Kras^{G12D/+}$; $Mx1Cre^{tg}$/+, WT, and Water) followed by representative embyros from 2 litters. Data representative of data from 3 experiments and 5 embryos. Gel split as not adjacent to ladder.

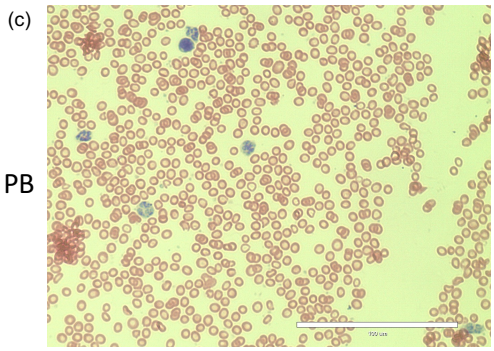


Appendix 1.3: CD71 and CD31 staining on EMPs. Representative flow plots from CD71 fluoresence minus one (FMO) and WT embryo (n=7), pregated on EMPs. Data from two separate experiments.



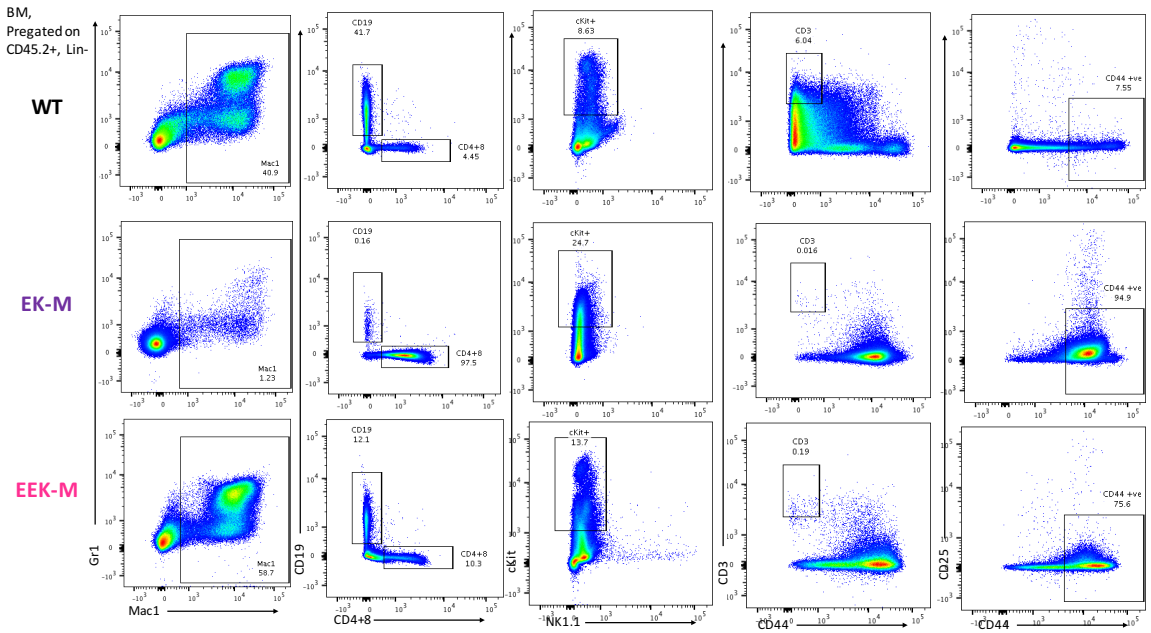
Appendix 1.4: Example gating strategy for lineage readout panel. Representative flow plot from PB readout at 6 weeks post-transplant.



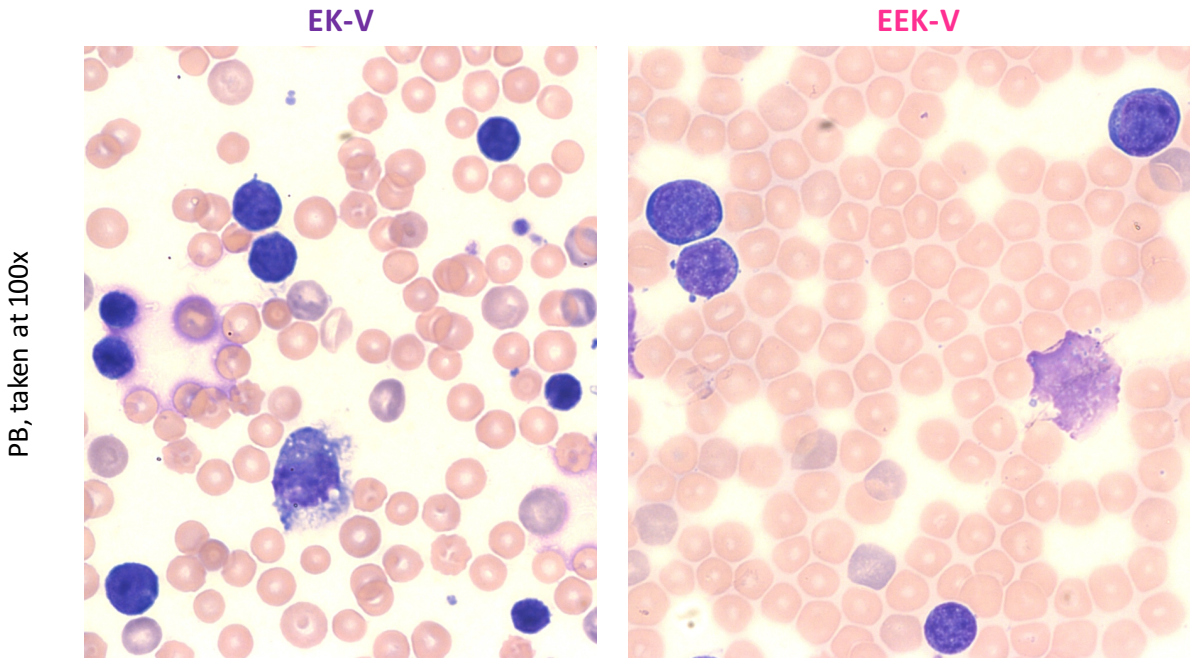


Appendix 1.5: Summary of cause of death from EEK-V mouse which engrafted (a) PB flow cytometry plot showing expansion of Gr1+, Mac1+ population, shown in (b) in BM. (c) PB morphology showing poorly stained slide but with vacuolation of myeloid cells

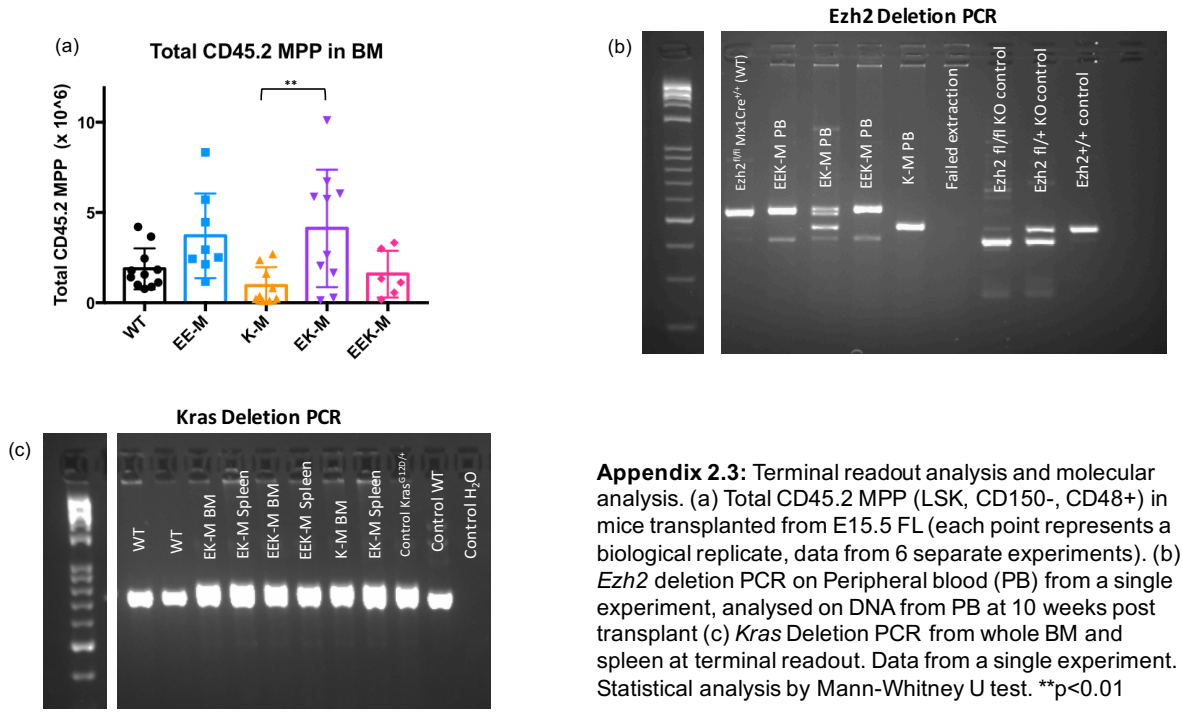
Appendix 2: Mx1Cre



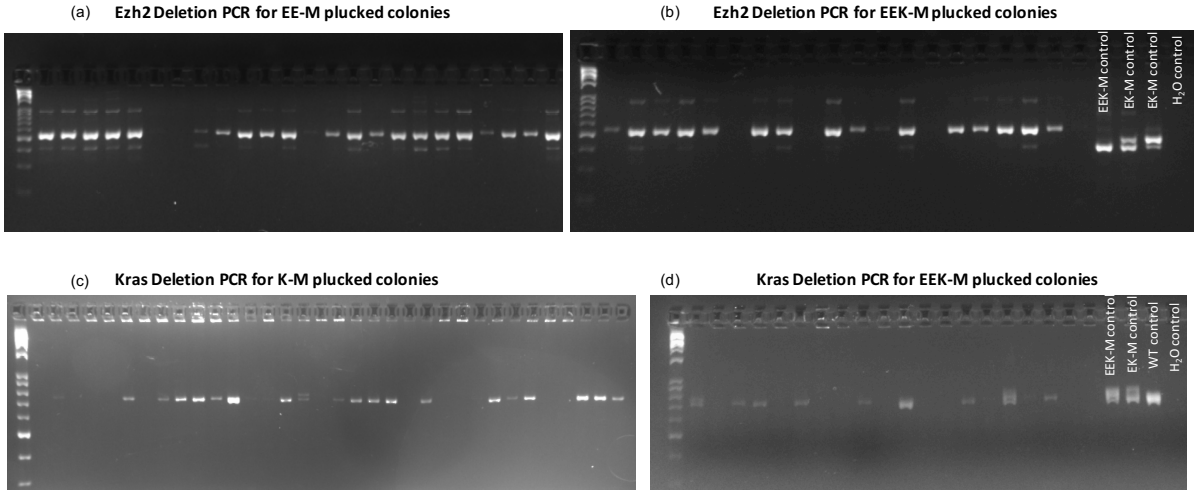
Appendix 2.1: Summary of lineage markers in BM. Showing example flow plots from BM on extended lineage and standard lineage panels to assess mice with negative population on standard lineage panel. WT (n=1), EK-M (n=2), EEK-M (n=2). Different phenotypes observed included complete lack of markers, and only CD44 positivity (as per EEK-M mouse). EK-M shown for example of CD4+8 and CD44 staining.



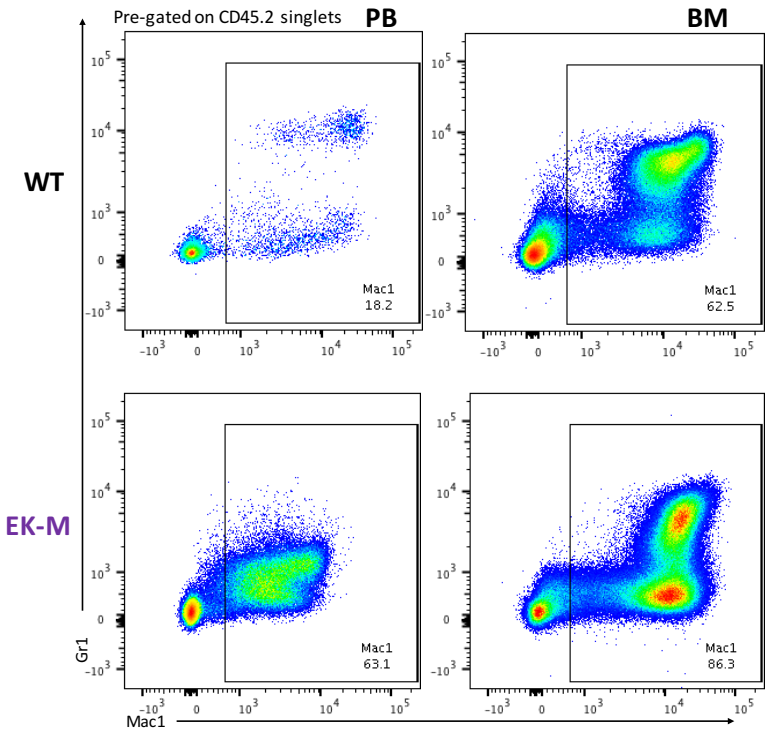
Appendix 2.2: Example morphology from T-cell leukaemic mice. EK-V mouse with 'traditional' CD4+8 positive T-cell leukaemia and EEK-V (n=1) mouse (flow data in appendix 2.1) showing similar morphology with T-cell blasts. Taken at 100x magnification.



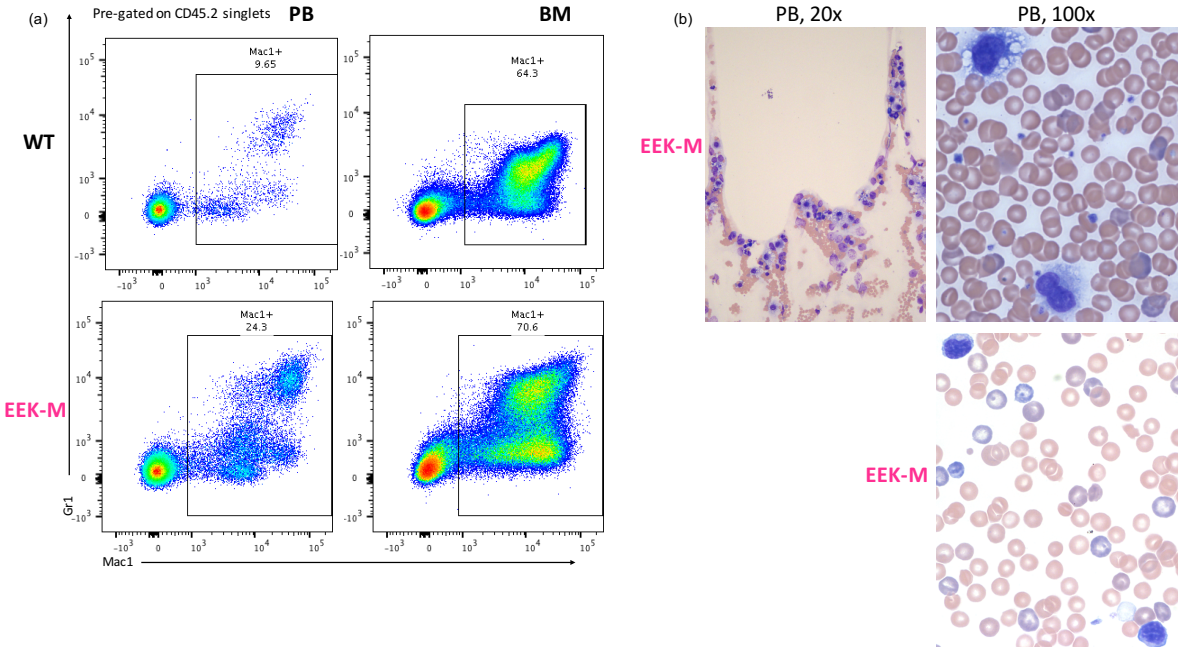
Appendix 2.3: Terminal readout analysis and molecular analysis. (a) Total CD45.2 MPP (LSK, CD150-, CD48+) in mice transplanted from E15.5 FL (each point represents a biological replicate, data from 6 separate experiments). (b) *Ezh2* deletion PCR on Peripheral blood (PB) from a single experiment, analysed on DNA from PB at 10 weeks post transplant (c) *Kras* Deletion PCR from whole BM and spleen at terminal readout. Data from a single experiment. Statistical analysis by Mann-Whitney U test. **p<0.01



Appendix 2.4: Deletion PCRs on DNA from single cell derived plucked colonies. *Ezh2* deletion PCR from plucked colonies from EE-M FL (a) and EEK-M FL (b) and *Kras*^{G12D} deletion PCR for colonies K-M FL (c) and EEK-M FL (d). Each well represents DNA from a single cell derived colony, except for controls (marked). Data representative of n=1 each, however representative line from each gel taken and ~96 colonies analysed per genotype.

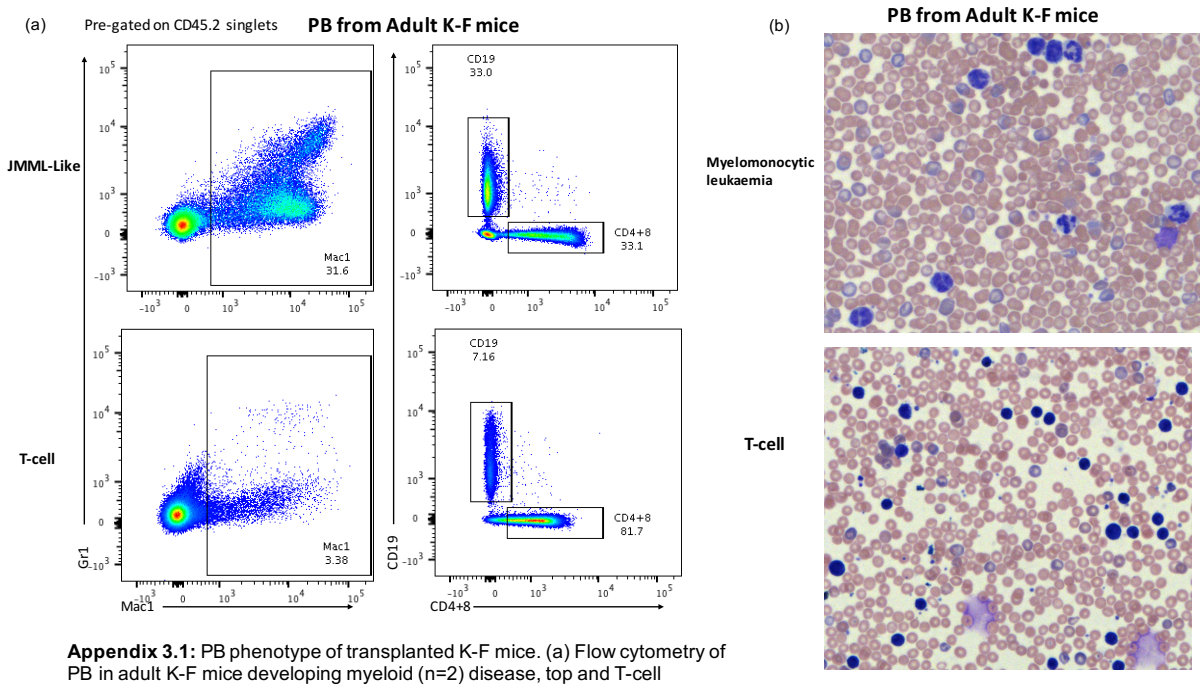


Appendix 2.5: Uninduced primary Mx1Cre mice develop leukaemia. (a) Example flow cytometry plots from 6month old WT (n=2) and EK-M at termination ~15 weeks (n=1), another EK-M mouse was found dead.

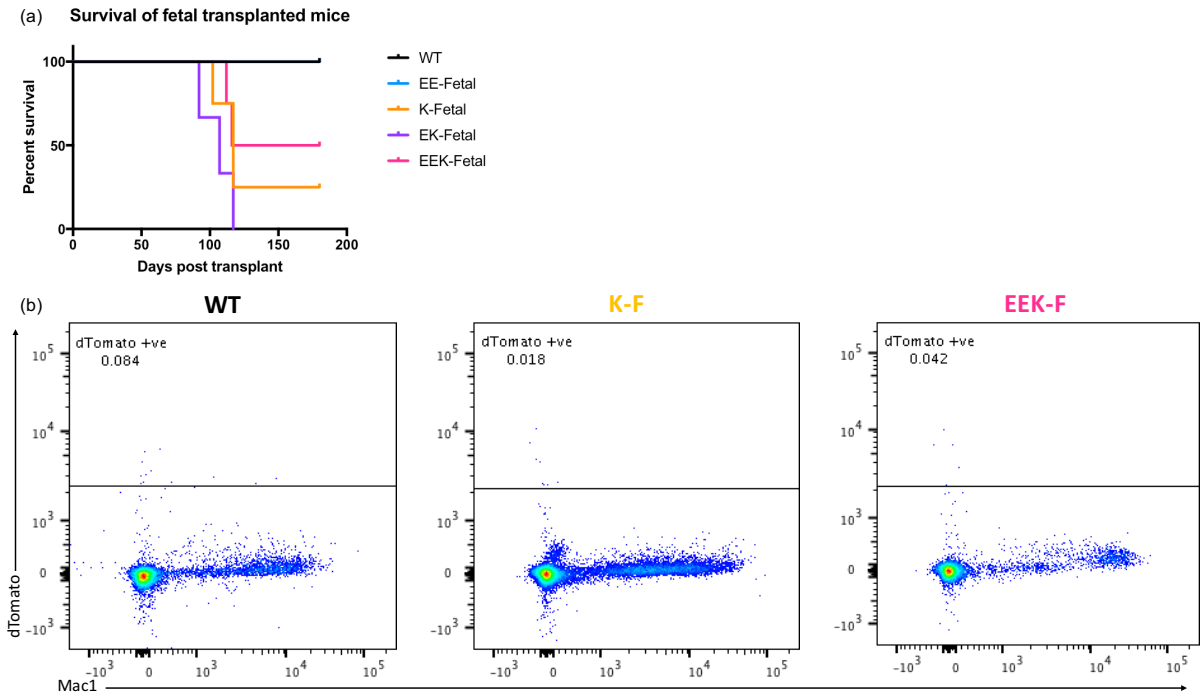


Appendix 2.6: Induced primary adult mice develop a myelomonocytic phenotype. (a) Example flow cytometry plots from WT (n=4, n=3 for BM) and EEK-M at termination (n=4). (b) PB morphology from the other 2 EEK-M mice (n=3) showing extensive macrophages in one and small monocytes in the other. Pictures taken at 20x and 100x.

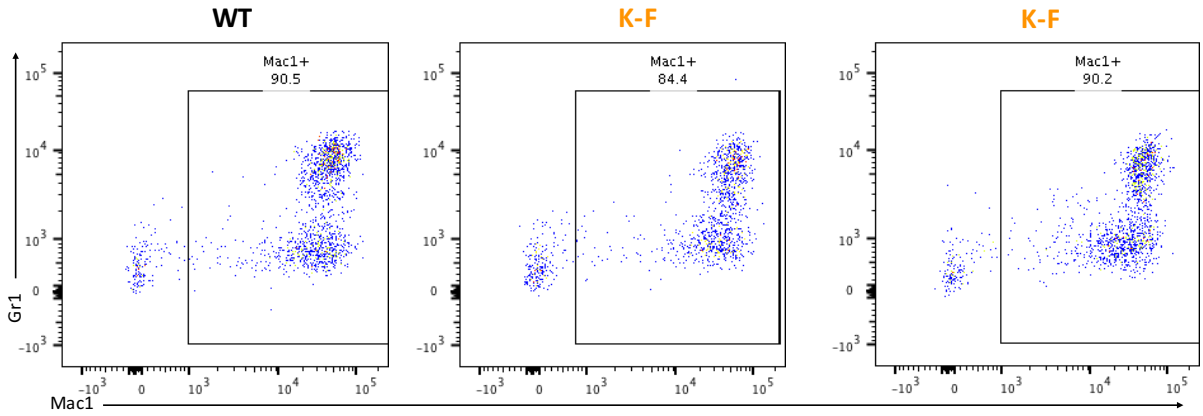
Appendix 3: Fgd5CreERT2 optimisation



Appendix 3.1: PB phenotype of transplanted K-F mice. (a) Flow cytometry of PB in adult K-F mice developing myeloid (n=2) disease, top and T-cell leukaemia (n=7). (b) PB films showing myeloid (n=1) and T-cell disease (n=1) in transplanted K-F mice. Data from two separate experiments.

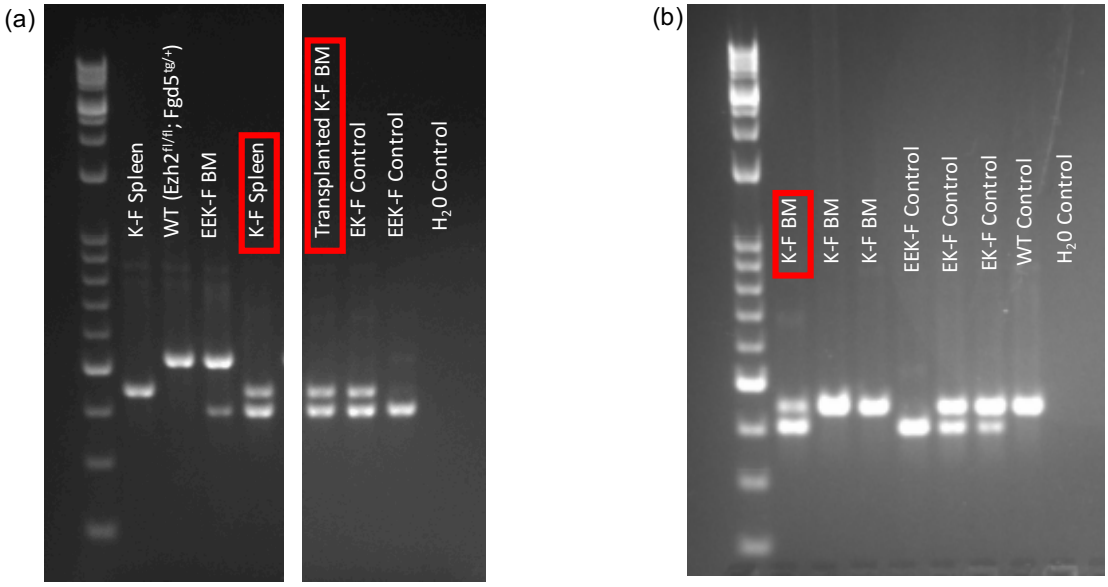


Appendix 3.2: Spontaneous dTomato expression in mice transplanted with Fgd5CreERT2 induced BM. (a) Survival of fetal mice from two experiments showing long term survival of Fgd5CreERT2 induced CD45.2 engrafted mice, data from two separate experiments. (b) Example flow cytometry plots at 8 weeks post transplant from (Fgd5CreERT2$^{+/+}$, dTomato$^{+/+}$; n=4) and expression and Kras transgenic mice (n=4) from FL induction. Example flow cytometry plots from a single experiment.

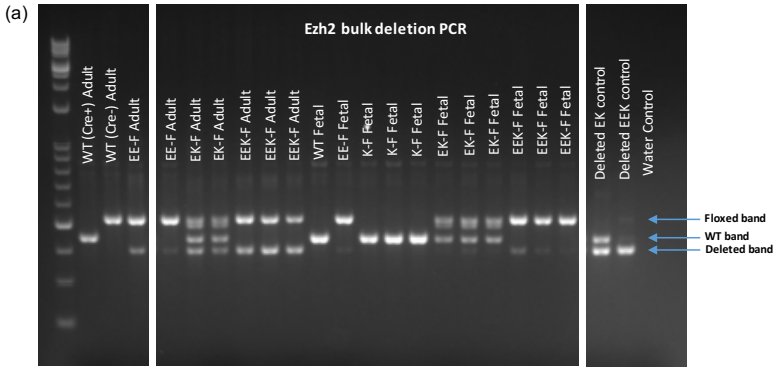


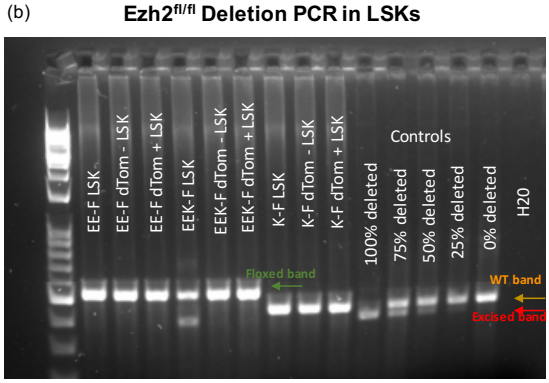
Appendix 3.3: BM at E19.5 following induction at E12.5 and E13.5 with 4mg tamoxifen showing representative flow cytometry plots of WT (n=2) and K-F (n=2) from a single experiments on BM, showing a myeloid BM drive, but no difference between the WT and Kras mutant mice.

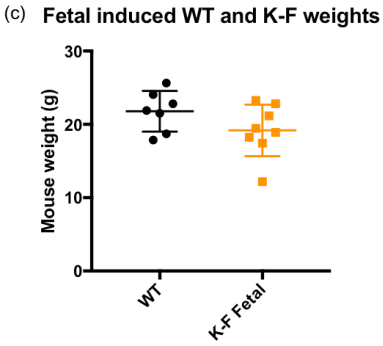
Appendix 4: Fgd5CreERT2 primary mice



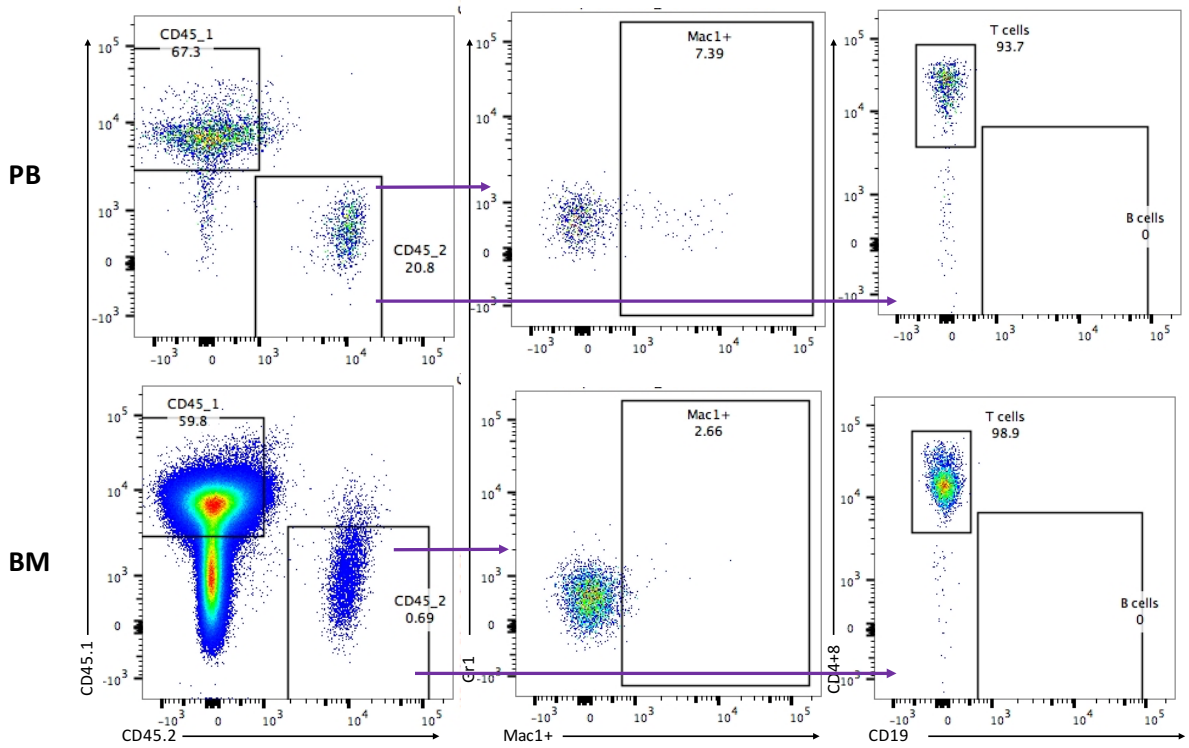
Appendix 4.1: Ezh2 deletion PCR used to exclude germline deletion mouse. (a) Ezh2 deletion PCR on primary mice and transplanted mice. Red boxes mark excluded mouse, supposedly K-F genotype but showing deleted *Ezh2* band suggesting germline deletion. Mother of primary mouse from Vav-Cre colony, known for deletion PCR. Gel split to show ladder and controls. (b) Ezh2 deletion PCR from primary mice showing DNA extracted from cryopreserved BM from induced littermates of excluded mouse (red box)



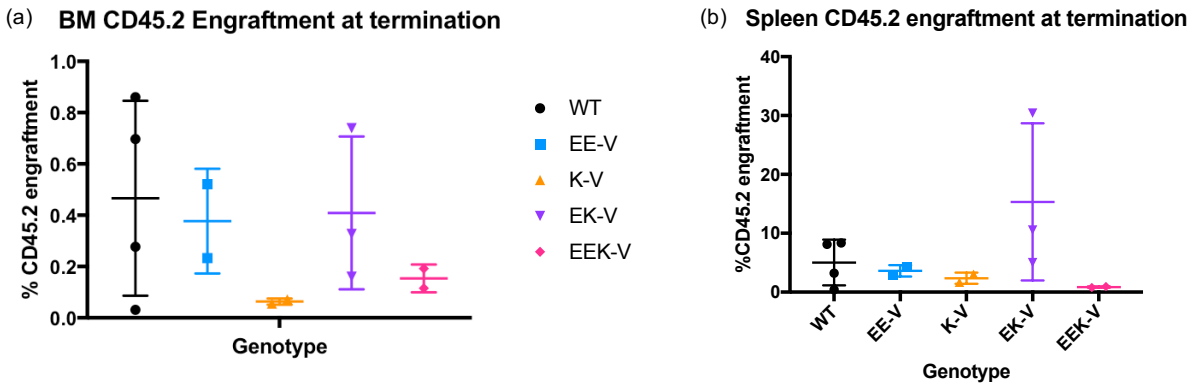




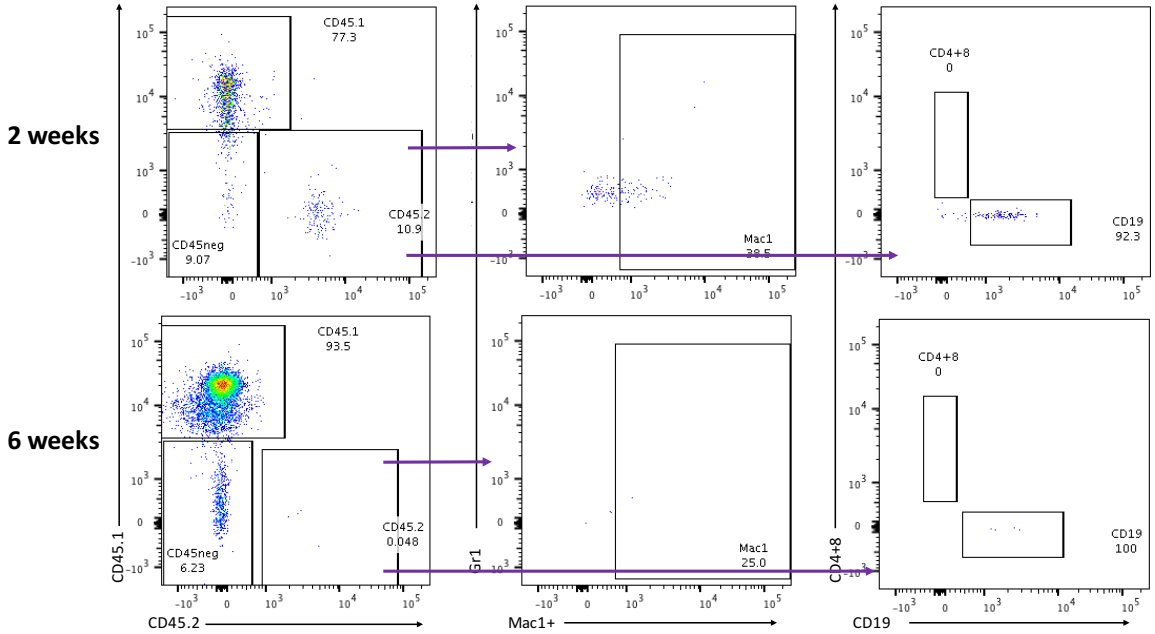
Appendix 4.2: Ezh2 is deleted in the tissues at terminal readout of primary mice. (a) *Ezh2* deletion PCR (top) in spleen of mice at terminal readout. Genotypes shown in figure and bands marked. Gel split to show relevant data. (b) Ezh2 deletion PCR in 100 FACS sorted LSKs following whole genome amplification (c) Weight (g) of WT and K-F fetal induced mice at terminal readout. WT mice littermates of K-F mice.



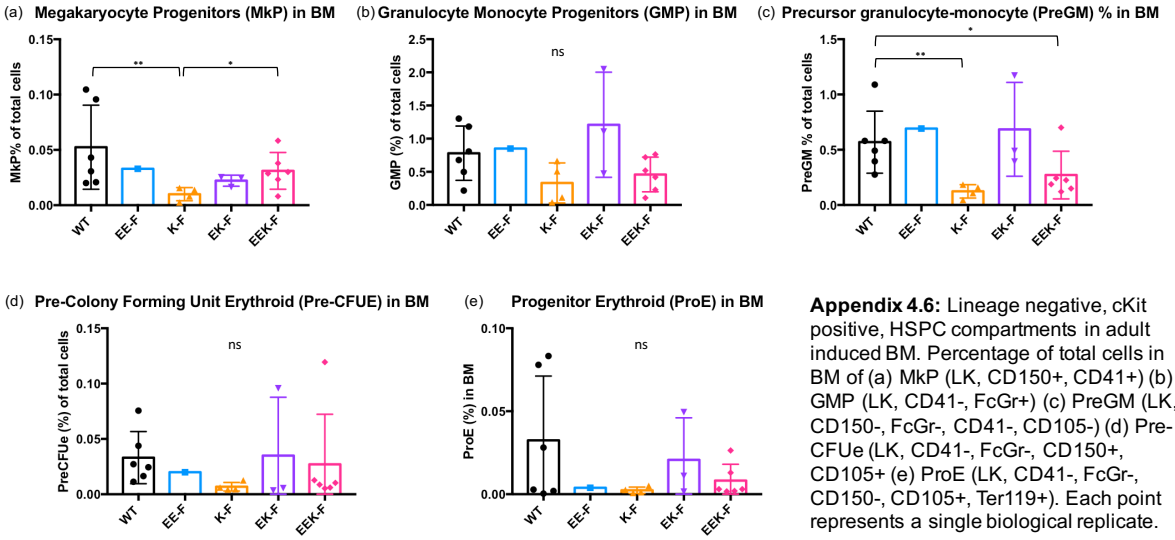
Appendix 4.3: PB and BM at death from CD45.1 mouse transplanted with WT YS. PB (top) and BM (bottom) both showing CD45.2 population with T-cell predominance. Demonstrating long term potential for expansion of YS transplanted cells.



Appendix 4.4: Long term engraftment of YS mice. (a) BM CD45.2 engraftment at terminal readout (>150 days post transplant) of CD45.1 NSG mice transplanted with CD45.2 E10.5 YS and (b) Splenic engraftment of these mice. Each data point represents a single mouse. Data pooled from 5 experiments.



Appendix 4.5: Transient engraftment at 2weeks and 6 weeks following transplantation of BM from primary YS transplants K-F leukaemic mouse. Showing 1 replicate of 3, 2/3 had no engraftment. By 8 weeks there was no remaining CD45.2 engraftment and the recipient mice lived to 16 weeks.



Appendix 4.6: Lineage negative, cKit positive, HSPC compartments in adult induced BM. Percentage of total cells in BM of (a) MkP (LK, CD150+, CD41+) (b) GMP (LK, CD41-, FcGr+) (c) PreGM (LK, CD150-, FcGr-, CD41-, CD105-) (d) Pre-CFUe (LK, CD41-, FcGr-, CD150+, CD105+ (e) ProE (LK, CD41-, FcGr-, CD150-, CD105+, Ter119+). Each point represents a single biological replicate.

Appendix 5: Methods

(a)

KAPA PCR protocol		
Mastermix		**Volume**
H2O (uL)		9 - (primers)
KAPA mix (uL)		10
Primers (10µM)		1.25 per primer
DNA (uL)		1
Total 19uL of master mix + 1uL undiluted DNA per sample		
PCR program		
95ºC	1 min	
95ºC	10 sec	
60ºC	10 sec	30x
72ºC	10 sec	
10ºC	hold	

(b)

Protocol	Primers	Primer sequence
dTomato	oIMR9020	AAG GGA GCT GCA GTG GAG TA
	oIMR9021	CCG AAA ATC TGT GGG AAG TC
	oIMR9103	GGC ATT AAA GCA GCG TAT CC
	oIMR9105	CTG TTC CTG TAC GGC ATG G
Ezh2	Ezh2 F	CTGCTCTGAATGGCAACTCC
	EZH2 R:	GGTCACTGGGTTCTTTCTAAGG
Ezh2 Deletion PCR	Fw1	ATGGGCCTCATAGTGACAGG
	Rv1	CTGCAAGTGGTTGGGACTCT
	Rv2	GTGCAGGTCAGTCAGCAACT
GenCre	Cre-Fw	CGT TTT CTG AGC ATA CCT GGA
(for Tie2, Fgd5, Mx1Cre)	Cre-Rv	ATT CTC CCA CCG TCA GTA CG
Kras$^{LSL-G12D}$	y117	CTA GCC ACC ATG GCT TGA GT
	y118	ATG TCT TTC CCC AGC ACA GT
	y116	TCC GAA TTC AGT GAC TAC AGA TG
Kras Deletion PCR	KLSLfw3	AAGCAAGGCA GAAGTCACAGAGG
	LoxedRasRv	TCCGAATTCAGTGACTACAGATGTACAGAG
Vav-iCre	Vav Cre Fw	AGATGCCAGGACATCAGGAACCTG
	Vav Cre Rv	ATCAGCCACACCAGACACAGAGATC

Appendix 5.1: PCR protocol and primers. (a) PCR protocol used for genotyping PCRs with total volume 20microL, made up with ddH20. PCR protocol shown at bottom. (b) Table of primers used and sequences.

Lineage Panel		BV650	AF700	APC	PECy7	APC-eF780	PB	PO	PE	FITC	PECy5	PBS per tube
		CD45.1	CD45.2	Mac1	CD19 (ID3)	CD4 & CD8	NK1.1	Gr1	cKit	ter119	7AAD	
		50	100	400	500	400	1200	200	200	200	200	
Dilution for 20X		2.5	5	20	25	20	60	10	10	10		
FMO BV650			1.25	1.25	1.25	1.25	1.25	1.25	1.25	1.25		2.5
FMO AF700		1.25		1.25	1.25	1.25	1.25	1.25	1.25	1.25		2.5
FMO APC		1.25	1.25		1.25	1.25	1.25	1.25	1.25	1.25		2.5
FMO PECy7		1.25	1.25	1.25		1.25	1.25	1.25	1.25	1.25		2.5
FMO APC-eF780		1.25	1.25	1.25	1.25		1.25	1.25	1.25	1.25		2.5
FMO PB		1.25	1.25	1.25	1.25	1.25		1.25	1.25	1.25		2.5
FMO PO		1.25	1.25	1.25	1.25	1.25	1.25		1.25	1.25		2.5
FMO PE		1.25	1.25	1.25	1.25	1.25	1.25	1.25		1.25		2.5
FMO FITC		1.25	1.25	1.25	1.25	1.25	1.25	1.25	1.25			2.5
FMO PECy5		1.25	1.25	1.25	1.25	1.25	1.25	1.25	1.25	1.25		1.25
Sample **(1X)**		1.25	1.25	1.25	1.25	1.25	1.25	1.25	1.25	1.25		13.75
Sample x	30	37.5	37.5	37.5	37.5	37.5	37.5	37.5	37.5	37.5		412.5
Total Ab dilution		50	50	50	50	50	50	50	50	50		
Make up extra	15	65	65	65	65	65	65	65	65	65		
Predilution Ab		26.00	13.00	3.25	2.60	See below	1.08	6.50	6.50	6.50		
Predilution PBS		39.00	52.00	61.75	62.40	60.67	63.92	58.50	58.50	58.50		
						CD4 1/1200, CD8 1/400						
					CD4	1.083						
					CD8	3.25						

Appendix 5.2: Example flow cytometry panel set up. Showing makeup of fluoresence minus one (FMO) controls and fluorochromes/conjugates for each colour.

Pooled 0.2x TaqMan Assay Mix										
Pool Taqman Gene Expression Assays (Applied Biosystems) and then dilute with TE buffer so that each assay is at a final concentration of 0.2x										
	assay 1	5								
	assay 2	5								
	assay 96	5								
	TE	20								
	TTL	500								
RT-Mix	**1 sample**	**18**	**reactions**	**x1.2**	96 well plate		**Pre-amplification PCR programme**			
CellsDirect 2x Reaction Mix	5		90	108			RT	50 ºC	15min	
Ambion's SUPERase12-In	0.1		1.8	2.16			Inactivation of RT/activation of Taq enzyme	95 ºC	2min	
TE Buffer	1.2		21.6	25.92			Specific target amplification	95 ºC	15sec	16 cycles
0.2x Assay mix	2.5		45	**54**				60 ºC	4min	
RT	1.2		21.6	**25.92**						
TTL	10		180	216						
Taq Mix for no RT ctrls	**1 sample**	**3**	**reactions**	**x1.2**						
CellsDirect 2x Reaction Mix	5		15	18						
Ambion's SUPERase12-In	0.1		0.3	0.36						
TE Buffer	1.2		3.6	4.32						
0.2x Assay mix	2.5		7.5	**9**						
Taq Mix (40% Taq + 60% TE)	1.2		3.6	**4.32**						
TTL	10		30	36						
How many assays	**6**	**Volume assays**		**TE to add**	**Final volume required**		**Final Dilution obtained**			
4	2	8		192	200		100			
Assays Used	EZH2 1: Mm00468449_m1	EZH2 2: Mm00468464_m1	GAPDH	ACTB						

Appendix 5.3: Protocol used for *Ezh2* qPCR assays. Showing method for making assay mix, reverse transcriptase (RT) and RT-negative controls. Also showing PCR programmes and assays used.

Bibliography

Abdel-Wahab O, Adli M, LaFave LM, et al. ASXL1 mutations promote myeloid transformation through loss of PRC2-mediated gene repression. *Cancer Cell*. 2012;22(2):180-193.

Akutagawa J, Huang TQ, Epstein I, et al. Targeting the PI3K/Akt pathway in murine MDS/MPN driven by hyperactive Ras. *Leukemia*. 2016;30(6):1335-1343.

An W, Mohapatra BC, Zutshi N, et al. VAV1-Cre mediated hematopoietic deletion of CBL and CBL-B leads to JMML-like aggressive early-neonatal myeloproliferative disease. *Oncotarget*. 2016;7(37):59006-59016.

Anastassiadis K, Fu J, Patsch C, Hu S, Weidlich S, Duerschke K, Buchholz F, Edenhofer F, Stewart AF. Dre recombinase, like Cre, is a highly efficient site-specific recombinase in E. coli, mammalian cells and mice. Dis Model Mech. 2009 Sep-Oct;2(9-10):508-15.

Araki T, Mohi MG, Ismat FA, et al. Mouse model of Noonan syndrome reveals cell type- and gene dosage-dependent effects of Ptpn11 mutation. *Nat Med*. 2004;10(8):849-85.

Aricò M, Biondi A, Pui CH. Juvenile myelomonocytic leukemia. *Blood*. 1997;90(2):479-488.

Azcoitia V, Aracil M, Martinez AC, Torres M. The homeodomain protein Meis1 is essential for definitive hematopoiesis and vascular patterning in the mouse embryo. *Dev Biol*. 2005;280:307–320.

Bader-Meunier B, Tchernia G, Miélot F, et al. Occurrence of myeloproliferative disorder in patients with Noonan syndrome. *J Pediatr*. 1997;130(6):885-889.

Balazs AB, Fabian AJ, Esmon CT, Mulligan RC. Endothelial protein C receptor (CD201) explicitly identifies hematopoietic stem cells in murine bone marrow. *Blood*. 2006;107(6):2317-2321.

Basak A, Munschauer M, Lareau CA, et al. Control of human hemoglobin switching by LIN28B-mediated regulation of BCL11A translation. *Nat Genet*. 2020;52(2):138-145.

Basel-Vanagaite L. Acute lymphoblastic leukemia in Weaver syndrome. *Am J Med Genet A*. 2010;152A(2):383-386.

Basheer F, Giotopoulos G, Meduri E, et al. Contrasting requirements during disease evolution identify EZH2 as a therapeutic target in AML. *J Exp Med*. 2019;216(4):966-981.

Baumann I, Bennett JM, Niemeyer CM. Thiele J. Juvenile myelomonocytic leukaemia. In: Swerdlow SH, Campo E, Harris NL, et al, eds. WHO Classification of Tumors of Haematopoietic and Lymphoid Tissues. Lyon, France: International Agency for Research on Cancer (IARC); 2017:89-92.

Barker JE. Development of the mouse hematopoietic system. I. Types of hemoglobin produced in embryonic yolk sac and liver. *Dev Biol*. 1968;18(1):14-29.

Beaudin AE, Boyer SW, Perez-Cunningham J, et al. A Transient Developmental Hematopoietic Stem Cell Gives Rise to Innate-like B and T Cells. *Cell Stem Cell*. 2016;19(6):768-783.

Béguelin W, Teater M, Gearhart MD, et al. EZH2 and BCL6 Cooperate to Assemble CBX8-BCOR Complex to Repress Bivalent Promoters, Mediate Germinal Center Formation and Lymphomagenesis. *Cancer Cell*. 2016;30(2):197-213.

Bergstraesser E, Hasle H, Rogge T, et al. Non-hematopoietic stem cell transplantation treatment of juvenile myelomonocytic leukemia: a retrospective analysis and definition of response criteria. *Pediatr Blood Cancer*. 2007;49(5):629-633.

Berrozpe G, Bryant GO, Warpinski K, et al. Polycomb Responds to Low Levels of Transcription. *Cell Rep*. 2017;20(4):785-793.

Bhatnagar N, Nizery L, Tunstall O, Vyas P, Roberts I. Transient Abnormal Myelopoiesis and AML in Down Syndrome: an Update. *Curr Hematol Malig Rep*. 2016;11(5):333-341.

Böiers C, Carrelha J, Lutteropp M, et al. Lymphomyeloid contribution of an immune-restricted progenitor emerging prior to definitive hematopoietic stem cells. *Cell Stem Cell*. 2013;13(5):535-548.

Boland MJ, Hazen JL, Nazor KL, Rodriguez AR, Gifford W, Martin G, Kupriyanov S, Baldwin KK. Adult mice generated from induced pluripotent stem cells. *Nature*. 2009 Sep 3;461(7260):91-4.

Booth CAG, Barkas N, Neo WH, et al. Ezh2 and Runx1 Mutations Collaborate to Initiate Lympho-Myeloid Leukemia in Early Thymic Progenitors. *Cancer Cell*. 2018;33(2):274-291.e8.

Boultwood J, Perry J, Pellagatti A, et al. Frequent mutation of the polycomb-associated gene ASXL1 in the myelodysplastic syndromes and in acute myeloid leukemia. *Leukemia*. 2010;24(5):1062-1065.

Bowie MB, McKnight KD, Kent DG, McCaffrey L, Hoodless PA, Eaves CJ. Hematopoietic stem cells proliferate until after birth and show a reversible phase-specific engraftment defect. *J Clin Invest*. 2006;116(10):2808-2816.

Bowie MB, Kent DG, Dykstra B, et al. Identification of a new intrinsically timed developmental checkpoint that reprograms key hematopoietic stem cell properties. *Proc Natl Acad Sci U S A*. 2007;104(14):5878-5882.

Braun BS, Tuveson DA, Kong N, et al. Somatic activation of oncogenic Kras in hematopoietic cells initiates a rapidly fatal myeloproliferative disorder. *Proc Natl Acad Sci U S A*. 2004;101(2):597-602.

Brenner S, Whiting-Theobald N, Kawai T, et al. CXCR4-transgene expression significantly improves marrow engraftment of cultured hematopoietic stem cells. *Stem Cells*. 2004;22(7):1128-1133.

Brown P. Treatment of infant leukemias: challenge and promise. *Hematology Am Soc Hematol Educ Program*. 2013;2013:596-600.

Brown P, Pieters R, Biondi A. How I treat infant leukemia. *Blood*. 2019;133(3):205-214.

Buijs A, Bruin M. Fusion of FIP1L1 and RARA as a result of a novel t(4;17)(q12;q21) in a case of juvenile myelomonocytic leukemia. *Leukemia*. 2007;21(5):1104-1108.

Busch K, Klapproth K, Barile M, et al. Fundamental properties of unperturbed haematopoiesis from stem cells in vivo. *Nature*. 2015;518(7540):542-546.

Busque L, Gilliland DG, Prchal JT, et al. Clonality in juvenile chronic myelogenous leukemia. *Blood*. 1995;85(1):21-30.

Cao R, Wang L, Wang H, et al. Role of histone H3 lysine 27 methylation in Polycomb-group silencing. *Science*. 2002;298(5595):1039-1043.

Castleberry RP, Emanuel PD, Zuckerman KS, et al. A pilot study of isotretinoin in the treatment of juvenile chronic myelogenous leukemia. *N Engl J Med*. 1994;331(25):1680-1684.

Castro-Malaspina H, Schaison G, Passe S, et al. Subacute and chronic myelomonocytic leukemia in children (juvenile CML). Clinical and hematologic observations, and identification of prognostic factors. *Cancer*. 1984;54(4):675-686.

Carrelha J, Meng Y, Kettyle LM, et al. Hierarchically related lineage-restricted fates of multipotent haematopoietic stem cells. *Nature*. 2018;554(7690):106-111.

Caye A, Strullu M, Guidez F, et al. Juvenile myelomonocytic leukemia displays mutations in components of the RAS pathway and the PRC2 network. *Nat Genet*. 2015;47(11):1334-1340.

Caye A, Rouault-Pierre K, Strullu M, et al. Despite mutation acquisition in hematopoietic stem cells, JMML-propagating cells are not always restricted to this compartment [published correction appears in Leukemia. 2020 Jan 31;:]. *Leukemia*. 2020;34(6):1658-1668.

Chan G, Kalaitzidis D, Usenko T, et al. Leukemogenic Ptpn11 causes fatal myeloproliferative disorder via cell-autonomous effects on multiple stages of hematopoiesis. *Blood*. 2009;113(18):4414-4424.

Chang T, Krisman K, Theobald EH, et al. Sustained MEK inhibition abrogates myeloproliferative disease in Nf1 mutant mice [published correction appears in J Clin Invest. 2016 Jan;126(1):404]. *J Clin Invest*. 2013;123(1):335-339.

Chen MJ, Li Y, De Obaldia ME, et al. Erythroid/myeloid progenitors and hematopoietic stem cells originate from distinct populations of endothelial cells [published correction appears in Cell Stem Cell. 2012 Mar 2;10(3):345-6].

Cheshier, S. H., Morrison, S. J., Liao, X. and Weissman, I. L. (1999). In vivo proliferation and cell cycle kinetics of long-term self-renewing hematopoietic stem cells. *Proc. Natl. Acad. Sci. USA* 96,3120 -3125

COOKE JV. Chronic myelogenous leukemia in children. *J Pediatr*. 1953;42(5):537-550.

Cseh A, Niemeyer CM, Yoshimi A et al . Bridging to transplant with azacitidine in juvenile myelomonocytic leukemia: a retrospective analysis of the EWOG-MDS study group. *Blood* 2015; 125: 2311–3.

Cumano A, Dieterlen-Lievre F, Godin I. Lymphoid potential, probed before circulation in mouse, is restricted to caudal intraembryonic splanchnopleura. *Cell*. 1996;86(6):907-916.

Cumano A, Ferraz JC, Klaine M, Di Santo JP, Godin I. Intraembryonic, but not yolk sac hematopoietic precursors, isolated before circulation, provide long-term multilineage reconstitution. *Immunity*. 2001;15(3):477-485.

Czermin B, Melfi R, McCabe D, Seitz V, Imhof A, Pirrotta V. Drosophila enhancer of Zeste/ESC complexes have a histone H3 methyltransferase activity that marks chromosomal Polycomb sites. *Cell*. 2002;111(2):185-196.

Davé UP, Jenkins NA, Copeland NG. Gene therapy insertional mutagenesis insights. *Science*. 2004;303(5656):333.

de Boer J, Williams A, Skavdis G, Harker N, Coles M, Tolaini M, Norton T, Williams K, Roderick K, Potocnik AJ, Kioussis D. Transgenic mice with hematopoietic and lymphoid specific expression of Cre. *Eur J Immunol*. 2003 Feb;33(2):314-25.

de Bruijn MF, Speck NA, Peeters MC, Dzierzak E. Definitive hematopoietic stem cells first develop within the major arterial regions of the mouse embryo. *EMBO J.* 2000;19(11):2465-2474.

De Raedt T, Beert E, Pasmant E, et al. PRC2 loss amplifies Ras-driven transcription and confers sensitivity to BRD4-based therapies. *Nature*. 2014;514(7521):247-251.

Deevy O, Bracken AP. PRC2 functions in development and congenital disorders. *Development*. 2019;146(19):dev181354.

Dick JE. Normal and leukemic human stem cells assayed in SCID mice. *Semin Immunol*. 1996;8(4):197-206.

Di Genua C, Norfo R, Rodriguez-Meira A, et al. Cell-intrinsic depletion of Aml1-ETO-expressing pre-leukemic hematopoietic stem cells by K-Ras activating mutation. *Haematologica*. 2019;104(11):2215-2224.

Dong L, Yu WM, Zheng H, et al. Leukaemogenic effects of Ptpn11 activating mutations in the stem cell microenvironment. *Nature*. 2016;539(7628):304-308.

Drissen R, Buza-Vidas N, Woll P, et al. Distinct myeloid progenitor-differentiation pathways identified through single-cell RNA sequencing. *Nat Immunol*. 2016;17(6):666-676.

Dzierzak E, Speck NA. Of lineage and legacy: the development of mammalian hematopoietic stem cells. *Nat Immunol*. 2008;9(2):129-136.

Dzierzak E, Bigas A. Blood Development: Hematopoietic Stem Cell Dependence and Independence. *Cell Stem Cell*. 2018;22(5):639-651.

Duncan, I. M. Polycomblike: a gene that appears to be required for the normal expression of the bithorax and antennapedia gene complexes of Drosophila melanogaster. *Genetics.* 1982;102:49 -70.

Emanuel PD, Bates LJ, Castleberry RP, Gualtieri RJ, Zuckerman KS. Selective hypersensitivity to granulocyte-macrophage colony-stimulating factor by juvenile chronic myeloid leukemia hematopoietic progenitors. *Blood*. 1991;77(5):925-929.

Emanuel PD, Shannon KM, Castleberry RP. Juvenile myelomonocytic leukemia: molecular understanding and prospects for therapy. *Mol Med Today*. 1996;2(11):468-475.

Epelman S, Lavine KJ, Beaudin AE, et al. Embryonic and adult-derived resident cardiac macrophages are maintained through distinct mechanisms at steady state and during inflammation. *Immunity*. 2014;40(1):91-104.

Ernst P, Fisher JK, Avery W, Wade S, Foy D, Korsmeyer SJ. Definitive hematopoiesis requires the mixed-lineage leukemia gene. *Dev Cell*. 2004;6:437–443.

Ezhkova E, Lien WH, Stokes N, Pasolli HA, Silva JM, Fuchs E. EZH1 and EZH2 cogovern histone H3K27 trimethylation and are essential for hair follicle homeostasis and wound repair. *Genes Dev*. 2011;25(5):485-498.

Flotho C, Valcamonica S, Mach-Pascual S, et al. RAS mutations and clonality analysis in children with juvenile myelomonocytic leukemia (JMML). *Leukemia*. 1999;13(1):32-37.

Flotho C, Kratz CP, Bergsträsser E, et al. Genotype-phenotype correlation in cases of juvenile myelomonocytic leukemia with clonal RAS mutations. *Blood*. 2008;111(2):966-968.

Ford AM, Ridge SA, Cabrera ME, et al. In utero rearrangements in the trithorax-related oncogene in infant leukaemias. *Nature*. 1993;363(6427):358-360.

Fraser CC, Kaneshima H, Hansteen G, Kilpatrick M, Hoffman R, Chen BP. Human allogeneic stem cell maintenance and differentiation in a long-term multilineage SCID-hu graft. *Blood*. 1995;86(5):1680-1693.

Furlan I, Batz C, Flotho C et al . Intriguing response to azacitidine in a patient with juvenile myelomonocytic leukemia and monosomy 7. *Blood* 2009; 113: 2867–8.

Gagne AL, Maguire JA, Gandre-Babbe S, et al. Generation of a human Juvenile myelomonocytic leukemia iPSC line, CHOPi001-A, with a mutation in CBL. *Stem Cell Res*. 2018;31:157-160.

Gale KB, Ford AM, Repp R, et al. Backtracking leukemia to birth: identification of clonotypic gene fusion sequences in neonatal blood spots. *Proc Natl Acad Sci U S* A. 1997;94(25):13950-13954.

Gan T, Jude CD, Zaffuto K, Ernst P. Developmentally induced Mll1 loss reveals defects in postnatal haematopoiesis. *Leukemia*. 2010;24(10):1732-174

Gandre-Babbe S, Paluru P, Aribeana C, et al. Patient-derived induced pluripotent stem cells recapitulate hematopoietic abnormalities of juvenile myelomonocytic leukemia. *Blood*. 2013;121(24):4925-4929.

Gazit R, Mandal PK, Ebina W, et al. Fgd5 identifies hematopoietic stem cells in the murine bone marrow. *J Exp Med*. 2014;211(7):1315-1331.

Gibson WT, Hood RL, Zhan SH, et al. Mutations in EZH2 cause Weaver syndrome. *Am J Hum Genet*. 2012;90(1):110-118.

Gitler AD, Kong Y, Choi JK, Zhu Y, Pear WS, Epstein JA. Tie2-Cre-induced inactivation of a conditional mutant Nf1 allele in mouse results in a myeloproliferative disorder that models juvenile myelomonocytic leukemia. *Pediatr Res*. 2004;55(4):581-584.

Göllner S, Oellerich T, Agrawal-Singh S, et al. Loss of the histone methyltransferase EZH2 induces resistance to multiple drugs in acute myeloid leukemia. *Nat Med*. 2017;23(1):69-78.

Gomez Perdiguero E, Klapproth K, Schulz C, et al. Tissue-resident macrophages originate from yolk-sac-derived erythro-myeloid progenitors. *Nature*. 2015;518(7540):547-551.

Greaves MF, Maia AT, Wiemels JL, Ford AM. Leukemia in twins: lessons in natural history. Blood. 2003;102(7):2321-2333.

Greaves M. A causal mechanism for childhood acute lymphoblastic leukaemia [published correction appears in Nat Rev Cancer. 2018 May 30;:]. *Nat Rev Cancer*. 2018;18(8):471-484.

Gupta RK, Qureshi A, Choi JK. Histologic findings in skin biopsy in a JMML rash: a case report and review of literature. *Pediatr Dev Pathol*. 2014;17(2):130-133.

Gustafsson B, Hellebostad M, Ifversen M, Sander B, Hasle H. Acute respiratory failure in 3 children with juvenile myelomonocytic leukemia. *J Pediatr Hematol* Oncol. 2011 Dec;33(8):e363-7.

Hacein-Bey-Abina S, Von Kalle C, Schmidt M, et al. LMO2-associated clonal T cell proliferation in two patients after gene therapy for SCID-X1 [published correction appears in Science. 2003 Oct 24;302(5645):568]. *Science*. 2003;302(5644):415-419.

HARDISTY RM, SPEED DE, TILL M. GRANULOCYTIC LEUKAEMIA IN CHILDHOOD. *Br J Haematol*. 1964;10:551-566.

Hasegawa D, Bugarin C, Giordan M, et al. Validation of flow cytometric phospho-STAT5 as a diagnostic tool for juvenile myelomonocytic leukemia. *Blood Cancer J.* 2013;3(11):e160.

Hasle H. Myelodysplastic syndromes in childhood--classification, epidemiology, and treatment. *Leuk Lymphoma*. 1994;13(1-2):11-26.

Hasle H, Wadsworth LD, Massing BG, McBride M, Schultz KR. A population-based study of childhood myelodysplastic syndrome in British Columbia, Canada. *Br J Haematol*. 1999;106(4):1027-1032.

Hasle H. Malignant diseases in Noonan syndrome and related disorders. *Horm Res*. 2009;72 Suppl 2:8-14.

Helsmoortel HH, Bresolin S, Lammens T, et al. LIN28B overexpression defines a novel fetal-like subgroup of juvenile myelomonocytic leukemia. *Blood*. 2016;127(9):1163-1172.

Herviou L, Cavalli G, Cartron G, Klein B, Moreaux J. EZH2 in normal hematopoiesis and hematological malignancies. *Oncotarget*. 2016;7(3):2284-2296.

Hidalgo I, Herrera-Merchan A, Ligos JM, et al. Ezh1 is required for hematopoietic stem cell maintenance and prevents senescence-like cell cycle arrest. *Cell Stem Cell*. 2012;11(5):649-662.

Hock H, Hamblen MJ, Rooke HM, Schindler JW, Saleque S, Fujiwara Y, Orkin SH. Gfi-1 restricts proliferation and preserves functional integrity of haematopoietic stem cells. *Nature*. 2004a;431:1002–1007.

Hoeffel G, Chen J, Lavin Y, et al. C-Myb(+) erythro-myeloid progenitor-derived fetal monocytes give rise to adult tissue-resident macrophages. *Immunity*. 2015;42(4):665-678.

Johnson L, Mercer K, Greenbaum D, et al. Somatic activation of the K-ras oncogene causes early onset lung cancer in mice. *Nature*. 2001;410(6832):1111-1116.

Jordan CT. The leukemic stem cell. *Best Pract Res Clin Haematol.* 2007;20(1):13-18.

Kamminga LM, Bystrykh LV, de Boer A, et al. The Polycomb group gene Ezh2 prevents hematopoietic stem cell exhaustion. *Blood*. 2006;107(5):2170-2179.

Khalaf WF, White H, Wenning MJ, Orazi A, Kapur R, Ingram DA. K-Ras is essential for normal fetal liver erythropoiesis. *Blood*. 2005;105(9):3538-3541.

Kiel MJ, Yilmaz OH, Iwashita T, Yilmaz OH, Terhorst C, Morrison SJ. SLAM family receptors distinguish hematopoietic stem and progenitor cells and reveal endothelial niches for stem cells. *Cell*. 2005;121(7):1109-1121.

Kim E, Ilagan JO, Liang Y, et al. SRSF2 Mutations Contribute to Myelodysplasia by Mutant-Specific Effects on Exon Recognition. *Cancer Cell*. 2015;27(5):617-630.

Kim I, Yilmaz OH, Morrison SJ. CD144 (VE-cadherin) is transiently expressed by fetal liver hematopoietic stem cells. *Blood*. 2005;106(3):903-905.

Kim I, Saunders TL, Morrison SJ. Sox17 dependence distinguishes the transcriptional regulation of fetal from adult hematopoietic stem cells. *Cell*. 2007;130(3):470-483.

Kim KH, Roberts CW. Targeting EZH2 in cancer. *Nat Med*. 2016;22(2):128-134.

Kimura Y, Sugita Y, Seki R, Inada H, Arakawa F, Kiyasu J, Takeuchi M, Hashikawa K, Aoki R, Niino D, Ohshima K. Infant juvenile myelomonocytic leukemia (JMML) with rapid infiltration of multiple organs. *Pathol Int*. 2010 Apr;60(4):333-5.

Kisanuki YY, Hammer RE, Miyazaki J, Williams SC, Richardson JA, Yanagisawa M. Tie2-Cre transgenic mice: a new model for endothelial cell-lineage analysis in vivo. *Dev Biol*. 2001 Feb 15;230(2):230-42.

Kollmann TR, Kim A, Zhuang X, Hachamovitch M, Goldstein H. Reconstitution of SCID mice with human lymphoid and myeloid cells after transplantation with human fetal bone marrow without the requirement for exogenous human cytokines. *Proc Natl Acad Sci U S A*. 1994;91(17):8032-8036.

Kühn R, Schwenk F, Aguet M, Rajewsky K. Inducible gene targeting in mice. *Science*. 1995 Sep 8;269(5229):1427-9.

Labuhn M, Perkins K, Matzk S, et al. Mechanisms of Progression of Myeloid Preleukemia to Transformed Myeloid Leukemia in Children with Down Syndrome. *Cancer Cell*. 2019;36(3):340.

Le DT, Kong N, Zhu Y, et al. Somatic inactivation of Nf1 in hematopoietic cells results in a progressive myeloproliferative disorder. *Blood*. 2004;103(11):4243-4250.

Lee ML, Yen HJ, Chen SJ, Hung GY, Tsao PC, Soong WJ. Juvenile Myelomonocytic Leukemia in a Premature Neonate Mimicking Neonatal Sepsis. *Pediatr Neonatol*. 2016;57(2):149-152.

Lee SC, Miller S, Hyland C, et al. Polycomb repressive complex 2 component Suz12 is required for hematopoietic stem cell function and lymphopoiesis. *Blood*. 2015;126(2):167-175.

Lee YT, de Vasconcellos JF, Yuan J, et al. LIN28B-mediated expression of fetal hemoglobin and production of fetal-like erythrocytes from adult human erythroblasts ex vivo. *Blood*. 2013;122(6):1034-1041.

Lewis EB. A gene complex controlling segmentation in Drosophila. *Nature*. 1978;276(5688):565-570.

Li Q, Haigis KM, McDaniel A, et al. Hematopoiesis and leukemogenesis in mice expressing oncogenic NrasG12D from the endogenous locus. *Blood*. 2011;117(6):2022-2032.

Li Q, Bohin N, Wen T, et al. Oncogenic Nras has bimodal effects on stem cells that sustainably increase competitiveness. *Nature*. 2013;504(7478):143-147.

Lipka DB, Witte T, Toth R, et al. RAS-pathway mutation patterns define epigenetic subclasses in juvenile myelomonocytic leukemia. *Nat Commun*. 2017;8(1):2126.

Lizen B, Claus M, Jeannotte L, Rijli FM, Gofflot F. Perinatal induction of Cre recombination with tamoxifen. *Transgenic Res*. 2015 Dec;24(6):1065-77.

Locatelli F, Niemeyer C, Angelucci E, et al. Allogeneic bone marrow transplantation for chronic myelomonocytic leukemia in childhood: a report from the European Working Group on Myelodysplastic Syndrome in Childhood. *J Clin Oncol*. 1997;15(2):566-573.

Locatelli F, Nöllke P, Zecca M, et al. Hematopoietic stem cell transplantation (HSCT) in children with juvenile myelomonocytic leukemia (JMML): results of the EWOG-MDS/EBMT trial. *Blood*. 2005;105(1):410-419.

Locatelli F, Crotta A, Ruggeri A et al . Analysis of risk factors influencing outcomes after cord blood transplantation in children with juvenile myelomonocytic leukemia: a EUROCORD, EBMT, EWOG-MDS. CIBMTR study. *Blood* 2013; 122: 2135–41.

Locatelli F, Niemeyer CM. How I treat juvenile myelomonocytic leukemia. *Blood*. 2015;125(7):1083-1090.

Loh ML, Vattikuti S, Schubbert S, et al. Mutations in PTPN11 implicate the SHP-2 phosphatase in leukemogenesis. *Blood*. 2004;103(6):2325-2331.

Lord A, personal communication from Karolinska Institutet. June 2017. Karolinska SOP for tamoxifen preparation 2016_10_28.

Lorenzana A, Lyons H, Sawaf H, Higgins M, Carrigan D, Emanuel PD. Human herpesvirus 6 infection mimicking juvenile myelomonocytic leukemia in an infant. *J Pediatr Hematol Oncol*. 2002;24(2):136-141.

Louka E, Povinelli B, Meira AR. Heterogeneous disease-propagating stem cells in juvenile myelomonocytic leukemia. *BioRXiv*. 2019; May 07. https://doi.org/10.1101/628479.

Lund K, Adams PD, Copland M. EZH2 in normal and malignant hematopoiesis. *Leukemia*. 2014;28(1):44-49.

Lutz P, Zix-Kieffer I, Souillet G, et al. Juvenile myelomonocytic leukemia: analyses of treatment results in the EORTC Children's Leukemia Cooperative Group (CLCG). *Bone Marrow Transplant*. 1996;18(6):1111-1116.

Lyubynska N, Gorman MF, Lauchle JO, et al. A MEK inhibitor abrogates myeloproliferative disease in Kras mutant mice. *Sci Transl Med*. 2011;3(76):76ra27.

MacMillan ML, Davies SM, Orchard PJ, Ramsay NK, Wagner JE. Haemopoietic cell transplantation in children with juvenile myelomonocytic leukaemia. *Br J Haematol*. 1998;103(2):552-558.

Madisen L, Zwingman TA, Sunkin SM, Oh SW, Zariwala HA, Gu H, Ng LL, Palmiter RD, Hawrylycz MJ, Jones AR, Lein ES, Zeng H. A robust and high-throughput Cre reporting and characterization system for the whole mouse brain. *Nat Neurosci*. 2010 Jan;13(1):133-40.

Majewski IJ, Ritchie ME, Phipson B, et al. Opposing roles of polycomb repressive complexes in hematopoietic stem and progenitor cells. *Blood*. 2010;116(5):731-739.

Manabe A, Okamura J, Yumura-Yagi K, et al. Allogeneic hematopoietic stem cell transplantation for 27 children with juvenile myelomonocytic leukemia diagnosed based on the criteria of the International JMML Working Group. *Leukemia*. 2002;16(4):645-649.

Margueron R, Li G, Sarma K, et al. Ezh1 and Ezh2 maintain repressive chromatin through different mechanisms. *Mol Cell*. 2008;32(4):503-518.

Margueron R, Reinberg D. The Polycomb complex PRC2 and its mark in life. *Nature*. 2011;469(7330):343-349.

Mass E, Jacome-Galarza CE, Blank T, Lazarov T, Durham BH, Ozkaya N, Pastore A, Schwabenland M, Chung YR, Rosenblum MK, Prinz M, Abdel-Wahab O, Geissmann F. A somatic mutation in erythro-myeloid progenitors causes neurodegenerative disease. Nature. 2017 Sep 21;549(7672):389-393.

Matsuda K, Shimada A, Yoshida N, et al. Spontaneous improvement of hematologic abnormalities in patients having juvenile myelomonocytic leukemia with specific RAS mutations. *Blood*. 2007;109(12):5477-5480.

Matsuda K, Sakashita K, Taira C, et al. Quantitative assessment of PTPN11 or RAS mutations at the neonatal period and during the clinical course in patients with juvenile myelomonocytic leukaemia. *Br J Haematol*. 2010;148(4):593-599.

Matsumoto K, Miki J, Matsuzaki S, Koike K, Saida T. Skin infiltration of juvenile myelomonocytic leukemia. *J Dermatol*. 2004;31(9):748-751.

McGrath KE, Frame JM, Fromm GJ, et al. A transient definitive erythroid lineage with unique regulation of the β-globin locus in the mammalian embryo. *Blood*. 2011;117(17):4600-4608.

McGrath KE, Frame JM, Fegan KH, et al. Distinct Sources of Hematopoietic Progenitors Emerge before HSCs and Provide Functional Blood Cells in the Mammalian Embryo. *Cell Rep*. 2015;11(12):1892-1904.

Medvinsky A, Dzierzak E. Definitive hematopoiesis is autonomously initiated by the AGM region. *Cell*. 1996;86(6):897-906.

Melo-Cardenas J, Xu Y, Wei J, et al. USP22 deficiency leads to myeloid leukemia upon oncogenic Kras activation through a PU.1-dependent mechanism. *Blood*. 2018;132(4):423-434.

Migliaccio G, Migliaccio AR, Petti S, et al. Human embryonic hemopoiesis. Kinetics of progenitors and precursors underlying the yolk sac----liver transition. *J Clin Invest*. 1986;78(1):51-60.

Mikkola HK, Orkin SH. The journey of developing hematopoietic stem cells. *Development*. 2006;133(19):3733-3744.

Miyauchi J, Asada M, Sasaki M, Tsunematsu Y, Kojima S, Mizutani S. Mutations of the N-ras gene in juvenile chronic myelogenous leukemia. *Blood*. 1994;83(8):2248-2254.

Mochizuki-Kashio M, Mishima Y, Miyagi S, et al. Dependency on the polycomb gene Ezh2 distinguishes fetal from adult hematopoietic stem cells [published correction appears in *Blood*. 2012 Jul 26;120(4):924]. *Blood*. 2011;118(25):6553-6561.

Mohi MG, Williams IR, Dearolf CR, et al. Prognostic, therapeutic, and mechanistic implications of a mouse model of leukemia evoked by Shp2 (PTPN11) mutations. *Cancer Cell*. 2005;7(2):179-191.

Montecino-Rodriguez E, Fice M, Casero D, Berent-Maoz B, Barber CL, Dorshkind K. Distinct Genetic Networks Orchestrate the Emergence of Specific Waves of Fetal and Adult B-1 and B-2 Development. *Immunity*. 2016;45(3):527-539.

Moore, M.A.S. and Metcalf, D. Ontogeny of the Haemopoietic System: Yolk Sac Origin of In Vivo and In Vitro Colony Forming Cells in the Developing Mouse Embryo*. *British Journal of Haematology*. 1970;18: 279-296.

Moritake H, Ikeda T, Manabe A, Kamimura S, Nunoi H. Cytomegalovirus infection mimicking juvenile myelomonocytic leukemia showing hypersensitivity to granulocyte-macrophage colony stimulating factor. *Pediatr Blood Cancer*. 2009;53(7):1324-1326.

Morrison SJ, Hemmati HD, Wandycz AM, Weissman IL. The purification and characterization of fetal liver hematopoietic stem cells. *Proc Natl Acad Sci U S A*. 1995;92(22):10302-10306.

Müller J, Hart CM, Francis NJ, et al. Histone methyltransferase activity of a Drosophila Polycomb group repressor complex. *Cell*. 2002;111(2):197-208.

Murakami N, Okuno Y, Yoshida K, et al. Integrated molecular profiling of juvenile myelomonocytic leukemia. *Blood*. 2018;131(14):1576-1586.

Muto T, Sashida G, Oshima M, et al. Concurrent loss of Ezh2 and Tet2 cooperates in the pathogenesis of myelodysplastic disorders. *J Exp Med*. 2013;210(12):2627-2639.

Nakagawa M, Kitabayashi I. Oncogenic roles of enhancer of zeste homolog 1/2 in hematological malignancies. *Cancer Sci*. 2018;109(8):2342-2348.

Nambu M, Shimizu K, Ito S, Ohta S. A case of juvenile myelomonocytic leukemia with ocular infiltration. *Ann Hematol*. 1999;78(12):568-570.

Neo WH, Booth CAG, Azzoni E, et al. Cell-extrinsic hematopoietic impact of Ezh2 inactivation in fetal liver endothelial cells. *Blood*. 2018;131(20):2223-2234.

Niemeyer CM, Arico M, Basso G, et al. Chronic myelomonocytic leukemia in childhood: a retrospective analysis of 110 cases. European Working Group on Myelodysplastic Syndromes in Childhood (EWOG-MDS). *Blood*. 1997;89(10):3534-3543.

Niemeyer CM, Kratz CP. Paediatric myelodysplastic syndromes and juvenile myelomonocytic leukaemia: molecular classification and treatment options. *Br J Haematol*. 2008;140(6):610-624.

Niemeyer CM. RAS diseases in children. *Haematologica*. 2014;99(11):1653-1662.

Niemeyer CM. JMML genomics and decisions. *Hematology Am Soc Hematol Educ Program*. 2018;2018(1):307-312.

North TE, de Bruijn MF, Stacy T, et al. Runx1 expression marks long-term repopulating hematopoietic stem cells in the midgestation mouse embryo. *Immunity*. 2002;16(5):661-672.

Ntziachristos P, Tsirigos A, Van Vlierberghe P, et al. Genetic inactivation of the polycomb repressive complex 2 in T cell acute lymphoblastic leukemia. *Nat Med*. 2012;18(2):298-301.

Oberlin E, Tavian M, Blazsek I, Péault B. Blood-forming potential of vascular endothelium in the human embryo. *Development*. 2002;129(17):4147-4157.

O'Byrne S, Elliott N, Rice S, et al. Discovery of a CD10-negative B-progenitor in human fetal life identifies unique ontogeny-related developmental programs. *Blood*. 2019;134(13):1059-1071.

Oguro H, Ding L, Morrison SJ. SLAM family markers resolve functionally distinct subpopulations of hematopoietic stem cells and multipotent progenitors. *Cell Stem Cell*. 2013;13(1):102-116.

Okuda T, Vandeursen J, Hiebert SW, Grosveld G, Downing JR. AML1, the target of multiple chromosomal translocations in human leukemia, is essential for normal fetal liver hematopoiesis. *Cell*. 1996;84:321–330.

Olk-Batz C, Poetsch AR, Nöllke P, et al. Aberrant DNA methylation characterizes juvenile myelomonocytic leukemia with poor outcome. *Blood*. 2011;117(18):4871-4880.

Ooi AG, Karsunky H, Majeti R, et al. The adhesion molecule esam1 is a novel hematopoietic stem cell marker. *Stem Cells*. 2009;27(3):653-661.

Osawa M, Hanada K, Hamada H, Nakauchi H. Long-term lymphohematopoietic reconstitution by a single CD34-low/negative hematopoietic stem cell. *Science*. 1996;273(5272):242-245.

Oshima M, Hasegawa N, Mochizuki-Kashio M, et al. Ezh2 regulates the Lin28/let-7 pathway to restrict activation of fetal gene signature in adult hematopoietic stem cells. *Exp Hematol*. 2016;44(4):282-96.e3.

Owen G, Lewis IJ, Morgan M, Robinson A, Stevens RF. Prognostic factors in juvenile chronic granulocytic leukaemia. *Br J Cancer Suppl*. 1992;18:S68-S71.

Palis, J., Robertson, S., Kennedy, M., Wall, C. and Keller, G., 1999. Development of erythroid and myeloid progenitors in the yolk sac and embryo proper of the mouse. *Development*, *126*(22), pp.5073-5084.

Papaemmanuil E, Gerstung M, Malcovati L, et al. Clinical and biological implications of driver mutations in myelodysplastic syndromes. *Blood*. 2013;122(22):3616-3699.

Papaemmanuil E, Gerstung M, Bullinger L, et al. Genomic Classification and Prognosis in Acute Myeloid Leukemia. *N Engl J Med*. 2016;374(23):2209-2221.

Park IK, Qian D, Kiel M, Becker M, Pihalja M, Weissman IL, Morrison SJ, Clarke M. Bmi-1 is required for the maintenance of adult self-renewing hematopoietic stem cells. *Nature*. 2003;423:302–305.

Passmore SJ, Hann IM, Stiller CA, et al. Pediatric myelodysplasia: a study of 68 children and a new prognostic scoring system. *Blood*. 1995;85(7):1742-1750.

Passmore SJ, Chessells JM, Kempski H, Hann IM, Brownbill PA, Stiller CA. Paediatric myelodysplastic syndromes and juvenile myelomonocytic leukaemia in the UK: a population-based study of incidence and survival. *Br J Haematol*. 2003;121(5):758-767.

Pérez B, Kosmider O, Cassinat B, et al. Genetic typing of CBL, ASXL1, RUNX1, TET2 and JAK2 in juvenile myelomonocytic leukaemia reveals a genetic profile distinct from chronic myelomonocytic leukaemia. *Br J Haematol*. 2010;151(5):460-468.

Pietras EM, Reynaud D, Kang YA, et al. Functionally Distinct Subsets of Lineage-Biased Multipotent Progenitors Control Blood Production in Normal and Regenerative Conditions. *Cell Stem Cell*. 2015;17(1):35-46.

Porcher C, Swat W, Rockwell K, Fujiwara Y, Alt FW, Orkin SH. The T cell leukemia oncoprotein SCL/tal-1 is essential for development of all hematopoietic lineages. *Cell*. 1996;86:47–57.

Pronk CJ, Rossi DJ, Månsson R, et al. Elucidation of the phenotypic, functional, and molecular topography of a myeloerythroid progenitor cell hierarchy. *Cell Stem Cell.* 2007;1(4):428-442.

Randall TD, Weissman IL. Phenotypic and functional changes induced at the clonal level in hematopoietic stem cells after 5-fluorouracil treatment. *Blood*. 1997;89(10):3596-3606.

REISMAN LE, TRUJILLO JM. Chronic granulocytic leukemia of childhood. Clinical and cytogenetic studies. *J Pediatr*. 1963;62:710-723.

Rinke J, Chase A, Cross NCP, Hochhaus A, Ernst T. EZH2 in Myeloid Malignancies. *Cells*. 2020;9(7):E1639. Published 2020 Jul 8.

Roberts I, Alford K, Hall G, et al. GATA1-mutant clones are frequent and often unsuspected in babies with Down syndrome: identification of a population at risk of leukemia. *Blood*. 2013;122(24):3908-3917.

Roberts I, Izraeli S. Haematopoietic development and leukaemia in Down syndrome. *Br J Haematol*. 2014;167(5):587-599.

Roberts I, Fordham NJ, Rao A, Bain BJ. Neonatal leukaemia [published correction appears in Br J Haematol. 2019 Jul;186(1):196]. *Br J Haematol*. 2018;182(2):170-184.

Röttgers S, Gombert M, Teigler-Schlegel A, et al. ALK fusion genes in children with atypical myeloproliferative leukemia. *Leukemia*. 2010;24(6):1197-1200.

Rowe RG, Wang LD, Coma S, et al. Developmental regulation of myeloerythroid progenitor function by the Lin28b-let-7-Hmga2 axis. *J Exp Med*. 2016;213(8):1497-1512.

Sabnis AJ, Cheung LS, Dail M, et al. Oncogenic Kras initiates leukemia in hematopoietic stem cells. *PLoS Biol*. 2009;7(3):e59.

Sakashita K, Matsuda K, Koike K. Diagnosis and treatment of juvenile myelomonocytic leukemia. *Pediatr Int*. 2016;58(8):681-690.

Sankaran VG, Menne TF, Xu J, et al. Human fetal hemoglobin expression is regulated by the developmental stage-specific repressor BCL11A. *Science*. 2008;322(5909):1839-1842.

Sankaran VG, Xu J, Orkin SH. Advances in the understanding of haemoglobin switching. *Br J Haematol*. 2010;149(2):181-194.

Sashida G, Wang C, Tomioka T, et al. The loss of Ezh2 drives the pathogenesis of myelofibrosis and sensitizes tumor-initiating cells to bromodomain inhibition. *J Exp Med*. 2016;213(8):1459-1477.

Schuettengruber B, Cavalli G. Recruitment of polycomb group complexes and their role in the dynamic regulation of cell fate choice. *Development*. 2009;136(21):3531-3542.

Schwenk F, Kuhn R, Angrand PO, Rajewsky K, Stewart AF. Temporally and spatially regulated somatic mutagenesis in mice. *Nucleic Acids Res*. 1998 Mar 15;26(6):1427-32.

Score J, Hidalgo-Curtis C, Jones AV, et al. Inactivation of polycomb repressive complex 2 components in myeloproliferative and myelodysplastic/myeloproliferative neoplasms. *Blood*. 2012;119(5):1208-1213.

Shen X, et al. EZH1 mediates methylation on histone H3 lysine 27 and complements EZH2 in maintaining stem cell identity and executing pluripotency. *Mol Cell*. 2008;32:491–502.

Shannon KM, O'Connell P, Martin GA, et al. Loss of the normal NF1 allele from the bone marrow of children with type 1 neurofibromatosis and malignant myeloid disorders. *N Engl J Med*. 1994;330(9):597-601.

Shimizu T, Kubovcakova L, Nienhold R, et al. Loss of Ezh2 synergizes with JAK2-V617F in initiating myeloproliferative neoplasms and promoting myelofibrosis. *J Exp Med*. 2016;213(8):1479-1496.

Shyh-Chang N, Daley GQ. Lin28: primal regulator of growth and metabolism in stem cells. *Cell Stem Cell*. 2013;12(4):395-406.\\ Simon JA, Kingston RE. Mechanisms of polycomb gene silencing: knowns and unknowns. *Nat Rev Mol Cell Biol*. 2009;10(10):697-708.

SIMINOVITCH L, MCCULLOCH EA, TILL JE. THE DISTRIBUTION OF COLONY-FORMING CELLS AMONG SPLEEN COLONIES. J Cell Comp Physiol. 1963;62:327-336.

Sinka L, Biasch K, Khazaal I, Péault B, Tavian M. Angiotensin-converting enzyme (CD143) specifies emerging lympho-hematopoietic progenitors in the human embryo. *Blood*. 2012;119(16):3712-3723.

Smith LB, Valdes Y, Check WE, Britt PM, Frankel LS. Juvenile myelomonocytic leukemia presenting with facial nerve paresis: a unique presentation. *J Pediatr Hematol Oncol*. 2007;29(11):770-773.

Sonoda Y. Human CD34-negative hematopoietic stem cells: The current understanding of their biological nature. *Exp Hematol*. 2021 Apr;96:13-26.

Spangrude GJ, Heimfeld S, Weissman IL. Purification and characterization of mouse hematopoietic stem cells [published correction appears in Science 1989 Jun 2;244(4908):1030]. *Science*. 1988;241(4861):58-62.

Stieglitz E, Taylor-Weiner AN, Chang TY, et al. The genomic landscape of juvenile myelomonocytic leukemia [published correction appears in Nat Genet. 2015 Nov;47(11):1333] [published correction appears in Nat Genet. 2016 Jan;48(1):101]. *Nat Genet*. 2015;47(11):1326-1333.

Su IH, Basavaraj A, Krutchinsky AN, et al. Ezh2 controls B cell development through histone H3 methylation and Igh rearrangement. *Nat Immunol*. 2003;4(2):124-131.

Su IH, Dobenecker MW, Dickinson E, et al. Polycomb group protein ezh2 controls actin polymerization and cell signaling. *Cell*. 2005;121(3):425-436.

Tang P, Gao C, Li A, Aster J, Sun L, Chai L. Differential roles of Kras and Pten in murine leukemogenesis. *Leukemia*. 2013;27(5):1210-1214.

Tarnawsky SP, Yoshimoto M, Deng L, Chan RJ, Yoder MC. Yolk sac erythromyeloid progenitors expressing gain of function PTPN11 have functional features of JMML but are not sufficient to cause disease in mice. *Dev Dyn*. 2017;246(12):1001-1014.

Tarnawsky* SP, Kobayashi M, Chan RJ, Yoder MC. Mice expressing KrasG12D in hematopoietic multipotent progenitor cells develop neonatal myeloid leukemia. *J Clin Invest*. 2017;127(10):3652-3656.

Tarnawsky SP, Yu WM, Qu CK, Chan RJ, Yoder MC. Hematopoietic-restricted Ptpn11E76K reveals indolent MPN progression in mice. *Oncotarget*. 2018;9(31):21831-21843.

Tasian SK, Casas JA, Posocco D, et al. Mutation-specific signaling profiles and kinase inhibitor sensitivities of juvenile myelomonocytic leukemia revealed by induced pluripotent stem cells. *Leukemia*. 2019;33(1):181-190.

Tavian M, Hallais MF, Péault B. Emergence of intraembryonic hematopoietic precursors in the pre-liver human embryo. *Development*. 1999;126(4):793-803.

Tsai FY, Keller G, Kuo FC, Weiss M, Chen J, Rosenblatt M, Alt FW, Orkin SH. An early haematopoietic defect in mice lacking the transcription factor GATA-2. *Nature*. 1994;371:221–226.

Ved N, Curran A, Ashcroft FM, Sparrow DB. Tamoxifen administration in pregnant mice can be deleterious to both mother and embryo. *Lab Anim*. 2019;53(6):630-633.

Vo LT, Kinney MA, Liu X, et al. Regulation of embryonic haematopoietic multipotency by EZH1. *Nature*. 2018;553(7689):506-510.

Wang J, Kimura T, Asada R, Harada S, Yokota S, Kawamoto Y, Fujimura Y, Tsuji T, Ikehara S, Sonoda Y. SCID-repopulating cell activity of human cord blood-derived CD34- cells assured by intra-bone marrow injection. *Blood*. 2003 Apr 15;101(8):2924-31.

Wang H, Wang L, Erdjument-Bromage H, et al. Role of histone H2A ubiquitination in Polycomb silencing. *Nature*. 2004;431(7010):873-878.

Warren AJ, Colledge WH, Carlton MB, Evans MJ, Smith AJ, Rabbitts TH. The oncogenic cysteine-rich LIM domain protein rbtn2 is essential for erythroid development. *Cell*. 1994;78(1):45-57.

Xie H, Xu J, Hsu JH, et al. Polycomb repressive complex 2 regulates normal hematopoietic stem cell function in a developmental-stage-specific manner. *Cell Stem Cell*. 2014;14(1):68-80.

Xu B, On DM, Ma A, et al. Selective inhibition of EZH2 and EZH1 enzymatic activity by a small molecule suppresses MLL-rearranged leukemia. *Blood*. 2015;125(2):346-357.

Yabe M, Sako M, Yabe H, et al. A conditioning regimen of busulfan, fludarabine, and melphalan for allogeneic stem cell transplantation in children with juvenile myelomonocytic leukemia. *Pediatr Transplant*. 2008;12(8):862-867.

Yabe M, Ohtsuka Y, Watanabe K et al . Transplantation for juvenile myelomonocytic leukemia: a retrospective study of 30 children treated with a regimen of busulfan, fludarabine, and melphalan. *Int. J. Hematol*. 2015; 101: 184–90.

Yamada M, Hatta T, Otani H. Mouse exo utero development system: protocol and troubleshooting. *Congenit Anom (Kyoto)*. 2008 Dec;48(4):183-7.

Yang Y, Akada H, Nath D, Hutchison RE, Mohi G. Loss of Ezh2 cooperates with Jak2V617F in the development of myelofibrosis in a mouse model of myeloproliferative neoplasm. *Blood*. 2016;127(26):3410-3423.

Ye R, Wang QA, Tao C, Vishvanath L, Shao M, McDonald JG, Gupta RK, Scherer PE. Impact of tamoxifen on adipocyte lineage tracing: Inducer of adipogenesis and prolonged nuclear translocation of Cre recombinase. *Mol Metab*. 2015 Aug 29;4(11):771-8.

Yoder MC, Hiatt K. Engraftment of Embryonic Hematopoietic Cells in Conditioned Newborn Recipients. *Blood* 1997; 89 (6): 2176–2183.

Yoshida N, Yagasaki H, Xu Y, et al. Correlation of clinical features with the mutational status of GM-CSF signaling pathway-related genes in juvenile myelomonocytic leukemia. *Pediatr Res*. 2009;65(3):334-340.

Yoshimi A, Kamachi Y, Imai K, et al. Wiskott-Aldrich syndrome presenting with a clinical picture mimicking juvenile myelomonocytic leukaemia. *Pediatr Blood Cancer*. 2013;60(5):836-841.

Yoshimi A, Balasis ME, Vedder A, et al. Robust patient-derived xenografts of MDS/MPN overlap syndromes capture the unique characteristics of CMML and JMML [published correction appears in Blood. 2017 Sep 28;130(13):1602]. *Blood*. 2017;130(4):397-407. doi:10.1182/blood-2017-01-763219

Yoshimoto M, Montecino-Rodriguez E, Ferkowicz MJ, et al. Embryonic day 9 yolk sac and intra-embryonic hemogenic endothelium independently generate a B-1 and marginal zone progenitor lacking B-2 potential. *Proc Natl Acad Sci U S A*. 2011;108(4):1468-1473.

Zhang Y, Taylor BR, Shannon K, Clapp DW. Quantitative effects of Nf1 inactivation on in vivo hematopoiesis. *J Clin Invest*. 2001;108(5):709-715.

Zhang J, Socolovsky M, Gross AW, Lodish HF. Role of Ras signaling in erythroid differentiation of mouse fetal liver cells: functional analysis by a flow cytometry-based novel culture system. *Blood*. 2003;102(12):3938-3946.

Zhang J, Wang J, Liu Y, et al. Oncogenic Kras-induced leukemogeneis: hematopoietic stem cells as the initial target and lineage-specific progenitors as the potential targets for final leukemic transformation. *Blood*. 2009;113(6):1304-1314.

Zhang Y, Patel S, Abdelouahab H, et al. CXCR4 inhibitors selectively eliminate CXCR4-expressing human acute myeloid leukemia cells in NOG mouse model. *Cell Death Dis*. 2012;3(10):e396.

A final acknowledgement to the 4510 mice, with which I (eventually) gained some ease:

A mouse should be handled with utmost care,
To avoid a nasty bite,
The nip of a digit holds naught to fear,
But that one may die from fright.

THE END